Investigating the renogenic potential of mesenchymal stem cells

Thesis submitted in accordance with the requirements of the University of Liverpool for the degree of Doctor in Philosophy

by

Maria Kuźma-Kuźniarska

May 2011

Contents

Acknowledgments

I would like to thank my supervisors Patricia Murray and David Edgar for their support during this project as well as all my collaborators in the KIDSTEM network. Especially, I would like to thank Christos Xinaris, Veronika Ganeva, Sandra Rak-Raszewska and Monika Wozińska for all the great scientific and not only scientific discussions.

I would like to thank Jarek Lipski for his support during the whole project and his help in the final stages of thesis preparation (for non-computer people like me).

Finally, I would like to thank to my parents for their support.

Glossary of common abbreviations

AFSC amniotic fluid stem cells
BSA bovine serum albumin
BMP bone morphogenetic protein
cDNA complementary DNA
CFDA SE carboxyfluorescein diacetate succinimidyl ester
DAPI 4',6-diamidino-2-phenylindole
DMEM Dulbecco's Modified Eagle Medium
DNA deoxyribonucleic acid
E embryonic day
EDTA ethylenediaminetetraacetic acid
ESC embryonic stem cells
FCS fetal calf serum
GAPDH glyceraldehyde 3-phosphate dehydrogenase
GDNF glial cell-derived neurotrophic factor
GFP green fluorescent protein
h hours
HBSS Hanks’s buffered saline solution
HSC hematopoietic stem cell
IM intermediate mesoderm
NKC neonatal kidney cells
MEF mouse embryonic fibroblast
min minutes
MM metanephric mesenchyme
MSC mesenchymal stem cells
PBS phosphate buffered saline
PCR polymerase chain reaction
PFA paraformaldehyde
RNA ribonucleic acid
sec seconds
QD quantum dot
TAE tris-acetate EDTA
TGF transforming growth factor
UB ureteric bud

Abstract

Mesenchymal stem cells (MSCs) are a multipotent cell population which have been described to exert renoprotective and regenerative effects in experimental models of kidney injury. In addition, it was recently shown that human MSCs are able to contribute to the development of both renal tubules and glomeruli. These results suggest that MSCs might be potential candidates for stem cell-based de novo renal tissue generation. The current study was aimed at re-evaluating the renogenic capacity of mouse and human bone marrow-derived MSCs. In order to elucidate the renogenic potential of MSCs, a novel method of embryonic kidney culture was used that is based on disaggregation of mouse kidney rudiments and their subsequent re-aggregation in the presence of cells from different origins to form kidney chimeras. Initially, MSCs did show expression of some genes involved in renal development; however, neither mouse nor human cells expressed important renal development genes, such as Wt1 and Pax2. Accordingly, MSCs were demonstrated to have low renogenic potential in the chimeric kidney model as they did not engraft into ureteric buds, the precursors of collecting duct system, and were only occasionally found in the condensing metanephric mesenchyme, which gives rise to nephrons. In addition, the incorporation of MSCs into embryonic kidneys had some detrimental effect on metanephric development. This effect was mediated through a paracrine action of the cells, as conditioned medium derived from mouse MSCs was demonstrate to reduce ureteric bud branching in *in vitro* kidney rudiment culture. On the contrary, mouse neonatal kidney cells did engraft into the condensing mesenchyme of chimeric kidneys and were subsequently found in some developing nephron-like structures. Regarding the potential of mouse embryonic stem cells to contribute to renal development in the re-aggregated kidney chimeras, the cells were found to some extent in both the condensing mesenchyme and the laminin-positive tubular compartment of chimeric

kidneys, possibly the ureteric buds. No negative effect on kidney development was observed using the neonatal kidney cells as well as the embryonic stem cells. Ultimately it has been shown that the pre-conditioning of mouse MSCs with medium derived from mouse neonatal kidney cells facilitated the engraftment of MSCs into condensing mesenchyme of chimeric kidneys. It also prevented the negative action of MSCs on kidney development confirmed in the *in vitro* kidney rudiment culture. MSCs were demonstrated to up-regulate *GDNF* expression upon the pre-conditioning which is important factor for outgrowth and branching of ureteric buds. In conclusion, although pre-conditioning of the MSCs with medium derived from kidney cells was able to improve considerably the renogenic potential of the cells in the chimeric kidney, MSCs demonstrate a relatively low renogenic potential and for this reason are not good candidates for regenerative approaches aimed at recapitulation of nephrogenesis.

Statement of authorship

This thesis is submitted for the degree of Doctor in Philosophy at the University of Liverpool. The research work presented here, which includes the analysis of all samples, interpretation of the data and writing of the thesis, was performed by the author.

Chapter 1: Introduction

1.1. Overview of the anatomy and function of the adult kidney

Kidneys remove waste products from blood. They also produce hormones, like erythropoietin and maintain homeostasis by regulating fluid balance, acid-base balance and blood pressure. The nephron is the structural and functional unit of the kidney. It consists of renal tubules, including the proximal tubule, limbs of the loop of Henle and the distal tubule, as well as the renal corpuscle formed by the Bowman's capsule and the glomerulus. The role of the glomerulus is to produce an ultrafiltrate, in the process called glomerular filtration, which becomes urine once it is concentrated by the renal tubules, while the collecting duct system of the kidney is connecting the nephrons to the ureters. The kidneys, together with ureters, bladder and urethra, form the urinary system (Figure 1.1a) (Vize Peter 2003).

A kidney contains a cortex and a medulla, as demonstrated in the Figure 1.1b. In the renal cortex, glomeruli, proximal and distal tubules, loops of Henle and collecting ducts are found (Figure 1.1b). The medulla is divided into outer medulla, containing the proximal and distal tubules, the loops of Henle and the collecting ducts, while the inner medulla harbours the loops of Henle and large collecting ducts that empty into the minor calyces (Figure 1.1b). The renal interstitium is present in both the renal cortex and medulla and contains fibroblasts, lymphocyte-like cells, pericytes and the extracellular matrix (Vize Peter 2003; Cullen-McEwen et al. 2005). Fibroblasts are the most abundant cell population producing the extracellular matrix (Vize Peter 2003). In addition, the medulla can be organized into several renal pyramids connecting to the minor calyces and renal columns which are formed between the pyramids by cortical tissue.

Accordingly, the urine flows from the medulla into the minor calyces, which open into the major calyces and subsequently into the renal pelvis. The renal pelvis is connected to the ureters and the urine flows into the bladder (Figure 1.1a) (Vize Peter 2003).

As mentioned earlier, the role of the glomerulus is to perform filtration. The blood enters the kidney though the renal arteries, which divide subsequently into arterioles that enter and exit the Bowman's capsule at the vascular pole (Figure 1.2a). In the Bowman's capsule the glomerular arterioles branch into glomerular capillaries. Mesangial cells found between glomerular capillaries maintain the structural integrity of the glomerulus. Later, the blood from the glomerular arteriole is transported to the peritubular capillaries which recover water, salts and other compounds reabsorbed by the tubular epithelium. The glomerular filtration proceeds through a filtration barrier consisting of glomerular capillaries with many fenestrations, the glomerular basement membrane and the podocytes. The filtration barrier allows separation of blood cells and large macromolecules from the ultrafiltrate. Podocytes are specialized cells of the Bowman's capsule which wrap around the glomerular capillaries using foot processes. The filtration proceeds through slits in the foot processes and subsequently the ultrafiltrate is collected in the Bowman's space. Figure 1.2b shows a schematic representation of the filtration barrier. The glomerular filtration is regulated by vasoconstriction and dilation of afferent and efferent arterioles, which together with the distal tubule, form the juxtaglomerular apparatus at the vascular pole of the renal corpuscle (Vize Peter 2003).

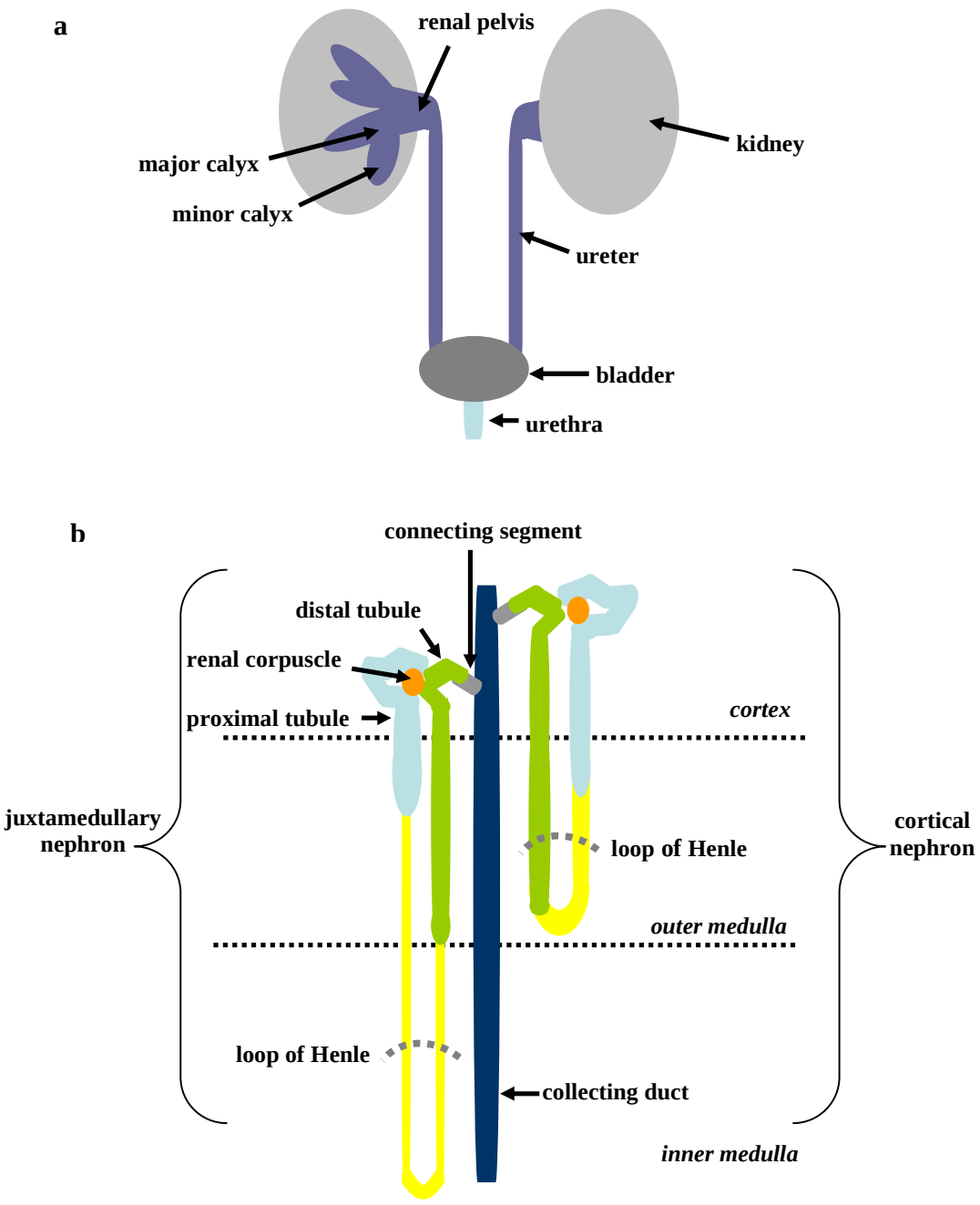

Figure 1.1 Schematic representation of the urinary system and kidney parenchyma. (a) The urinary system, including the minor and major calyx and renal pelvis. (b) The components of renal parenchyma, the cortex and medulla, with two types of nephron found in the kidneys.

a

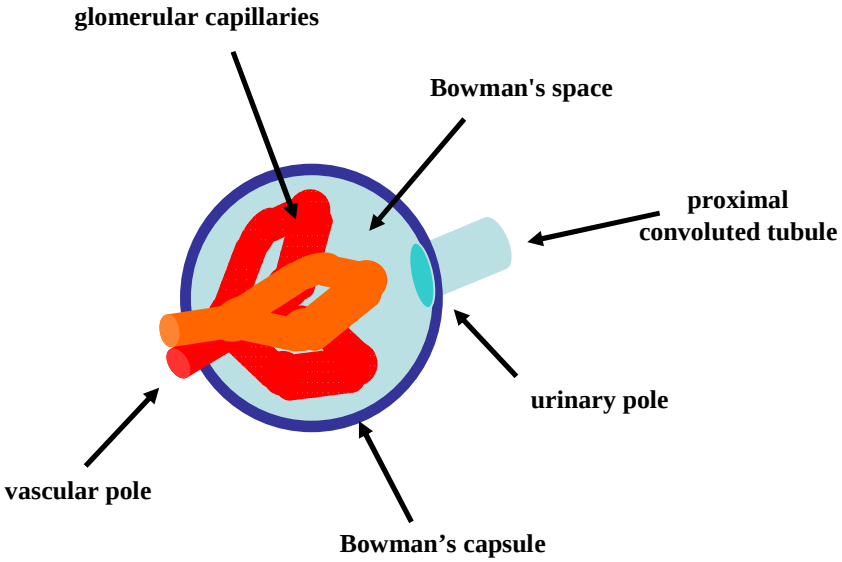

b

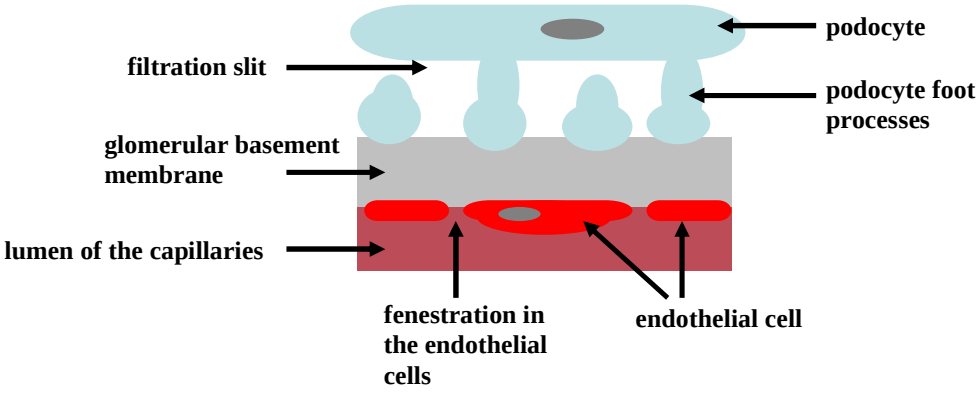

Figure 1.2 A schematic representation of the renal corpuscle (a) and the filtration barrier found in the glomerulus (b).

From the Bowman's space, the ultrafiltrate enters the proximal tubule at the urinary pole (Figure 1.2a). The proximal tubule consists of a convoluted and a straight part. In the proximal tubules, reabsorption of water as well as amino acids, glucose, creatinine, bicarbonate, phosphate, potassium, calcium, sodium and chloride occurs. The epithelial cells of proximal tubules have a brush border of microvilli which enhance the reabsorption. They also express many proteins related to transport, such as aquaporin-1, a water channel protein responsible for water transport across the tubule. The proximal tubule is also the site of secretion of uric acid and the site of ammonia production (Vize Peter 2003).

The ultrafiltrate from the proximal tubule passes next through the loops of Henle which consist of the thin descending limb, permeable to water and ions, the thin ascending limb, permeable to salts but less permeable to water, and the thick ascending limb, impermeable to water but able to actively transport salts. The thick ascending limb is the largest site of sodium and chloride reabsorption after the proximal tubule. The loop of Henle is also the regulatory site of magnesium excretion. In addition there are two main populations of nephrons in the kidney depending on the length of the loop of Henle. Cortical nephrons have shorter loops in comparison to juxtamedullary nephrons (Vize Peter 2003).

Subsequently, the ultrafiltrate reaches the distal tubule which is impermeable to water but reabsorbs salts. The distal tubule is divided into the straight and convoluted portion. At the point where the ascending straight part of the distal tubule reaches the glomerulus, the *macula densa* is formed, which is a component of the juxtaglomerular apparatus. The distal tubule is also the regulatory site for calcium extraction. The intermediate zone between the distal convoluted tubule and the collecting duct is called the connecting segment and contains cells that have the

characteristics of both distal tubule cells as well the collecting duct cells (Vize Peter 2003).

The collecting duct is divided into the following segments: cortical, outer medullar and inner medullary and papillary. These segments increase in size towards the papilla where the medulla empties urine into the minor calyx. The principal and intercalated cells are two cell types that are distinguished in the collecting duct. The principal cells, expressing aquaporin-2, are specialized in water transport, while the intercalated cells play a role in maintaining the acid-base balance by secreting bicarbonate into the collecting duct. In the medullary segment of the collecting duct, the reabsorption of sodium, chloride and water occurs (Vize Peter 2003).

1.2. Kidney development

The urinary system is derived during embryogenesis from the intermediate mesoderm (IM) which is located between the somitic and lateral plate mesoderm. Figure 1.3a demonstrates the localization of the IM in a developing mouse embryo before the nephric duct is formed at embryonic day (E) 8. Kidney development is characterized by the sequential appearance of three excretory organs, namely the pronephros, mesonephros, and finally the metanephros, which is the permanent kidney in amniotes. A central role in nephrogenesis is played by the nephric duct, which is responsible for the formation of the collecting duct system. The pronephros develops in the anterior part of the duct whereas the mesonephros is located more caudally. Ultimately, the metanephros arises caudal to the mesonephros (Saxen 1987; Vize Peter 2003). Figure 1.3b demonstrates the sequential development of the mouse pronephros, mesonephros and metanephros.

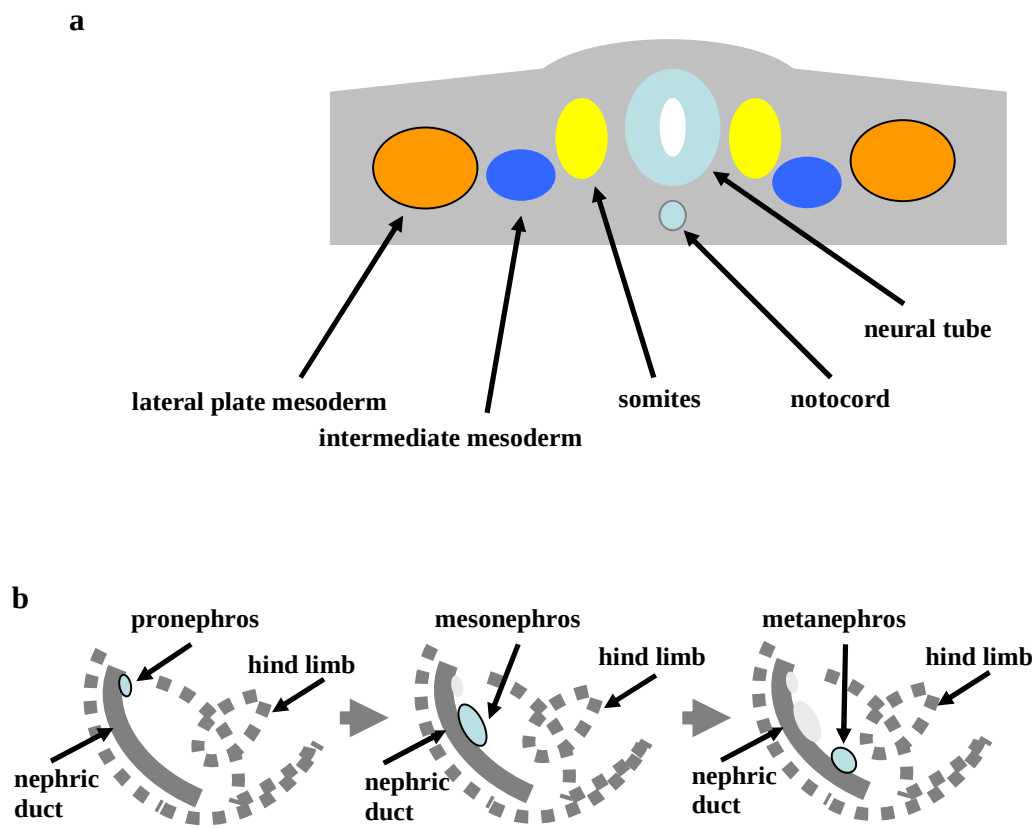

Figure 1.3 Schematic representation of kidney development in amniotes. (a) Localization of intermediate mesoderm within a mouse embryo before E8. (b) Sequential appearance of the pronephros, mesonephros and the metanephros in a mouse embryo.

1.2.1. Pronephros

The pronephric kidney (pronephros) is the most primitive kidney and contains a single nephron which filters blood. However, as there is no Bowman's space, the filtrate from the glomus (glomerulus) is collected from an open cavity by ciliated tubules called nephrostomes which are connected to pronephric tubules. Pronephric tubules contain a proximal segment which resorbes solute, and a distal segment which resorbes water. Subsequently the urine passes through the nephric duct, also called the pronephric duct, to the cloaca. Pronephroi are present during the urinary tract development in mammals but they are rudimentary and undergo early degeneration

in comparison with well-developed pronephroi found in fish and amphibians. In mice, the pronephros appears around E8. Accordingly, the pronephros functions as an excretory organ in the larval stages of lower vertebrates. In adult fish the pronephros becomes a lymphoid organ, similar as in the amphibians, where it becomes the site of hematopoiesis (Saxen 1987; Vize Peter 2003).

1.2.2. Mesonephros

The mesonephric kidney (mesonephros) is a temporary organ that precedes the development of the permanent kidney in mammals. However, it is the definitive excretory organ in adult amphibians and some fish, such as the zebrafish. The mesonephros is characterized by a linear series of nephrons that are linked to the nephric duct, called at this stage of development, the Wolffian duct. The mesonephric nephron consists of a glomerulus, proximal and distal tubule. Some important differences exist between the nephrons found in the mesonephric kidneys and the nephrons of a permanent kidney. Accordingly, mesonephric nephrons have poor fenestration of the capillaries and they lack the juxtaglomerular apparatus. The mesonephros emerges in mice at E9.5. The mesonephros undergoes degeneration during embryogenesis in mammals. The degradation is partial in males and the remaining mesonephric tubules form parts of the ducts in the gonads. The role of the Wolffian duct during mesonephric kidney development is not only restricted to its function as a urinary drain. The Wolffian duct plays an important part in the induction of mesonephric devolvement, possibly utilizing the same molecular mechanisms found during the development of the permanent kidney (Saxen 1987; Vize Peter 2003).

1.2.3. Metanephros

The metanephric kidney (metanephros) becomes the permanent kidney in mammals. It is the most complex kidney, and unlike the mesonephros, has a branched structure. The metanephros starts to develop in mice at E11 and its development continues postnatally for approximately 1 week. The development of the adult kidney starts with the invasion of the ureteric bud (UB) into the surrounding metanephric mesenchyme (MM). UB is an epithelial outgrowth of the posterior end of the Wolffian duct and is a precursor of the collecting duct system, while MM is involved in nephron formation. Aspects of metanephric development, which include the formation of the collecting duct, nephron and stroma in the metanephros, are discussed in the following sections.

1.2.3.1. Collecting duct system development

The collecting ducts develop from the UB, which is the derivative of the nephric duct. The outgrowth of the UB is induced by the MM and starts with the formation of an epithelial bud from the Wolffian duct. In mouse, the UB forms at E10, and at E11, invades the MM. Further interaction between the UB and MM triggers the UB to branch dichotomously. By E11.5, the UB forms a T-shaped tubule. At the same time, the UB induces the MM to form nephrons and further branching morphogenesis occurs. Later during development, the UB branches less and several nephrons start to form at the same level, joining to the same collecting duct. Figure 1.4 demonstrates the branching morphogenesis of a UB during mouse metanephric kidney development. Ultimately, the UB develops into the collecting ducts, calyces, renal pelvis and the ureter (Vize Peter 2003; Dressler 2006).

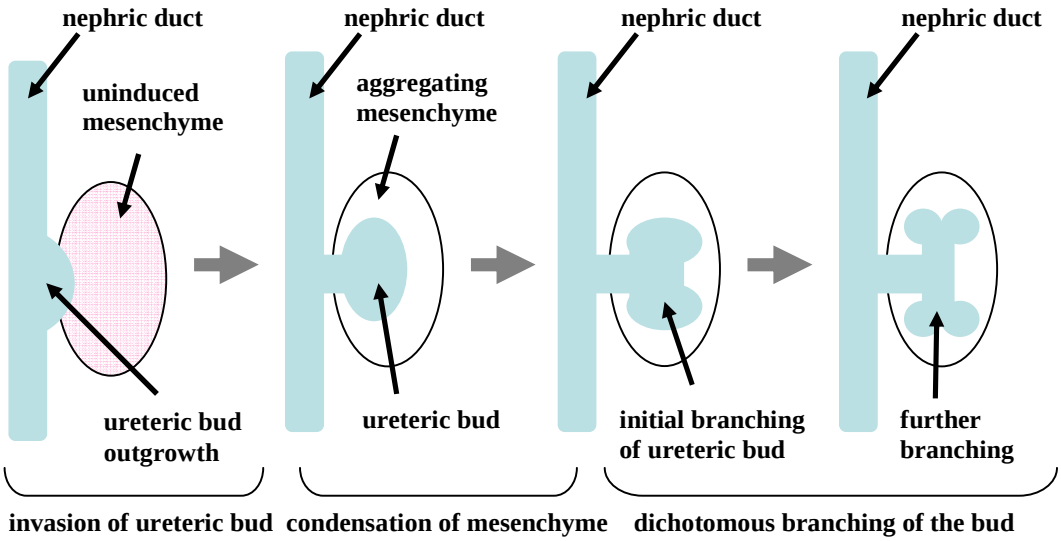

Figure 1.4 The branching morphogenesis of the UB.

1.2.3.2. Nephron development

The interaction between UB and MM stimulates the uninduced MM to condense in the proximity of the UB tips and subsequently form nephrons. In the mouse, the MM starts to condense in the proximity of the UB tips around E11. Accordingly, the condensing MM undergoes epithelial conversion, generating renal vesicles. This transition is characterised by important changes in the expression of extracellular matrix proteins. The uninduced MM expresses collagen type I and III, as well as fibronectin, which are not found in condensing MM. Conversely, the condensation of MM is accompanied by expression of laminin, a component of the epithelial basement membrane (Horster et al. 1999; Dressler 2006). Furthermore it has been described that α1 chain of laminin-1 is highly expressed during early epithelial development and it is also the major chain found in adult kidneys (Ekblom et al. 2003). Subsequently, renal vesicles are converted into comma (C)-shaped bodies. At this stage the developing nephrons start to fuse with the UBs. Next, the C-shaped bodies develop into the S-shaped bodies (Horster et al. 1999; Dressler 2006). The

formation of the early nephron, including the renal vesicle, C-shaped and S-shaped body stage, is depicted in Figure 1.5a. The proximal end of the S-shaped body forms the renal corpuscle, whereas the distal end fused with UB epithelium forms the renal tubule. Around the vascular cleft found in the proximal end of the S-shaped body the Bowman's capsule is formed. Accordingly, the outer cell layer of the proximal end of the S-shaped body develops into the Bowman's capsule epithelium whereas the internal cell layer becomes the podocytes (1.5b) (Horster et al. 1999; Vize Peter 2003; Dressler 2006). The glomerular basement membrane is derived from both the extracellular matrix of the forming capillary endothelium and the podocytes (Vize Peter 2003). Subsequently, the endothelial precursors invade the forming nephron at the vascular cleft to form the glomerular capillary loops (Figure 1.5b). The glomerular endothelial and mesangial cells are most likely of extrarenal origin. However, there is also some evidence that the MM contains endothelial progenitors (Vize Peter 2003). Ultimately, the S-shaped body also forms the proximal tubule, the loop of Henle, distal tubule and the connecting segment. However there is not much data on the pattering of the emerging renal tubules (Vize Peter 2003).

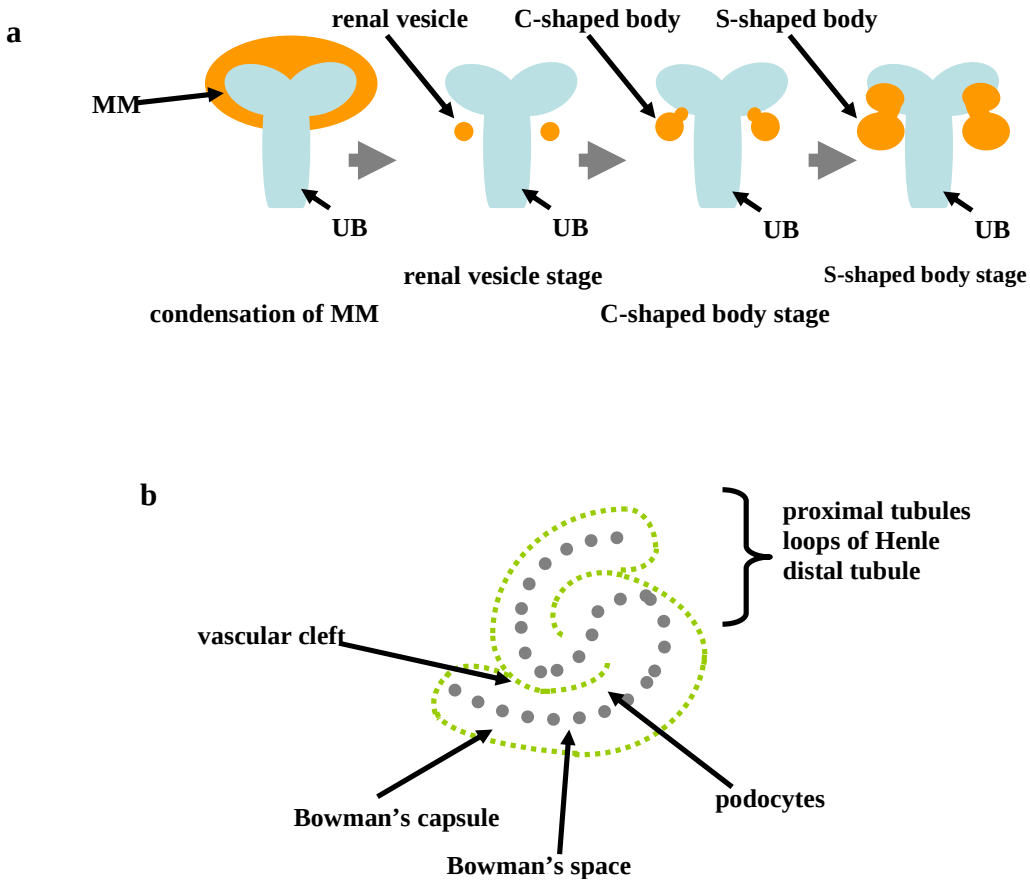

Figure 1.5 Schematic representation of early nephron development. (a) Formation of the renal vesicle, C-shaped and S-shaped body (in orange). The ureteric bud is shown in blue. (b) A developing the S-shaped body. As demonstrated, the proximal end of the S-shaped body will develop into renal corpuscle and the distal into different renal tubules.

1.2.3.3. Development of the renal stroma

An important compartment in the developing metanephros, which is implicated in regulation of UB branching and mesenchymal-to-epithelial transition of the MM, is the renal stroma. The localization of the stromal compartment in a mouse metanephros is depicted in Figure 1.6. After the UB has invaded the MM and induced MM to condense around its tips, formation of two mesenchymal compartments can be determined in the metanephros. Accordingly, the condensing MM closely surrounding the bud tip will form the nephrons, and the peripheral cells will become

the stromal cells (Figure 1.6). Later, the stromal cells are found surrounding the UB branches and forming nephrons (Figure 1.6). These cells are called the primary renal interstitium. As renal tubules develop, a secondary interstitium is formed; the cortical stroma and the medullary stroma (Cullen-McEwen et al. 2005). Earlier it has been proposed that renal stromal cells could be neural crest derivates, as the stromal cells were found to express neurofilaments (Sainio et al. 1994). However, recent results in chicken, presented by Guillaume *et al.*, showed that the renal stroma mainly originates from paraxial mesoderm (Guillaume et al. 2009).

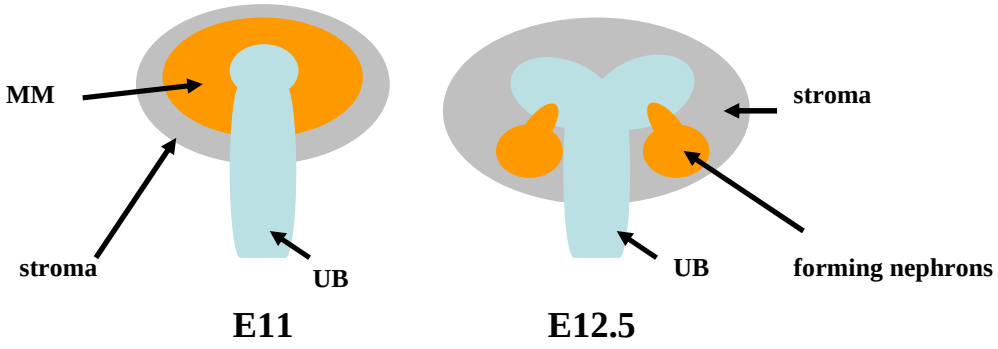

Figure 1.6 Localisation of stroma in developing mouse metanephros at the onset of metanephric development at E11 and later at E12.5.

1.2.3.4. Genes important during metanephric development

A number of genes are implicated in the development of the metanephric kidney (Dressler 2009). In order to ensure that the metanephros develops in the correct location at the posterior end of IM, metanephric development requires a tight regulation of key transcription factors along the mediolateral and anteroposterior axis (Dressler 2009). For example *Eya1* (Sajithlal et al. 2005) and *Hox11* paralogs (Mugford et al. 2008) play a crucial role in determining the region of IM that will become MM. Hox11 proteins, together with Eya1 and Pax2, form a transcriptional complex which activates expression of genes such as *glial cell line-derived neurotrophic factor* (*Gdnf*) in the posterior intermediate mesoderm, thus triggering the start of metanephric development

(Gong et al. 2007). Other genes that positively regulate expression of *Gdnf* include *Six2* and *Sall1* (Saavedra et al. 2008). Metanephric development is initiated with the interaction between the UB and MM. Gdnf plays a crucial role in this interaction as the binding of Gdnf to the tyrosine kinase receptor, Ret, is responsible for UB outgrowth and branching (Vega et al. 1996; Sainio et al. 1997). Furthermore, some genes have been demonstrated to take part in later metanephric development. For instance, it has been shown that Notch2 signalling plays role in nephron patterning. Accordingly, kidneys of Notch2-deficient kidneys do not develop proximal tubules, although they form distal tubules (Cheng et al. 2007). Finally, it is important to note that some genes involved in metanephric development are not exclusively found in the metanephros. Genes such as Pax2 were also demonstrated to be expressed during development of the pronephros and mesonephros (Dressler et al. 1990). An overview of several important signalling pathways and genes involved in metanephric development is presented below.

Gdnf signalling

The initial outgrowth and subsequent branching of the UB is induced by the glial cell line-derived neurotrophic factor (Gdnf) that is expressed by MM adjacent to the UB. Gdnf is a member of the transforming growth factor-β (TGF-β) superfamily and was identified by its ability to promote the survival of dopaminergic neurons (Saavedra et al. 2008). During metanephric development, Gdnf binds to the tyrosine kinase receptor, Ret, which is found at the tips of the UB and stimulates UB branching (Vega et al. 1996; Sainio et al. 1997). Ret activates various signalling pathways, such as p38 mitogen activated protein kinase (MAPK) and c-Jun N-terminal kinase (JNK) pathways (Takahashi 2001). Another receptor taking part in the interaction is the glycosylphosphatidylinositol (GPI)-anchored Gdnf receptor-α (GFR-α) which is expressed in

both UB and MM (Sainio et al. 1997). *Gdnf*-null mice do not develop a UB. The uninduced MM undergoes apoptosis, consequently leading to complete renal agenesis at birth (Sanchez et al. 1996). Similarly, in the *Ret*-deficient mice, the kidneys were also absent. However, occasionally some rudimentary dysplastic kidneys with large areas of undifferentiated mesenchyme were observed in the mutant animals (Schuchardt et al. 1994). The phenotype of *GFR-α* null mouse was consistent with *Ret* knockout, demonstrating lack of kidneys or renal dysgenesis (Enomoto et al. 1998).

Sall1

Similarly to *Gdnf*, the transcription factor, *Sall1*, a homologue of the *Drosophila* region-specific homeotic gene *spalt*, is important for regulating the initial interactions between MM and UB during UB outgrowth (Nishinakamura et al. 2001). *Sall1* expression starts at E10.5 in mice. At E11.5 *Sall1* is expressed in mesonephric tubules, Wolffian ducts, and in the metanephric mesenchyme but not in the UBs. Later, *Sall1* expression is observed in the condensing MM around the UBs and in comma-shaped bodies. *Sall1*-null mice display kidney agenesis, or severe dysgenesis, characterized by a disorganized renal structure, shrunken glomeruli, necrotic proximal tubules and multiple cysts. The ureteric bud in the *Sall1*-null animals either does not invade the MM or does not induce MM condensation. Impaired branching is observed in mutant mice (Nishinakamura et al. 2001). Mutations of *SALL1* in humans cause the Townes-Brocks syndrome, an autosomal dominant disease characterized by dysplastic ears, preaxial polydactyly, imperforate anus, and kidney and heart anomalies (Kohlhase et al. 1998).

Lim1

Another essential gene in renal development is the LIM-class homeobox gene, *Lim 1*. *Lim1* displays a broad expression profile during nephrogenesis. Its expression starts in the IM and is subsequently restricted to the nephric duct and UB. *Lim1* expression is also present at different stages of nephron formation, including pretubular aggregates, comma-shaped and S-shaped bodies. Subsequently, postnatal *Lim1* expression is found in collecting ducts and cortical tubules but remains downregulated in mature glomeruli (Karavanov et al. 1998; Kobayashi et al. 2005). *Lim*-/- mice lack head structures and die at E10. However, some stillborn *Lim1*-/- pups were shown to not have developed kidneys (Shawlot and Behringer 1995). In addition, in E9.5 *Lim1*-null mice, the expression of Pax2, an important transcription factor during nephrogenesis, is only found in the posterior region of the IM in comparison with wild type mice where Pax2 expression was demonstrated along the entire length of the IM (Tsang et al. 2000).

Wnt signalling

During metanephric development, Wnt signalling is observed at different stages of MM development and in ureteric buds (Maretto et al. 2003; Iglesias et al. 2007). Experiments in mice demonstrated that Wnt signalling can be observed in the nephric duct. However, by E16.5, it becomes restricted to the UB tips of branching UBs and the distal part of the S-shaped body. It has been demonstrated that in UB cells, the inactivation of β-catenin, which mediates Wnt signalling, impairs UB branching during nephrogenesis, and consequently, leads to lower numbers of nephrons and collecting ducts in kidneys of new born mice (Bridgewater et al. 2008). Wnt4 is a member of the Wnt gene family. During metanephric development it is expressed in condensed MM. Its expression persists in vesicles, C- and S-shaped bodies. *Wnt4*-deficient mice

develop small kidneys which are composed of undifferentiated MM and branches of collecting duct. Initial condensation of MM occurs in the *Wnt4*-deficient mice. However, no C-shaped and S-shaped bodies are detected in the E15 kidneys, while branching morphogenesis is preserved (Stark et al. 1994). The forced expression of *Wnt4* in the NIH3T3 mouse embryonic fibroblast line was sufficient to elicit tubulogenesis in co-cultured MM. Accordingly, it has been shown that *Wnt4* expression induces MM to condense, form epithelial structures and finally display glomeruli, similar as the induction with the spinal cord (Kispert et al. 1998). Another member of the Wnt family is *Wnt9b*, inactivation of which leads to renal agenesis in mice. Wnt9b is expressed in collecting ducts. Further studies on *Wnt9b* mutant mice demonstrated that *Wnt9b* is important for establishing planar cell polarity in the renal tubules (Karner et al. 2009).

Pax2

Pax2, a pair box gene, is expressed in the UB, condensing mesenchyme and developing nephrons (Dressler et al. 1990; Dressler and Douglass 1992). Experiments in mice showed that Pax2 can be detected also in adult kidney in the collecting duct cells. In addition, some cells in the inner medulla and thin descending limb of loop of Henle were also demonstrated to express Pax2 (Cai et al. 2005). *Pax2*-null mice lack kidneys. Accordingly, no Wolffian duct elongation is found at E10.5 and the parts of the Wolffian duct that form initially, subsequently degenerate in *Pax2*-deficient mice at E12.5. In addition, no mesonephric tubules are detected in mutant embryos. *Pax-2*$^{+/-}$ mice develop hypoplastic kidneys with smaller calyces and a decreased number of developing nephrons (Torres et al. 1995). *Pax2*-deficient mutants do not express *Gdnf* (Brophy et al. 2001).

Wt1

The *Wilms' tumor* gene, *Wt1*, encodes a transcription factor that plays a number of crucial roles throughout nephrogenesis, and ablation of *Wt1* leads to renal agenesis (Kreidberg et al. 1993). Expression of *Wt1* has been associated with both condensing mesenchyme and developing nephrons (Armstrong et al. 1993; Mundlos et al. 1993). Some *Wt1* expression can be observed prior to the onset of nephrogenesis, both in the IM and uninduced MM (Armstrong et al. 1993). During kidney development, *Wt1* expression becomes restricted to the precursors of podocytes in the S-shaped bodies in both the metanephros and mesonephros. *Wt1* expression persists in the podocytes throughout adulthood (Mundlos et al. 1993). In *Wt1*-deficient mice, fewer mesonephric tubules are detected. Further, at E11.5, the UB is absent in the mutant mice and the MM is undergoing apoptosis. Ultimately, at E12, the MM is completely degenerated (Kreidberg et al. 1993). *Pax2*, *Six2* and *Gdnf* are however expressed in the MM of mutant embryos, suggesting that *Wt1*-deficient MM acquired already features of the nephrogenic lineage and possibly for this initial process, Wt1 is not required. Nevertheless, *Wt1*-deficient MM could not be induced by UB to undergo tubulogenesis *in vitro* (Donovan et al. 1999).

Six2

Six2 expression is found in the MM before UB invasion as well as the induced MM surrounding the UB. However, its expression is downregulated in cells undergoing subsequent mesenchymal-to-epithelial transition. Inactivation of *Six2* expression in mice leads at E11.5 to formation of premature renal vesicles surrounding the UB. Also, $Six2^{-/-}$ kidneys do not demonstrate branching of the UB (Self et al. 2006). Six2 regulates the expression of *Gdnf* in the MM (Brodbeck et al. 2004). Ultimately, the Six2 expressing cells were shown to gives rise to all nephron-specific cell

types within the metanephros (Kobayashi et al. 2008).

Osr1

Osr1 is *odd-skipped related 1* gene encoding a transcriptional regulator. The *Osr1*-expressing precursor population in the IM was shown to gives rise to most cells found within the developing metanephros, including the collecting duct epithelium, nephrons and interstitial mesenchyme, mesangial and smooth muscle cells. Still, it was demonstrated that *Osr1*-expressing precursors for nephron and interstitial mesenchyme separate before the start of metanephric development (Mugford et al. 2008). In E9.5 mice, *Osr1* expression is present in intermediate and lateral plate mesoderm. Its expression is also found in undifferentiated mesonephric mesenchyme and tubules. At the onset of metanephric development, *Osr1* is expressed in the MM but is absent in the UB. Later it is expressed in the condensing mesenchyme that surrounds the branching UB, but is down-regulated in pre-tubular aggregates, C-shaped and S-shaped bodies (James et al. 2006). *Osr1*-null mice lack kidneys as no MM and UB development occurs in the embryos (Wang et al. 2005). No expression of *Six2*, *Eya1*, *Gdnf*, *Pax2* and *Sall1* was found in the metanephric region in the mutant mice (James et al. 2006).

Eya1

Eya1 is a homologue of the *Drosophila eyes absent* gene. *Eya1* expression is first observed at around E8.5 in the intermediate mesoderm and subsequently becomes restricted to a region where the UB forms. During the early stage of metanephric development, *Eya1* is expressed in both uninduced and induced MM but not in UB (Sajithlal et al. 2005). Eya1+/− mice were demonstrated to have renal defects, such as renal hypoplasia and unilateral agenesis, while Eya1−/− mice completely lacked kidneys and ureters (Xu et al. 1999). In the *Eya1*-deficient

mouse embryos, *Ret* expression is observed in the Wolffian duct but no UB outgrowth occurs (Sajithlal et al. 2005). Subsequently, in the absence of the UB, the MM undergoes apoptosis. Complete degeneration of the MM is observed by E12.5 (Xu et al. 1999).

Hox11 paralogs

Hox genes encode transcription factors that play an essential role in patterning of the body axes during embryonic development. As *Hox11* paralogous genes are redundant, the knockouts of *Hox11* result in incompletely penetrant phenotypes. Accordingly, *Hoxa11/Hoxd11*-deficient mice display hypoplastic kidneys, whereas *Hoxa11*/*Hoxc11*/*Hoxd11*-deficient mice completely lack kidneys. Accordingly, no UB formation is observed in triple mutants. This is accompanied by the lack of *Six2* and *Gdnf* expression in the MM (Wellik et al. 2002). Hox11 paralogous proteins were demonstrated to form a complex with Pax2 and Eya1, which activates the expression of Six2 and Gdnf in the MM (Gong et al. 2007).

Notch2 signalling

Notch genes encode single-transmembrane receptors. It has been demonstrated that disruption of Notch2 receptor expression in the metanephric mesenchyme disrupts nephrogenesis. Accordingly, *Notch2*-deficient mice at birth displayed smaller kidneys with no glomeruli or proximal tubules. The mutant mice demonstrated normal condensation of MM and subsequent transition to epithelium, however no segmentation of the nephron into proximal and distal tubules occurred in the kidneys (Cheng et al. 2007).

Bmp4

Like Gdnf, bone morphogenetic protein 4 (Bmp4) is a member of the TGF-β superfamily. At

E12.5 *Bmp4*is expressed in the stromal mesenchymal cells. In addition, at E14.5, expression is seen in the S-shaped bodies. The Bmp receptor gene, *Alk3,* is ubiquitously expressed during kidney development, while *Alk6* is expressed in the Wolffian duct and in UBs. *Bmp4*$^{+/-}$ mice display renal abnormalities similar to human congenital anomalies of the kidney and urinary tract (CAKUT), categorized as dysplastic kidneys, hydronephrosis or duplex kidney with bifid ureters (Miyazaki et al. 2000). *In vitro* it was demonstrated that Bmp4 promotes growth and elongation of UBs, but also inhibits condensation of MM and promotes expansion of the peripheral stromal compartment (Miyazaki et al. 2000; Raatikainen-Ahokas et al. 2000; Miyazaki et al. 2003).

Bf2

Brain factor 2, Bf2, (*Foxd1*) encodes a transcription factor expressed in stromal cells that in mouse kidneys at E11.5 form a ring of stromal mesenchyme around the Pax2 positive nephrogenic mesenchyme. Later, *Bf2* expression is found in cells surrounding the condensing MM and at the periphery of the kidney rudiment. Mice carrying a *Bf2*-null mutation show abnormalities in development of both the collecting duct system and nephrons. The number of nephrons is reduced, as large amounts of condensing mesenchyme are still present in the kidneys at birth. Further, the number of UB branches is diminished. The expression of *Ret* in mutant kidneys is not restricted to UB tips in the cortex, as it is in wild type E14.5 kidneys, but is found along the branches in both cortical and medullary regions (Hatini et al. 1996).

Rarβ2

Retinoid acid receptor β 2 (*Rarβ2*) expression is found in mouse metanephroi as early as E11. *Rarβ2* is associated with stromal cells surrounding the UB and MM, where its expression co-localizes with the other stromal marker, *Bf-2*. During the later stages of nephrogenesis, *Rarβ2* is

expressed in stromal cells found in the developing cortex and medulla. It is also expressed in the subcapsular region, again co-localizing with *Bf2* (Mendelsohn et al. 1999). In mice lacking *Rarβ2* along with other retinoid acid receptors, *Rarα1* and *Rarα2*, the kidneys at birth display diminished numbers of nephrons and UB branches (Mendelsohn et al. 1994). It has been demonstrated that in these mutant kidneys, starting from E12, *Ret* expression in the UB tips is downregulated, leading to reduced UB branching. Furthermore, the stromal cells are abnormally distributed, forming a thick peripheral stromal layer in the E14 mutant kidneys (Mendelsohn et al. 1999).

1.2.3.5. Metanephric kidney as a model for *in vitro* nephrogenesis

Metanephric kidney is good model for studying *in vitro* nephrogenesis. For *in vitro* culture, metanephric kidneys can be obtained from mouse embryos at E10.5 when the UB has just invaded the MM, or at E11.5 when the UB has branched once. Following isolation, the kidney rudiments are cultured at the gas/medium interface. For this reason, the embryonic kidneys are placed on a filter supported by a metal grid which is submerged in growth medium (Davies 2010). After 4 to 5 days, the *in vitro* cultured E11.5 rudiment reaches a similar development stage as the E14 metanephros (Vize Peter 2003). The rudiments can be also cultured on a glass surface in the presence of a low volume of medium. One of the advantages of this culture method is the fact that the metanephroi develop a clear anatomical cortico-medullary zonation with extended loops of Henle (Sebinger et al. 2010). In addition, it is possible to trigger *in vitro* the development of MM into nephrons in the absence of the UB. It has been shown that spinal cord induces MM development similar to UB (Davies 2010).

1.3. Mesenchymal stem cells and their role in kidney repair and regeneration

1.3.1. Characteristics of mesenchymal stem cells

Mesenchymal stem cells (MSCs) are described as an adult stem cell population that possesses the capability to highly proliferate *in vitro* and differentiate into multiple lineages. They were initially isolated by Friedenstein (Friedenstein et al. 1974) who has shown that bone marrow contains an adherent heterogeneous fraction of cells with the ability to rapidly multiply and differentiate (Prockop 1997). Although MSCs have been demonstrated to primarily give rise to fat, bone and cartilage (Pittenger et al. 1999; Peister et al. 2004), there exist reports describing a much broader differentiation potential of the cells, such as myogenic (Dezawa et al. 2005), neuronal (Woodbury et al. 2000) and pancreatic lineages (Xie et al. 2009). Furthermore, the plasticity of MSCs is accompanied by immunosuppressive properties of the cells (Le Blanc and Ringden 2007). The following characteristics have been proposed as the minimal criteria for identification of human MSCs: plastic adherence, expression of surface markers such as CD105, CD73 and CD90, as well as adipogenic, osteogenic and chondrogenic differentiation potential (Dominici et al. 2006). In addition, since bone marrow-derived MSCs are commonly isolated by their ability to adhere to plastic culture dishes, the presence of contaminating hematopoietic cells in such cultures has been documented (Phinney et al. 1999). For this reason, negative selection using immunodepletion of cells expressing hematopoietic markers, such as CD45, is employed in order to enrich the cultures for MSCs (Baddoo et al. 2003). Although bone marrow is commonly described as a niche for MSCs, it is possible to establish MSC cultures from various other tissues and organs, like lung or kidney. These cells share common MSC features although their differentiation capabilities may differ depending on the source of isolation (da Silva Meirelles et

al. 2006; Kern et al. 2006). Recently, it was shown that MSCs could be obtained from different foetal tissues. Accordingly, it was possible to establish human MSCs from foetal bone marrow, lung or liver (Campagnoli et al. 2001; in 't Anker et al. 2003).

It is important to note that for both mouse and human bone marrow-derived MSCs, subpopulations with higher plasticity have been isolated (Kucia et al. 2006; Anjos-Afonso and Bonnet 2007). Mouse bone marrow-derived MSCs capable of differentiation into all three germ-layer lineages are named very small embryonic-like (VSEL) stem cells. These cells resemble embryonic stem cells in their morphology and express embryonic stem cell markers, such as Oct4, SSEA-1 and Nanog (Kucia et al. 2006). A similar subpopulation of cells has been described by Anjos-Afonso and Bonnet, who called these cells the most primitive mesenchymal progenitors in the adult murine bone marrow compartment (Anjos-Afonso and Bonnet 2007). In humans, bone marrow-derived MSCs that maintain the ability to proliferate rapidly and differentiate into a wide range of lineages, among them neurons and pancreatic islet cells, have been named marrow-isolated adult multilineage inducible cells (MIAMI) (D'Ippolito et al. 2004).

1.3.2. Mesenchymal stem cells in kidney disease

In the literature, there are a number of reports showing the existence of extra-renal cells within the kidney (Ito et al. 2001; Poulsom et al. 2001; Gupta et al. 2002). The presence of male extrarenal cells in male patients receiving transplantation of female kidneys was established by some authors (Poulsom et al. 2001; Gupta et al. 2002). Subsequent results demonstrated that these cells could originate from the bone marrow. Accordingly, experiments in mice showed that the kidneys of female recipients of male bone marrow contained male cells within the renal tubules and glomeruli (Poulsom et al. 2001). A similar experiment was performed in rats:

labelled rat bone marrow was transplanted into irradiated recipient rats, and following, the induction of glomerulonephritis, the labelled bone marrow-derived cells were found in the glomeruli of injured rats and were described to provide structural support for glomerular capillaries (Ito et al. 2001). Others showed that wild type bone marrow cells injected into collagen type IV α3 knockout mice with progressive glomerulonephritis (a model of Alport syndrome), resulted in improved renal histology and function (Prodromidi et al. 2006). From this study, as well as from other studies, it was not entirely clear which bone marrow-derived population, i.e., the MSCs or the hematopoietic stem cells (HSCs), was responsible for the positive outcome. Subsequently, many authors concentrated on evaluating the contribution of bone marrow-derived MSCs to renal regeneration and it was demonstrated that MSCs can indeed protect mice from tubular damage and renal function deterioration in various experimental models of acute renal injury (Herrera et al. 2004; Morigi et al. 2004; Togel et al. 2005; Bi et al. 2007; Semedo et al. 2007; Togel et al. 2007; Qian et al. 2008; Li et al. 2010). Some of the data suggested also that MSCs are able, at least to some extent, to engraft into damaged kidneys and differentiate towards tubular cells (Herrera et al. 2004; Morigi et al. 2004; Qian et al. 2008; Li et al. 2010).

As demonstrated by Morigi *et al.,* mouse bone morrow-derived MSCs injected into mice 24h after induction of acute renal injury following subcutaneous injection of cisplatin, improved renal function, as well as prevented tubular damage at the peak of cisplatin injury at day 4. In addition, MSC administration was demonstrated to induce proliferation of tubular cells in cisplatin-treated mice. Furthermore, injected MSC were found in the proximal and distal tubules kidneys of cisplatin-treated animals. The MSCs engrafted among tubular cells and accordingly, stained with

Lens culinaris lectin, which binds to the brush border of the tubular epithelium. Even 29 days after the injury, the cells were still detected within the tubular epithelium. In the same study it was also demonstrated that administration of HSCs does not protect mice from renal function and tissue damage in the cisplatin-induced injury model. Nevertheless, occasional engraftment of HSCs into injured tubules was observed (Morigi et al. 2004). More recently, Morigi and the co-workers demonstrated the effectiveness of human cord blood-derived MSCs in ameliorating cisplatin-induced kidney injury. MSCs were injected into severe combined immunodeficiency (SCID) mice following cisplatin treatment. At the peak of injury the tubular damage was reduced in the kidneys of animals receiving MSCs. Importantly, the injection of the cells was able to improve the survival of cisplatin-treated mice. Consequently, MSCs were demonstrated to inhibit cisplatin-induced damage by reducing oxidative damage and apoptosis in the kidneys of cisplatin-treated animals. The injured kidneys receiving MSCs also demonstrated an increase in tubular cell proliferation, as well as having a high number of tubules positive for the serine/threonine protein kinase Akt, which mediates anti-apoptotic effects. Additionally, the injured kidneys treated with MSCs showed up-regulation in expression of *hepatocyte growth factor*, a factor responsible for anti-apoptotic effects during kidney injury. Nevertheless, regarding the engraftment and differentiation potential of human MSCs in the injured renal tissue, the cells were mainly found in the peritubular areas and only rarely engrafted in the tubules or glomeruli (Morigi et al. 2010).

The data obtained in cisplatin-induced injury were confirmed in the model of glycerol-induced acute renal failure, where enhanced functional and structural recovery was accompanied with engraftment of MSCs into the injured tubules (Herrera et al. 2004; Qian et al. 2008).

Accordingly, Herrera *et al.* investigated the effect of administration of mouse bone morrow-derived MSCs in acute injury induced by intramuscular injection of glycerol in the mice. Similarly as in the cisplatin model, MSCs were demonstrated to increase tubular cell proliferation. Furthermore, MSCs were detected in the tubular epithelium of glycerol injured kidneys expressing cytokeratin, suggesting that some of the MSCs were possibly differentiating into tubular epithelial cells (Herrera et al. 2004). Others demonstrated that human foetal bone marrow-derived MSCs administrated into rats with glycerol-induced acute renal failure enhanced tubular cell proliferation, which was accompanied by engraftment of MSCs into injured tubules. Consequently, the integrated cells acquired expression of *aquaporin-1* and *parathyroid hormone receptor 1* as well as stained positively for cytokeratin, suggesting epithelial differentiation of engrafted MSCs (Qian et al. 2008).

Interestingly, it has been observed that following intravenous injection, MSCs homed to the kidney of mice with induced renal injury; however, they failed to localize to the kidneys of uninjured mice (Herrera et al. 2004). Subsequently, efforts have been made to elucidate the mechanism underlying homing of MSCs into injured kidneys. Some results suggest that the homing to injured tissues depends on chemotactic factors. MSCs migrate *in vitro* in response to some growth factors, such as platelet-derived growth factor (PDGF)-AB and insulin-like growth factor-1. In addition, pre-treatment with inflammatory cytokines, such as the tumor necrosis factor-α (TNF-α), enhances MSC migration. Also, an increase in migration of the cells towards chemokines, like stromal-derived factor-1, upon stimulation with TNF-α has been described (Ponte et al. 2007). In the model of glycerol-induced acute renal failure it was shown that the interaction between CD44, expressed on MSCs, and its ligand, hyaluronic acid, is responsible for

localization of the cells to the injury site. Accordingly, CD44-positive MSCs were detected in the peritubular capillaries and interstitium in kidneys of glycerol-treated mice, whereas only rarely, CD44-negative MSCs were found in the renal tissue of injured animals (Herrera et al. 2007). In the same study it was demonstrated that CD44-positive MSCs were also present to some extent in glomeruli and within the tubular epithelium (Herrera et al. 2007).

Other reports have shown renoprotective effects of MSC administration in the ischemia-reperfusion model of acute kidney injury (Togel et al. 2005; Semedo et al. 2007; Togel et al. 2007; Li et al. 2010). For instance, Togel and co-workers demonstrated that injection of rat bone marrow-derived MSCs into the carotid artery in the ischemia-reperfusion model in rats improves renal function. In addition, the injured kidneys of animals receiving MSCs showed higher tubular cell proliferation and less apoptosis in comparison with injured kidneys of animals receiving no MSCs. After administration of rat MSCs, the injured kidneys also showed reduced expression of the pro-inflammatory cytokines, *TNF-α* and *interleukin-1β,* and an increase in expression of the anti-inflammatory molecule, *interleukin-10*. Furthermore, no MSCs were identified in the injured kidneys after 3 days from administration of the cells, strongly suggesting a differentiation-independent mechanism of MSC action (Togel et al. 2005).

MSCs were demonstrated to also have some renoprotective action in the experimental model of glomerulonephritis. Accordingly, rat bone marrow-derived MSCs were injected into the renal artery of rats with mesangioproliferative anti-Thy1.1 glomerulonephritis. Following injection, the cells were detected in glomeruli. Accordingly, MSC administration led to a reduction of mesangiolysis and increased intra-glomerular and glomerular cell proliferation. Most of the MSCs found in the glomeruli, however, did not express the endothelial marker, JG12, or the

mesangial marker, α-smooth muscle actin (α-SMA). In addition, MSCs were found *in vitro* to secrete high amounts of vascular endothelial growth factor and transforming growth factor-β1 (Kunter et al. 2006). Similar results were observed in a progressive rat model of glomerulonephritis. In this model, anti-Thy1.1 mesangioproliferative glomerulonephritis was induced after a right-sided uninephrectomy. Following the injury, rat MSCs were injected intra-arterially into the left kidney. After administration, MSCs localized to glomeruli and ameliorated acute renal failure by enhancing the functional recovery. In addition, more glomeruli were counted in kidneys of animals receiving MSCs following the injury (Kunter et al. 2007).

Ultimately, MSCs derived from adipose tissue were used in kidney injury models to test their contribution to regeneration. Mouse adipose-derived MSCs were injected in mice following cisplatin-induced renal injury. Subsequently, the cells were shown to increase functional and structural recovery and improve the survival of injured animals in a similar manner as bone marrow-derived MSCs. Interestingly, despite the renoprotective effect, no cells were found engrafted into the renal tissue in this study (Bi et al. 2007). On the other hand, human adipose-derived MSCs were demonstrated to engraft into the renal tubular epithelium, replacing dead tubular cells in mice with induced ischemia–reperfusion injury: in this study, it appeared that the MSCs, helped maintain the structural integrity of the damaged tubules, facilitating regeneration (Li et al. 2010).

1.3.3. Mesenchymal stem cells kidney specific kidney differentiation *in vitro*

Some reports have suggested that MSCs can also be differentiated directly towards kidney-specific cell types *in vitro* (Qian et al. 2008; Singaravelu and Padanilam 2009; Matsushita et al. 2010). Rat bone marrow-derived MSCs were reported to acquire expression of *aquaporin-1*

(*AQP1*) following *in vitro* co-culture with glycerol-injured rat kidney tissue. MSCs were indirectly co-cultured for up to 7 days with injured kidney tissues obtained from rats that underwent glycerol-induced kidney injury 48 h before the co-culture. Accordingly, MSCs became more rounded, and thus morphologically, became more similar to renal tubular epithelial-like cells and started to express *AQP1*. The analysis showed also that MSCs were induced to express high levels of *cytokeratin* when incubated with injured tissue (Qian et al. 2008). Similarly, it was shown that co-culture with injured cortical tubular epithelial cells induced mouse MSCs to acquire a tubular epithelial-like phenotype and express *AQP1* and *kidney-specific cadherin* (Singaravelu and Padanilam 2009). It has been also described that MSCs can acquire a phenotype similar to juxtaglomerular cells which are specialized renal endocrine cells that express renin. As the expression of renin is regulated by the nuclear hormone receptor, liver X receptor-α (LXR-α), the treatment with 22-hydroxycholesterol or cyclic adenosine monophosphate (cAMP), which are the natural ligands for LXR-α, was demonstrated to increase the expression of renin in both mouse and human bone marrow-derived MSCs. In addition, stimulation with a synthetic ligand for LXR-α resulted in a significant increase in renin expression in the studied cells. Furthermore, mouse MSCs over-expressing the liver X receptor-α, were shown to produce, accumulate and subsequently release renin into the culture medium (Matsushita et al. 2010).

Finally, an MSC-like population obtained from human glomeruli was demonstrated to differentiate into kidney-specific cell types upon stimulation. Accordingly, in the presence of PDGF-BB and TGF-β1, the cells acquired a mesangial-like phenotype, characterized by the expression of α-smooth muscle actin (α-SMA) and angiotensin II receptor 1. Furthermore, they

were shown to contract in response to simulation with angiotensin II. On the other hand, in the presence of all-trans retinoic acid, MSCs were demonstrated to express cytokeratin as well as podocyte-specific markers such as podocin, nephrin and synaptopodin (Bruno et al. 2009).

1.3.4. Mesenchymal stem cells in nephrogenesis

The expression of the following early kidney markers was recently confirmed in primary mouse bone marrow-derived MSC: *Eya1*, *Six2*, *Osr1*, *cadherin 11*, *Gdnf*, *Wnt4* and *Bf2* (Lusis et al. 2010). The first attempt to introduce MSCs into embryonic kidney in order to evaluate the contribution of MSCs to kidney development was made by Yokoo and co-workers (Yokoo et al. 2005). Human bone marrow-derived MSCs were injected into the IM of rat embryos at the site of nephrogenesis before the initiation of metanephric development. Subsequently, the embryos were cultured for 48 h *ex utero,* followed by the isolation of metanephroi and further *in vitro* culture of kidney rudiments harbouring MSCs for another 6 days. Figure 1.7 illustrates briefly the technique used by Yokoo and co-workers. Using this system, human MSCs were shown to contribute to the development of both the glomerular and tubular epithelium, as well as the interstitium of metanephric kidneys. Two genes expressed during early ureteric bud and nephron development, *Kir6.1* and *SUR2*, were initially detected in human MSCs prior to their integration into kidney rudiments (Yokoo et al. 2005). Integration of human MSCs into renal structures was accompanied by expression of the podocyte-specific genes, *nephrin, podocin* and *glomerular epithelial protein 1,* and tubular epithelial cell-specific markers, *AQP1, 1α hydroxlyase, parathyroid hormone receptor 1* and HCO_3^- *co-transporter* (Yokoo et al. 2005; Yokoo et al. 2006). Moreover, the metanephroi containing integrated human MSCs were transplanted into the omentum of recipient rats and after 2 weeks became vascularised and were able to produce fluid

similar to urine (Yokoo et al. 2006). Importantly, in order to increase the number of MSC-derived renal structures, in all experiments, human MSCs were transduced with a virus encoding human GDNF (Yokoo et al. 2005; Yokoo et al. 2006). At the same time it has been shown that simple injection of human MSCs into an isolated kidney rudiment followed by *in vitro* culture for 6 days is insufficient to trigger differentiation of the cells, as the MSCs remained aggregated, did not disperse and consequently did not form any recognizable renal structures. MSCs also failed to express kidney specific genes (Yokoo et al. 2005). Experiments performed by Yokoo *et al*. led to the conclusion that MSCs can be reprogrammed towards nephron-specific cell types when put into an appropriate embryonic environment (Yokoo et al. 2005; Yokoo et al. 2006).

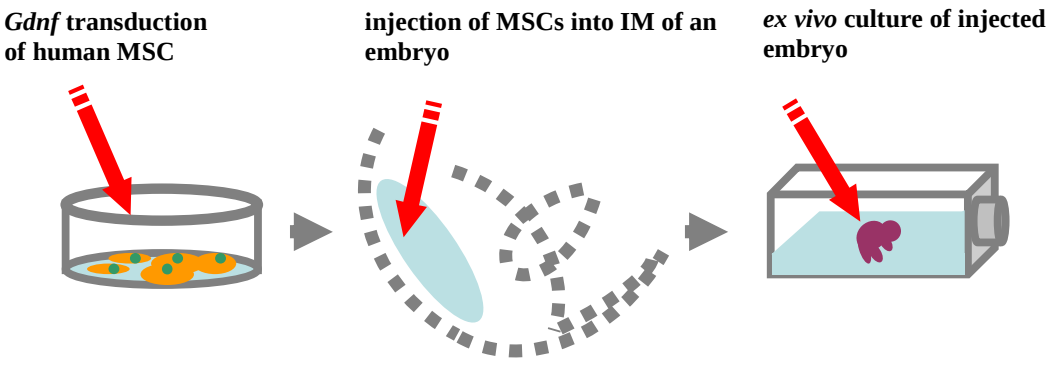

Figure 1.7 Technique used by Yokoo and co-workers to integrate successfully human MSCs into rodent metanephric kidneys

Efforts have also been made using a similar methodology described by Yokoo *et al.* to induce human MSCs to take part in the formation of the kidney collecting duct system (Fukui et al. 2009). Consequently, human bone marrow-derived MSCs expressing chicken Pax2 were transplanted into the region of the chicken embryo that was described to contain collecting duct progenitors. Human MSCs transfected with chicken Pax2 acquired expression of *SALL1* and *WNT4*, and 24h following transplantation, were shown to migrate along the elongating Wolffian

duct. Subsequently, on the 2nd day following transplantation, integration of human cells into the duct epithelia occurred accompanied by the acquisition of *LIM1* expression by the cells. In these experiments, although MSCs were demonstrated to integrate into the Wolffian duct, at the same time, it was shown that they were unable to incorporate into the ureteric bud, which gives rise directly to the collecting ducts of the adult kidney (Fukui et al. 2009).

In addition, Yokoo and co-workers administered human MSCs, using the methodology earlier described (Figure 1.7), into Fabry mice which accumulate glycosphingolipids in the kidneys due to lack of α-galactosidase A enzyme. Accordingly, analysed metanephroi harbouring engrafted human MSCs showed increased α-galactosidase A enzyme activity compared with untreated metanephroi. This was accompanied by a marked reduction in the levels of glycosphingolipids in ureteric buds and S-shaped bodies in the metanephric kidneys containing human MSCs (Yokoo et al. 2005). Furthermore, human MSCs isolated from foetal blood were transplanted into the offspring of pregnant mice carrying a deletion in the alpha2 chain of the procollagen type I gene (Guillot et al. 2008). The transplantation was performed intra-peritoneally *in utero* at embryonic day (E) 13.5-15. Mice harbouring this defect were shown previously to display skeletal fragility as well as developing glomerulopathy due to deposition of abnormal homotrimeric collagen type I in the kidneys. Accordingly, injected human MSCs were found engrafted into the foetal glomeruli, localizing among mesangial cells, in the offspring of *colIα2*-deficient mice analysed between 1-12 weeks of age. The injection of human MSCs was shown to reduce the occurrence of abnormal collagen depositions in renal glomeruli in the offspring of *colIα2*-deficient mice. In addition, the presence of the α2 chain of type I collagen was detected in the kidneys (Guillot et al. 2008). Nevertheless, it is important to mention that transplantation of human MSCs into wild-

type animals, without any defects, did not result in the engraftment of the cells. This result highlights again the essential role of renal injury for homing and engraftment of MSCs in the kidneys (Guillot et al. 2008).

1.3.5. Controversies regarding the renoprotective and renogenic action of mesenchymal stem cells

Observations made by several groups highlighted the potential role of bone marrow cells in renal regeneration (Ito et al. 2001; Poulsom et al. 2001; Gupta et al. 2002; LeBleu et al. 2009). However, at least two populations found in the bone marrow, namely the MSCs and HSCs, may be involved in the regeneration. According to data presented by Morigi *et al*., MSCs have the potential to engraft in the proximal and distal tubules and ameliorate kidney injury in the cisplatin-induced kidney injury, while HSCs demonstrate only occasional engraftment into injured tubules and no renoprotective capacity. Contradictory results were published by Fang *et al*., comparing the engraftment potential of MSCs and hematopoietic lineage marrow cells in $HgCl_2$-induced acute tubular injury in mice. Upon injury, mouse hematopoietic cells were found in renal tubules, while mouse MSCs only occasionally engrafted into the interstitium of the injured kidneys (Fang et al. 2008). The differences discussed above could arise due to dissimilar approaches used to induce kidney injury, like cisplatin and $HgCl_2$ (Fang et al. 2008). It is also worth mentioning that different MSC populations were injected in both studies. Morigi *et al*. used short-term cultures of MSCs still harbouring CD45-positive contaminating hematopoietic cells, while Fang *et al*. administered cells obtained from a long-term culture of MSC containing no CD45-positive cells (Morigi et al. 2004; Fang et al. 2008).

In summary, the renoprotective effects of MSCs in kidney injury have been confirmed; however,

not all authors could demonstrate the engraftment of MSCs into renal structures, as observed by Morigi *et al.* and Herrera *et al.* (Herrera et al. 2004; Morigi et al. 2004). In contrast, there is a vast body of evidence showing a differentiation-independent action of MSCs in experimental models of acute kidney injury and it appears that the paracrine activity of MSCs plays the major role in achieving the enhanced recovery from kidney injury (Togel et al. 2005; Bi et al. 2007; Imberti et al. 2007; Semedo et al. 2007; Togel et al. 2007; Togel et al. 2009). Accordingly, it has been demonstrated that injection of rat bone marrow-derived MSCs in the model of ischemia-reperfusion acute renal failure was able to improve renal function, despite that only a small number of MSCs was detected in the injured renal tissue (Togel et al. 2005). Furthermore, it has been shown that injection of conditioned medium derived from mouse MSCs is able, in a similar manner as the injection of the cells, to reduce kidney injury in cisplatin-induced acute renal failure. These results were also repeated in an *in vitro* model where conditioned medium derived from mouse MSCs was shown to increase the survival of immortalized mouse proximal tubule cells treated with cisplatin (Bi et al. 2007). Subsequently, some factors secreted by MSCs were identified that mediate the enhanced recovery, like the insulin-like growth factor-1 (IGF-1) and vascular endothelial growth factor (VEGF) (Imberti et al. 2007; Togel et al. 2009). Both were confirmed to be present in conditioned medium of MSCs (Kunter et al. 2006; Togel et al. 2007). Accordingly, the inhibition of VEGF expression in rat bone marrow-derived MSCs resulted in reduced functional renal recovery following ischemia-reperfusion injury (Togel et al. 2009). In addition, the inhibition of IGF-1 expression in mouse bone marrow-derived MSCs led to lower renoprotective potential of the cells following cisplatin-induced injury (Imberti et al. 2007).

Furthermore, a recent study demonstrated poor survival of MSCs during acute kidney injury. Rat

bone marrow-derived MSC were injected intravenously into rats following ischemia-reperfusion injury. The analysis revealed that 1 h after injection, most of the cells were trapped in the lung or liver, and only very few cell could be detected in the injured kidney, where they were detected only in the tubulointerstitial areas. No beneficial effect of MSC administration on renal function was observed. Direct injection of MSCs into the renal parenchyma did result in higher numbers of cells detected in the injured kidneys and improved renal function in the injured animals. Still, MSCs were unable to repopulate the kidney in the longer term. In addition, many cells were found in the lungs or liver. The authors of this study conclude that the type of renal injury model might have an impact on the engraftment potential of the cells (Burst et al. 2010). Similar observations were made by Ninichuk *et al*. who found that while the administration of mouse bone-marrow MSCs reduced fibrosis, it did not protect mice lacking collagen type IV α-3 from renal failure (Ninichuk et al. 2006).

Finally, as demonstrated by Kunter *et al.*, administration of MSCs in the rat model of progressive glomerulonephritis results in short-term renoprotective effects, but in the long-term, has a detrimental effect on the kidneys (Kunter et al. 2007). Accordingly, injured kidneys receiving MSCs expressed significantly more collagen types I, III, and IV and α-SMA, 60 days after the onset of injury, suggesting a fibrotic response in MSC-treated kidneys. Furthermore, at day 60, adipocyte-like cells were detected in about 20% of the glomeruli of MSC-treated kidneys. The vacuoles present in these cells stained with Oil Red O which detects intracellular lipid droplets normally observed in adipocytes. Importantly, these cells contained the fluorescent marker used for tracking MSCs, strongly suggesting that the cells were MSCs that had differentiated towards the adipogenic lineage. The areas containing adipocyte-like cells were surrounded by a matrix

containing collagen types I, III, IV and cells expressing α-SMA as well as by some monocytes/macrophages (Kunter et al. 2007).

1.4. Other stem cells/progenitors in kidney repair and regeneration

In the section 1.3 the characteristics of MSCs and as well as their kidney regenerative potential have been discussed. MSCs are an adult stem cell population, similarly as hematopoietic stem cells, and therefore they have only a limited differentiation potential. On the contrary, other stem cell type the embryonic stem cells (ESCs) are pluripotent. They possess the capacity to differentiate into all three embryonic germ layers. Although ESCs seem to be an ideal tool for regenerative approaches, there are several essential issues associated with the use of the cells for the purpose of regenerative medicine, such as the ethical considerations, as a therapy involving human ESCs would implicate destruction of human embryos. Except ethical issues, ESCs were found to form tumours when transplanted *in vivo*. Therefore only already committed populations of differentiated ESCs might be used for clinical applications. Further, differently as in case of MSCs that have low immunogenicity, transplantation of ESCs into patients would need to be accompanied by immunosuppression (Brignier and Gewirtz 2010). As demonstrated by Nussbaum *et al* transplantation of mouse allogeneic ESCs in the heart not only resulted in formation of teratomas but also triggered an immune response against the cells. The authors suggested that the immunogenicity of the ESCs derived cells increases in presence of inflammatory cytokines (Nussbaum et al. 2007). Except ESCs there exists another source of pluripotent cells that might be used in the future for therapy, namely the induced pluripotent stem cells (iPSCs). These cells display similar characteristics to ESCs but are created from somatic cells by transfer of particular genes. In this case it is possible to obtain patient specific cells with

high differentiation potential (Brignier and Gewirtz 2010). Nevertheless, it has been demonstrated that also iPSCs might have immunogenic potential *in vivo* (Zhao et al. 2011). Recently, a new population of stem cells has been identified, namely the amniotic fluid stem cells (AFSCs). AFSCs are a stem cell population that combines the features of embryonic and adult stem cells. The undifferentiated cells expand extensively and can be induced to differentiate towards several lineages, including the neuronal, hepatic and osteogenic lineages (De Coppi et al. 2007).Accordingly other stem cell/progenitor populations were demonstrated to be involved the enhanced recovery in models of acute renal injury, similarly as it has been described for MSCs (Bussolati et al. 2005; Dekel et al. 2006; Gupta et al. 2006; Sagrinati et al. 2006; Hauser et al. 2010; Lee et al. 2010). Similarly, other stem cell/progenitor types were shown to have potential to contribute to metanephric development following injection into kidney rudiments (Kim and Dressler 2005; Steenhard et al. 2005; Challen et al. 2006; Maeshima et al. 2006; Perin et al. 2007; Vigneau et al. 2007). In the following sections, a brief summary is given of the outcomes of administration of other stem cells and progenitors in the models of acute renal injury, and their *in vitro* differentiation potential towards renal cell types. Table 1.1 summarizes different methodologies used to assess the renogenic potential of progenitors, including MSCs, in the metanephric environment.

1.4.1. Kidney progenitors

Multipotent renal progenitor cells (MRPC) were isolated from adult rat kidneys. When MRPC were injected into the kidneys of rats with ischemia-reperfusion injury, they became incorporated into renal tubules in the cortex and outer medulla and expressed the proximal tubule marker, *Phaseolus vulgaris* erythroagglutinin, and the distal tubule marker, peanut agglutinin, as well as

the epithelial cell marker, zona occludens-1 (ZO-1). In addition, when injected under the capsule of rat kidneys, undifferentiated MRPC were shown to form nodules and cyst-like structures, and integrated into the renal tubules and formed multiple tubular-like structures. It has also been attempted to differentiate MRPC toward a renal cell lineage using a combination of fibroblast growth factor 2, TGF-β and leukaemia inhibitory factor. Under these conditions, the cells started to grow in aggregates and express cytokeratin and ZO-1 (Gupta et al. 2006). Another renal progenitor population that was demonstrated to engraft into damaged kidneys was derived from the adult mouse. These cells were shown to express the stem cell antigen-1 (Sca-1) and lacked CD45 expression. Also, the $Sca\text{-}1^{+}CD45^{-}$ population was demonstrated to incorporate into renal tubules in mice in the ischemia-reperfusion injury model (Dekel et al. 2006). Direct injection of other murine progenitors, such as mouse kidney progenitor cells (MKPC), was demonstrated to protect mice with ischemia-reperfusion renal injury from the renal function deterioration and to improve renal structure following the injury. In consequence, the mice with renal injury that received MKPC survived longer then untreated mice. Ultimately MKPC after injection into the medulla of normal mice were found incorporated into vessels and capillaries as well as into distal tubules and Henle's loop expressing Tamm-Horsfall glycoprotein (THP) (Lee et al. 2010).

Several groups have demonstrated the significance of a renal progenitor population expressing the CD133 antigen in the amelioration of acute kidney injury and *in vitro* differentiation (Bussolati et al. 2005; Sagrinati et al. 2006; Lazzeri et al. 2007; Ronconi et al. 2009). Accordingly, human CD133-positive renal progenitors derived from the cortex of normal human kidney were injected into mice with glycerol-induced acute kidney injury. The cells were found in the proximal and distal tubules of injured kidneys where they expressed the epithelial marker,

cytokeratin. In addition, the CD133-positive cells were shown to undergo *in vitro* epithelial differentiation upon stimulation with hepatocyte growth factor (HGF) and fibroblast growth factor-4, as the cells started to express cytokeratin, E-cadherin and ZO-1, as well as renal markers such as alkaline phosphatase, amino peptidase A, normally found in proximal tubular epithelial cells, and the thiazide-sensitive NaCl co-transporter present in distal tubular epithelial cells. When injected into severe combined immunodeficiency (SCID) mice, they also showed spontaneous *in vivo* differentiation towards tubular epithelia, characterized by the formation of tubular-like structures with a lumen harbouring cells that display short microvilli and tight junctions, and accompanied by the expression of cytokeratin, thiazide-sensitive NaCl co-transporter and alkaline phosphatase (Bussolati et al. 2005). Sagrinati *et al*. demonstrated that $CD24^{+}133^{+}$ human adult stem cells derived from the Bowman's capsule can ameliorate glycerol-induced kidney injury and subsequently engraft into both proximal and distal tubules following injury. Differentiation towards tubular cells was accompanied by the acquisition of the expression of alkaline phosphatase and THP as well as the up-regulation of other renal markers like aminopeptidase A, AQP1, AQP3, and the thiazide-sensitive Na/Cl transporter. Finally, the tubular-like cells also acquired the ability to respond to angiotensin II with intracellular calcium influx (Sagrinati et al. 2006). Correspondingly, the behaviour of adult human $CD133^{+}CD24^{+}$ cells derived from the Bowman's capsule was assessed in a model of adriamycin-induced renal injury in mouse. The administration of the cells led to enhanced functional and structural recovery of the injured kidneys. Accordingly, the cells were present in glomerular structures, expressing the podocyte-specific markers synaptopodin, WT1, nephrin, and podocin, as well tubules expressing binding sites for *Lotus tetragonolobus* agglutinin (LTA), a marker for proximal tubules. Furthermore, $CD133^{+}CD24^{+}$ cells were differentiated *in vitro* towards the tubular lineage using

HGF, and towards the podocyte lineage using vitamin D3 and retinoic-acid. Accordingly, tubular differentiation resulted in the acquisition of binding of LTA as well as up-regulation of the expression proximal tubule-specific genes, including aminopeptidase A, aquaporin-1, aquaporin-3, and thiazide-sensitive Na/Cl transporter. At the same time, following podocyte differentiation, the cells started to express podocyte markers like nephrin, WT1, synaptopodin and podocin (Ronconi et al. 2009). Finally, a similar population of cells was derived from human foetal kidneys. In the glycerol-induced kidney injury model in SCID mice, the cells incorporated into tubules stained with the proximal tubule marker, LTA, and the collecting duct marker, *Dolichos biflorus* agglutinin. The cells improved the function as well as the structural recovery of the kidneys following the treatment with glycerol. Finally, following *in vitro* stimulation, the cells were shown to up-regulate expression of some important kidney genes, such as aminopepetidase A, aquaporin 1 and 3, thiazide-sensitive Na/Cl, megalin or THP (Lazzeri et al. 2007).

Ultimately, kidney-derived progenitors have been demonstrated to harbour the potential to contribute to the development of different compartments during nephrogenesis when injected into metanephroi (Challen et al. 2006; Maeshima et al. 2006; Ward et al. 2011) (Table 1.1). Among several types of renal progenitor populations, the label-retaining tubular cells (LRTC), or kidney side population (SP), showed renogenic potential. On the 5^{th} day following injection into E15 rat kidney rudiment, the LRTC were found in and around the ureteric buds, as well as in tubules positive for LTA (Maeshima et al. 2006). Similarly, the SP cells (isolated from adult mouse kidneys using their ability to efflux the Hoechst dye), were shown to have the potential to contribute to kidney development. After 3 days from the injection of the cells into mouse E12.5 metanephroi, SP cells were found in UBs stained with calbindin and Pax2, as well as in MM

stained with Wt1 and Pax2. Importantly, it was shown that the kidney main population cells (i.e., the cells that were unable to efflux the Hoechst dye) were also able to engraft into UB and MM, albeit at a much lower percentage than the SP cells (Challen et al. 2006). Finally, human CD133/1^{+} kidney progenitors isolated from both the papilla and the cortex were injected into E12.5 mouse kidney rudiments. Accordingly, the cells demonstrated an ability to engraft into the tubular compartment of the metanephric kidney after 3 days of culture (Ward et al. 2011).

1.4.2. Amniotic fluid stem cells

Similar to MSCs and kidney progenitors, human AFSC were described to enhance functional and structural recovery of mouse kidneys following glycerol-induced acute renal failure. Furthermore, it has been demonstrated that following their administration, the AFSCs differentiated into renal tubules as they stained positively with peanut agglutinin and *Dolichos biflorus* agglutinin in the damaged kidneys (Perin et al. 2010). Interestingly, the intravenous injection of human AFSCs was demonstrated to lead to a more rapid recovery of renal function in glycerol-induced acute kidney injury in comparison to MSCs. In addition, in these experiments, MSCs were demonstrated to induce more effectively the proliferation of tubular cells, while AFSC had a more pronounced anti-apoptotic effect on injured kidneys (Hauser et al. 2010). Ultimately, AFSCs were demonstrated to contribute to developing renal structures following injection into mouse metanephric kidneys. Accordingly, after 5 days from injection, human AFSCs were found integrated into stroma and the renal vesicle, C- and S-shaped bodies. This was accompanied by expression of some human kidney-associate genes, such as *ZO-1, claudin* and *GDNF* (Perin et al. 2007) (Table 1.1). Recently, another group confirmed these results by demonstrating that human AFSCs could contribute to nephron formation as well as to ureteric

bud structures during metanephric development (Siegel et al. 2010) (Table 1.1).

1.4.3. Embryonic stem cells

Regarding embryonic stem cells (ESCs) or ESC-derivatives, the cells were injected into developing metanephroi, similarly as for kidney progenitors and AFSCs, but were found primarily in tubular compartments (Kim and Dressler 2005; Steenhard et al. 2005; Vigneau et al. 2007) (Table 1.1). The injection of undifferentiated ESCs into E13 mouse kidney rudiments resulted after 5 days of culture, in the formation of large tubule-like structures consisting of cells displaying apical microvilli, junctional complexes and basal bodies, surrounded by a basement membrane. Furthermore, such ESC-derived structures stained with LTA, a marker for proximal tubules. It has been also observed that ESCs did not mix with native kidney cells to create chimeric tubules in the metanephroi. In addition, injected ESCs were rarely observed in developing glomeruli (Steenhard et al. 2005). Other groups injected pre-differentiated ESCs into kidney rudiments (Kim and Dressler 2005; Vigneau et al. 2007). For instance, Kim and Dressler used undifferentiated ESCs to form embryoid bodies (EBs), which after 5 days of culture, were further induced with retinoic acid, activin-A and bone morphogenic protein-7. Following the induction, the cells started to express genes involved in early kidney development, such as *Pax2*, *Wt1*, *Wnt4*, *Lim1*, *Six2*, *Eya1* and *Gdnf*. These differentiated ESCs engrafted into tubules of E12.5 mouse kidney rudiments after 5 days of *in vitro* culture. Furthermore, tubules generated by the differentiated cells stained with laminin and LTA. In addition, EB-derived cells that were not induced with the nephrogenic cocktail had a lower ability to incorporate into tubules and were found mainly in non-tubular structures (Kim and Dressler 2005). Another group demonstrated that if ESCs were differentiated towards an early renal phenotype prior to their injection into the

E11.5 kidney rudiment, the cells were found in pretubular aggregates after 4 days of culture. Accordingly, when injected into the kidneys of newborn mice, the cells incorporated into proximal tubules. The cells used in these experiments were derived from EBs, similarly as in the previous study, but with the difference that they were cultured in the presence of activin-A for 4 days before injection. This resulted in high expression levels of the nascent mesodermal marker, *brachyury*, which was subsequently used to divide the EB cell population in two separate fractions. Interestingly, in comparison to the *brachyury* positive fraction, which integrated into proximal tubules, the *brachyury* negative cells integrated into ureteric buds (Vigneau et al. 2007). Recently, it has been shown that conditioned medium from a UB culture can trigger ESCs previously induced by retinoic acid and activin, to differentiate towards a renal phenotype, as assessed by expression of WT1, Pax2 and binding of *Dolichos biflorus* agglutinin (Ren et al. 2010).

Table 1.1 Different techniques used to introduce stem cell/progenitor populations into the embryonic kidney environment with the aim of differentiating them towards a kidney-specific phenotype.

Stem cell/progenitor	No. of cells	Outcome	Methodology	Reference
Human MSCs	1000	Glomerular and tubular epithelium and interstitium	Injection into intermediate mesoderm of a rat embryo or E13 rat kidney	Yokoo et al. 2005; Yokoo et al. 2006
Human MSCs	50-100	Wolffian duct	Injection into intermediate mesoderm of a chicken embryo	Fukui et al. 2009
Human AFSCs	1000	Stroma, renal vesicle, C- and S-shaped bodies	Injection into E12.5-E18 mouse kidney rudiment	Perin et al. 2007
Human AFSCs	10 000	Developing nephron, UB	Recombination of AFSCs with E11.5 mouse kidney cells (1:10)	Siegel et al. 2010
Human kidney progenitors	4500	Integration into tubules	Injection into E12.5 mouse kidney rudiment	Ward et al. 2011
Mouse ESCs	1500	Proximal tubules	Injection into E12-E13 mouse kidney rudiment	Steenhard et al. 2005
Mouse ESC-derived progenitors	1000-2000	Proximal tubules	Injection into E12.5 mouse kidney rudiment	Kim and Dressler 2005
Mouse ESC-derived progenitors	300	Pretubular aggregates	Injection into E11.5 mouse kidney rudiment	Vigneau et al. 2007
Mouse kidney progenitors	100	Ureteric buds and condensing metanephric mesenchyme	Injection into E12.5 mouse kidney rudiment	Challen et al. 2006
Rat kidney progenitors	200	Interstitium, ureteric buds, proximal tubules	Injection into E15 rat kidney rudiment	Maeshima et al. 2006

Aim of the study

The aim of the study is to investigate the potential of mesenchymal stem cells (MSCs), a multipotent cell population (Prockop 1997), to contribute to *in vitro* nephrogenesis by differentiating into kidney-specific cell types in a metanephric environment of mouse kidney rudiment. MSCs might be potential candidates for stem cell-based renal tissue generation as they not only exert renoprotective effects in different acute kidney injury models, but also engraft into the tubules of injured kidneys, and to some extent, differentiate into tubular epithelial cells (Herrera et al. 2004; Morigi et al. 2004; Qian et al. 2008; Li et al. 2010). Moreover, human MSCs were shown to give rise to nephron-specific cell types after they underwent specific reprogramming in the embryonic environment of the metanephric kidney (Yokoo et al. 2005; Yokoo et al. 2006). Additionally, human MSCs were shown to ameliorate renal pathologies when incorporated into embryonic kidneys containing renal defects (Yokoo et al. 2005; Guillot et al. 2008). Nevertheless to achieve a significant contribution of MSCs to metanephric development, a sophisticated methodology is required, as demonstrated by Yokoo *et al*. (Yokoo et al. 2005). Since the direct injection of human MSCs into the developing kidney *in vitro*, is insufficient to enable MSC differentiation, the cells need to be genetically modified to over-express glial cell-derived neurotrophic factor before they are injected into the intermediate mesoderm of an embryo, followed by *ex utero* culture of the embryos (Yokoo et al. 2005; Yokoo et al. 2006; Fukui et al. 2009). The current study is therefore aimed at re-evaluating the renogenic capacity of mouse and human bone marrow-derived MSCs using a much simpler protocol described by Unbekandt and Davies, which is based on disaggregation and subsequent re-aggregation of mouse metanephroi (Unbekandt and Davies 2010). This new methodology allows incorporation

of cells from different origins into kidney rudiments to form kidney chimeras and to determine the contribution of the cells to nephrogenesis in an *in vitro* environment, which mimics metanephric development. Furthermore, in this study an attempt will be made to enhance the potential of MSCs to engraft into structures of developing kidney chimeras by incubating the cells with conditioned medium from a kidney cell culture. The use of conditioned medium to induce differentiation of MSCs has been described before. It has been demonstrated that MSCs can adopt the characteristics of the cells from which the conditioned medium was derived (Rivera et al. 2006; Pan et al. 2008; Baer et al. 2009; Schittini et al. 2010). The conditioned medium from neonatal kidney cells will be used in this study to pre-condition both mouse and human MSCs and accordingly the renogenic potential of pre-conditioned MSC will be evaluated. Finally, the paracrine activity of MSCs was shown to play a major role in promoting recovery from kidney injury (Togel et al. 2005; Bi et al. 2007; Imberti et al. 2007; Semedo et al. 2007; Togel et al. 2007; Togel et al. 2009). However, it is not clear what effect factors secreted by MSCs might have on embryonic kidneys. Therefore the paracrine action of MSCs on metanephric kidneys will be additionally assessed in this study.

The following is a summary of the most important issues addressed in this study:

- the ability of the MSC to contribute to developing renal structures in a chimeric kidney culture assay based on the protocol of Unbekandt and Davies

- the potential of other cells, such as embryonic stem cells and neonatal kidney cells, to contribute to developing renal structures using the protocol of Unbekandt and Davies

- the renogenic potential of MSCs pre-treated with conditioned medium derived from

neonatal kidney cells using the protocol of Unbekandt and Davies

- the effects exerted by MSCs on embryonic kidney development

Chapter 2: Material and methods

2.1. Primary cells and stem cell lines

2.1.1. Mesenchymal stem cells

Mouse mesenchymal stem cells

Mouse mesenchymal stem cells (MSCs) used in this study were the D1 MSC line, derived from bone marrow of BALB/c mice (Diduch et al. 1993). The D1 line was purchased from ATCC (CRL-12424).

Human mesenchymal stem cells

Primary human MSCs were obtained from bone marrow of healthy donors following immunodepletion of CD45 cells. Human MSCs were purchased from Lonza (Lonza Walkersville, Inc., USA)

2.1.2. Mouse embryonic fibroblasts

Mouse embryonic fibroblasts (MEFs) were isolated from mouse embryos at embryonic day (E) 11.5-12.5. The isolation protocol is described in section 2.2.8.

2.1.3. Mouse embryonic stem cells

Mouse embryonic steam cells (ESCs) used here were the E14 line, established from mouse strain 129/Ola by Martin Hooper (Hooper et al. 1987). E14 ESCs were obtained from Mark Boyd at the University of Liverpool.

2.1.4. Mouse neonatal kidney cells

Mouse neonatal kidney cells (NKCs) were derived from kidney of CD-1 mice by Cristina Fuente Mora at the University of Liverpool (Mora 2009). The isolation protocol is briefly described in section 2.2.5.

2.2. Cell culture

2.2.1. Cell thawing protocol

In order to thaw cells employed in this study, cryovials containing frozen cells were removed from the liquid nitrogen container and promptly transferred into a water bath at 37°C. As soon as the cells thawed, the cell suspension was transferred into a 15ml conical tube (Greiner Bio One, UK) filled with pre-warmed standard culture medium (see section 2.11.1). Subsequently the cells were centrifuged at 400*g* for 2.5 min and the supernatant discarded. Accordingly the cell pellet was resuspended in appropriate culture medium and placed in a humidified incubator (Thermo Fisher Scientific Inc., USA) at 37°C, 5% CO_2 (v/v) in air.

2.2.2. Cell freezing protocol

In order to freeze cells used in this study, the medium was aspirated, the cell cultures were washed once with Dulbecco's Phosphate Buffered Saline (PBS) without $CaCl_2$ and $MgCl_2$ (Sigma-Aldrich, USA) and subsequently incubated with 0.25% trypsin/EDTA (Sigma-Aldrich) solution at 37°C for 1-5 min. Depending on size of the culture dish, an appropriate volume of trypsin/EDTA solution was added. Accordingly, cells cultured in 3.5 cm dishes were incubated with 0.5ml of 0.25% trypsin/EDTA solution. Next, the trypsin reaction was stopped by adding 1ml of pre-warmed standard culture medium (see section 2.11.1) to the dish. The obtained cell

suspension was transferred into a 15ml conical tube and centrifuged at 400*g* for 2.5 min. Following the centrifugation, the supernatant was discarded and the cell pellet resuspended in Recovery™ Cell Culture Freezing Medium (Invitrogen, USA). Accordingly, cells obtained form 3.5 cm dish were resuspended with 1ml of the Recovery™ Cell Culture Freezing Medium. The cell suspension was then divided between two cryovials (Corning, Holland), which were then left overnight in a freezing container (Nalgene, Denmark) filled with isopropanol (Sigma-Aldrich) at -80°C, to facilitate slow freezing of the cells. Next day the cryovials were transferred into a liquid nitrogen container.

2.2.3. Cell passaging

All cells used in this study were adherent cells. In order to passage the cells, culture medium was aspirated and the cultures were washed once with PBS without $CaCl_2$ and $MgCl_2$. Next the cultures were incubated with 0.25% trypsin/EDTA (Sigma-Aldrich) solution at 37°C for 1-5 min. The appropriate volume of trypsin/EDTA solution was added to sufficiently cover the cells. In order to stop the action of trypsin 1ml of pre-warmed standard culture medium (see section 2.11) was added to the dishes. Next the cell suspension was transferred into a 15ml conical tube and centrifuged at 400*g* for 2.5 min. The supernatant was discarded and the cell pellet resuspended in warmed culture medium. D1 cells and NKCs were resuspended in standard culture medium (see section 2.11.1); human MSCs were resuspended in culture medium provided by the manufacturer (Lonza); MEFs were resuspended in MEF culture medium (see section 2.11.1); ESCs in ESC culture medium (see section 2.11.1). Usually the cells were passaged in 1 to 3 or 1 to 4 ratios. In order to obtain exact number of cells following detachment, the cells were counted beforehand using a Neubauer haemocytometer (Hausser Scientific, USA).

2.2.4. Routine mesenchymal stem cell culture

Mouse mesenchymal stem cells

D1 cells were cultured in standard culture medium (see section 2.11.1) on uncoated plastic culture dishes (Nunc, Denmark) in a humidified incubator at 37°C, 5% CO_2. The cells were passaged 1 to 3 or 1 to 4 every 2-3 days according to the protocol in section 2.2.3. D1 cells were used be between 10^{th} and 30^{th} passage.

Human mesenchymal stem cells

Human MSCs were cultured according to the manufacturer's instructions (Lonza). In brief, the cells were maintained in Mesenchymal Stem Cell Growth Medium (MSCGM™) on uncoated plastic culture dishes (Nunc) in a humidified incubator at 37°C, 5% CO_2. The medium was changed every 3-4 days. The cells were passaged approximately once a week when the cultures reached around 90% confluency. Subsequently the cells were seeded, according to the instructions provided by Lonza, at 5,000-6,000 cells per cm^2 of surface area. Human cells were used up to 8^{th} passage.

2.2.5. Preparation of mouse neonatal kidney cells

NKC cultures were first established by Cristina Fuente Mora at the University of Liverpool (Mora 2009). In brief, the cells were isolated from kidneys of 2–6 days old CD-1 mice, cut into <1 mm pieces and incubated for 20 min at 37°C in 1mg/ml collagenase type I (Sigma-Aldrich) and 0.1mg/ml deoxyribonuclease I (Sigma-Aldrich) in Hank's Buffered Salt Solution (HBSS) containing calcium and magnesium (Invitrogen). The suspension was washed with HBSS and incubated with 0.5mM EDTA (Sigma-Aldrich) for 20 min at 37°C. Next the suspension was

passed through 21-gauge and 23-gauge hypodermic needles (Becton Dickinson, USA), centrifuged at 200*g* and resuspended in HBSS cells were passed though a 30μm pre-separation filter. The obtained cell suspension was cultured on fibronectin coated dishes in the presence of conditioned medium derived from the STO embryonic mouse fibroblast cell line.

2.2.6. Routine mouse neonatal kidney cell culture

NKCs used in this study were cultured under previously described conditions (Mora 2009). Accordingly NKCs were maintained in standard culture medium (see section 2.11.1) on uncoated plastic culture dishes (Nunc) a humidified incubator at 37°C, 5% CO_2. The cells were passaged 1 to 3 or 1 to 4 every 2-3 days as described in the protocol in section 2.2.3. The cells were used be between 5^{th} and 15^{th} passage.

2.2.7. Gelatinization of culture dishes

Some culture dishes were coated with 0.1% (w/v) gelatine solution (see section 2.11.2) before seeding the cells. Accordingly, 3.5 cm culture dishes were incubated with 2ml of the gelatine solution in room temperature for 15 min. Subsequently, the dishes were washed 3 times with warm PBS and used to culture MEFs and ESCs.

2.2.8. Preparation of mouse embryonic fibroblasts

MEF cultures were established as follows: CD-1 E11.5-12.5 mouse embryos were decapitated, eviscerated and minced into small pieces. After that, they were incubated with 0.25% trypsin/EDTA (Sigma-Aldrich) at 37°C for 20-30 min. The reaction was stopped by adding MEF culture medium (see section 2.11.1). The obtained cell suspension was allowed to adhere to a 10 cm culture dish (Corning) in 37°C, 5% CO_2 humidified incubator for 3-4 days. Subsequently

when the primary cultures reached around 90% of confluency they were passaged 1 to 3 on gelatinized dishes. When the cultures reached passage 4 they were treated with 20µg/ml mitomycin C (Sigma-Aldrich) which covalently binds to the DNA crosslinking complementary DNA strands thus preventing further proliferation of the treated cells. To obtain appropriate concentration of mitomycin for a 10 cm culture dish, 5ml of MEF medium was mixed with 100µl of previously prepared 2mg/ml mitomycin C in PBS. Next, the treated cells were incubated for 2-3 h in a humidified incubator at 37°C, 5% CO_2. After the incubation, the cells were washed three times with PBS and were prepared for freezing as described in section 2.2.2. The cells were frozen at a final cell density of 2 million cells in 1ml of freezing recovery medium per cryovial. In order to be used in subsequent experiment, the mitomycin C treated MEFs, also referred as inactivated MEFs, were thawed according to the protocol in section 2.2.1.

2.2.9. Routine mouse embryonic fibroblast culture

In this study, inactivated MEFs were used as feeder layers for mouse ESCs and to obtain conditioned medium for mouse MSC stimulation. The cells were thawed using the protocol described in section 2.2.1. The cells were then seeded on 3.5 cm gelatinized dishes (Nunc) (see section 2.2.7). From each cryovial 3 dishes were prepared. The cells were allowed to attach overnight in a humidified incubator at 37°C, 5% CO_2 before use. Accordingly, the inactivated MEFs were maintained in MEF medium in 37°C, 5% CO_2 humidified incubator for a maximum of 2 weeks. The medium was changed every other day.

2.2.10. Routine mouse embryonic stem cell culture

Mouse ESCs were cultured on a monolayer of inactivated MEFs in ESC culture medium (see section 2.11.1) in humidified incubator at 37°C, 5% CO_2. The medium was changed every

other day. The cells were passaged 1 to 4 every 3-4 days (see section 2.2.3). To ensure absence of the fibroblasts in the recombination experiments (in the chimeric kidney assay, see section 2.6), ESCs were cultured in the presence of ESC culture medium on gelatinized dishes but in the absence of feeder cells for two subsequent passages. The cells were used between 10^{th} and 20^{th} passage.

2.3. Conditioned medium treatment

2.3.1. Conditioned medium preparation

In this study, different conditioned media were used to stimulate either D1 cells or intact kidney rudiments. In order to obtain conditioned medium from NKCs (NKC CM), sub-confluent cultures of NKCs were cultured in standard culture medium for 2 days before medium collection. In order to obtain conditioned medium from MEFs, confluent inactivated MEF were maintained in MEF culture medium for 2 days before the collection. Ultimately, in order to derive conditioned medium from D1 cells (MSC CM), sub-confluent cultures of D1 cells were cultured in standard culture medium for 1 day before the collection. The collected conditioned media were centrifuged at maximum speed in a table-top centrifuge for 3 min. Subsequently, the supernatant was collected and filtered with 0.22µm syringe filter (Sartorius Stedim Biotech GmbH, Germany). Conditioned media were then stored in -20°C. Before use, they were thawed and mixed with fresh standard culture medium in a ratio of 1:1. In order to achieve different concentrations of NKC CM, Vivaspin centrifugal ultra-filtration devices (Sartorius Stedim Biotech GmbH, Germany) were used.

2.3.2. Stimulation with conditioned medium

Stimulation of mesenchymal stem cells

In order to increase renogenic potential of D1 cells, the cells were stimulated with NKC CM for 4 days. Accordingly, $2.5x10^5$ D1 cells were seeded in an uncoated 3.5 cm culture dish (Nunc) in the presence of NKC CM 1:1 mixed with standard culture medium and incubated for 4 days in humidified incubator at 37°C, 5% CO_2. The conditioned medium was replaced with a fresh mix on the second day of culture. Subsequently the same conditions were used to stimulate D1 cells with MEF CM. In order to pre-condition human MSCs, sub-confluent human cultures were used. The cells were incubated with NKC CM 1:1 mixed with standard culture medium for 4 days in a humidified incubator at 37°C, 5% CO_2.

Stimulation of intact kidney rudiments

In order to assess if MSCs may exert an indirect effect on metanephric development *in vitro*, intact kidney rudiments were cultured for 3 days in the presence of conditioned medium derived from D1 cells (MSC CM) or D1 cells previously stimulated with NKC CM (sMSC CM). MSC CM used in these experiments was obtained from sub-confluent MSCs cultures after 1 day of conditioning. In order to collect sMSC CM, D1 cultures were first stimulated with NKC CM for 4 days. The cultures were subsequently washed with PBS and the medium was changed to standard culture medium. After 1 day the conditioned media was collected and prepared for stimulation. Accordingly E11.5 kidney rudiments obtained from littermate embryos were cultured in the presence of MSC CM or sMSC CM mixed 1:1 with standard culture medium for 3 days. The condition for embryonic kidney culture is described in detail in section 2.5.2.

2.4. *In vitro* multilineage differentiation protocols

2.4.1. Adipogenesis assay

Mouse mesenchymal stem cells

The adipogenic assay was performed as described previously by Peister *et al* (Peister et al. 2004). Accordingly confluent D1 cultures were stimulated twice a week with adipogenic inductive media (see section 2.11.1). After 2 weeks the cells were fixed with 4% paraformaldehyde (w/v) (PFA) (see section 2.11.2) for 10 min and subjected to analysis. At the same time the non-induced cells were cultured in standard culture medium. Intracellular lipid vacuoles were detected using Oil Red O staining. Accordingly the cells were covered with 0.5% (w/v) Oil Red O solution (see section 2.11.1) diluted 3:2 in water before use. For a 3.5 cm culture dish 1ml of Oil Red O solution was used. The dishes were incubated for 15 min at room temperature. In this solution lipid droplets were stained red. Subsequently the cells were washed several times with large volumes of H_20 to get rid of excess of the solution. Finally 1ml of H_20 was added to the dishes and images of stained cultures were acquired using Leica DM2500 microscope and DFC350FX camera.

Human mesenchymal stem cells

Human MSCs were confirmed to undergo adipogenesis using Differentiation Media BulletKit® (PT-3004) supplied by Lonza according to manufacturer's instructions. In brief, the adipogenic assay was started when human MSC reached confluency. Three cycles of induction/maintenance were performed using the adipogenic inductive and maintenance medium. Each cycle consisted of incubating the cells with supplemented adipogenesis induction medium (Lonza) for 3 days

followed by 1-3 days of culture in supplemented with adipogenic maintenance medium (Lonza). At the same time, non-induced control cells were cultured in maintenance medium only. Finally, the cells were cultured for the next 7 days in maintenance medium, replaced every 2-3 days. The lipid vacuoles were detected as described above for mouse MSCs, using the Oil Red O solution (see section 2.11.1) after the cells were fixed with 4% PFA.

2.4.2. Osteogenic assay

Mouse mesenchymal stem cells

The osteogenic assay was performed as described previously by Peister *et al* (Peister et al. 2004). Confluent D1 cultures were stimulated twice a week with osteogenic inductive media (see section 2.11.1). At the same time the non-induced cells were cultured in standard culture medium. After 2 weeks the cells were fixed with 4% PFA for 10 min and calcium deposits visualised using 2% (w/v) Alizarin Red S solution (see section 2.11.2) adjusted to pH 4.2 with ammonium hydroxide (Sigma-Aldrich). For a 3.5 cm culture dish 1ml of Alizarin Red S solution was added. The dishes were incubated for 20 min at room temperature. Extracellular calcium deposits produced by osteoblasts were stained red/orange. Subsequently the cells were washed several times with large volumes of H_20 to get rid of excess of the solution. Finally 1ml of H_20 was added to the dishes and images of stained cultures were acquired using Leica DM2500 microscope and DFC350FX camera.

Human mesenchymal stem cells

Human MSCs were confirmed to undergo osteogenesis using Differentiation Media BulletKit® (PT-3002) supplied by Lonza according to manufacturer's instructions. In brief, human MSCs

were plated at a density of $3.1x10^3$ per cm^2 of tissue culture surface area in Mesenchymal Stem Cell Growth Medium (Lonza). The cells were allowed to adhere for 24 h. In order to induce osteogenic differentiation the growth medium was replaced with osteogenesis induction medium (Lonza) and the cells were cultured in the inductive medium for the next 2 weeks. Medium was changed every 3-4 days. The non-induced control human MSCS were maintained for the same period of time in growth medium. The calcium deposits were detected as described above for mouse MSCs, using Alizarin Red S solution (see section 2.11.2) after the cells were fixed with 4% PFA.

2.4.3. Chondrogenic assay

The chondrogenic assay was performed as described by Peister *et al* (Peister et al. 2004). Accordingly, $3x10^5$ D1 cells were spun down to form a pellet at the bottom of a 15ml polypropylene tube. The supernatant was carefully discarded, in order not to disturb the pellet and 0.5ml of chondrogenic inductive media (see section 2.11.2) was added. The cells were then stimulated twice a week with this medium. After 2 weeks the micromass (pellet) culture was fixed with 4% PFA for 20 min and 10μm cryosections were prepared. For this purpose the micromasses were washed with PBS 3x10 min and incubated overnight in 15% (w/v) sucrose solution (see section 2.11.2) at 4°C. The sucrose solution was aspirated and the micromasses then embedded using cryo-embedding medium (Bright Instrument Ltd., UK) and frozen using liquid nitrogen-chilled isopentane (Sigma-Aldrich). Frozen cultures were cut at -20°C using a cryostat (HM505, Microm International, Germany) with C35 Feather microtome blades (VWR, UK). Subsequently the sections were transferred onto subbed glass microscope slides 76x26x0.8mm (VWR). Frozen sections were stored at -20°C. The subbed slides were prepared as follows:

slides were soaked for 10-15 min in absolute ethanol (University of Liverpool solvent service) and washed 5x in distilled water. Then they were treated with a solution of 0.5% (w/v) porcine gelatine (Sigma-Aldrich) and 0.05% (w/v) CrKSO4 (Sigma-Aldrich) in distilled water for 25 sec and allowed to dry before being stored for future use. In order to visualize chondrogenic differentiation, 1% (w/v) Alcian Blue solution (see section 2.11.2) was used to detect extracellular proteoglycans. Accordingly the frozen sections were incubated with 0.1N HCl (Invitrogen) for 5 min in room temperature prior staining. Next the solution was applied onto sections and incubated for 30 min at room temperature. Finally the sections were washed twice with 0.1N HCl. The images of stained sections were acquired using Leica DM2500 microscope and DFC350FX camera.

2.5. Cell labelling

2.5.1. Quantum dot labelling

For Quantum dot (QD) labelling, the Qtracker® 655 Cell Labelling Kit (Invitrogen) was used according to manufacturer's instructions. First, 1µl of component A (QD nanocrystals) and 1µl of component B (carrier) were mixed in a microcentrifuge tube and incubated for 5 min at room temperature. In order to obtain the 10nM final concentration of the QDs for labelling, 200µl of standard culture medium was added to mixed components and subsequently vortexed for 30 sec at room temperature. The labelling solution was added to a suspension of the appropriate cell type and incubated in humidified incubator at 37°C, 5% CO_2 for 45-60 min. In order to obtain the cell suspension, the adherent cultures of MSCs, NKCs or ESCs were treated with 0.25% trypsin/EDTA as described in section 2.2.3 before QD labelling. Following labelling, the cells were centrifuged at 400*g* for 3 min and the supernatant aspirated. Finally, the cells were washed

four times with standard culture medium to remove any QDs that had not incorporated into the cells. In order to test efficiency of QD-labelling, labelled D1 cells were resuspended in 2ml of standard culture medium, seeded at $2.5x10^5$ on uncoated 3.5 cm culture dishes and cultured for 5 days at 37°C, 5% CO_2. Ultimately, QD-labelled cells resuspended in standard culture medium were used in the chimeric kidney assay (see section 2.6).

2.5.2. CFDA SE labelling

For CFDA SE (carboxyfluorescein diacetate succinimidyl ester) labelling, the Vybrant® Cell Tracer Kit (Invitrogen) was used. Initially 10mM CFDA SE stock solution was prepared by dissolving the contents of Component A (CFDA SE) in 90μl of Component B (dimethyl sulfoxide). Next, the stock solution was diluted to reach 0.5μM working concentration in high glucose Dulbecco's Modified Eagle Medium (Sigma-Aldrich). The labelling was performed on D1 cells in suspension, similarly as described for QD labelling. Accordingly, cells were incubated with the labelling solution in a humidified incubator at 37°C, 5% CO_2 for 45 min. Subsequently the cells were centrifuged at 400*g* for 5 min and the supernatant aspirated. They were washed three times with standard culture medium. Next the cells were seeded at $2.5x10^5$ on uncoated 3.5 cm culture dishes and cultured for 5 days at 37°C, 5% CO_2, in order to compare the effectiveness of labelling with CFDA SE and QDs.

2.5.3. Lentiviral transduction

For constitutive expression of green fluorescent protein (GFP), mouse MSCs were transduced with pHR-SFFV-GFP a lentiviral vector encoding enhanced GFP under the spleen focus-forming virus (SFFV) promoter. The lentiviral supernatant, containing the GFP vector, was obtained from Sokratis Theocharatos at the University of Liverpool. Before the transduction, D1 cells were

seeded at $2.5x10^5$ on uncoated 3.5 cm culture dishes in standard culture medium and allowed to adhere for 1 h. Next the medium was discarded and the cells were maintained for 6 h in the presence of 200µl lentivirus supernatant mixed with 1800µl standard culture medium in humidified incubator at 37°C, 5% CO_2. Following the incubation the medium was replaced with standard culture medium and the transduced cells were cultured for 3 days at 37°C, 5% CO_2. On the third day GFP expression was verified using Leica DMIL fluorescent microscope (Leica, Germany). GFP-transduced D1 cells were cultured as described for non-modified cells in section 2.2.4.

2.5.4. Immunostaining of human mesenchymal stem cells

In this study a mouse anti-human nuclei antibody was used to detect human MSCs. First the suitability of the antibody was determined in a monolayer culture in a 3.5 cm culture dish. Accordingly, the culture medium was discarded and human MSCs were fixed with -20°C 100% methanol (Sigma-Aldrich) for 10 min at room temperature. Next, the methanol was aspirated and the fixed cells washed with PBS (see section 2.11.2) for 30 min at room temperature. Subsequently, the PBS was aspirated and the cells were incubated in the blocking solution containing 0.1% (v/v) Triton X-100 (Sigma-Aldrich) and 10% (v/v) goat serum (Sigma-Aldrich) in PBS for 45 min which was then replaced with primary antibody solution containing 0.1% (v/v) Triton X-100 and 1% (v/v) goat serum in PBS and 1:200 diluted mouse anti-human nuclei antibody (MAB1281, Millipore). The cells were incubated with the primary antibody solution overnight at 4°C in a humidified chamber. Next day the cells were washed 1 h in PBS and subsequently incubated with secondary antibody solution containing 0.1% (v/v) Triton X-100 and 1% (v/v) goat serum in PBS and 1:500 diluted goat anti-mouse Alexa Fluor488 antibody

(A21121, Invitrogen) for 2 h at room temperature in a humidified chamber in dark. Then the cells were washed for 30 min with PBS and incubated for 10 min in dark in the presence of 4',6-diamidino-2-phenylindole (DAPI) (Invitrogen) diluted 1:100 000 in PBS in order to visualize nuclei of the cells. Finally, the cells were washed three times with PBS and mounted with 80% (v/v) glycerol (Sigma-Aldrich) in PBS and cover slips. Stained human MSC cultures were observed using Leica DM2500 microscope and images were acquired using the DFC350FX camera. Blocking solution and subsequent primary and secondary antibody solutions were centrifuged before use at 13 400*g* for 5 min in a table-top centrifuge (Sanyo, Japan). A control was included where the primary antibody was omitted from the primary antibody solution. Ultimately the anti-human nuclei antibody was used to detect human MSCs in the kidney chimeras, according to the protocol described in section 2.7.1.

2.6. Metanephric kidney culture

2.6.1. Dissection of mouse kidney rudiments

In order to obtain kidney rudiments in this study, mouse embryos were dissected from timed-mated pregnant CD1 mice (Charles River) at embryonic day (E) 11.5 and 13.5. The dissection protocol was performed as described earlier by Davies (Davies 2010). Accordingly, mice were sacrificed by cervical dislocation and the uterine horns were removed and placed into a 50ml conical tube at 4°C. Subsequently the uterine horns were transferred into a dish with cold high glucose Dulbecco's Modified Eagle Medium (DMEM) (Sigma-Aldrich) and the embryos were removed from the uteri and cleaned from extra-embryonic membranes using forceps and small scissors. Then the embryos were decapitated and the caudal parts were removed and transferred to a new dish filled with DMEM. The tail was removed and the caudal parts were placed on their

dorsal side and cut sagittally in half, then the kidney rudiments were dissected using 27 gauge hypodermic needles (Becton Dickinson) under a stereoscopic microscope Nikon SMZ1000 (Nikon Instruments Inc., USA). Following isolation, the kidney rudiments were transferred into dishes filled with DMEM using a glass pipette and placed in a humidified incubator at 37°C, 5% CO_2. Kidney rudiments dissected using the protocol described above were *in vitro* cultured (see section 2.5.2), as well as used for the chimeric kidney assay (see section 2.6) or RNA extraction (see section 2.8.1)

2.6.2. Culture of mouse kidney rudiments *in vitro*

In order to culture *in vitro* kidney rudiments dissected mouse embryonic kidneys were transferred using a glass pipette onto a 1.2μm membrane filter (Millipore, USA) and placed on a Trowell screen (a grid made from stainless steel mesh (Sigma-Aldrich)) (Figure 2.1). The grid supports kidney growth as the culture has to be performed at the gas/medium interface (Davies 2010). Embryonic kidneys were cultured in the presence of standard culture medium (see section 2.11.1) at the gas/medium interface in 37°C, 5% CO_2 humidified incubator. The intact kidney rudiments were analysed using immunostaining, as described in section 2.7.

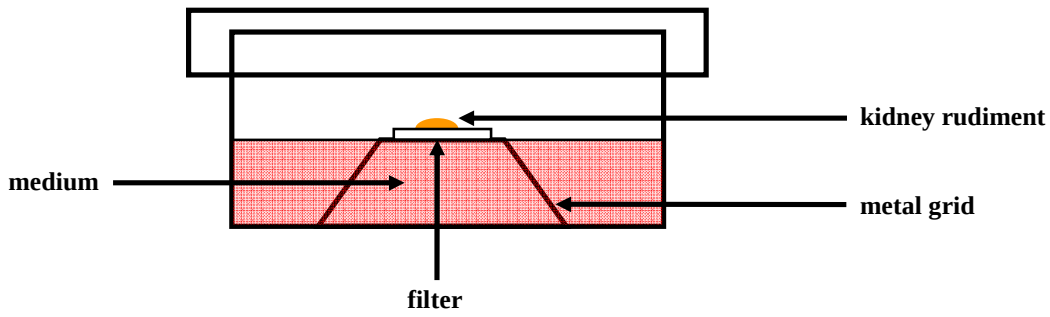

Figure 2.1 Culture condition for kidney rudiments *in vitro*.

2.7. Chimeric kidney assay

Disaggregation, subsequent re-aggregation and culture of re-aggregated mouse embryonic kidneys has been reported previously (Unbekandt and Davies 2010). In the current study this protocol was used to incorporate different stem cells into mouse kidney rudiments. Accordingly the embryonic kidneys were dissected from embryos at E11.5 from pregnant CD-1 mice (Charles River), as described in section 2.5.1. Kidney rudiments were transferred into a 1.5ml microcentrifuge tube (Eppendorf, Germany) and disaggregated using 1ml of 0.25% trypsin/EDTA (Sigma-Aldrich) in high glucose Dulbecco's Modified Eagle Medium (Sigma-Aldrich) for 4 min at 37°C. After the incubation, the rudiments were mixed using a Gilson pipette. If no single cell suspension was obtained after the first incubation step, the rudiments were incubated for an additional 1-2 min at 37°C. Next the embryonic kidney cell suspension was spun down at 400*g* for 2 min, the trypsin/EDTA discarded and 1ml of standard culture medium (see section 2.11.1) was used to resuspend the cells. This was followed by incubation for 5 min at 37°C. After that the suspension was spun down at 400*g* for 2 min and resuspended in 200µl of standard culture medium. Finally, kidney cells were counted using a haemocytometer. Labelled stem cell suspension was mixed with the embryonic kidney cell suspension in a ratio of 1:5 to reach approximately 100 000 cells in total. The recombined cells were spun down at 400*g* for 2 min to form a pellet which was then transferred using a glass pipette on a 1.2µm membrane filter (Millipore) supported by a metal grid. Re-formed embryonic kidneys containing labelled stem cells were cultured for 5 or 7 days in standard culture medium at the gas/medium interface in 37°C, 5% CO_2 humidified incubator, as demonstrated in section 2.5.2. For the first 24h the standard culture medium was supplemented with 5µM Y-27632 Rho kinase inhibitor

(Calbiochem) to promote the survival of the reformed kidneys (Unbekandt and Davies 2010). Medium was changed every second day. After 5 or 7 days the chimeras were immediately fixed with 100% methanol or 4% PFA and analysed using immunostaining (see section 2.8).

2.8. Immunostaining of intact kidney rudiments and kidney chimeras

In this study both intact kidney rudiments and re-aggregated kidney chimeras were fixed with ice-cold (stored at -20°C) 100% methanol for 10 min at room temperature in the dark. An exception was made for chimeras harbouring D1 cells expressing GFP as it was found that the GFP signal was lost after methanol treatment. Accordingly such chimeras were fixed with 4% PFA in PBS for 30 min at room temperature in the dark. In order to perform the fixation step the culture medium was aspirated and replaced with either methanol or PFA until the filters with cultured kidney rudiments and chimeras started to float. After the fixation specimens were transferred into 1.5ml microcentrifuge tubes and subsequently washed with PBS for 30 min and blocked with a blocking solution containing 10% (v/v) goat serum and 0.1% (v/v) Triton X100 in PBS for 45 min at room temperature in the dark. Next the specimens were transferred into primary antibody solution containing 0.1% (v/v) Triton X-100 and 1% (v/v) goat serum in PBS and appropriate antibody or antibodies to incubate overnight at 4°C in dark. All primary antibodies used in this study and their working concentrations are listed in Table 2.1. In addition, for chimeras harbouring human MSCs, an anti-human antibody (MAB1281, Chemicon) was included in the primary antibody solution, diluted 1:200. Subsequently the specimens were washed for 1 h in PBS and incubated with secondary antibody solution containing 0.1% (v/v) Triton X-100 and 1% (v/v) goat serum in PBS and appropriate secondary antibody or antibodies overnight at 4°C in the dark. All secondary antibodies used in this study and their working

concentrations are listed in Table 2.2. In order to visualize human MSCs in the kidney chimeras, goat anti-mouse Alexa Fluor488 antibody (A2112, Invitrogen) was added to the secondary antibody solution diluted 1:500 in the mix. Finally, the stained kidneys and chimeras were washed for 30 min with PBS at room temperature in dark and mounted using 80% (v/v) glycerol (Sigma-Aldrich) in PBS and cover slips. Nail polish was applied onto edges of cover slips to seal the samples. Accordingly the slides were stored in at 4°C in dark. Blocking solution and subsequent primary and secondary antibody solutions were spun down before use at 13 400*g* for 5 min in a table-top centrifuge (Sanyo). Controls consisted of samples where primary antibody was omitted. The images were acquired using Leica AOBS SP2 confocal laser scanning microscope (Leica).

2.9. Confocal imaging

The confocal analysis was performed on whole mount re-aggregated kidneys and kidney chimeras. The images were acquired either as xyz stacks or single plane in the 1024x1024 format. In order to simplify the statistical analysis of MSC integration into kidney structures, only single plane images were used in the study. In order to obtain images containing merged green, red and blue channels ImageJ software was used. To obtain xyz stacks (3D Series) the beginning and end of the 3D series was determined using the Leica software. In order to define the frequency of sampling required to capture the z resolution, the optimal number of sections suggested by the software was selected. For imaging of AlexaFluor488 (excitation/emission of 495/519nm), enhanced GFP (excitation/emission of 488/507nm), as well as quantum dots (excitation/emission of 488/655nm) the argon laser was used. The helium-neon laser and the ultraviolet laser were used for imaging of AlexaFluor594 (excitation/emission of 590/617nm) and AlexaFluor350

(excitation/emission of 346/442nm), respectively. For each sample the gain and offset were adjusted separately. To regulate the intensity of the acquired signal, the Q-LUT option was used in the Leica software. Consequently, the regions containing signal were set up not to have any green, while the background intensity was set up as green pixels. Further, only few saturated, blue pixels were allowed in the areas containing signal. Other parameters used to acquire the images included: beam expander – 6, scan speed – 400Hz, pinhole – airy, frame average – 4, line average – 2.

Table 2.1 Primary antibodies used for immunostaining of kidney chimeras

Antibody	Type	Concentration	Supplier
anti-Wt1	mouse IgG1 monoclonal	1:500	05-753/Upstate
anti-Wt1	rabbit IgG polyclonal	1:200	SC-192/Santa Cruz Biotechnology
anti-laminin	rabbit IgG polyclonal	1:1000	L9393/Sigma-Aldrich
anti-calbindin	mouse IgG1 monoclonal	1:500	ab9481/Abcam
anti-Six2	rabbit IgG polyclonal	1:200	11562-1-AP/Proteintech
anti-human nuclei	mouse IgG1 monoclonal	1:200	MAB1281/Millipore

Table 2.2 Secondary antibodies used for immunostaining of kidney chimeras

Antibody	Type	Concentration	Supplier
anti-rabbit AlexaFluor350	goat IgG	1:500	A11046/Invitrogen
anti-mouse AlexaFluor350	goat IgG1	1:500	A21120/Invitrogen
anti-mouse AlexaFluor488	goat IgG1	1:500	A21121/Invitrogen
anti-mouse AlexaFluor594	goat IgG1	1:500	A21125/Invitrogen
anti-rabbit AlexaFluor594	chicken IgG	1:500	A21442/Invitrogen

2.10. Molecular biology

2.10.1. RNA extraction

Total RNA was isolated using TRIzol® reagent (Invitrogen) according to manufacturer's instructions. In brief, in order to extract RNA from cells, culture medium was aspirated and the cells were washed with PBS. After the PBS was discarded 1ml of TRIzol® reagent was directly

add to the cultures and gently mixed until a homogenous suspension was obtained. The lysed cells were subsequently transferred to a 1.5ml microcentrifuge tube. In order to extract RNA from embryonic kidneys, kidney rudiments were collected at the bottom of a microcentrifuge tube and 1ml of TRIzol® reagent was added. The suspension was vigorously mixed using Gilson pipette until a homogenous suspension was obtained. Next 200µl of chloroform (Sigma-Aldrich) was added to the homogenous mixture. The tubes were shaken for 15 sec and subsequently centrifuged at 12,000*g* for 15 min at 4°C. Following the centrifugation step three phases could be distinguished. For the purpose of RNA extraction only the upper aqueous phase was collected. Nevertheless it is possible to perform sequential precipitation of RNA, DNA and proteins from a single sample using the TRIzol® reagent. According to the manufacturer's instructions, RNA is obtained from the aqueous layer using isopropanol, while the DNA can be precipitated with ethanol from the two other phases, namely the interphase and the organic layer. Subsequently proteins are precipitated from the phenol-ethanol supernatant layer left over after the DNA precipitation step. In order to obtain RNA, the upper phase was transferred into a new microcentrifuge tube containing 1µg/µl of glycogen (Boehringer Mannheim GmbH, Germany) and an equal volume of isopropanol (Sigma-Aldrich) (approximately 0.5ml) was added. Next the solution was mixed 6 times by inversion. Following overnight incubation at -20°C, the solution was centrifuged at 12,000*g* for 10 min at 4°C and the supernatant was discarded. The obtained pellet was then washed with 1ml of cold 75% (v/v) ethanol (Sigma-Aldrich) in nuclease-free water (Sigma-Aldrich) and centrifuged at 4,400*g* for 5 min at 4°C. Finally, the ethanol was discarded and the pellet was allowed to air dry for few minutes at room temperature. The pellets, depending on size, were dissolved in 15-25µl nuclease free water (Sigma-Aldrich) and subjected

to DNase treatment (see section 2.9.2).

2.10.2. DNase treatment

Before cDNA synthesis, DNase treatment was performed in order to remove contaminating genomic DNA from RNA samples. Accordingly, 8μl RNA, extracted as described above, was placed in 0.2ml microfuge tubes and incubated with 1μl of DNaseI (1000U/ml) (Promega, USA) and 1μl DNase buffer (Promega) at 37°C for 30 min. In order to stop DNase treatment, 1μl of STOP buffer (Promega) was added and the tubes incubated for 15 min at 60°C. DNase inactivation is important, as the remaining active DNase might affect subsequent PCR reactions. The DNase-treated RNA was immediately used for cDNA synthesis (see section 2.9.3) or stored in -20°C until further use.

2.10.3. cDNA synthesis

In order to synthesize cDNA, a mix was prepared consisting of 5μl of DNase-treated RNA, 2μl of 100ng/μl random hexamers (ABgene, UK) and 5μl nuclease-free water (Sigma-Aldrich). This mix was incubated at 80°C for 3 min and subsequently chilled on ice for 1 min and the contents were collected by brief centrifugation. Next 4μl of 5x 1st strand buffer (Invitrogen), 2μl dithiothreitol (DDT) (0.1M) (Invitrogen) and 1μl of 10mM dNTP mix (Bioline, UK) were mixed together. In order to facilitate of the random hexamers annealing to RNA, the solution was incubated at 42°C for 2 min. Then 1μl of reverse transcriptase SuperScript III (200U/μl) (Invitrogen) was added to the mixture and the solution was incubated at 42°C for 50 min. In this time reverse transcriptase, which is a DNA polymerase, catalyzed the synthesis of a complementary DNA (cDNA) from the RNA template. Finally, the reverse transcriptase was inactivated at 65°C for 10 min, followed by short incubation on ice and collection of the contents

by brief centrifugation. The nucleic acid concentration was determined using NanoDrop™ 1000 spectrophotometer (Thermo Fisher Scientific Inc.) and diluted using nuclease-free water to a final concentration of 250ng/µl before the use.

2.10.4. Primers

Primers used in this study were purchased from Sigma-Aldrich. Details of primer sequences and product length are shown below (Table 2.3). The primers were designed to span different exons to minimize the risk of genomic DNA amplification. All primers were delivered in lyophilised form. Accordingly, they were reconstituted using nuclease-free water to reach the working concentration of 6.25pmol/µl. Products of all in house designed primers were sequenced by the Sequencing Service, University of Dundee, UK.

Table 2.3 Mouse primer sequences

Gene	Sequence	Product length (bp)	Annealing temperature (°C)/cycle number	Source
Wt1	F: CCAGTGTAAAACTTGTCAGCGA R: TGGGATGCTGGACTGTCT	234	60/33	Yamamoto et al. 2006
Pax2	F: AAGTTCAGCAGCCTTTCCAC R: GCCCTCAGACACATCTCTTA	274	62/33	In house
Six2	F: GCCTGCGAGCACCTCCACAAGAAT R: CACCGACTTGCCACTGCCATTGAG	522	67/33	Fogelgren et al. 2008
Gdnf	F: TGCCAGCCCAGAGAATTCCA R: AGCCTTCTACTCCGAGACAG	216	62/33	In house
Lim1	F: CAACATGCGTGTTATCCAGG R: CTTGCGGGAAGAAGTCGTAG	239	63/33	Yamamoto et al. 2006
Sall1	F: GCACATGGGAGGCCAGATCC R: GGAAGCGTCCGCTGACTTGG	181	62/33	In house
Osr1	F: GCAGCGACCCTCACAGAC R: GCCATTCACTGCCTGAAGGA	169	62/33	In house

Bf2	F: GGTGAAGCCGCCCTACTC R: AGGTTGTGACGGATGCTGTT	162	62/35	In house
Rarβ2	F: CTCTCAAAGCCTGCCTCAGT R: GTGGTAGCCCGATGACTTGT	182	62/35	Ulven et al. 2000
Bmp4	F: GCGCCGTCATTCCGGATTAC R: CATTGTGATGGACTAGTCTG	402	63/33	Luppen et al. 2008
Ret	F: GCGTCAGGGAGATGGTAAAG R: CATCAGGGAAACAGTTGCAG	217	62/33	In house
Gapdh	F: TGAAGCAGGCATCTGAGGG R: CGAAGGTGGAAGAGTGGGAG	102	56/33	In house

Table 2.4 Human primer sequences

Gene	**Sequence**	**Product length (bp)**	**Annealing temperature (°C)/cycle number**	**Source**
WT1	F: GGCATCTGAGACCAGTGAGAA R: GAGAGTCAGACTTGAAAGCAGT	483	62/33	In house
PAX2	F: CATCAAGCCGGGTGTGATC R: GATTCTGTTGATGGAAGAGACGC	184	62/33	In house
OSR1	F: GTTCCCTCATGTCATTCAACC R: CCCACAGGTTCTATTAGCA	542	62/33	In house
SALL1	F: GCTTTCACGACTAAAGGCAATCTT R: GAGCGCTGCTGCATACTGAT	216	62/33	In house
GAPDH	F: GTGGTCTCCTCTGACTTCAA R: TCTCTTCCTCTTGTGCTCTT	211	62/33	In house

2.10.5. Polymerase chain reaction

Polymerase chain reaction (PCR) was used to assess expression of different kidney-specific genes in MSCs. The reactions were prepared according to the following protocol. Each 25µl reaction mix contained 17µl nuclease-free water (Sigma-Aldrich), 2.5µl 10x NH_4 Reaction buffer

(Bioline), 0.5µl $MgCl_2$ (25mM) (Bioline), 0.5µl dNTP mix (10mM) (Bioline), 1µl forward primer (6.25pmol/µl) (Table 2.3), 1µl reverse primer (6.25pmol/µl) (Table 2.3), 2µl template (250ng/µl) and 0.5µl Taq DNA Polymerase (Bioline). *Glyceraldehyde 3-phosphatedehydrogenase* (Gapdh) was used as a reference gene throughout all experiments (Table 2.3). *Gapdh* is a housekeeping gene, which expression remains constant in the cells. Consequently it can be used to compare expression levels of other genes between different samples. In addition, a no-template control (a reaction mix prepared without cDNA) was included in each experiment, in order to detect potential contamination. The template prepared from E13.5 kidney rudiments was used as positive control. All mixes were prepared in 0.2ml tubes on ice and briefly spun down before being transferred to a GeneAmp PCR Systems 9700 thermal cycler (Applied Biosystems, USA). The conditions used to perform PCR reactions were set as described below. The exact number of cycles performed with given primers and their annealing temperatures are shown in Table 2.3. All PCR reactions started with the initial incubation for 5 min at 95°C, followed by 33-35 cycles (depending on primer pair used) with each cycle consisting of denaturation of cDNA template, followed by annealing of the primers and subsequent elongation of the complementary DNA strand. Accordingly, the samples were heated for 6 sec at 95°C for denaturation, then incubated for 30 sec at 56-67°C (depending on primer used) for annealing followed by 30 sec at 72°C for elongation. After the last cycle the samples were maintained for another 5 min at 72°C to ensure final elongation. PCR reactions were stored at 4°C before analysis.

2.10.6. Electrophoresis

In order to analyse PCR results, electrophoresis using agarose gels was performed. Accordingly, for each gel 120ml of 2% (w/v) agarose solution (Bioline) in 1x TAE buffer (see section 2.11.2)

was prepared. The solution was then heated to dissolve agarose and following cooling; 2µl ethidium bromide solution (10mg/ml) (Sigma-Aldrich) was added to the solution and poured into a tray with inserted comb. Any bubbles that were created during pouring the gel were pushed to the side using a disposable pipette tip. The agarose gel was left to set for at least 30 min and subsequently transferred to a tank filled with 1x TAE. 10µl of each PCR sample was mixed with 2µl of 6X loading dye (see section 2.11.2) before loading onto the gel. Accordingly the electrophoresis was set for 30 min and 140V. Hyperladder IV (Bioline) was used as a DNA molecular weight marker. The gels were analyzed using Chemi Imager 4400 UV transilluminator (Alpha Innotech Corporation, USA).

2.10.7. Real-time polymerase chain reaction

Real-time (quantitative) PCR using SYBR green was performed in order to quantify differences in expression levels of *Gdnf* and *Bmp4* between unstimulated and NKC CM- stimulated D1 cells. In order to prepare 20 µl of reaction mix, 10 µl of SYBR Green JumpStart Taq Ready Mix (Sigma-Aldrich), 1µl forward primer (6.25pmol/µl) (Table 2.3), 1µl reverse primer (6.25pmol/µl) and 1µl of template and 7µl nuclease-free water (Sigma-Aldrich) were combined. However, in order to prevent differences in amount of cDNA added, a general master mix was prepared which was then used to prepare all PCR reactions. Each time 11µl of mix containing the Jump Start Taq Read Mix and template was combined with a mix containing 9µl of specific primers mixed with water. In all experiments expression levels of *Gdnf* or *Bmp4* gene were compared to the expression levels of a reference gene, *Gapdh* (Table 2.3). In addition, a no-template control was included in each experiment to detect any contamination. For each PCR reaction duplicates of technical replicates were performed. All mixes were prepared in 0.2ml tubes on ice and briefly

spun down before transferred to a Rotor-Gene 3000 centrifugal real-time cycler (Corbett Research, Australia) with Rotor Gene Software (Version 6). The conditions used to perform quantitative PCR reactions were set as described below. First in order to activate the DNA polymerase an initial incubation for 10 min at 95^{o}C was performed, followed by 35 cycles consisting of 6 sec at 95^{o}C for denaturation, then 30 sec at 62^{o}C for annealing and finally 30 sec at 72^{o}C for elongation. SYBR Green fluorescence was measured at the end of the each 72^{o}C step. Initially, the amplicons were analysed using agarose gel electrophoresis (see section 2.9.6). However, additionally for each experiment a melting curve for each PCR reaction following the final cycle was generated, to assess the presence of non-specific products and primer dimers. The melting curve analysis was performed using the Rotor-Gene software. Accordingly the melting curve was generated between 72ºC and 95ºC with 1ºC rise per each step.

2.10.8. Efficiency of the real-time polymerase chain reaction

In order to quantify expression, efficiency of *Gapdh*, *Gdnf* and *Bmp4* primers in the PCR reactions had to be determined. Accordingly, real-time PCR reactions were performed using serial dilutions of the template from E13.5 kidney rudiment and each primer pair. Serial dilutions of the template in water were prepared as follows: undiluted template, 1/5, 1/25, 1/125, 1/625 and 1/3125. Triplicates of technical replicates were performed. The conditions for the real-time PCR were the same as above (see section 2.9.7). SYBR Green fluorescence was measured at the end of each elongation step. When a primer yields a 2-fold increase in the amount of PCR product in every cycle its efficiency is 2 thus the efficiency of the primers is 100%. In this study the determined efficiencies of the primers for *Gapdh*, *Gdnf* and *Bmp4* were 1.95, 1.7 and 1.9 respectively. The Rotor-Gene software was used for analysis.

2.10.9. Quantification of real-time polymerase chain reaction

Suitability of SYBR green for quantitative PCR was demonstrated before (Simpson et al. 2000). During the exponential phase of the real time PCR reaction, the increase in fluorescence emitted from SYBR Green bound to double-stranded DNA is also exponential. The cycle threshold (Ct) value indicates the start of the exponential phase and depends on the number of copies of target sequence initially present in the PCR mix. If a particular cDNA is highly abundant then the Ct value will be low as the exponential phase is reached sooner than for a less abundant template. The Rotor-Gene software was used to determine Ct values in all experiments. Subsequently Pfaffl method (Pfaffl 2001) was used to quantify relative expression levels between unstimulated and NKC CM stimulated-D1 cells. In this method a relative expression ratio is established based on PCR efficiency (*E*) and the crossing point (CP) at which the fluorescence was detected to raise above the background fluorescence, i.e., the Ct value (Pfaffl 2001). The Pfaffl's equation is shown below.

$$\mathbf{ratio} = \frac{(E_{\mathbf{target}})^{\Delta \mathbf{Ct}_{\mathbf{target}}\,\mathbf{(control\text{-}sample)}}}{(E_{\mathbf{ref}})^{\Delta \mathbf{Ct}_{\mathbf{ref}}\,\mathbf{(control\text{-}sample)}}}$$

As demonstrated in the equation, the relative expression ratio of a target gene is normalised with the expression of an endogenous reference gene transcript. The E_{target} is the real-time PCR efficiency of target gene transcript whereas the E_{ref} is the real-time PCR efficiency of a reference gene transcript. The ΔCt_{target} is the Ct difference of control – sample of the target gene transcript and the ΔCt_{ref} is the Ct difference of control – sample of reference gene transcript. In the current study the ratio was calculated based on the *E* and the Ct difference of the target genes *Gdnf* or *Bmp4* in unstimulated D1 cells versus NKC CM stimulated D1 cells and the *E* and the CP

difference of *Gapdh* of the unstimulated D1 cells versus NKC CM stimulated cells.

2.11. Statistical analysis

Statistical analysis was performed using Student's *t*-test. Differences between samples were expressed as mean of standard error. $P<0.05$ was considered as significant.

2.12. Culture media and buffers

2.12.1. Culture media

Standard culture medium

- High glucose Dulbecco's Modified Eagle Medium (DMEM) (Sigma-Aldrich)
- 10% (v/v) foetal calf serum (FCS) (PAA Laboratory)
- 2mM L-glutamine (Invitrogen)
- 1% (v/v) penicillin/streptomycin (Sigma-Aldrich)

MEF culture medium

- High glucose DMEM (Sigma-Aldrich)
- 10% (v/v) FCS (PAA Laboratory)
- 2mM L-glutamine (Invitrogen)
- 1% (v/v) penicillin/streptomycin (Sigma-Aldrich)

- 1% (v/v) non-essential amino acids (Sigma-Aldrich)
- 0.01% (v/v) 50mM 2-mercaptoethanol (Invitrogen)

ESC culture medium

- High glucose DMEM (Sigma-Aldrich)
- 10% (v/v) FCS (PAA Laboratory)
- 2mM L-glutamine (Invitrogen)
- 1% (v/v) penicillin/streptomycin (Sigma-Aldrich)
- 0.15% (v/v) 100mM monothioglycerol (Sigma-Aldrich)
- 1000U/ml leukaemia inhibitory factor (LIF) (Chemicon)

Adipogenic inductive medium

- High glucose DMEM (Sigma-Aldrich)
- 10% (v/v) FCS (PAA Laboratory)
- 2mM L-glutamine (Invitrogen)
- 1% (v/v) penicillin/streptomycin (Sigma-Aldrich)
- 1nM dexamethasone (Sigma-Aldrich)
- 5µg/ml insulin (Sigma-Aldrich)

- 0.5μM 3-isobutyl-1-methylxanthine (IBMX) (Sigma-Aldrich)
- 50μM indomethacin (Sigma-Aldrich)

Osteogenic inductive medium

- High glucose DMEM (Sigma-Aldrich)
- 10% (v/v) FCS (PAA Laboratory)
- 2mM L-glutamine (Invitrogen)
- 1% (v/v) penicillin/streptomycin (Sigma-Aldrich)
- 20mM β-glycerol phosphate (Sigma-Aldrich)
- 0.5μM L-ascorbic acid sodium (Sigma-Aldrich)
- 1nM dexamethasone (Sigma-Aldrich)
- 50ng/ml thyroxine (Sigma-Aldrich)

Chondrogenic inductive medium

- High glucose DMEM (Sigma-Aldrich)
- 2mM L-glutamine (Invitrogen)
- 1% (v/v) penicillin/streptomycin (Sigma-Aldrich)
- 500 ng/ml bone morphogenetic protein 6 (R and D)

- 10 ng/ml transforming growth factor β-3 (R and D)
- 0.1nM dexamethasone (Sigma-Aldrich)
- 50µg/ml L-ascorbic acid sodium (Sigma-Aldrich)
- 40µg/ml proline (Sigma-Aldrich)
- 1x ITS+3 liquid media supplements comprising: insulin, transferring, selenious acid, bovine serum albumin, linoleic acid and oleic acid (Sigma-Aldrich)
- 100µg/ml sodium pyruvate (Sigma-Aldrich)

2.12.2. Buffers and solutions

0.1% (w/v) gelatine solution

- 1g porcine gelatine type A (Sigma-Aldrich)
- 1L distilled H_20

The solution was autoclaved before use.

4% (w/v) paraformaldehyde

- 4g PFA (Sigma-Aldrich)
- 100ml PBS

The solution was heated to 60-70ºC and ultimately the pH was adjusted to 7.4-7.6.

0.5% (w/v) Oil Red O solution

- 0.5g Oil Red O (Sigma-Aldrich)
- 100ml isopropanol (Sigma-Aldrich)

The solution was filtered using Whatman paper and diluted 3:2 in H_20 before use.

2% (w/v) Alizarin Red S solution

- 2g Alizarin Red S (Sigma-Aldrich)
- 100ml distilled H_2O

The solution was filtered using Whatman paper and the pH adjusted to 4.1-4.3 with 5% ammonium hydroxide.

15% (w/v) sucrose solution

- 15g sucrose (Sigma-Aldrich)
- 100ml PBS

The solution was autoclaved before use.

Subbing solution

- 2.5g porcine gelatine type I (Sigma-Aldrich)
- 500ml distilled H_2O
- 0.25g $CrKSO_4x12H_2O$ (Sigma-Aldrich)

1% (w/v) Alcian Blue solution

- 1g Alcian Blue (Sigma-Aldrich)
- 100ml 0.1N HCl pH 1 (Invitrogen)

The solution was filtered using Whatman paper before use.

Phosphate buffered saline

- 6mM Na_2HPO_4 (Sigma-Aldrich)
- 2mM KCl (Sigma-Aldrich)
- 0.137M NaCl (Sigma-Aldrich)

The pH was adjusted to 7.4.

TAE buffer (50x)

- 40mM Tris base (Sigma-Aldrich)
- 20mM glacial acetic acid (AnalarR)
- 0.5M EDTA (Sigma-Aldrich)
- up to 1L distilled H_20

The pH was adjusted to 8.0. Before use the buffer was diluted.

Gel loading buffer (6x)

- 3ml glycerol (Sigma-Aldrich)
- 25mg bromophenol blue (Sigma-Aldrich)
- 10ml distilled H_20

Chapter 3: Differentiation potential of mesenchymal stem cells and their labelling methods

3.1. Introduction

The aim of the study is to investigate the potential of MSC to contribute to kidney development in an *in vitro* model of nephrogenesis. Accordingly, the capacity of MSCs to become integrated into developing renal structures and their subsequent differentiation into specific kidney phenotypes will be tested. The objective of the first part of the chapter is therefore to demonstrate multilineage differentiation potential of MSCs employed in this study by performing adipogenic, osteogenic and chondrogenic differentiation assays. The ability of MSCs to undergo *in vitro* adipogenesis, osteogenesis and chondrogenesis upon stimulation with appropriate inductive medium is widely used for identification and characterisation of MSC populations (Pittenger et al. 1999; Peister et al. 2004). Nevertheless, different MSC populations might differ substantially in their differentiation potential (Peister et al. 2004; Anjos-Afonso and Bonnet 2007). It has been described that MSCs isolated from various mouse strains have different abilities to differentiate (Phinney et al. 1999; Peister et al. 2004). It was demonstrated that bone marrow-derived MSCs isolated from Bl/6 mice more readily undergo osteogenic differentiation than from BALB/c mice which in turn have higher adipogenic potential. MSCs isolated from Bl/6 and BALB/c have also lower chondrogenic potential in comparison with MSCs derived from FVB/N and DBA1 mice (Peister et al. 2004). In addition, over time the number of broad flattened and slowly growing cells increases over rapidly expanding spindle-shaped cells in the MSC culture (Digirolamo et al. 1999). It has been shown that different morphologies relate to dissimilar differentiation potential of the cells. Cultures harbouring thin spindle-shaped MSCs differentiate more readily towards

adipocytes, whereas cultures composed of wider spindle-shaped cells have greater chondrogenic potential (Sekiya et al. 2002). Even cells derived from the same MSC colony can vary in their differentiation potential (Digirolamo et al. 1999; Pittenger et al. 1999). Moreover the differentiation capability and expansion potential of the cells decreases with increasing passage number (Digirolamo et al. 1999). Finally, the proliferation and differentiation abilities of bone marrow-derived MSCs depend also on the age of the donor and tend to decline with increasing age of donor (Kretlow et al. 2008). Infrequently, MSCs have been described to spontaneously differentiate. For instance, osteogenic differentiation was observed in high passage human MSC cultures in the absence of inductive medium (Digirolamo et al. 1999). In current study a clonal multipotent stromal stem cell line called D1 and human primary MSCs were employed. D1 were demonstrated previously to undergo adipogenic, osteogenic and chondrogenic differentiation (Diduch et al. 1993; Juffroy et al. 2009). Similarly human MSCs were demonstrated to have adipogenic, osteogenic and chondrogenic differentiation potential (Prockop 1997).

The second part of this chapter is aimed at establishing the most appropriate method for labelling of MSCs. This is important as the renogenic potential of the MSCs will be investigated by incorporating the cells into mouse kidney rudiments to generate kidney chimeras. It is therefore necessary to use a labelling method that will enable MSCs to be distinguished from the kidney cells. There exists a range of labelling methods available for imaging cells. When choosing appropriate fluorophores for staining, some important aspects such as brightness or resistance to photobleaching of the particular fluorophore need to be taken into consideration, as the properties among different fluorophores can vary significantly (Schroeder 2008). To date, MSCs have been successfully labelled with a number of transient labels, including fluorescent dyes such as the

green cell tracer carboxyfluorescein diacetate succinimidyl ester (CFDA SE) which reacts with intracellular amines (Togel et al. 2005), and the red fluorescent cell linker PKH26 that is incorporated into the cell membrane (Morigi et al. 2010), or nanoparticles such as quantum dots (QDs) (Rosen et al. 2007) and superparamagnetic iron oxide nanoparticles (SPIONs) (Jendelova et al. 2004). It has been also possible to introduce fluorescent proteins into MSCs by genetically modifying the cells to stably express fluorescent proteins, like the green fluorescent protein (GFP) (Fukui et al. 2009). Finally, staining using species-specific antibodies can be used for detecting human MSCs in some experimental settings (Azizi et al. 1998; Jeong et al. 2009). For this study, the following labelling methods for mouse MSCs will be investigated for their suitability; namely, transient labelling using CFDA SE or QDs, and permanent labelling using genetically encoded GFP. For human MSCs, the suitability of post-staining using a species specific antibody to a human nuclear antigen will be evaluated.

CFDA SE (carboxyfluorescein diacetate succinimidyl ester) is a non-fluorescent membrane-permeant dye, which in the intracellular environment, becomes fluorescent 5-(and-6)-carboxyfluorescein succinimidyl ester, due to removal of acetate groups by esterases. This molecule is not only less membrane permeant than the CFDA SE, but also reacts with intracellular amine groups, forming a range of fluorescent conjugates. CFDA SE can be used for tracking non-dividing cells over a long period of time; however, its intensity in proliferating cells is reduced after each cell division (Parish 1999). Nevertheless, several groups have successfully used CFDA SE for tracking MSCs (Togel et al. 2005; Kucerova et al. 2007; Fiorina et al. 2009).

QDs are fluorescent nanocrystals that are synthesised from semiconductor materials. They have proven to be ideal probes for sensitive fluorescent imaging. As QDs are highly photostable, they

are resistant to photobleaching, whereas the high fluorescence intensity of the nanoparticles enables sensitive detection. Furthermore QDs show broad absorption but narrow emission spectra, which facilitates simultaneous detection of multiple colours (Pinaud et al. 2006; Solanki et al. 2008). QDs have been used for imaging a variety of cell types, including HeLa cells (Jaiswal et al. 2003), cardiac myocytes (Koshman et al. 2008) and embryonic stem cells (Lin et al. 2007). Human MSCs labelled with commercially available QDs were shown to maintain their normal rate of proliferation, and their multilineage differentiation potential. Importantly, the stained cells were able to retain the label up to 8 weeks (Rosen et al. 2007). Further, Moioli *et al* showed that human MSCs labelled with bioconjugated QDs maintain multilineage differentiation potential. Additionally, no difference in viability and proliferation of the cells following the staining was noticed (Shah et al. 2007). Another study using commercially available QDs demonstrated high labelling efficiency with minimal cytotoxic effects on rat MSCs (Muller-Borer et al. 2007). Similarly as for CFDA SE, progressive loss of QDs from QD-labelled cells was demonstrated (Rosen et al. 2007; Pi et al. 2010).

In contrast to fluorescent dyes and nanoparticles, GFP labelling requires some genetic modification in order to achieve stable expression of fluorescent protein. As a consequence, no loss of signal due to cell division occurs (Schroeder 2008). It has been reported that hematopoietic stem cells have been successfully modified to express GFP without any noticeable effects on their characteristics, such as long-term multilineage potential (Tao et al. 2007). MSCs isolated from GFP transgenic animals have been shown to display the same features as cells isolated from non-transgenic animals (Raimondo et al. 2006; Ripoll and Bunnell 2009). Ripoll and Brunnell, who used MSCs isolated from enhanced GFP transgenic mice, showed that

expression of GFP in the cells did not alter their adipogenic and osteogenic potential. Similarly, the surface expression marker profile of GFP MSCs remained unchanged (Ripoll and Bunnell 2009). Apart from cells that can be directly isolated from GFP transgenic mice, MSCs can be transfected with GFP encoding plasmids to trigger GFP expression (Min et al. 2002; Song and Tuan 2004). Such cells have been subsequently used for *in vivo* tracking of MSCs in injured porcine myocardium (Min et al. 2002) or *in vitro* studies on transdifferentiation potential of MSCs (Song and Tuan 2004). Another method of introducing GFP into MSCs takes advantage of viral transduction: here, the cells are infected with a virus encoding GFP (Lu et al. 2005; Yang et al. 2009). For example, this method of labelling has been used for imaging MSCs in a spinal cord injury model (Lu et al. 2005). Finally, although GFP expression was not described to affect multilineage differentiation potential of MSCs, GFP presence was found to have some adverse effects on the kidney, as a GFP transgenic mouse strain was shown to display renal defects (Guo et al. 2007). An earlier study showed also that expression of enhanced GFP or GFP fusion proteins lead to suppression of NF-κB and JNK signalling pathways in the HEK2934-T cells, a human embryonic kidney cell line (Baens et al. 2006).

Finally, staining for human specific antigens can be used for detection of human primary MSCs. Previously such staining was performed to track human bone marrow–derived MSCs in rat brain (Azizi et al. 1998) and in rat degenerated tailbone disc (Jeong et al. 2009). In this way cells do not undergo modifications that could cause loss of differentiation potential, as the immunostaining is performed at the end of the assay. Also, no progressive loss of the label can occur during culture period. However, confirmation of the specificity of the antibody is crucial for effective detection.

The aim of this chapter is to confirm the multilineage potential of the MSC used in this study and to determine the most appropriate labelling method for further experiments. In order to study the potential of MSC to differentiate into kidney-specific cell types in the kidney chimeras, first the multipotency of MSCs will be confirmed to ensure that employed cells have the potential to differentiate. Accordingly, the adipogenic, osteogenic and chondrogenic capacity of MSCs will be assessed using standard differentiation protocols. In order to examine the contribution of MSCs to developing kidney structures, MSCs will require labelling to discriminate them from kidney cells. Several labelling methods can be used for labelling of MSCs, as described above. To elucidate the most appropriate labelling method for MSCs, labelling with CFDA SE, QDs, GFP and staining with species-specific antibody will be performed.

3.2. Results

In this chapter, the adipogenic, osteogenic and chondrogenic differentiation potential of MSCs used throughout this study is investigated, in order to ensure that the cells display typical MSC multipotency. Furthermore, different MSC labelling methods are evaluated to identify which methods are likely to be appropriate for identifying MSCs within the chimeric kidneys. Transient labelling using CFDA SE or QDs, permanent labelling using genetically encoded GFP and staining with species-specific antibody are compared.

3.2.1. The multilineage differentiation potential of the mouse D1 MSC line

In order to prevent problems caused by contamination with hematopoietic cells and the heterogeneity of mouse MSC cultures, a clonal multipotent stromal stem cell line called D1 has been employed in this study. This line was derived from the bone marrow of the BALB/c mice and displays common MSC features (Diduch et al. 1993). D1 have the typical spindle-shaped

morphology and demonstrate characteristic adipogenic, osteogenic and chondrogenic differentiation potential (Diduch et al. 1993; Juffroy et al. 2009). D1 cells have been used before in stem cell-based applications aimed at bone formation (Shen et al. 2002; Juffroy et al. 2009). The cells form uniform, adherent monolayer cultures with cells displaying characteristic spindle-shaped morphology, as demonstrated in Figure 3.1.

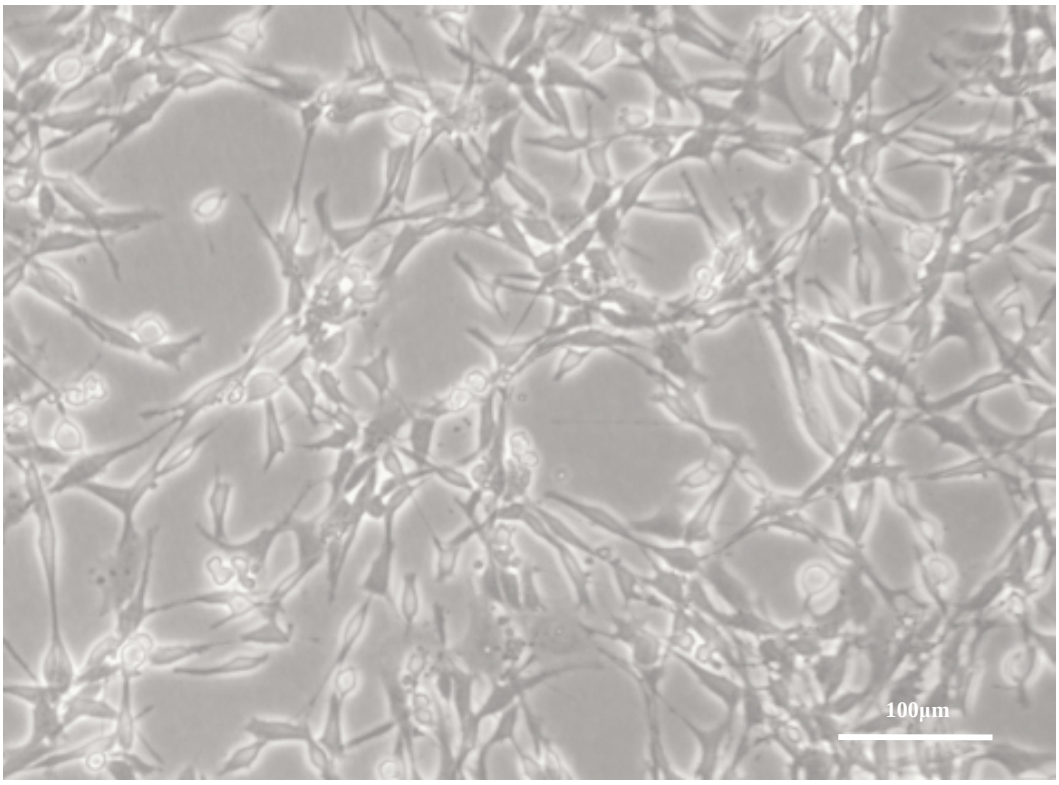

Figure 3.1 Morphology of D1 cells, a mouse bone marrow-derived MSC line.

To confirm the differentiation potential of the D1 cells used in this study, subconfluent D1 cultures were stimulated for two weeks with adipogenic and osteogenic inductive media, as described before by Peister et al (Peister et al. 2004). Unstimulated cultures were treated identically, except that they were plated in complete culture medium. After approximately 1 week of stimulation with adipogenic inductive media, lipid vacuoles become visible inside some of the

induced D1 cells, indicating the start of adipogenic differentiation. Subsequent staining with Oil Red on day 14 confirmed the presence of lipid vacuoles, as shown in Figure 3.2a. Meanwhile, the unstimulated D1 cells did not show any vacuole formation (Figure 3.2b).

As depicted in Figure 3.2c, the stimulation with osteogenic inductive medium for 14 days resulted in characteristic extracellular calcium deposits in the cultures visualized with Alizarin Red, confirming the osteogenic potential of D1 cells. No deposits were detected in cultures of unstimulated cells maintained in normal growth medium for 14 days (Figure 3.2d).

To achieve chondrogenic differentiation, MSCs were cultured as a micromass in the presence of chondrogenic inductive media, as described previously (Peister et al. 2004). In brief, D1 cells were spun down to form a pellet and subsequently cultured at the bottom of a 15ml tube in the presence or absence of inductive media for 14 days. An important feature of chondrogenic differentiation is the production of extracellular proteoglycans which can be detected with Alcian Blue solution (Karlsson et al. 2007). In order to detect chondrogenic differentiation Alcian Blue staining was performed on 10 µm frozen sections prepared from fixed micromass cultures. Proteoglycans, visualised by blue staining, were detected in the periphery of the pellet formed with the stimulated D1 cells, as shown in Figure 3.2e. No significant staining occurred in sections of control pellets cultured in the absence of inductive media (Figure 3.2f). In addition, it was found that the micromass culture induced with chondrogenic medium was noticeably larger than control. The difference in size can be observed with the representative micromass section (Figure 3.2e and f).

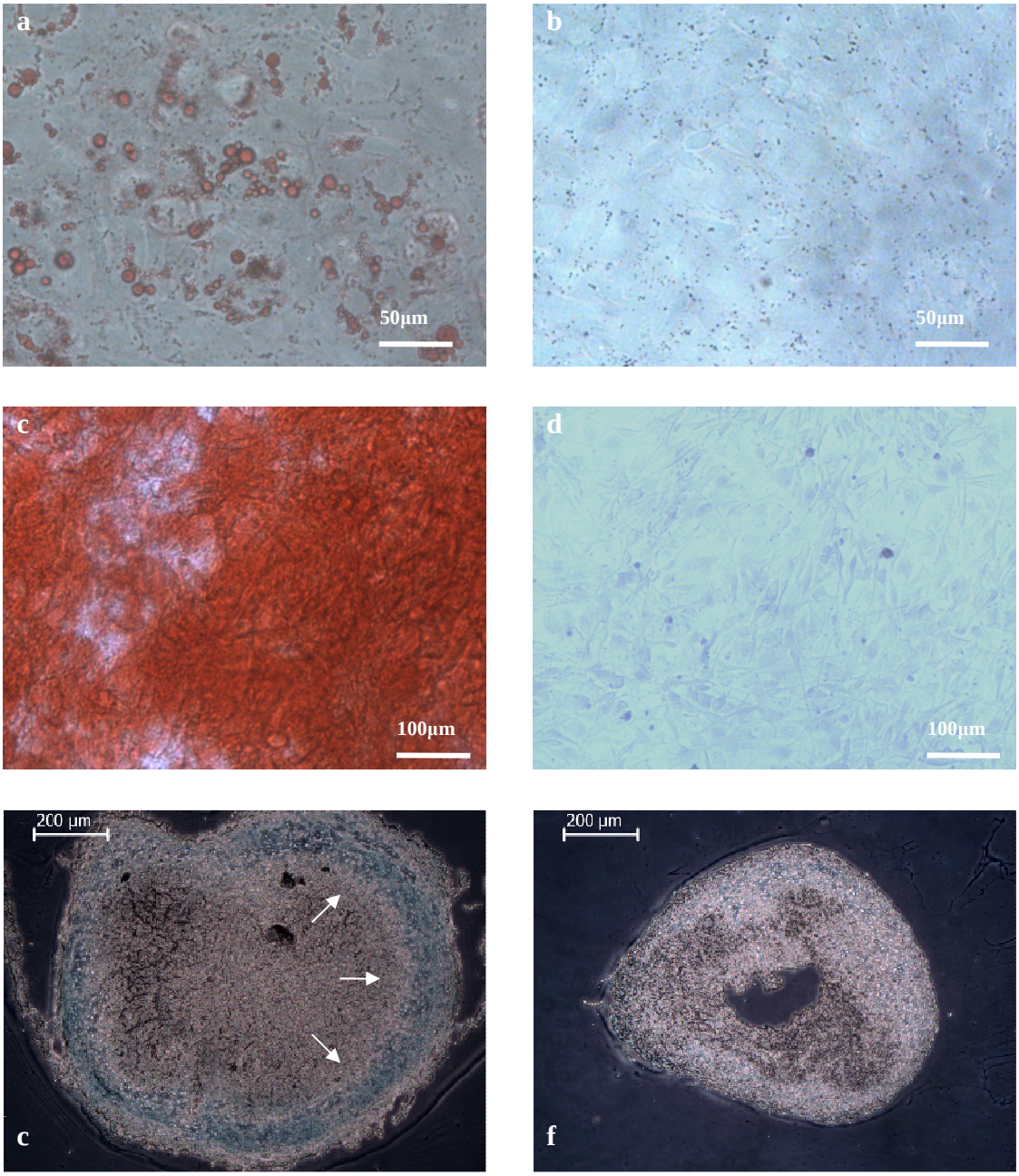

Figure 3.2 Confirmation of multilineage differentiation potential of D1 cells following stimulation with inductive media. (a) Following 14 days culture in adipogenic inductive medium, D1 cells displayed lipid vacuoles that stained positively with Oil Red. (b) Oil Red staining of control D1 culture (D1 cells cultured in standard culture medium) showed that no lipid vacuoles had formed. (c) Following 14 days culture in osteogenic inductive medium, Alizarin Red staining showed the presence of extracellular calcium deposits in D1 culture. (d) Alizarin Red staining of control D1 cells showed that no calcium deposits were present in the culture. (e) Following 14 days of micromass culture in chondrogenic inductive medium, Alcian Blue staining of frozen sections showed positive staining in the periphery of the pellet (arrows), indicating that cartilage proteoglycans were present. (f) Alcian Blue staining of control micromass sections showed no evidence of cartilage proteoglycans.

In summary, D1 cells demonstrated adipogenic, osteogenic and chondrogenic differentiation potential *in vitro*. The multipotency of D1 cells was therefore confirmed.

The multilineage differentiation potential of human MSCs

Bone marrow-derived human primary MSCs depleted of hematopoietic cells were purchased from Lonza. An important concern regarding primary human MSCs is the loss of multipotency of the cells following prolonged *in vitro* culture (Digirolamo et al. 1999). It has been shown that human MSCs can reach senescence after several passages (Baxter et al. 2004). In order to avoid problems associated with prolonged culture, in this study human MSCs were used only at low passage numbers. Human cells were cultured and subsequently differentiated towards adipogenic and osteogenic lineages according to instructions provided by the supplier. In standard culture conditions human MSCs displayed the same characteristic spindle shaped morphology despite being larger than the mouse MSC (Figure 3.3).

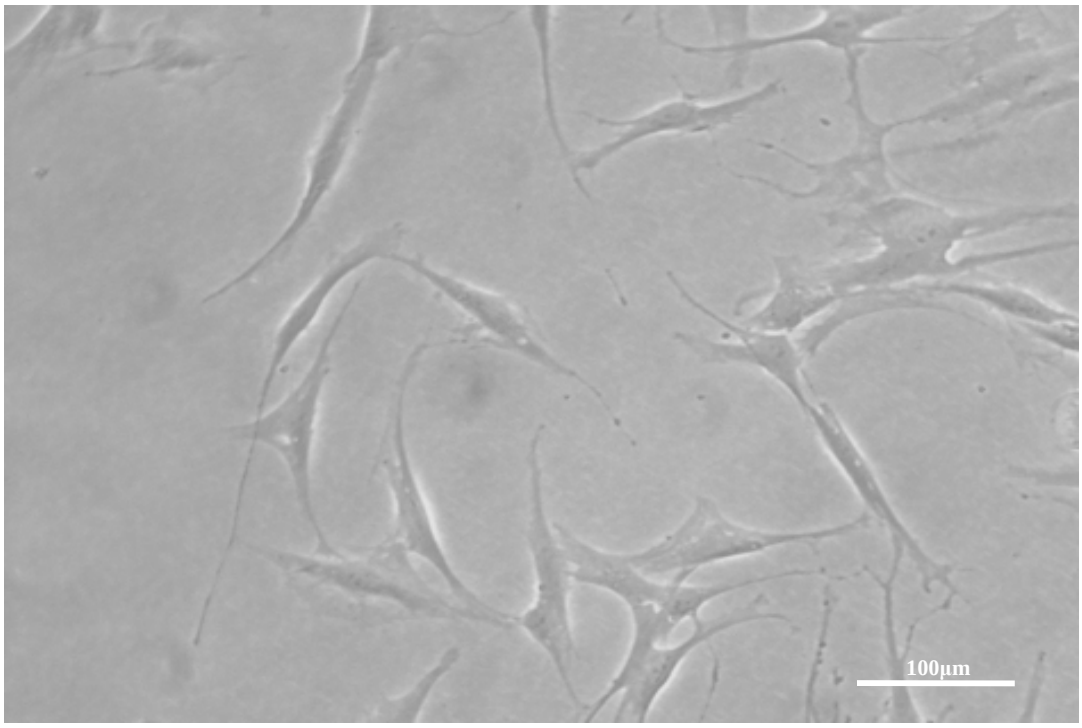

Figure 3.3 Morphology of human bone marrow-derived MSCs.

In order to confirm the adipogenic differentiation potential of these cells, confluent human MSCs (passage 4) were stimulated with adipogenic inductive medium for 3 days followed by stimulation with adipogenic maintenance medium for 1-3 days. Three cycles of stimulation with inductive and subsequently maintenance medium were performed. Finally, the cells were cultured one week in adipogenic maintenance medium. The cells not subjected to adipogenic induction were cultured in adipogenic maintenance medium for the same period of time. As shown in Figure 3.4a, following 20 days of culture, staining with Oil Red confirmed the presence of lipid vacuoles in the stimulated human MSCs. No vacuole formation occurred in controls that were cultured in maintenance medium only (Figure 3.4b).

To confirm the osteogenic potential of the human MSC, the cells were cultured for 14 days in osteogenic inductive medium, following which they were stained with Alizarin Red to detect the

presence of calcium deposits. Human MSCs cultured in the inductive medium demonstrated evidence of calcium deposits (Figure 3.4c), whereas no deposits were detected in controls that were cultured in normal growth medium for 14 days (Figure 3.4d).

Accordingly human MSCs were shown to display adipogenic and osteogenic differentiation capacity *in vitro*. No chondrogenic assay was performed for human MSCs. Herewith the differentiation potential of mouse and human MSCs was confirmed.

3.2.2. Identification of suitable labelling method for tracking of MSCs

As mentioned in the introduction, several labelling methods can be utilized for imaging MSCs. For the purpose of this study, the suitability of the following methods has been assessed for detecting MSC following their incorporation into mouse kidney rudiment chimeras: (i) labelling with the vital cell tracker, CFDA SE; (ii) QD labelling; (iii) lentiviral transduction with GFP, (iv) staining with a species-specific antibody which was used only in conjunction with human MSCs.

In the first instance, the suitability of two transient labelling methods was assessed, in order to avoid potential problems associated with genetic modification. To be effective, the labelling method would need to show high labelling efficiency and low cytotoxicity. Furthermore, as the concentration of non-genetically encoded fluorophores is reduced with each cell division (Schroeder 2008), it was important to find a labelling method that would enable detection after several days of culture. A comparison was made between two transient labelling methods, CFDA SE and QDs, in order to elucidate their suitability for long term tracking. D1 cells were labelled with 10 µM CFDA SE or 10 nM QDs according to manufacturer's instructions.

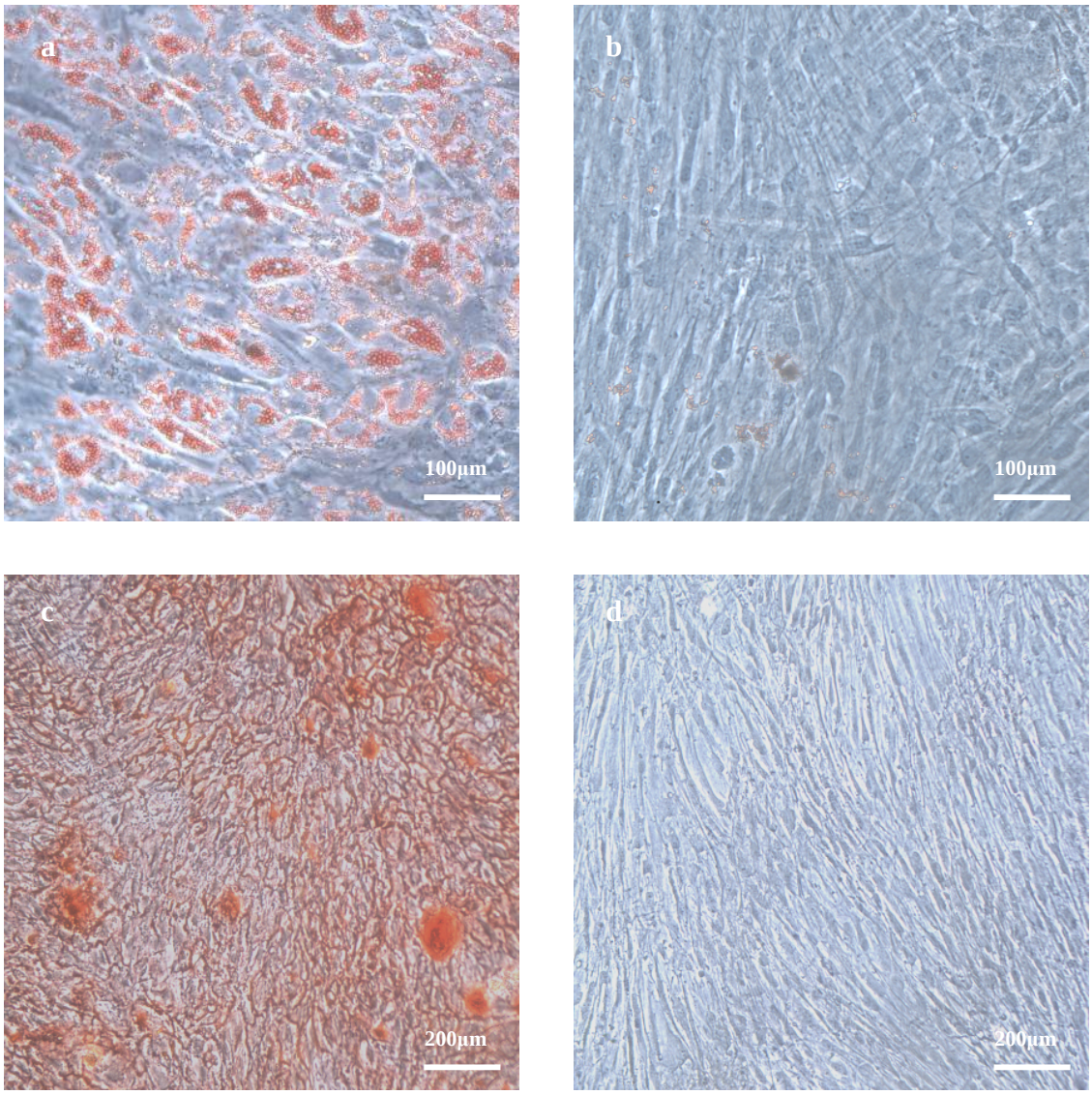

Figure 3.4 Confirmation of multilineage differentiation potential of human primary MSCs following stimulation with inductive media. (a) Stimulated with adipogenic inductive medium human MSCs after 3 cycles of adipogenic induction and subsequent week of culture in maintenance medium accumulated lipid vacuoles that stained positively with Oil Red. (b) Oil Red staining in the absence of stimulation: no lipid vacuoles were present in human MSCs cultured in maintenance medium only for the same period of time. (c) Alizarin Red staining indicated the presence of extracellular calcium deposits in human MSC cultures stimulated with osteogenic inductive medium after 14 days of culture. (d) Alizarin Red staining in control MSCs maintained in standard culture medium showed that no calcium deposits were present after 14 days of culture.

No visible difference in labelling efficiency was detected when the cells were analyzed directly after staining. All cells were stained following labelling with either CFDA SE (Figure 3.5a and b) or QDs (Figure 3.5e and f). Since CFDA SE interacts with intracellular molecules upon labelling, a diffuse cytoplasmic staining was observed (Figure 3.5a and b), whereas QDs showed a patchy pattern as nanoparticles tend to be unequally distributed in the cells (Figure 3.5e and f). After 5 days of standard culture no obvious cytotoxic effect was observed in any of the conditions. However, only the cells incubated with QDs remained labelled. As shown in Figure 3.5e-h QD staining remained intense, although in comparison to day 0 notably fewer cells were labelled with QDs. CFDA SE, on the other hand, was not detectable on the 5th day following labelling (Figure 3.5c and d).

Stable transduction or transfection with GFP is an efficient labelling method that should not lead to loss of signal over a period of time as the cells constitutively express the fluorescent protein that is used to detect them (Schroeder 2008). In this study, a lentivirus encoding enhanced GFP under control of the spleen focus-forming virus (SFFV) promoter has been used to induce expression of GFP in mouse MSCs. D1 cells were incubated for 24h with lentiviral particles carrying GFP (obtained from Sokratis Theocharatos, University of Liverpool). On the 3rd day following transduction, the cells were analyzed for GFP expression. No visible signs of cytotoxicity were observed. As shown in Figure 3.6a and b, although the levels of expression varied between cells, all D1 cells after 3 passages from initial labelling still expressed GFP, and maintained GFP expression at least for the next 20 passages.

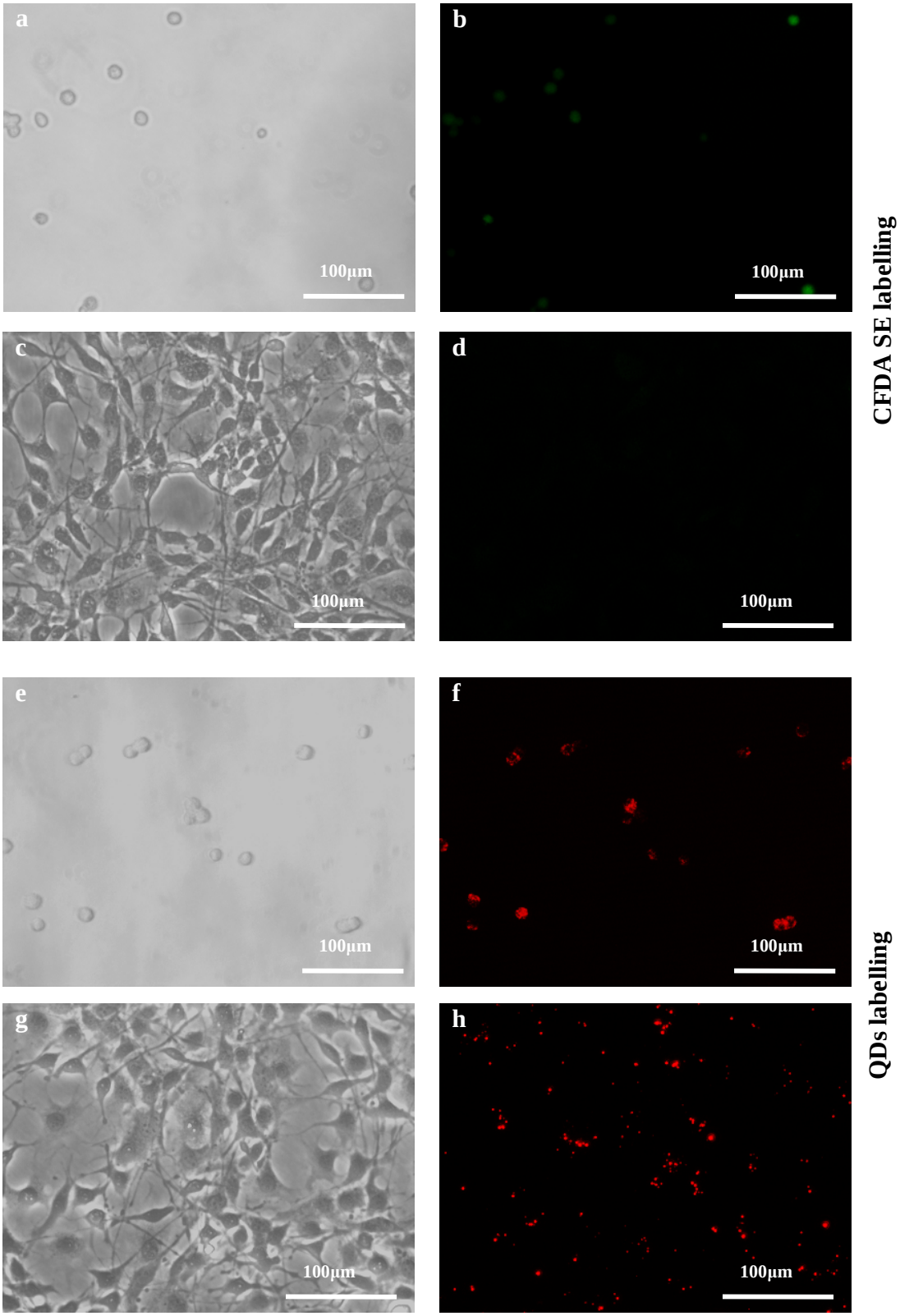

Figure 3.5 CFDA SE- and QD-labelling of D1 MSCs. (a-d) D1 cells stained with CFDA SE. (a) Bright field and (b) fluorescent image of the D1 cells stained with CFDA SE directly after labelling. (c) Bright field and (d) fluorescent image of the D1 cells stained with CFDA SE after 5 days. (e-h) D1 cells stained with QDs. (e) Bright field and (f) fluorescent image of the D1 cells stained with QDs directly after labelling. (g) Bright field and (h) fluorescent image of the D1 cells stained with QDs after 5 days.

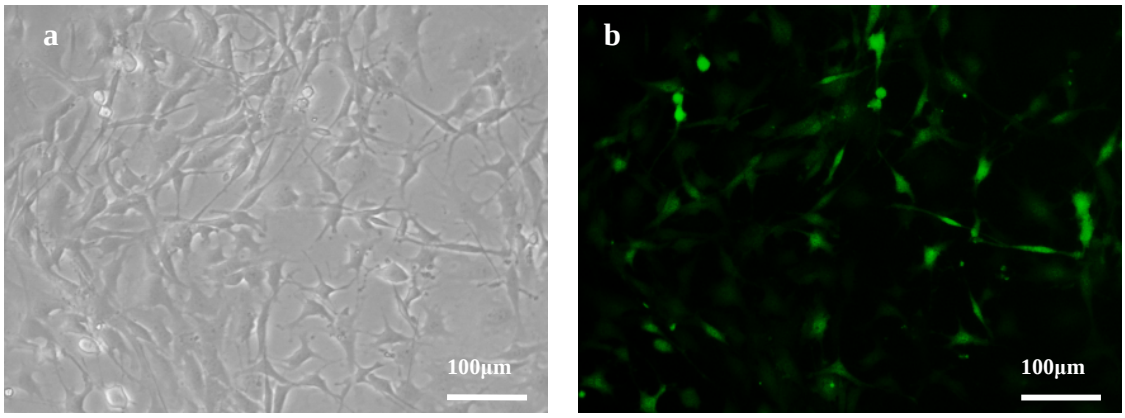

Figure 3.6 GFP labelling of D1 cells using lentiviral transduction. (a) Bright field and (b) fluorescent image of the D1 cells transduced with GFP.

Although it has been demonstrated that GFP MSCs are not affected by the enforced expression of fluorescent proteins and maintain adipogenic and osteogenic potential as well surface expression marker profile (Ripoll and Bunnell 2009), there are reports describing adverse effects associated with GFP expression (Baens et al. 2006; Guo et al. 2007). For this reason, the differentiation potential of transduced D1 cells was verified. GFP D1 cells were induced to undergo adipogenesis and osteogenesis in the presence of the appropriate inductive media, as described earlier in section 3.2.1. It was found that the GFP D1 cells were able to undergo both adipogenic (Figure 3.7a-d) and osteogenic (Figure 3.8e-f) differentiation, as visualized by Oil Red and Alizarin Red staining, respectively, whereas no staining was detected in uninduced cultures.

Above, three different labelling methods for tracking of D1 cells have been described. As the assessment of the renogenic potential of MSCs will require formation of kidney chimeras using mouse kidney cells, D1 cells, which are of mouse origin, could not be detected with a species-specific antibody. Nevertheless, a species-specific antibody can enable discrimination between human MSCs and mouse cells. To test the suitability of a human anti-nuclear antibody, human MSCs were immunostained using the human anti-nuclei antibody and co-stained with DAPI

(Figure 3.8a-c). No unspecific staining of human cells was detected when the primary antibody was omitted (Figure 3.8d-f). Further, the potential cross-reactivity of the antibody was tested on mouse cells. Using the protocol for formation of kidney chimeras described in the section 4.2.1 mouse embryonic kidneys were disaggregated and obtained kidney cells re-aggregated to form new kidneys in the absence of human MSCs. The re-aggregated mouse kidneys containing only mouse cells were stained subsequently with an antibody identifying expression of a nuclear kidney marker Wt1 and the antibody detecting human nuclei. Accordingly expression of Wt1 was observed; however, no expression of human nuclear antigen was found in the re-aggregated mouse kidney (Figure 3.9a-c). Some unspecific signal was detected in cytoplasm of the kidney cells.

In summary, several labelling methods were tested here for their suitability for imaging of MSCs, including labelling with CFDA SE, QDs, and GFP as well as staining with a species-specific antibody. For the purpose of this study labelling with QDs and viral transduction with GFP were identified as most suitable for tracking mouse MSCs. Furthermore the specificity of species-specific antibody for human MSC detection was assessed and subsequently proven to be suitable for human MSC tracking.

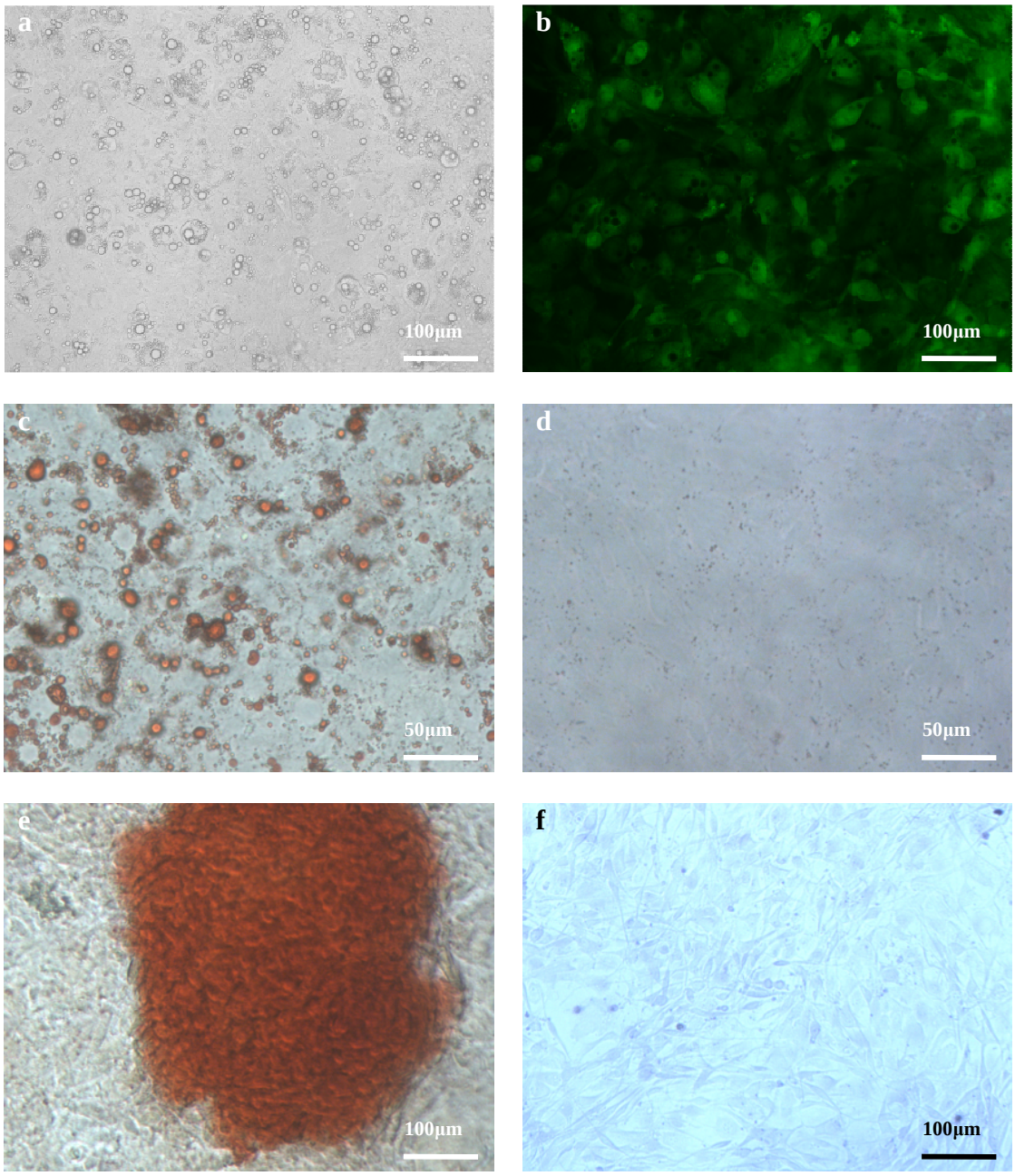

Figure 3.7 Confirmation of multilineage differentiation potential of GFP D1 cells (a) Stimulated with adipogenic inductive medium GFP D1 cells accumulate lipid vacuoles inside after 14 days of adipogenic induction. (b) GFP expression in induced towards adipocytes GFP D1 cells (in green). (c) Stimulated with adipogenic inductive medium GFP D1 cells display lipid vacuoles stained with Oil Red. (d) Oil Red staining of GFP D1 cells cultured in standard culture medium showed that no lipid vacuoles had formed. (e) Stimulated with osteogenic inductive medium GFP D1 cells show extracellular calcium deposits visualized using Alizarin Red staining after 14 days of osteogenic induction. (f) Alizarin Red staining of GFP D1 cells cultured in standard culture medium showed that no calcium deposits were present.

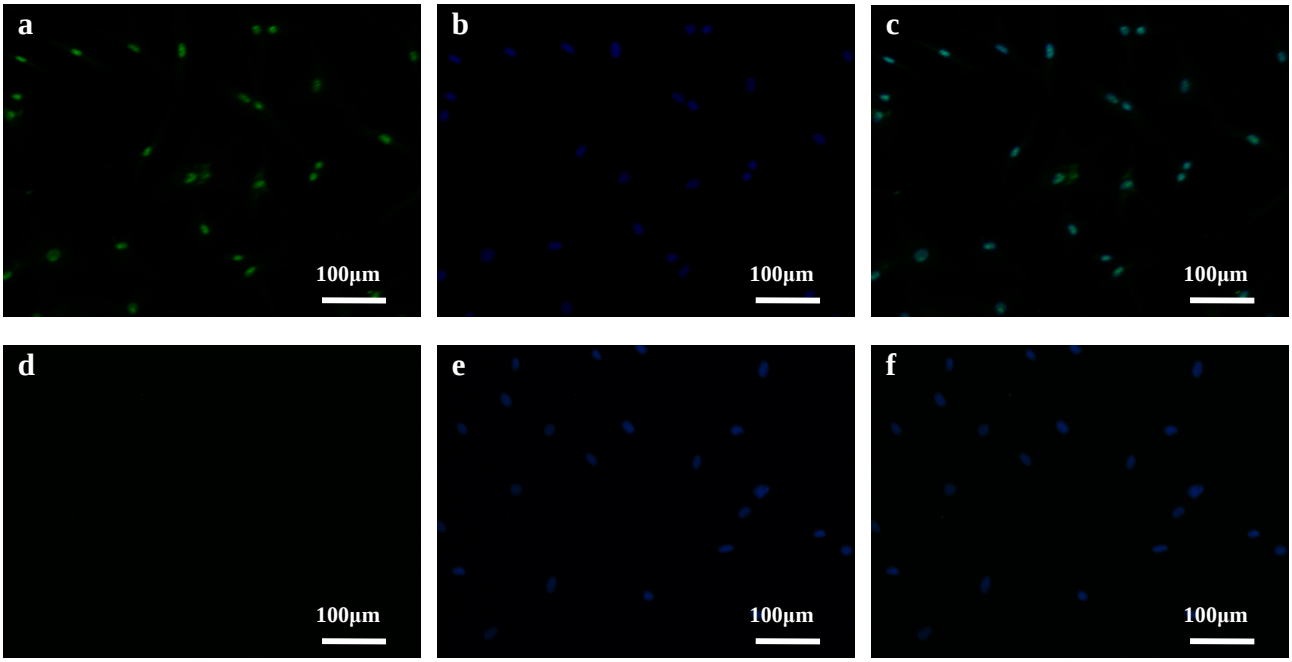

Figure 3.8 Staining of human MSCs using an anti-human nuclei antibody. (a) Human MSCs labelled with anti-human antibody. (b) Labelled human MSCs co-stained with DAPI. (c) Merged image of a and b indicates that all cells are labelled. (d) Human MSCs incubated only with appropriate secondary antibody; the anti-human antibody was omitted. (e) Human MSCs co-stained with DAPI (in blue). (f) Merged image of d and e.

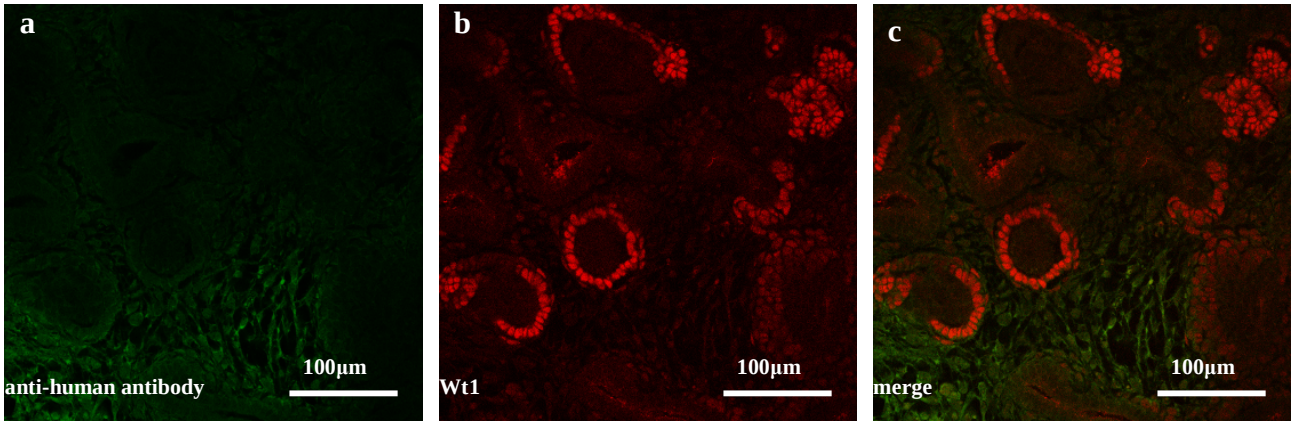

Figure 3.9 Assessment of specificity of anti-human nuclei antibody tested on mouse cells. (a) Staining using the antibody detecting human nuclei performed on the same re-aggregated kidney. (b) A re-aggregated mouse kidney stained with an antibody identifying expression of a nuclear kidney marker Wt1. (c) Merge.

3.3. Discussion

In this chapter the multipotency of the mouse and human MSCs that will be used in renogenic assays performed in subsequent chapters has been confirmed and different labelling methods for MSCs have been assessed. Both mouse and human MSCs showed considerable multilineage differentiation potential. Furthermore, QD staining and GFP transduction were proven to be suitable methods for mouse MSCs labelling, similarly as antibody staining for human MSCs.

3.3.1. The multilineage differentiation potential of MSCs

The multilineage differentiation potential of mouse D1 MSCs and primary human MSCs was confirmed in standard assays for adipogenesis, osteogenesis and chondrogenesis. Following induction with adipogenic medium, MSCs started accumulating lipid vacuoles, a feature of adipogenic differentiation, whereas stimulation with osteogenic medium resulted in the appearance of calcium deposits, which are characteristic for osteogenic differentiation. No spontaneous differentiation of unstimulated cells occurred, neither towards the adipogenic, nor osteogenic lineage. Moreover, the adipogenic and osteogenic potential of both mouse and human MSCs has been confirmed. In addition, both stimulated and unstimulated D1 cells formed stable pellets in chondrogenic culture condition. Alcian Blue staining confirmed the presence of proteoglycans in stimulated cells, indicating chondrocyte differentiation of mouse MSCs. Nevertheless only a small amount of proteoglycans was detected. D1 cells are derived from bone marrow of BALB/c mouse and MSCs isolated from this mouse strain have been described to produce little proteoglycans in response to chondrogenic culture conditions (Peister et al. 2004). No chondrogenic differentiation was attempted for human MSCs in this study; however it has been shown previously that human MSCs efficiently undergo chondrogenesis in micromass

culture. Accordingly human MSCs secrete proteoglycans and type II collagen and subsequently undergo hypertrophic differentiation, which is similar to the behaviour of chondrocytes *in vivo* (Mackay et al. 1998). Finally, another member of the laboratory, Laurence Glennon-Alty, demonstrated that human MSCs used in the current study are able to undergo chondrogenesis in the micromass culture condition (personal communication). In conclusion, MSCs employed in this study demonstrate genuine differentiation potential.

3.3.2. The labelling methods of MSCs

A number of labelling methods for MSCs was described in this chapter. Subsequently, D1 cells were labelled with CFDA SE, QDs and GFP, whereas human MSCs were stained with human specific antibody in order to elucidate the best labelling method for MSCs. All of the techniques have been employed previously in imaging of MSCs, as described in the introduction for this chapter.

According to results presented here, QDs have proven to be a more persistent labelling agent than CFDA SE, since CFDA SE could not be detected in D1 cells with fluorescent microscopy after 5 days of culture. CFDA SE loss of intensity, which led to exclusion of this labelling method from further experiments, has been demonstrated before in sheep MSCs after 8 days of culture (Weir et al. 2008). The loss of CFDA SE signal in D1 cells most likely occurred due to the high proliferation rate of the cells, as it was described that the intensity of this dye is reduced by half with every cell division (Lyons and Parish 1994).

In contrast, cells labelled with QDs remained stained after 5 days of culture. The localisation of QDs within D1 cells was perinuclear. QDs were shown previously to localise around the nucleus in MSCs (Muller-Borer et al. 2007; Rosen et al. 2007). According to Muller-Borer *et al* QDs

found in the perinuclear region represent aggregated nanoparticles in endosomal vesicles (Muller-Borer et al. 2007). Importantly, no loss of intensity of the QD-labelling occurred during the culture period. Nevertheless, fewer nanoparticles were detected inside the D1 cells after 5 days of *in vitro* culture than when observed directly after labelling. This is in agreement with Rosen *et al*, who showed progressive loss of QDs in human MSCs (Rosen et al. 2007). Loss of QD labelling was also reported in mouse embryonic stem cells (ESCs) (Lin et al. 2007; Pi et al. 2010) and mouse embryonic fibroblasts (MEFs) (Pi et al. 2010). In particular ESCs were demonstrated to rapidly lose the labelling within a few days of *in vitro* culture (Lin et al. 2007). MEFs are more likely to retain QD-labelling, since the decrease in the number of labelled cells over a period of time was smaller in MEFs than in ESCs (Pi et al. 2010). It was suggested that loss in QD-labelling in ESCs is not due to cell division, as treatment with mitomycin C which inhibited the proliferation of the cells did not prevent loss of labelling. Accordingly other mechanisms such as degradation and excretion of QDs were proposed. At the same time inhibition of proliferation did help to retain the labelling in MEFs; implying that proliferation rate of the cells may be linked to loss of QD-labelling and that there exist different mechanisms for QDs loss in different cells (Pi et al. 2010). In contrast, human MSCs were shown to retain the QDs for up to 44 days in culture (Rosen et al. 2007). As QD-labelled human MSCs were observed to divide only a few times during this period of time (Rosen et al. 2007), the retention of QDs in human MSCs might be also attributed to lower proliferation rate of the cells. D1 cells used in this study seemed to lose QDs more rapidly than described by Rosen *et al*. human MSCs. Although no direct comparison between QD-labelled D1 cells and human MSCs was attempted, it might be possible that D1 cells lose QDs more quickly due to a higher proliferation rate. D1 cells used in this study were robustly proliferating and therefore passaged regularly every 2-3 days in comparison to primary

human MSCs used also in this study which displayed a much lower proliferation rate and accordingly were sub-cultured approximately once a week.

An important issue regarding QDs is the potential transfer of nanoparticles from QD-loaded MSCs to other cells. It has been demonstrated that QDs can be transferred to other cells. Supernatants collected from the cultures of ESCs labelled with QDs were shown to contain QDs. Subsequently QDs derived from such supernatants were used to label MEFs in the presence of a labelling buffer (Pi et al. 2010). Nevertheless, Rosen *et al*. demonstrated that human MSCs labelled with QDs did not transfer QDs to unlabelled MSCs. Furthermore, no uptake of QDs by cardiac myocytes from mechanically disrupted QD-labelled human MSCs occurred (Rosen et al. 2007). Another study on QD-labelled rat MSCs showed that QDs are not transferred when co-cultured with cardiac myocytes (Muller-Borer et al. 2007). The transfer of QDs between the cells has not been addressed in this study.

There are a number of reports describing the use of GFP-labelled MSCs (Min et al. 2002; Lu et al. 2005; Fukui et al. 2009). Transduction with GFP have been shown to be an ideal method for long term tracking of bone marrow-derived stem cells, namely hematopoietic stem cells (HSCs) (Tao et al. 2007) and MSCs (Lu et al. 2005). In the current study the D1 cells were transduced with lentiviral particles carrying enhanced GFP to induce constitutive GFP expression in MSCs. GFP D1 cells maintained labelling over a long period of time following many passages. However, GFP expression might have some adverse effects on the cells (Baens et al. 2006; Guo et al. 2007). It has been shown that expression of enhanced GFP or GFP fusion proteins inhibits NF-κB and JNK signalling pathways in a human embryonic kidney cell line (Baens et al. 2006). Furthermore GFP transgenic mouse expressing the fluorescent protein under the control of β-

actin promoter were shown to display renal defects including increase in glomerular extracellular matrix, occasional mesangiolysis, and tubulointerstitial injury, which are accompanied by proteinuria. As it has been confirmed that the insertion of the transgene encoding GFP did not disrupt nor modify expression of adjacent genes, the authors suggested that high expression levels of GFP in the glomeruli might be responsible for the observed defects (Guo et al. 2007). In order to examine if stable GFP expression does not negatively affect D1 cells and hence alter their differentiation potential, GFP D1 cells were confirmed to undergo adipogenic and osteogenic degeneration in standard differentiation assays. The obtained results were in agreement with previous report showing that that expression of GFP in MSCs does not alter their adipogenic and osteogenic potential (Ripoll and Bunnell 2009). Nevertheless, it is difficult to speculate if GFP expression is going to influence D1 cells behaviour in the chimeric kidneys thus if GFP D1 cells will have similar differentiation potential towards kidney-specific phenotype as non-transduced cells.

Another concern regarding GFP labelling of D1 cells is that the GFP expression might be downregulated when the labelled cells start to differentiae into kidney-like cells making the detection of D1 cells impossible. None of the GFP transgenic mice was shown to ubiquitously express GFP in all its tissues. Accordingly transgenic mice expressing GFP under the control of a human ubiquitin C promoter showed absence of GFP signal in the renal tissue (Swenson et al. 2007). There is also a discrepancy in levels of GFP expression between different GFP transgenic mice in the same tissues. Different percentage of peripheral blood cells was detected to be positive for GFP in different transgenic mice (Swenson et al. 2007). It is therefore not clear if GFP D1 cells will not loss the expression when undergoing differentiation. In this study it was

demonstrated that GFP expression is maintained upon adipogenic differentiation of D1 cells, which implicates that GFP D1 cell, might continue the express GFP when differentiating into renal structures.

Finally, horizontal transfer of labels between cells via microvesicles should be taken in consideration. Microvesicles mediate intracellular communication by delivering proteins and mRNA between cells. Recently, it was demonstrated that microvesicles derived from human MSCs protect mice from tubular damage in glycerol-induced acute kidney injury (Bruno et al. 2009). However, at the same time it has been shown that cultured tubular cells can take up microvesicles labelled with PKH-26 dye and subsequently become labelled with PKH-26 (Bruno et al. 2009). Therefore, there also exists the possibility that GFP mRNA can be transferred to kidney cells resulting in inaccurate GFP labelling of other cells than MSCs.

In particular, for detection of human primary MSCs a staining for human antigen can be performed. It was demonstrated that human specific antibodies may be used for detection of human primary MSCs in fixed samples obtained from rats (Azizi et al. 1998; Jeong et al. 2009). Here the staining with human anti-nuclei antibody has been demonstrated as a suitable method for labelling human cells.

In conclusion, QDs have proven to be better labelling agent than CFDA SE, although some loss of QD-labelling did occur during the *in vitro* culture period. Nevertheless, D1 cells labelled with QDs retained sufficient nanoparticles to be used for imaging, allowing sensitive detection over a period of 5 days. Therefore QDs can be used to investigate the renogenic potential of D1 cells in short-time experiments. Genetic modification using lentiviral transduction of D1 cells provided a long-term labelling method which did not result in loss of signal due to proliferation of the

cells. However, since it was described that GFP expression in the kidneys of transgenic mice led to renal defect it is unknown if GFP expression in this setting might not also influence the course of MSC differentiation. For this reason two labelling methods, QDs and GFP, were chosen for tracking D1 cells in the chimeric kidneys. For human MSCs antibody staining against human nuclear antigen will be used to track the cells.

Chapter 4: Potential of MSCs to contribute to metanephric development using the novel chimeric kidney system

4.1. Introduction

In the previous chapter, the multilineage potential of MSCs employed in this study was confirmed. Further, different labelling methods were established for tracking the cells. In this chapter the potential of MSCs to contribute to metanephric development will be studied using an *ex vivo* model of mouse embryonic kidney development. As mentioned previously, direct injection of human MSCs into an *in vitro* developing kidney, widely used for other stem cell/progenitor populations, has proven to be insufficient to trigger MSC integration and subsequent differentiation towards nephron-like structures (Yokoo et al. 2005; Yokoo et al. 2006; Fukui et al. 2009). The sophisticated protocol developed by Yokoo *et al.* used to introduce MSCs into embryonic kidneys makes further investigation of their renogenic capacity difficult. The technique involves demanding experimental procedures such as injection of MSCs into intermediate mesoderm (IM) of an embryo, *ex utero* culture of the embryos with the transplanted cells, as well as altering the expression profile of the MSC by genetically modifying the cells so that they express GDNF (Yokoo et al. 2005; Yokoo et al. 2006; Fukui et al. 2009). Consequently no other reports have been published utilizing this particular methodology for differentiation of MSCs to kidney-specific cell types. Furthermore, therapeutic applications of engineered renal tissue comprising genetically modified MSCs would not be feasible in the near future due to the potential risks associated with viral insertion, such as the activation of proto-oncogenes (Mavilio and Ferrari 2008). Recently, Unbekandt and Davies described a new approach, which permits *ex vivo* generation of chimeric embryonic kidneys. This uncomplicated method is based on

disaggregation and subsequent re-aggregation of mouse metanephroi. Similar to an intact, whole embryonic kidney, the re-aggregated kidneys display normal morphology and marker expression characteristic of normal developing kidneys. The technique has been used to integrate kidney progenitor cells with down-regulated *Wt1* expression into a normal kidney rudiment in order to study nephron formation (Unbekandt and Davies 2010). Accordingly, this new methodology allows incorporation of cells from different origins into kidney rudiments and can be used to determine the contribution of MSCs to nephrogenesis in a controlled environment which mimics the metanephric development. As the protocol involves the disaggregation of the kidney rudiments, there are no problems with aggregation at the site of injection as observed previously by Yokoo *et al*. (Yokoo et al. 2005). In this chapter, the ability of MSCs to integrate into developing embryonic kidney structures will be evaluated using a modified chimeric kidney culture system based on the protocol of Unbekandt and Davies (Unbekandt and Davies 2010).

However, before performing the chimeric kidney culture, in order to establish if any kidney related genes might be already expressed by MSCs used in this study, the expression profile of a panel of key genes involved in kidney development will be compared to that of kidney rudiment cells. Expression of the following genes will be investigated: *Wt1, Six2, Pax2, Sall1, Lim1, Gdnf, Osr1, Bf2* and *Rarβ2*. A brief description of the metanephric kidney markers used in this study is given below (see also Chapter 1). Both *Wt1* and *Six2* are found in the mesenchyme that gives rise to nephrons. *Wt1* expression is associated with both condensing metanephric mesenchyme (MM) and developing nephrons but becomes restricted to the precursors of podocytes in the S-shaped bodies later on in development (Armstrong et al. 1993; Mundlos et al. 1993). Similarly, *Six2* is expressed in the nephron progenitor population within the cap mesenchyme (Kobayashi et al.

2008). *Pax2* shows a broader expression during metanephric development than *Wt1* and *Six2*, as it is expressed in the ureteric buds (UBs), condensing mesenchyme and developing nephrons (Dressler et al. 1990; Dressler and Douglass 1992). Other essential genes in metanephric development include *Sall1* and *Lim 1*. *Sall1* is expressed during all stages of nephron formation (Nishinakamura et al. 2001) whereas *Lim1* expression is found during nephron development and in UBs (Karavanov et al. 1998; Kobayashi et al. 2005). *Glial cell line-derived neurotrophic factor* (*Gdnf*) is a crucial gene expressed during early metanephric development, as it induces the initial outgrowth and subsequent branching of the UB. Accordingly, *Gdnf* is expressed by MM adjacent to UB (Vega et al. 1996; Sainio et al. 1997). Recently, *Osr1*-expression was associated with a precursor population in IM which gives rise to most cells found within the developing metanephros, including the collecting duct, nephrons and interstitial mesenchyme, mesangial and smooth muscle cells (Mugford et al. 2008). Finally, *Bf2* (*Foxd1*) is expressed in stromal cells during metanephric kidney development (Hatini et al. 1996). Similarly, *retinoid acid receptor β 2* (*Rarβ2*) is expressed in kidney stromal cells (Mendelsohn et al. 1999).

Ultimately, in order to examine the capacity of MSCs to become integrated into different renal structures in the chimeric kidneys, expression of Wt1 and Six2 as well as laminin and calbindin will be studied in the chimeras. Wt1 (Armstrong et al. 1993) and Six2 (Kobayashi et al. 2008) will be used as markers for nephrogenic MM. Subsequently, calbindin staining will be performed in order to discriminate UBs. Calbindin was demonstrated to be expressed in the developing collecting duct and in the most distal part of the renal tubules of emerging nephrons (Davies 1994). Finally, laminin staining will be used to visualize both UBs and developing nephron-like structures in the chimeras. Laminin is detected in UBs and along the borders of comma-shaped

and S-shaped bodies (Ekblom 1981).

Other cell types, namely a mouse embryonic stem cells (ESCs) line and mouse kidney progenitor cell line will be also tested using the chimeric kidney assay. Previously, ESCs and ESCs-derivatives were detected in the tubular compartment of metanephric kidneys following injection into a kidney rudiment (Kim and Dressler 2005; Steenhard et al. 2005; Vigneau et al. 2007). Subsequently, kidney-derived progenitors have been demonstrated to harbour the potential to contribute to different compartments of the developing kidney, and were shown to give rise to both nephrons and the collecting system after injection into metanephroi (Challen et al. 2006; Maeshima et al. 2006; Ward et al. 2011). Accordingly, the kidney progenitors that will be employed in this study are a population of mouse neonatal kidney cells (NKCs) derived by at the University of Liverpool by Cristina Fuente Mora (Mora 2009). The NKC population used here expresses *Wt1* and *Gdnf*, but not *Pax2*, and displays some heterogeneity in morphology suggestive of differentiation towards different renal-specific cell types. NKCs were also demonstrated to express a range of renal markers such as *synaptopodin* characteristic for podocytes, *desmin* found in mesangial cells, *megalin* and *zona occludens-1* expressed in tubular cells (Mora 2009).

The aim of the chapter is to assess renogenic potential of MSCs using a model of mouse embryonic kidney development. Ultimately the renogenic potential between MSCs, ESCs and NKCs will be compared using the same chimeric kidney assay and the results obtained here will be compared with existing evidence.

4.2. Results

In this chapter the capacity of mouse and human MSCs to contribute to nephrogenesis was evaluated using the novel chimeric kidney culture system (Unbekandt and Davies 2010). Initially, prior to integration into the kidney rudiments, the expression profile of MSCs in regard to genes expressed during early kidney development was determined. The ability of the MSC to integrate into developing renal structures and differentiate into kidney-specific cell types was then tested by performing a chimeric kidney culture assay based on the protocol of Unbekandt and Davies (Unbekandt and Davies 2010). Subsequently, using the same assay, the renogenic potential of the MSCs was compared with other stem cell types.

4.2.1. Chimeric kidney culture

The first aim of this chapter was to confirm that the *in vitro* development of re-aggregated E11.5 mouse kidney rudiments resembled that of intact rudiments. It is important because the purpose of this study is to assess the contribution of MSCs to nephrogenesis in an environment that closely mimics to the metanephric development. The re-aggregated kidneys were previously shown to display marker expression characteristic of normal developing kidneys, such as Wt1 (Unbekandt and Davies 2010). Here the expression of Wt1, Six2, calbindin and laminin is investigated in intact and re-aggregated embryonic kidneys.

Early stage mouse kidney rudiments can be obtained at embryonic day (E) 10.5 when the UB has just invaded the MM and no branching has occurred or at E11.5 when the UB has branched once. The rudiments are located close to the hind limb bud and can be distinguished by an opaque region of MM and the presence of the UB outgrowing from the Wolffian duct (Davies 2010). Figure 4.1a shows the localization of the metanephric kidney within a caudal part of an E11.5

embryo, and Figure 4.1b shows the morphology of the rudiments following dissection from the embryo.

E11.5 metanephroi were dissected and following 4 days of *in vitro* culture stained for several markers of early nephrogenesis. As demonstrated in Figure 4.2a and g, Wt1 expression was detected using two different antibodies. Its expression was present in condensing MM and forming nephrons with the highest levels of Wt1 expression in nascent podocytes. Further, Six2 was detected in condensing MM (Figure 4.2b). As shown in Figure 4.2d calbindin expression was found exclusively in UBs. Finally, laminin staining was evident in the basement membrane of the UBs and developing nephrons of the cultured metanephroi (Figure 4.2e). The undifferentiated MM or stroma did express neither laminin nor Wt1, Six2, calbindin. As demonstrated in Figure 4.2c, f and h appropriate negative controls, in which primary antibody was omitted, showed only weak background staining.

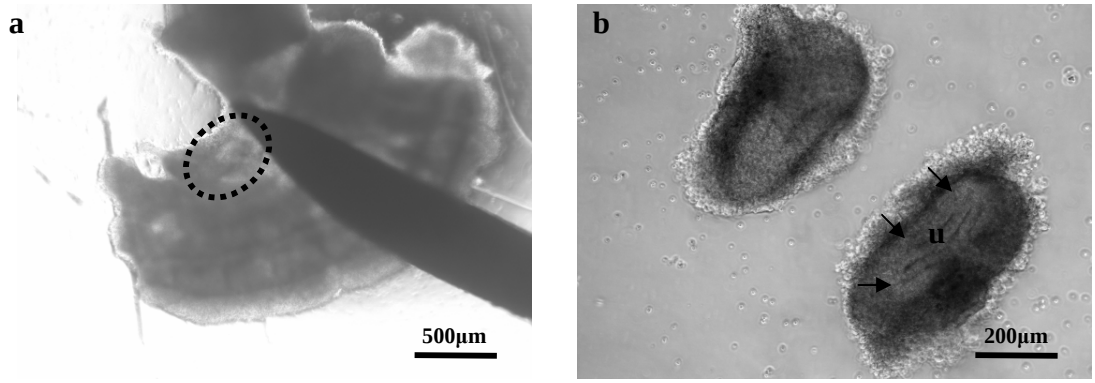

Figure 4.1 Morphology of mouse E11.5 kidney rudiment (bright field images). (a) Localization of mouse E11.5 metanephric kidney within the embryo (dashed line). Only the caudal part of an embryo is being shown. (b) Mouse E11.5 kidney rudiments after dissection consisting of T-shaped UB (u) and its surrounding MM (arrows).

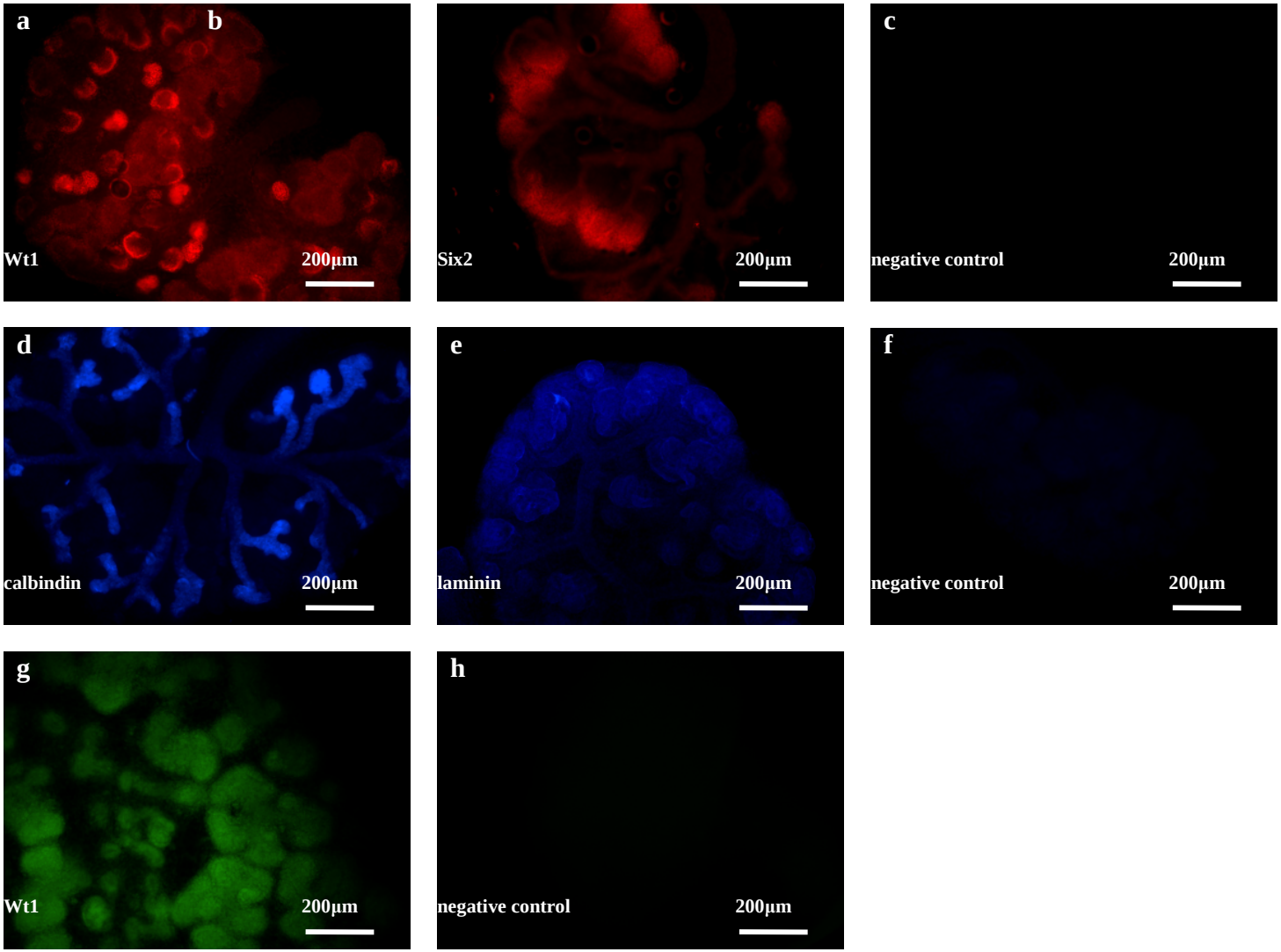

Figure 4.2 Expression of several markers of early nephrogenesis found in intact mouse metanephroi following 4 days of *in vitro* culture. Embryonic kidneys subsequent stained after for Wt1 (a and g), Six2 (b), calbindin (d) and laminin (e). Corresponding negative controls where the primary antibody was omitted are demonstrated: (c) Wt1 (in red), (h) Wt1 (in green), (c) Six2, (f) calbindin and (f) laminin.

Unbekandt and Davies developed a method which enables kidney chimeras to be re-formed from a suspension of individual kidney rudiment cells. In this method, following dissection, E11.5 kidneys are disaggregated and the resultant single cell suspension of kidney rudiment cells is pelletted to promote re-aggregation. The re-aggregated kidney is then cultured under the same conditions as an intact E11.5 kidney rudiment (Unbekandt and Davies 2010). Figure 4.3a-f shows such re-aggregated kidney after 4 days of *in vitro* culture. As demonstrated, the re-aggregated metanephros displays normal kidney development. Wt1 staining is detected in condensing MM as well as in forming nephrons whereas the laminin was found in the basement membranes surrounding emerging nephrons and UBs (Figure 4.3a-c). Subsequently, Six2 staining is detected in condensing MM, whereas calbindin staining is found in UBs (Figure 4.3d-f). No Wt1, laminin, Six2 or calbindin staining was detected in the stroma surrounding condensing MM and UBs (Figure 4.3a-f).

The presence of condensing MM around UB tips and early nephron formation demonstrates that kidney development was not disrupted by the disaggregation and re-aggregation protocol. This is also in accordance with data presented by Unbekandt and Davies (Unbekandt and Davies 2010). The re-aggregated embryonic kidney can act as a model for studying nephrogenesis *in vitro* and this model may be used to assess the renogenic potential of stem cells, similarly as the intact kidney.

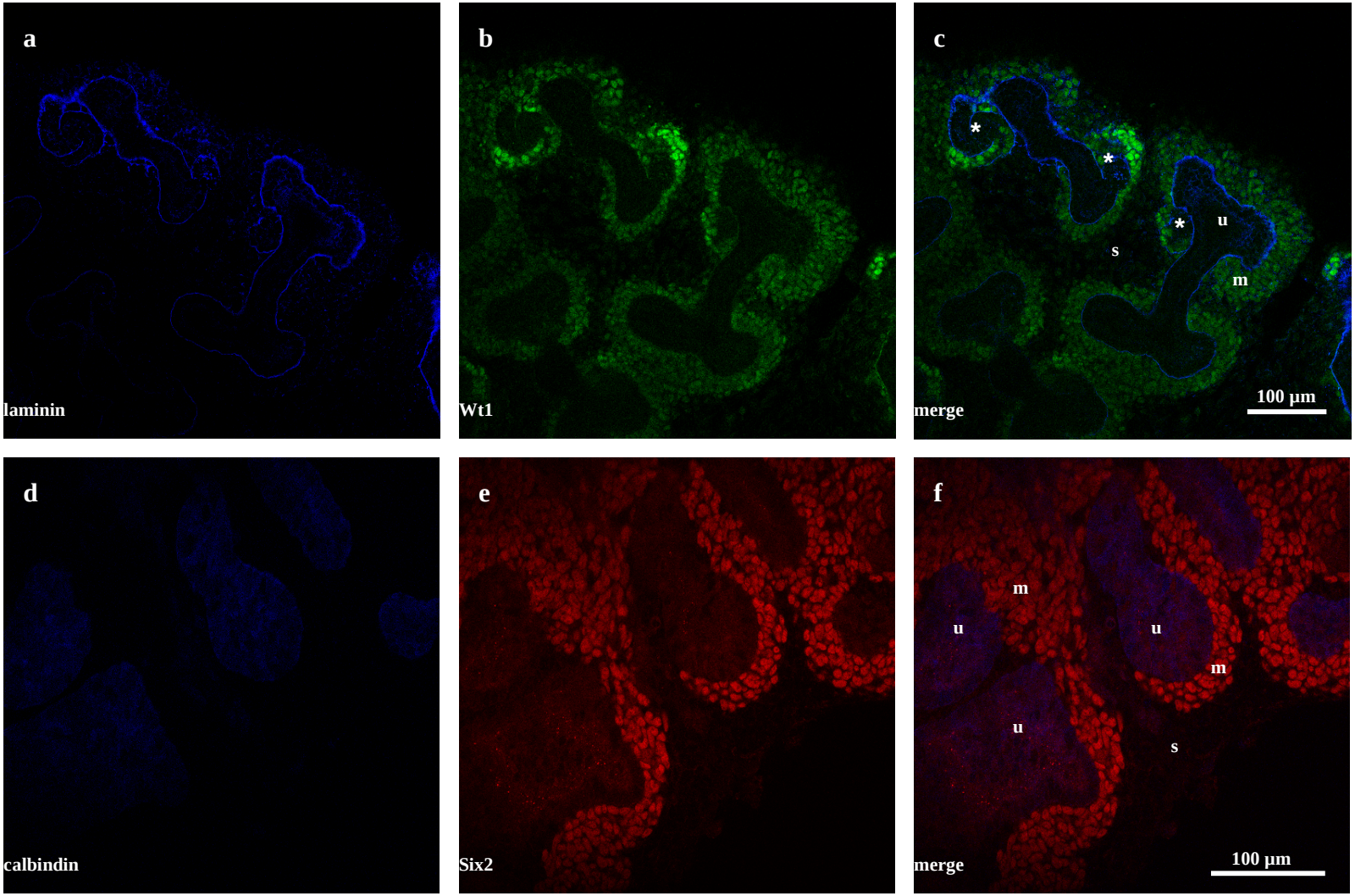

Figure 4.3 A re-aggregated mouse embryonic kidney cultured *in vitro* for 4 days. The re-aggregated kidney rudiment shows characteristic features of embryonic development during the *in vitro* culture period: branching UBs (u), condensing MM (m) and developing nephrons (*) surrounded by stromal cells (s). (a-c) Wt1 and laminin staining of a re-aggregated kidney rudiment, (d-f) Six2 and calbindin staining of a re-aggregated kidney rudiment.

4.2.2. Renogenic potential of D1 cells

Expression profile of D1 cells

In order to establish if any of the kidney related genes might be already expressed by MSCs before introducing them into the embryonic kidney environment, D1 MSCs were investigated for the expression of important markers found during nephrogenesis. To investigate the expression profile of D1 cells in regard to genes involved in nephrogenesis, semi-quantitative polymerase chain reaction (PCR) was performed. The following genes were selected for initial assessment, as all have been shown to play a crucial role in kidney development (see Chapter 1): *Pax2*, *Wt1*, *Six2*, *Sall1*, *Lim1*, *Gdnf*, *Osr1*, *Bf2* and *Rarβ2*. As demonstrated in Figure 4.4, the D1 cells displayed expression of several genes known to be important in the early stages of kidney development; namely, *Sall1*, *Lim1*, *Gdnf* and *Osr1*. Nevertheless, expression of other genes found during nephrogenesis like *Pax2*, *Wt1* and *Six2* was not detected (Figure 4.4). Additionally, expression of the stromal-specific genes, *Bf2* and *Rarβ2*, was analyzed in D1 cells. Accordingly, D1 cells did not show expression of *Bf2* or *Rarβ2* (Figure 4.4). *Glyceraldehyde 3-phosphate dehydrogenase* (*Gapdh*) was used as a reference gene for all samples.

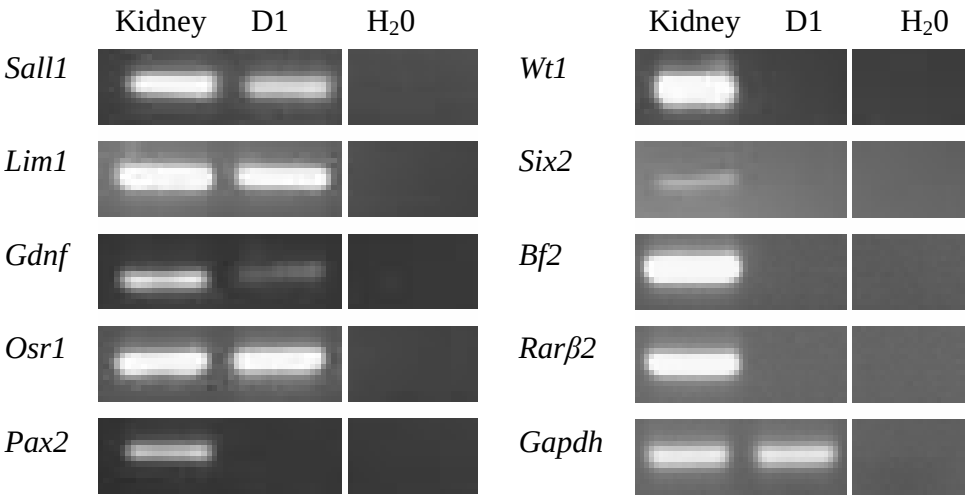

Figure 4.4 Gene expression profile of D1 cells (D1) compared with E13.5 kidney assessed using reverse transcription semi-quantitative PCR. D1 cells showed expression of several genes involved in kidney development. The reference gene is *Gapdh*. No template control was included (H_2O).

Chimeric kidney assay using D1 cells

As described earlier, the technique developed by Unbekandt and Davies will be used to introduce MSCs into the embryonic kidney environment, in order to assess their renogenic potential. In brief, labelled MSCs or other stem cells will be recombined with kidney rudiment cells derived from disaggregated E11.5 mouse embryonic kidneys. Following the aggregation step the obtained re-formed kidneys will be subsequently cultured for 4 days and analysed using a combination of antibody staining. Figure 4.5 highlights the essential steps of the recombination protocol.

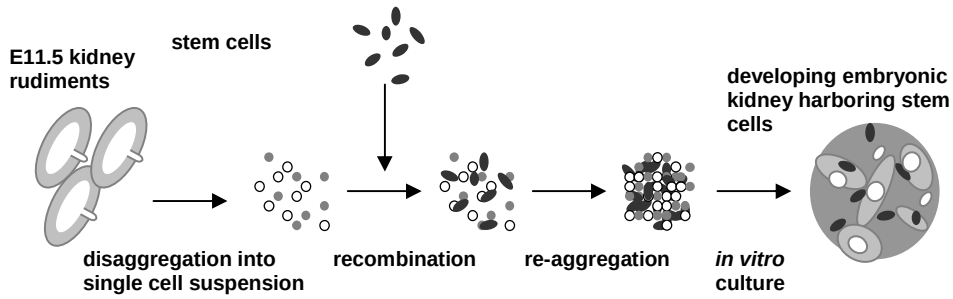

Figure 4.5 Schematic representation of the technique used to evaluate the contribution of stem cells to embryonic kidney development showing disaggregation of kidney rudiments and subsequent re-aggregation in the presence of labelled stem cells followed by *in vitro* culture.

D1 cells were recombined with kidney cells in all experiments in ratio of 1:5. Preliminary experiments performed with both mouse and human MSCs revealed that when lower ratios of MSCs were used for the recombination, such as 1:10, 1:20 and 1:100, only a few cells could be detected within the kidney chimeras (data not shown). For this reason a 1 to 5 ratio was chosen for the experiments. Since for each chimera a total of 100,000 cells was used, the approximate number of D1 cells recombined was 20,000. Upon the recombination MSCs were evenly distributed in the chimeras, mixing with rudiment kidney cells, hence no aggregates of MSCs were detected which could lead to impaired engraftment into renal structures (data not shown). In order to track D1 cells within the chimeric kidney the cells were labelled with either QDs or GFP, as described in section 3.2.3, and cultured for 4 days *in vitro*. The chimeras were then fixed and immunostained as demonstrated in section 4.2.1. Confocal microscopy was used to evaluate the localization of D1 cells within renal structures. After 4 days of chimeric kidney culture numerous laminin-positive structures were detected. This was accompanied by the expression of Wt1 in condensing MM (Figure 4.6). Some QD labelled cells were observed within the Wt1-positive

MM, hence the condensing MM, however most of the QD-labelled D1 cells were found in the Wt1- and laminin-negative compartment of developing chimeras, identified as stroma (Figure 4.6a-d). Further, no QD-labelled D1 cells were detected in the large laminin-positive structures, identified as the UBs (Figure 4.6 a-d). These results were confirmed using GFP-labelled D1 cells. Some GFP D1 cells were found within condensing MM, whereas the majority of the cells were detected in the stroma, where they appeared to form cell clusters (Figure 4.6 e-h).

In addition, it was observed that the integration of D1 cells might have a slight detrimental effect on the development of the chimeric kidneys. Chimeras harbouring D1 cells seemed to contain less condensing MM and nephrons in comparison with re-formed kidneys cultured in the absence of D1 cells. The negative effect on embryonic kidney development exerted by D1 cells will be investigated in more detail in Chapter 6.

Taken together, these data show that MSCs express some genes involved in early kidney development, such as *Gdnf, Sall1, Lim1* and *Osr1* but do not express important genes, like *Pax2, Six2* and *Wt1*. Furthermore, in the kidney chimeras D1 cells integrated into Wt1-positive condensing mesenchyme but not into laminin-positive structures, identified here as UBs. In addition, many recombined cells were found in the Wt1- and laminin-negative compartment of the chimeras where some clustering of the cells was observed. Finally, it is possible that the integration of D1 cells might have some negative effect on the development of the chimeras.

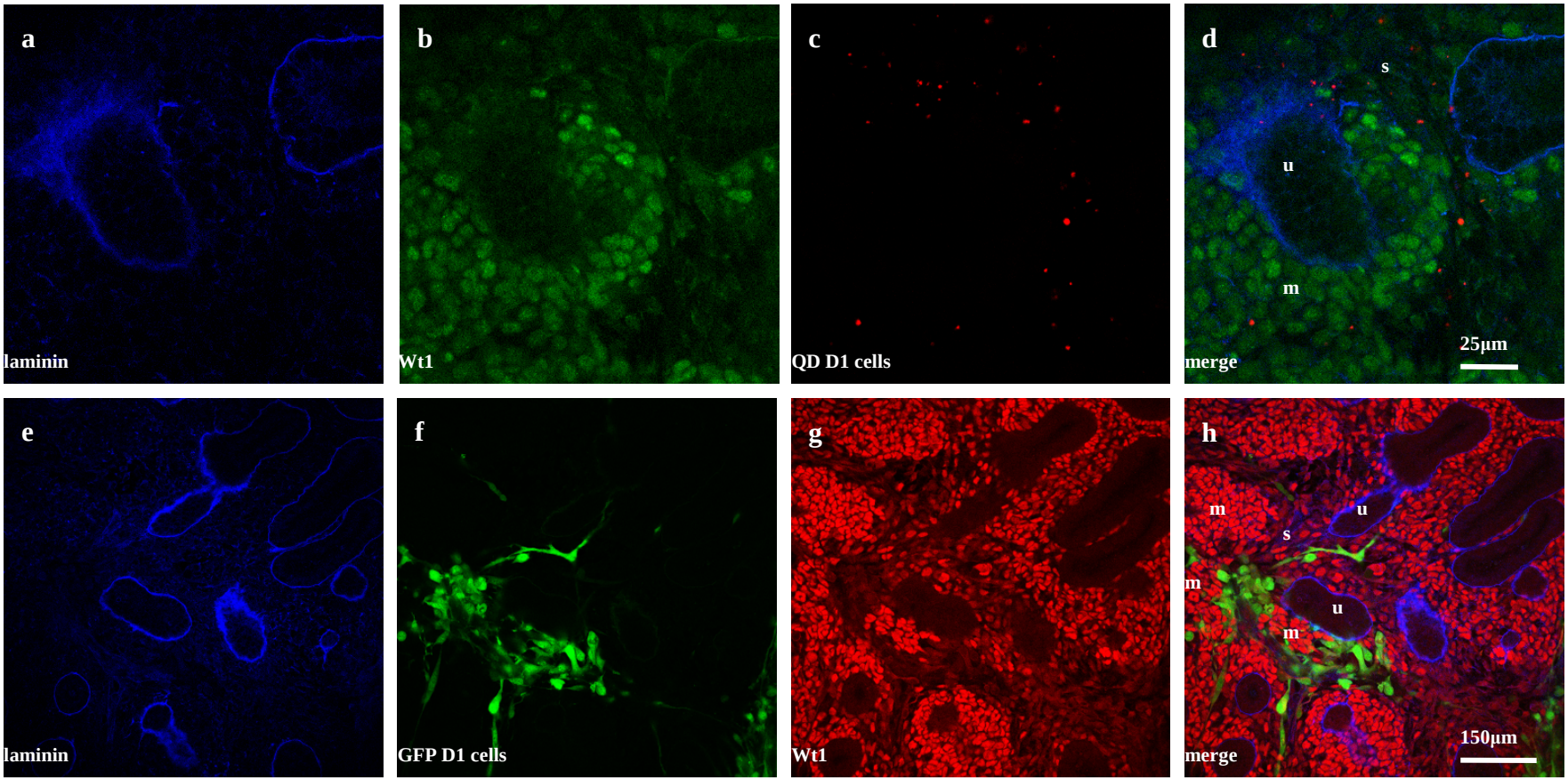

Figure 4.6 The contribution of D1 cells to nephrogenesis in chimeric kidneys after 4 days of *in vitro* culture. D1 cells were mainly found in stroma (s) and condensing MM of developing chimeras (m). No cells were found in UBs (u). Representative images of kidney chimeras are shown (at least 3 independent experiments were performed using each labelling method). (a-d) Engraftment potential of QD D1 cells (in red) into developing renal structures stained with Wt1 and laminin. (e-h) Engraftment potential of GFP D1 cells (in green) into developing renal structures stained with Wt1 and laminin.

4.2.3. Renogenic potential of human MSCs

Expression profile of human MSCs

The use of mouse MSCs for regeneration of human renal tissue in the future is rather unlikely. Ultimately human cells would be used for a purpose of such regenerative therapy. Therefore it is essential to determine human MSCs renogenic potential. The above results showed that D1 cells expressed several genes involved in nephrogenesis, such as *Osr1* and *Sall1*, but not *Pax2* or *Wt1* (Figure 4.4). Before performing the chimera assay to determine the renogenic potential of the human MSCs, expression of several metanephric markers was investigated in human MSCs. Similarly to mouse MSCs, no expression of *PAX2* or *WT1* was detected in human MSCs (Figure 4.7). As shown in the Figure 4.7 human MSCs did show expression of *OSR1* which was also found in D1 cells. However, in contrast to D1 cells, human cells did not express *SALL1* (Figure 4.7). *GAPDH* was used as reference gene for all samples and human proximal tubular cells (PTC) were used as a positive control.

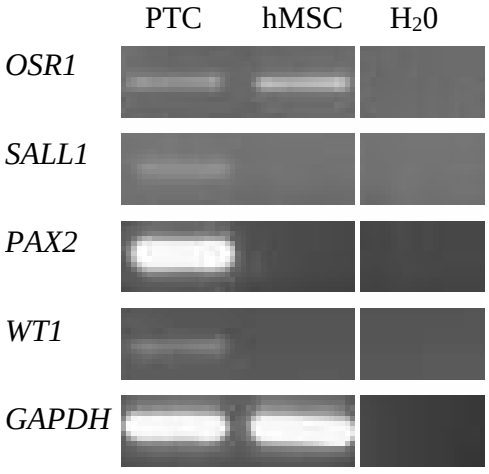

Figure 4.7 Gene expression profile of human MSCs (hMSC) compared with human proximal tubular cells (PTC) assessed using reverse transcription semi-quantitative PCR. The reference gene is *GAPDH*. No template control was included (H2O).

Chimeric kidney assay using human MSCs

In order to assess the renogenic potential of human MSCs, the same method described previously to generate chimeras harbouring D1 cells was utilized. Human MSCs were recombined with kidney cells in a ratio of 1 to 5. In order to track human MSCs within the chimeric kidney, the cells were immunostained with an anti-human nuclei antibody as described in section 3.2.3. After 4 days of chimeric kidney culture, some labelled cells were detected in the proximity of Wt1 positive structures, but never fully integrated into Wt1-expressing MM or developing nephrons. Human MSCs were predominantly found in the stromal compartment or outside the developing kidney, as shown in Figure 4.8a-c. It also appeared that human MSCs are mainly found in groups within the chimeras, similar to clusters of D1 cells, but less tightly packed (Figure 4.8a-c). As no staining for UBs was employed, the contribution of human cells to UB formation could not be assessed.

In addition, the recombination with human MSCs appeared to have also some negative effect on the development of chimeric kidneys, similar to D1 cells. Chimeras harbouring human MSCs seemed to contain less condensing MM and nephrons in comparison with re-formed kidneys cultured in the absence of human cells. The remaining Wt1-expressing regions often seemed to be disorganised. The negative effect exerted by human MSCs is described in Chapter 6.

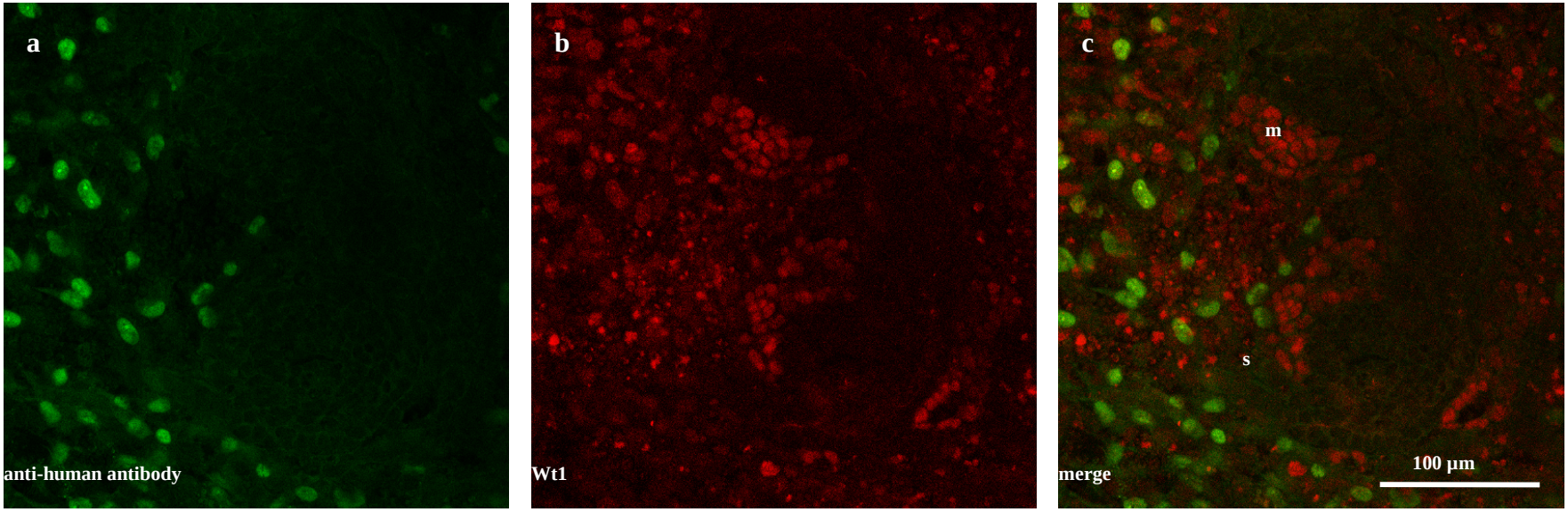

Figure 4.8 The contribution of human MSCs to nephrogenesis in chimeric kidneys after 4 days of *in vitro* culture. The cells were mainly found in stroma (s) and no integration occurred into Wt1-expressing condensing MM (m). A representative image of kidney chimera is shown (at least 3 independent experiments were performed). (a-c) Engraftment potential of human MSCs labelled with anti-human nuclei antibody (in green) into developing renal structures stained with Wt1.

In summary, human MSCs displayed similar expression profile to D1 cells, however they did not express *SALL1*. In the chimeric kidneys, numerous human cells were found in the Wt1- and laminin-negative compartment. Although some human MSCs were detected also in the proximity of Wt1-expressing structures, no definitive integration did occur. Finally, the integration of human MSCs might have some negative effect on the development of the chimeras similarly as observed for D1 cells.

4.2.4. Renogenic potential of other progenitors

In sections 4.2.2 and 4.2.3, the contribution to *in vitro* nephrogenesis of both mouse and human MSCs was assessed. Mouse MSCs could be found within the MM, which gives rise to nephrons, but the majority of the MSCs appeared to reside in the Wt1 and laminin-negative compartment, possibly the stromal compartment. Still, it is important to note that no marker for identifying the stromal compartment was employed in this study. Here the involvement of other stem cells/progenitors in the metanephric development was tested using the chimeric kidney culture system.

Accordingly, mouse ESCs were labelled with QDs and recombined in 1:5 ratios with E11.5 kidney rudiment cells to form chimeric kidneys. As shown in Figure 4.9a-h after 4 days of chimeric kidney culture QD-labelled ESCs were detected within Wt1-expressing condensing MM and laminin positive structures, possibly UBs. ESCs were also present in stroma but no cells were detected in nephron-like structures (Figure 4.9a-h).

Also, a cell population derived from mouse neonatal kidney, here referred as neonatal kidney cells (NKCs), was introduced into metanephric environment using the described chimeric culture system. NKCs have been established from a Pax2 expressing cell population isolated from a

disaggregated neonatal mouse kidney. These cells were described to spontaneously differentiate *in vitro* to generate cells with different renal phenotypes characteristic for podocyte-, mesangial- and tubular-like cells (Mora 2009). Following a 4 day culture period, QD-labelled NKCs integrated into condensing MM and developing nephron-like structures, as demonstrated in Figure 4.10a-h. Integration into UBs was rarely observed.

Finally, the integration of ESCs and NKCs did not appear to have an adverse affect on the chimeric kidney development. On the contrary, it seemed that more Wt1- and laminin-expressing structures were induced in the chimeras harbouring NKCs in comparison with the other stem cells tested.

In conclusion, both ESCs and NKCs were found in the Wt1-expressing compartment of chimeric kidneys. Presence of NKCs in the developing nephron-like structures was detected. Some ESCs were also present in laminin-positive structures. Both ESCs and NKCs were detected as well in the Wt1- and laminin-negative stromal compartment. Ultimately, the integration of ESCs and NKCs appeared not to have any negative effect on the development of the chimeras.

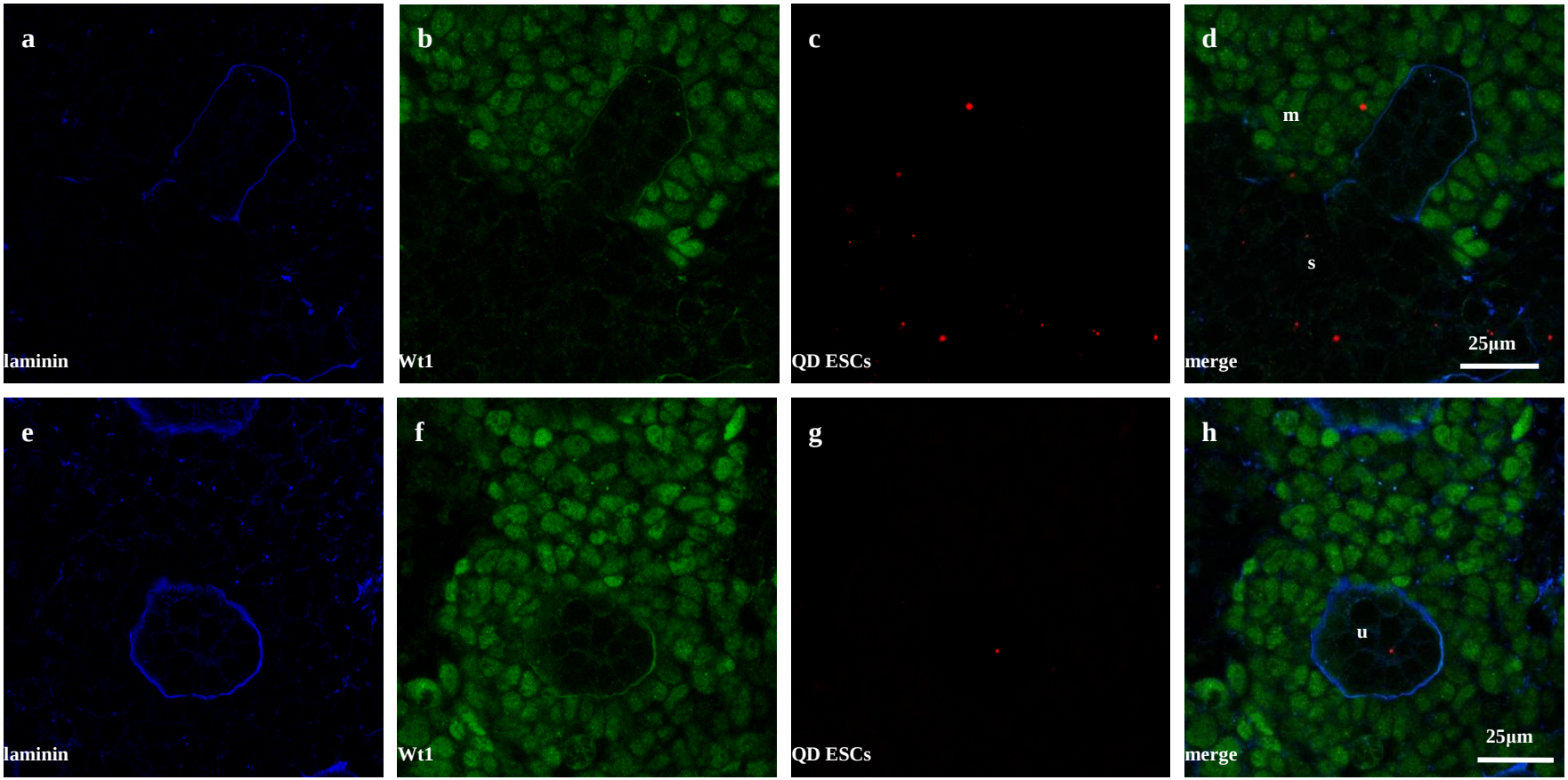

Figure 4.9 The contribution of mouse ESCs to nephrogenesis in chimeric kidneys after 4 days of *in vitro* culture. ESCs were found in stroma (s), condensing MM (m) and UBs (u) of developing chimeras. Representative images of kidney chimeras are shown (at least 2 independent experimenters were performed). (a-d) Engraftment potential of QD ESCs (in red) into condensing MM stained with Wt1. (e-f) Engraftment potential of QD ESCs (in red) into UBs stained with laminin.

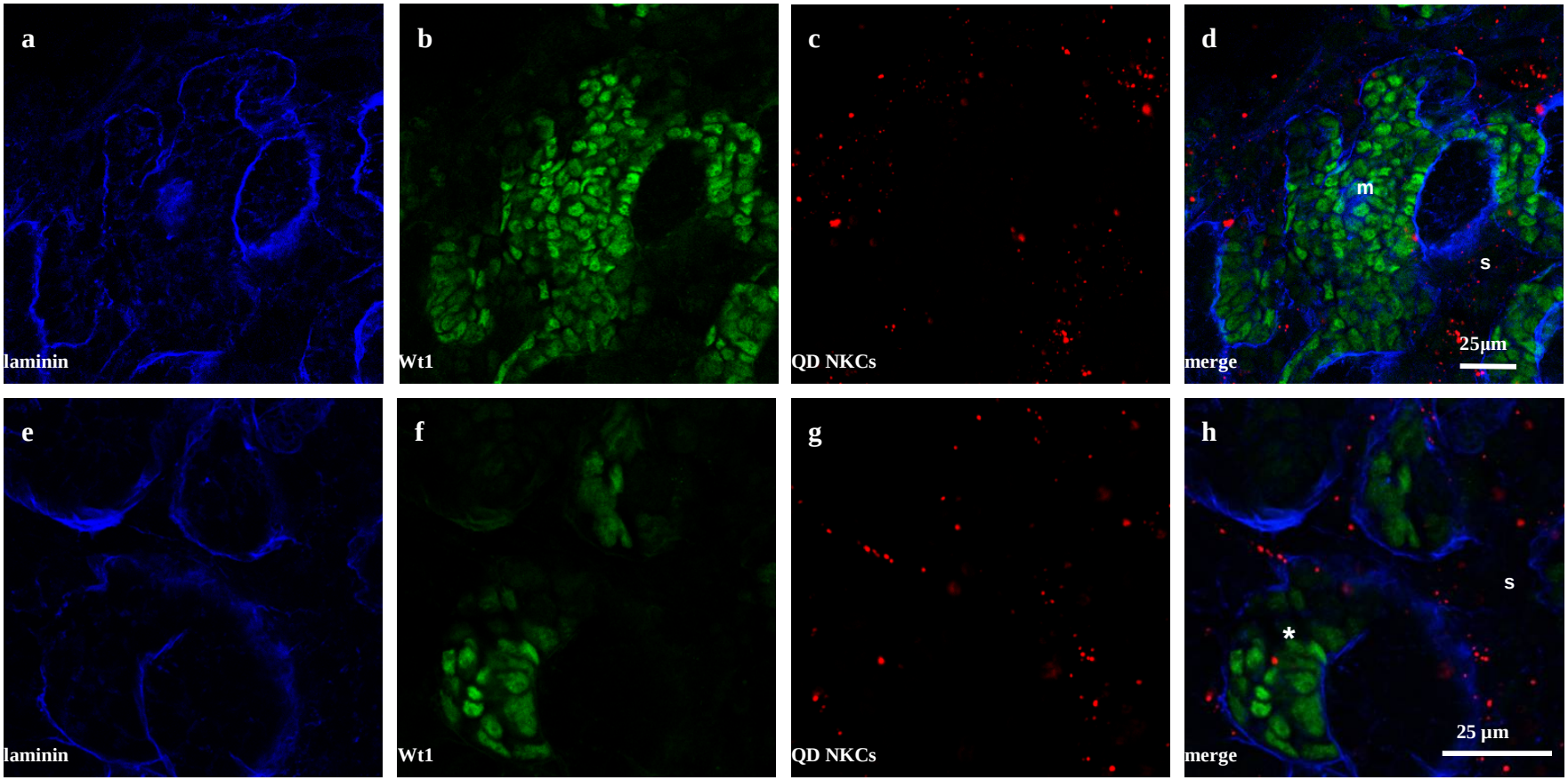

Figure 4.10 The contribution of mouse NKCs to nephrogenesis in chimeric kidneys after 4 days of *in vitro* culture. NKCs were found in stroma (s), condensing MM (m) and forming nephrons (*) of developing chimeras. Representative images of kidney chimeras are shown (at least 2 independent experimenters were performed). (a-d) Engraftment potential of QD NKCs (in red) into MM stained with Wt1. (e-f) Engraftment potential of QD NKCs (in red) into developing nephron-like structures stained with Wt1 and laminin.

4.3. Discussion

In this chapter the potential of mouse and human MSCs to contribute to renal development was evaluated using a novel method of embryonic kidney culture. Although D1 cells showed expression of some genes associated with early nephrogenesis, they did not express important genes, like *Pax2, Six2* and *Wt1*. In the chimeric kidney culture, D1 cells remained mainly within the Wt1- and laminin-negative compartment, although some D1 cells integrated into Wt1-expressing condensing MM. Nevertheless, the presence of MSCs within developing nephrons was not detected. When compared with mouse embryonic stem cells and mouse neonatal kidney cells, mouse MSCs behave comparable to neonatal kidney cells. Similarly to mouse MSCs, human MSCs did not show expression of *PAX2* and *WT1*. When recombined with embryonic kidney, they did not integrate into Wt1-exprssing condensing MM though several human cells were found in the proximity of Wt1 positive structures. Ultimately, the integration of mouse and human MSCs appeared to have some negative effect on the development of the chimeras.

4.3.1. Expression profile of MSCs

Expression of kidney related genes had previously been described in MSCs. Rat bone marrow-derived MSCs were shown to start expressing *aquaporin-1* when indirectly co-cultured with glycerol-injured rat kidney tissue (Qian et al. 2008). Similarly, indirect co-culture with injured cortical tubular epithelial cells induced expression of *aquaporin-1* and *kidney-specific cadherin* in mouse MSCs (Singaravelu and Padanilam 2009). As demonstrated by Yokoo *et al*., human bone marrow-derived MSCs transduced with GDNF and integrated into kidney rudiments, acquire expression of several kidney-specific markers that were previously not expressed in the cells, such as the podocyte specific genes, *nephrin, podocin* and *glomerular epithelial protein 1*, as well

as the tubular epithelial cell-specific markers, *aquaporin-1*, *1α hydroxlyase*, *parathyroid hormone receptor 1* and HCO_3^- *co-transporter* (Yokoo et al. 2005; Yokoo et al. 2006). Moreover, human bone marrow-derived foetal MSCs were demonstrated to express *aquaporin-1* and *parathyroid hormone receptor 1* after infusion into rats with glycerol-induced acute renal failure. Subsequently these cells were found integrated into tubular structures (Qian et al. 2008).

The expression of early embryonic kidney markers in MSC has not been thoroughly investigated until a recent paper from Lusis *et al*. identified a panel of embryonic kidney markers expressed in mouse MSCs (Lusis et al. 2010). Accordingly primary mouse bone-marrow-derived MSCs were shown to express *Eya1*, *Six1*, *Six2*, *Osr1*, *Pax8*, *cadherin 11*, *Gdnf*, *Wnt4*, *megalin* and *Foxd1*. In addition, no expression of *Wt1*, *Sall1*, *Hoxa11*, *Pax2* and *Lim1* was found in the cells. Moreover, human bone marrow-derived MSCs transfected with chicken Pax2 have been shown to express *SALL1*, *WNT4*, and *EMX2*. In addition, human MSCs over-expressing Pax2 were shown to acquire *LIM1* expression after integration into Wolffian duct epithelia (Fukui et al. 2009). Finally, two kidney-related genes were detected in human MSCs prior the incorporation into kidney rudiments*;* namely, *Kir6.1* and *SUR2* (Yokoo et al. 2005). The expression pattern of abovementioned genes in metanephric kidneys during nephrogenesis was described in detail in Chapter 1, except for *Emx2*, *Kir6.1* and *SUR2*. Accordingly, Emx2 was shown to be expressed in the ureteric buds and early epithelial structures derived from MM during mouse metanephric development (Pellegrini et al. 1997). Further, ATP-sensitive K+ channel subunits Kir6.1 and SUR2 were demonstrated to be expressed during early ureteric bud and nephron development and later in proximal tubules in rats (Braun et al. 2002).

In the current study, the expression profile of MSCs in regard to embryonic kidney markers has

been evaluated. The analysis demonstrated that D1 cells express a number of genes important for metanephric development; namely, *Osr1*, *Sall1*, *Lim1* and *Gdnf*. Mugford *et al*. showed that the Osr1-expressing progenitors give rise to the collecting duct epithelium, nephron and interstitial mesenchyme precursors (Mugford et al. 2008). Here, comparable expression levels of *Osr1* were found in D1 cells and E13.5 kidney. Similarly, human MSCs were demonstrated to express *OSR1*. This is in agreement with Lusis *et al*. demonstrating Osr1 expression in mouse MSCs (Lusis et al. 2010). Furthermore, D1 cells were found to express *Lim1*, which is detected in UBs and at different stages of nephron formation during nephrogenesis (Karavanov et al. 1998; Kobayashi et al. 2005), and *Sall1*, which is present during all stages of nephron development (Nishinakamura et al. 2001). *SALL1* was not detected in human MSCs though. *Lim1* and *Sall1* expression has not been reported previously in mouse MSCs (Lusis et al. 2010). Further the Gdnf/Ret signalling plays important role in UB outgrowth and the branching morphogenesis and Gdnf is normally expressed by mesenchymal cells during metanephric development (Sainio et al. 1997). D1 cells demonstrated expression of *Gdnf*, which is in accordance with previous results (Lusis et al. 2010).

As demonstrated, D1 cells show expression of a range of markers found in embryonic kidney. However it is important to note that all mentioned genes are not exclusively expressed during nephrogenesis. *Osr1* expression is found throughout limb and branchial arch development (So and Danielian 1999). Similar to *Osr1*, *Sall1* is expressed during limb development but also during heart development (Sweetman and Munsterberg 2006). Gdnf is a neurotrophic factor, which is an important survival factors for central and peripheral neurons. Gdnf and its receptors are expressed in developing tooth, limbs and submandibular gland (Golden et al. 1999). Finally *Lim1*

expression was found during neurogenesis (Barnes et al. 1994). Therefore an expression of following genes in D1 cells may not necessary reflect their renogenic potential.

According to the data provide here D1 cells do not express several genes essential for metanephric development, such as *Pax2*, *Wt1* and *Six2*. Pax2 is found in UB but also in condensing mesenchyme and developing nephrons (Dressler et al. 1990; Dressler and Douglass 1992). Similarly *Wt1* expression is present in condensing mesenchyme and developing nephrons (Armstrong et al. 1993; Mundlos et al. 1993). Both D1 cells and human MSCs did not express *Pax2* or *Wt1*, which is in agreement with previous results (Lusis et al. 2010). Furthermore, *Six2*, which is a maker for the nephron progenitor population (Kobayashi et al. 2008), was not expressed by D1 cells, although *Six2* expression in mouse MSCs was described previously (Lusis et al. 2010). Finally, the stromal compartment of metanephric kidneys is characterised by the expression of *Bf2* (Hatini et al. 1996) and *Rarβ2* (Abecassis et al. 2008). D1 cells did not express any of the markers, even though expression of *Foxd1* (*Bf2*) in primary mouse MSCs was documented (Lusis et al. 2010).

In conclusion, MSCs employed in this study express some early embryonic kidney genes. However there is a discrepancy between the expression profile of D1 cells and the profile described previously for mouse MSCs (Lusis et al. 2010). One explanation for this could be the fact that D1 cells used in this study are a cell line. For that reason their expression profile might slightly differ from primary MSCs used by Lusis and co-workers. Finally, there was also a difference in expression pattern of mouse and human MSCs which may influence their contribution to kidney development. It has been demonstrated that D1 cells express *Sall1* whereas human MSCs do not. Similarly *Lim1* expression was detected in D1 cells which was not found

previously in primary mouse and human MSCs (Fukui et al. 2009; Lusis et al. 2010).

4.3.2. Renogenic potential of MSCs

To be used for renal tissue engineering aimed at *de novo* nephrogenesis, MSCs should commit efficient and exclusively into kidney-specific cell types. Ideally, a large number of MSCs should be reprogrammed, as the random contribution of only a few cells would be insufficient for future regenerative purpose. Previously, only a sophisticated protocol was employed to introduce MSCs into embryonic kidneys (Yokoo et al. 2005), making further investigation of their renogenic capacity difficult. Here, in order to test the renogenic potential of MSCs, the cells were integrated into an embryonic kidney environment by performing chimeric kidney culture. Accordingly, mouse kidney rudiments obtained at E11.5 were disaggregated and re-aggregated in the presence of MSCs to form a chimeric embryonic kidney based on the novel chimeric kidney culture system described by Unbekandt and Davies (Unbekandt and Davies 2010). The chimeras were cultured similarly to intact metanephric kidneys and were confirmed to recapitulate normal kidney development, as described before (Unbekandt and Davies 2010). Both mouse and human MSCs were recombined with kidney cells in ratio 1:5, using a total of 100,000 cells, with each chimeric kidney containing approximately 20,000 MSCs. In comparison, in Yokoo`s experiments, only 1000 human MSCs were used (Yokoo et al. 2005). However, human MSCs were injected into rat intermediate mesoderm between the somite and lateral plate at the level of somite 29 which is a relatively small area (Yokoo et al. 2005). Following 4 days of *in vitro* culture, both QDs and GFP labelled D1 cells were found predominantly outside the developing chimeric kidney and in the laminin- and Wt1-negative compartment, identified here as stroma. Furthermore, some labelled cells were detected within condensing MM but they were not

observed in forming nephron-like structures. No labelled D1 cells were detected in laminin-positive and Wt1-negative tubular structures, which can be described as the UBs. Similar results were obtained with human MSCs. Human MSCs appeared larger than mouse kidney cells in the chimeras. Labelled with anti-human antibody, MSCs were found mainly outside the developing chimeric kidney or in the putative stromal compartment. Some human cells were found in the proximity of Wt1 positive structures but did not engraft into MM, suggesting that human MSCs display even lower integration potential into MM than mouse MSCs. In addition, some human cells seemed to divide in the chimeras. Nevertheless, this has not been further verified. In conclusion, it has been demonstrated that MSCs have a rather low renogenic potential in the chimeric kidney assay.

Previously it has been demonstrated by Yokoo *et al*. that MSCs can contribute to nephrogenesis integrating into both glomerular and tubular epithelium (Yokoo et al. 2005; Yokoo et al. 2006). These results differ from data obtained here using the chimeric kidney system. Nevertheless the absence of D1 cells from UBs is in accordance with earlier results showing that human MSCs are unable to fully contribute to development of the collecting duct system (Fukui et al. 2009). In previous experiments performed by Yokoo and co-workers, human MSCs over-expressing GDNF were injected into rat IM at the site of nephrogenesis before the initiation of metanephric development (Yokoo et al. 2005; Yokoo et al. 2006). In the system described in this study MSCs were recombined with embryonic kidneys that were isolated at the onset of metanephric development. Therefore, the embryonic signals that MSCs receive in this environment are different from signals found in IM. It has been shown that injection of human MSCs into an intact kidney rudiment is insufficient to trigger integration of MSCs. It is not clear however if

these cells were over-expressing GDNF (Yokoo et al. 2005). Moreover, human MSCs injected into intact metanephroi did not form any recognizable renal structures and remained aggregated (Yokoo et al. 2005). Similar results were found in this study, as the mouse MSCs appeared to form aggregates of cells within the chimeric kidney, even after they were recombined with a single cell suspension of kidney cells. These data confirm that the method by which MSCs are introduced into kidney, namely injection into intact metanephros or recombination with kidney cells is not essential for the integration of cells, but rather, the stage of metanephric development is important. Another reason for the low contribution of MSCs to nephron formation could be that the MSCs used here for creating the chimeras were not genetically modified to express high levels of GDNF. This modification has been demonstrated to be crucial for enhancing the number of integrated cells (Yokoo et al. 2005). It is also important to note that human MSCs were analyzed after 6 days of culture in Yokoo`s experiments (Yokoo et al. 2005) whereas the chimeric kidneys here were analysed after 4 days of *in vitro* culture. For this reason, cells observed in the condensing MM at this stage could possibly be found in developing nephrons later on. Nonetheless, as described in Chapter 6, no extensive nephron formation did take place after 7 days of chimeric kidney culture and subsequently no MSCs were found in nephron-like structures. Finally Yokoo *et al*. do not present an exact quantification of human MSC engraftment and differentiation (Yokoo et al. 2005); therefore, it is difficult to compare the number of cells integrated into different kidney compartments between the two protocols.

As demonstrated, mouse MSCs do not express kidney stroma markers, like *Bf2* and *Rarβ2* in standard *in vitro* culture. However, many mouse and human MSCs were localised in the stroma of kidney chimeras upon recombination. The relatively high prevalence of the MSCs in the

stroma of developing metanephroi, however, might not be too surprising, as both ESCs and NKCs that were used to form kidney chimeras were also found in high numbers in the stromal compartment of the developing chimeras. Further, it has been shown that even kidney-derived progenitors are to a great extent found in the stromal compartment (Challen et al. 2006; Maeshima et al. 2006; Lusis et al. 2010). Ultimately, it was not possible to conclude if cells remaining in the Wt1- and laminin-negative compartment are becoming stromal cells, due to lack of appropriate commercially available antibody. It might be also feasible that cells which were not found integrated into UBs or MM-derived structures remained undifferentiated. As no reliable marker for undifferentiated MSCs exists, it was not possible to investigate this option in chimeras harbouring MSCs.

Furthermore, it is also difficult to conclude if the integrated D1 cells expressed Wt1 after integration into condensing MM. The data obtained with QDs indicate that D1 cells indeed did express some Wt1. Nevertheless Wt1 expression could not be confirmed using the GFP-labelled cells. One possibility explaining the discrepancy might be that GFP expression in the cells suppresses Wt1. It has been demonstrated that GFP expression interferes with activation of NF-κB and JNK signalling pathways and stabilisation of p53 tumor suppressor in human embryonic kidney cells (Baens et al. 2006). Another possibility is that after labelling with QDs, some nanoparticles remain in the MSC cell suspension and during the recombination and a small fraction of kidney cells becomes labelled with these QDs. QDs might also be lost from D1 cells and subsequently transferred to kidney cells expressing Wt1 in the chimeras. Accordingly, it was shown that embryonic stem cells lose QDs and such QDs can be further utilized for labelling of other cells when additional labelling buffer is used (Pi et al. 2010).

In addition, both mouse and human MSCs had some detrimental effect on the development of chimeric kidneys. Kidneys harbouring MSCs appeared to contain less condensing MM and forming nephron-like structures in comparison with kidneys recombined in absence of MSCs or recombined with other cells, for example ESCs. The inhibited development of the chimeras might be responsible in part for poor integration of the cells. Ultimately the effect on metanephric development exert by MSCs is examined in Chapter 6.

In summary, although MSCs express some of early embryonic kidney genes their integration potential into renal structures remains low in the kidney chimeras. High prevalence of MSCs has been observed in the stromal compartment of the chimeras. Also some negative effects on metanephric development were associated with the integration of MSCs. In order to contribute to renal development MSCs most likely require complex reprogramming, similar to the one described by Yokoo *et al*. Perhaps pre-conditioning before performing the chimeric assay could help the cells to increase their renogenic potential.

4.3.3. Renogenic potential of other stem cells

Here ESCs and NKCs have been used to perform embryonic chimeras using the same methodology as for MSCs in order to compare integration potential of MSCs with other stem cells. Previously, both ESCs and kidney progenitors have been introduced into the embryonic kidney environment with the aim to investigate their capability to differentiate towards renal like structures. However none of the aforementioned cell types had previously been recombined with kidney cells using the novel chimeric kidney culture technique (Steenhard et al. 2005; Challen et al. 2006; Maeshima et al. 2006). Accordingly, Steenhard *et al*. introduced undifferentiated mouse ESCs into E13 mouse kidney rudiments using microinjection. After 5 days of *in vitro* culture,

ESCs were detected in large tubule-like structures surrounded by basement membranes and displaying apical microvilli. In the injected metanephroi ESCs did not mix however with native kidney cells to create chimeric tubules. They also were rarely observed in glomerular structures (Steenhard et al. 2005). ESC-derived renal structures stained positively with *Lotus tetragonolobus* (LTA) lectin, a marker for proximal tubules, but were negative for Tamm-Horsfall protein and *Dolichos biflorus* lectin, which are markers of distal tubule and collecting duct, respectively (Steenhard et al. 2005). Using the chimeric kidney system it was possible to demonstrate the presence of mouse ESCs in Wt1- and laminin-negative compartment, laminin positive tubular structures and condensing MM. No cells were detected among highly Wt1-expressing cells of emerging glomeruli in the developing nephron-like structures. These results are partially in agreement with previous data, since the presence of ESCs in proximal tubules could not be confirmed using the chimeras. Finally, in chimeric kidneys ESCs were able to become integrated into emerging renal structures and not only contribute to structures formed entirely from ESCs, as described by Steenhard *et al*. (Steenhard et al. 2005).

Apart from ESCs, various kidney progenitors have been demonstrated to contribute to *in vitro* kidney organogenesis. Among several types of renal progenitors, label-retaining tubular cells (LRTC) (Maeshima et al. 2006) and kidney site population (SP) (Challen et al. 2006) were demonstrated to have the capacity to integrate into metanephric kidney, thus contributing to embryonic kidney development. LRTC have been isolated from an adult rat kidney by using bromodeoxyuridine labelling method that enables identification of slowly dividing cells. They were shown to form tubule-like structures in three-dimensional culture conditions in the presence growth factors such as hepatocyte growth factor. After 5 days following the injection into E15 rat

kidney rudiment, the cells were found in the interstitium, ureteric buds, as well around ureteric buds and in tubules positive for LTA (Maeshima et al. 2006). Similarly, the SP population isolated by Challen *et al.* from adult mouse kidneys using the ability of some cells to efflux the Hoechst dye incorporated into the metanephric kidney. Following injection of the SP cells into mouse E12.5 metanephroi, the cells were detected in UB structures labelled with calbindin and Pax2 as well as in MM co-stained with Wt1 and Pax2 after 3 days of *in vitro* culture. Further, kidney cells which did not represent the capacity to efflux the dye did also engraft into UB and MM but at a much lower percentage than the SP population (Challen et al. 2006). Recently, human CD133/1+ kidney progenitors isolated from both papilla and cortex were shown to integrate into tubular compartment of metanephric kidney after 3 days of culture following injection into E.12.5 mouse kidney rudiments (Ward et al. 2011). Here a renal cell population, the NKCs, was introduced into metanephric environment using the described chimeric culture system. NKCs have been established from Pax2 expressing cell population isolated from disaggregated neonatal mouse kidney. The cells are not a clonal population and demonstrate *in vitro* different renal phenotypes characteristic for podocyte-, mesangial- and tubular-like cells (Mora 2009). Accordingly NKCs were found in Wt1- and laminin-negative compartment and Wt1- positive condensing MM of chimeric kidneys. Some NKCs were found in developing nephron-like structures. The cells were rarely detected in tubular laminin positive structures which can be associated with UBs. NKCs appear to share some similarities with cells of kidney side population which after injection into metanephric kidney were found in higher numbers in MM-derived structures in comparison with UBs (Challen et al. 2006).

Recently it has been demonstrated using the same system described by Unbekandt and Davies

that human amniotic fluid stem cells (AFSCs) can form kidney chimeras. Accordingly AFSCs were contributing to nephron formation as well as ureteric bud structures during metanephric development. AFSCs represent a novel stem cell population which combine the features of embryonic and adult stem cells (De Coppi et al. 2007). Human AFSCs were recombined with E11.5 kidney cells in a 1 to 10 ratio and subsequently the kidney chimeras were cultured for 4 days. The cells were detected in Pax2 and Wt1 positive structures. Further, this was accompanied by acquisition of expression of some important embryonic kidney markers, such as Pax2 (Siegel et al. 2010). Interestingly, a broader integration potential of human AFSCs encompassing both UBs and developing nephrons has been described using the chimeric kidney approach. Previously the cells were injected into E13 kidneys and found integrated into stroma and developing nephron structures after 5 days (Perin et al. 2007).

In conclusion, it was shown that different progenitor types have different abilities to contribute to *ex vivo* kidney development in the chimeric kidneys. In the chimeric kidneys NKCs behave comparable to D1 cells as both progenitor types were found in the condensing MM and did not integrate into UBs. However, NKCs could be detected in structures resembling developing nephrons, which was not the case for MSCs. It appears also that AFSCs have the broadest integration potential in the chimeras since they have been described to integrate into both UBs and nephron-like structures (Siegel et al. 2010). As some D1 cells were detected in the nephrogenic mesenchyme, it can be suggested that mouse MSCs do possess some renogenic potential. The subsequent chapter describes an attempt to increase the presence of MSCs in the condensing MM, thus facilitating the integration of MSCs into nephron-like structures.

Chapter 5: Potential of MSCs to contribute to metanephric development after stimulation with conditioned medium from neonatal kidney cells

5.1. Introduction

In Chapter 4 the ability of MSCs to integrate into developing embryonic kidney structures was evaluated using a novel chimeric kidney culture system. As described previously, direct injection of human MSCs into a rodent kidney rudiment is insufficient to elicit MSC integration into nephron-like structures; instead, the MSCs tended to aggregate at the injection site (Yokoo et al. 2005). For that reason, a new methodology developed by Unbekandt and Davies (Unbekandt and Davies 2010) was employed to determine the contribution of both mouse and human MSCs to nephrogenesis. As the protocol involved the disaggregation of the kidney rudiments and subsequent reformation of the kidney in the presence of stem cells, no aggregation at the site of injection could occur. Nevertheless, as demonstrated in the previous chapter, only infrequent engraftment of mouse MSCs into condensing metanephric mesenchyme (MM) was observed in the embryonic kidney chimeras. Furthermore, no human primary MSCs were found in the MM of the chimeras. This implies that in order to obtain full MSC incorporation into renal structures, MSCs require additional reprogramming, as demonstrated by Yokoo *et al*. (Yokoo et al. 2005). It appears that glial cell line-derived neurotrophic factor (GDNF) plays a crucial role in this process since it was shown that over-expression of GDNF in human MSCs before their introduction into the embryonic environment, considerably increases their integration potential into metanephric kidneys (Yokoo et al. 2005). GDNF is an important factor for ureteric bud (UB) outgrowth and branching (Vega et al. 1996; Sainio et al. 1997). The mechanism of action of GDNF involves activation of the tyrosine kinase receptor Ret, encoded by the *Ret* proto-oncogene (Trupp et al.

1996; Vega et al. 1996). In the subsequent chapter the possibility to induce a renal phenotype and subsequently improve the engraftment potential of MSCs into metanephric kidney will be investigated following pre-treatment of MSCs with conditioned medium obtained from kidney progenitor population.

The use of conditioned medium to trigger differentiation of MSCs has been attempted before (Rivera et al. 2006; Pan et al. 2008; Baer et al. 2009; Schittini et al. 2010). Conditioned medium from cardiac explants was used as a potential source of factors to induce differentiation of MSCs into cardiomyocyte-like cells, as it has been demonstrated to contain cytokines, growth factors and myocardial and metabolism-related proteins. Accordingly, the conditioned medium was shown to elicit phenotypic changes in the MSCs so that their morphology and marker expression profiles resembled those of cardiomyocyte-like cells (Schittini et al. 2010). Further, foetal liver-conditioned medium obtained from different developmental stages was assessed for induction of hepatic differentiation in MSCs: this study demonstrated that stimulation with conditioned medium from E13.5 liver culture was most effective in inducing morphological and functional changes in the MSCs, as well as changes in gene expression that were characteristic of hepatic differentiation (Pan et al. 2008). In addition, to induce a neuronal-like phenotype, MSCs were treated with conditioned medium derived from adult hippocampus, cortex or cerebellum, and muscle-derived conditioned medium was used as a negative control. All media tested, except the muscle-derived conditioned medium, induced a neuronal morphology and the expression of neuronal markers in MSCs (Rivera et al. 2006). Finally, conditioned medium from proximal tubular cells has been used to initiate differentiation of MSCs into epithelial-like cells. After incubation with the conditioned medium, changes in morphology and gene expression of the cells

occurred, indicating epithelialisation (Baer et al. 2009). In conclusion, these studies highlight that the fate of MSCs can be influenced by factors derived from various types of differentiated cells, and in most cases, the MSCs start to adopt the characteristics of the cells from which the factors are derived.

In this chapter, conditioned medium from neonatal kidney cells (NKC CM) will be tested for its ability to increase the renogenic potential of MSCs. NKCs used for obtaining conditioned medium are a heterogeneous population displaying features of podocytes, mesangial and renal tubular cells (Mora 2009). As demonstrated in the previous chapter, NKCs contribute considerably to nephron development in chimeric kidneys by integrating into condensing MM and developing nephron-like structures. Accordingly, NKC CM will be used to initiate differentiation of MSCs towards a renal phenotype in order to subsequently increase the renogenic potential of the cells in the recombination assay.

5.2. Results

In order to enhance the potential of MSCs to engraft into developing nephron structures, NKC CM has been employed to pre-condition both mouse and human MSCs. Initially, the multilineage differentiation potential of D1 cells pre-treated with NKC CM was assessed, followed by expression analysis of kidney-specific genes. Finally, the ability of pre-treated D1 cells and human MSCs to integrate into developing renal structures and differentiate into nephron-specific cell types was tested by performing the chimeric kidney culture assay.

5.2.1. The multilineage differentiation potential of D1 cells stimulated with NKC CM

In an attempt to increase their renogenic potential, D1 cells were incubated for 4 days with a 1:1

mix of conditioned medium obtained from a confluent NKC culture (NKC CM), and standard culture medium. In Figure 5.1, bright field images of unstimulated and stimulated D1 cultures show that there is a slight difference in morphology of D1 cells incubated in NKC CM compared to those cultured in standard culture medium: i.e., following stimulation with NKC CM, MSCs appeared more aligned than when cultured in standard medium.

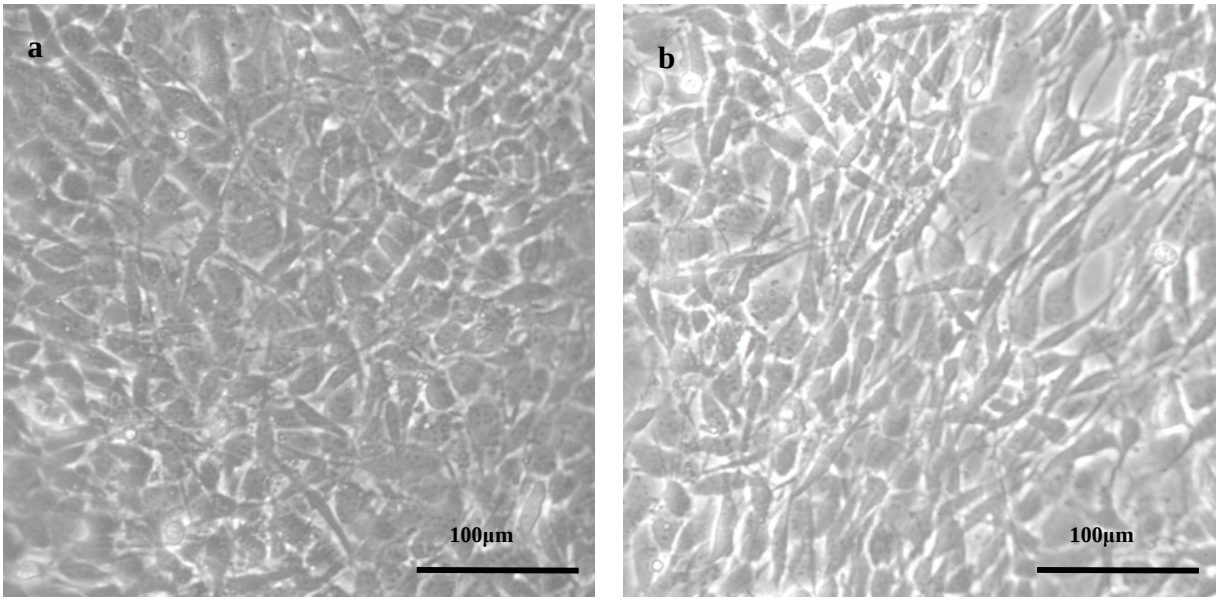

Figure 5.1 Morphology of D1 cells after stimulation with NKC CM. Representative images are shown (observed for more than 3 independent cultures). (a) Bright field image of the D1 cells cultured for 4 days in standard culture medium. (b) Bright field image of the D1 cells cultured in NKC CM.

To verify how the stimulation with NKC CM affects the multipotency of D1 cells, subconfluent D1 cultures were induced for two weeks to undergo adipogenic, osteogenic and chondrogenic differentiation using appropriate inductive media, as described in section 3.2.1. Figure 5.2 shows the adipogenic, osteogenic and chondrogenic potential of MSC stimulated with NKC CM compared to those cultured in standard medium.

Following induction with adipogenic medium, Oil Red staining on day 14 confirmed the presence

of lipid vacuoles in D1 cells that had been stimulated with NKC CM, and those cultured in standard medium, whereas in the absence of adipogenic medium, there was no evidence of lipid vacuoles (Figure 5.2a-d). It appeared, however, that D1 cells stimulated with NKC CM (Figure 5.2c) had a slightly lower adipogenic potential compared to controls, as fewer cells accumulated lipid vacuoles in comparison with unstimulated D1 cells (Figure 5.2a).

Further, 14 days following induction with osteogenic medium, Alizarin Red staining showed that both the control D1 cells and those stimulated with NKC CM were able to undergo osteogenesis (Figure 5.2e and g). Interestingly, under osteogenic conditions, some NKC CM-stimulated cells displayed vacuoles that appeared similar to lipid vacuoles found during adipogenesis, and these cells did not stain for Alizarin Red (Figure 5.2g insert). In the absence of osteogenic medium, no staining was detected in control cultures or in those stimulated with NKC CM (Figure 5.2f and h).

Finally, in order to confirm the chondrogenic differentiation potential of MSCs, a chondrogenic culture condition was employed, as described in section 3.2.1. Both unstimulated and NKC CM-stimulated D1 cells formed stable pellets and showed the presence of proteoglycans in the periphery of the pellet, as indicated by Alcian Blue staining (Figure 5.2i and k). No Alcian Blue staining was detected in pellets cultured in the absence of chondrogenic medium (Figure 5.2j and l).

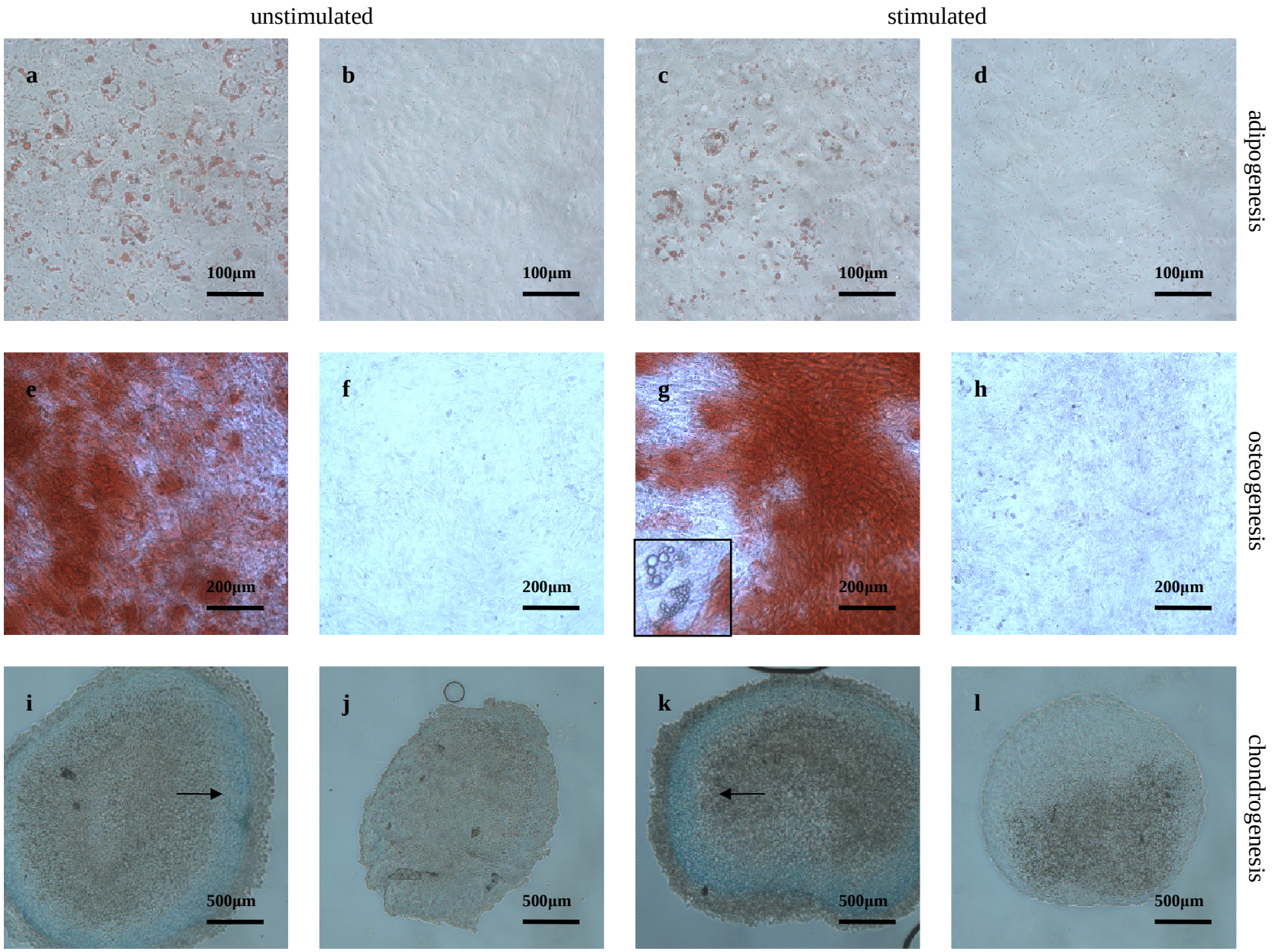
unstimulated
stimulated
a
b
c
d
100µm
adipogenesis
e
f
g
h
200µm
osteogenesis
i
j
k
l
500µm
chondrogenesis

Figure 5.2 Confirmation of multilineage differentiation potential of D1 cells treated with NKC CM for 4 days and subsequently induced with adipogenic, osteogenic and chondrogenic induction media. Representative images are shown. (a) After 14 days of stimulation with adipogenic inductive medium D1 cells displayed lipid vacuoles that stained positively with Oil Red. (b) Oil Red staining of D1 cells cultured in standard culture medium showed no lipid vacuole formation. (c) D1 cells pre-treated with NKC CM for 4 days and subsequently stimulated with adipogenic inductive medium for additional 14 days displayed lipid vacuoles. (d) In the absence of adipogenic medium, Oil Red staining demonstrated no lipid vacuole formation in cells pre-treated with NKC CM. (e) After 14 days of culture in osteogenic inductive medium, Alizarin Red staining showed the presence of extracellular calcium deposits in D1 cultures. (f) Alizarin Red staining of control D1 cells showed that no calcium deposits were present. (g) D1 cells pre-treated with NKC CM for 4 days and subsequently stimulated with osteogenic inductive medium show Alizarin Red staining detecting presence of calcium deposits. Occasionally some pre-treated D1 cells also displayed vacuoles comparable to lipid vacuoles found during adipogenesis (insert). (h) In the absence of osteogenic medium, Alizarin Red staining demonstrated no evidence of calcium deposits in cells pre-treated with NKC CM. (i) After 14 days of micromass culture in chondrogenic inductive medium, Alcian Blue staining showed positive staining in the periphery of the pellet, indicating cartilage formation. (j) In the absence of chondrogenic medium, Alcian Blue staining of D1 micromass sections showed no evidence of cartilage proteoglycans. (k) After 14 days of micromass culture in the presence of chondrogenic medium, NKC CM pre-treated of D1 cells showed evidence of cartilage formation at the periphery of the pellet, as indicated by Alcian Blue staining (arrow). (l) In the absence of chondrogenic medium, no Alcian Blue staining was detected in micromass sections of D1 cells pre-treated with NKC CM.

In summary, pre-treatment with NKC CM of D1 cells did not result in substantial morphological changes of the cells. Further, upon stimulation the cells maintained also their multilineage potential, as demonstrated in the adipogenic, osteogenic and chondrogenic assays.

5.2.2. Renogenic potential of D1 cells stimulated with NKC CM

Expression profile of D1 cells following treatment with NKC CM

Before performing chimeric kidney rudiment culture, the expression profile of D1 cells stimulated with NKC CM was assessed. D1 cells were stimulated with a mix of NKC CM and standard culture medium for 4 days, and subsequently, the expression of important early kidney markers was evaluated using semi-quantitative PCR. As demonstrated in Figure 5.3, stimulated D1 cells continued to express several genes essential for metanephric development, such as *Gdnf*, *Sall1*, *Lim1* and *Osr1*. Moreover, *Gdnf* expression appeared to be up-regulated in NKC CM-

stimulated cells in comparison with unstimulated MSCs. Furthermore, a slight downregulation of *Sall1* and *Lim1* expression was noted in NKC CM-stimulated cells. The incubation of D1 cells with NKC CM did not induce *Pax2, Wt1* or *Six2* expression. Expression of those genes was also not detected in unstimulated D1 cells (Figure 5.3). Interestingly, NKC CM-stimulated D1 cells did show weak expression of *Bf2* which was not detected in unstimulated cells (Figure 5.3). *Rarβ2* was not detected in either NKS CM-stimulated cells or unstimulated control D1 cells.

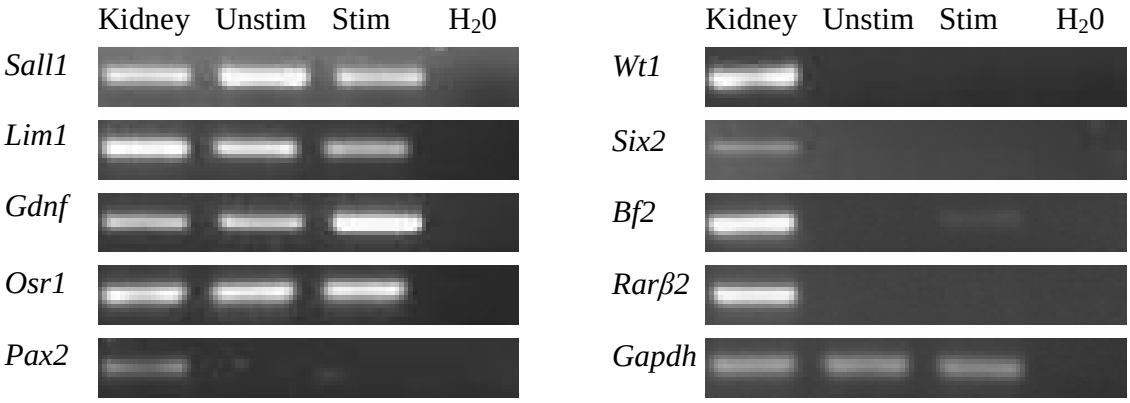

Figure 5.3 Comparison of gene expression related to metanephric development between D1 cells cultured in standard culture conditions and D1 cells following 4 days culture in NKC CM assessed using reverse transcription semi-quantitative PCR. E13.5 kidney was included as a positive control. *Gapdh* was used as reference gene. No template control was included (H_2O).

As the data obtained using semi-quantitative PCR showed up-regulation in *Gdnf* expression after KSC CM stimulation, quantitative PCR was performed to determine the extent of the up-regulation. Figure 5.4a shows a significant up-regulation of *Gdnf* expression after stimulation with NKC CM for 4 days in comparison to unstimulated cells ($p<0.01$, $n=6$). Further, *Gdnf* remained at significantly higher levels in the cells 24h after the NKC CM was changed to standard culture medium ($p<0.05$, $n=3$) (Figure 5.4b). Nevertheless, the increase in *Gdnf* expression in stimulated cells 24h after changing the medium to standard culture medium was less than that observed in MSCs cultured in the presence of NKC CM (Figure 5.4a and b). All

experiments were performed using *Gapdh* as a reference gene.

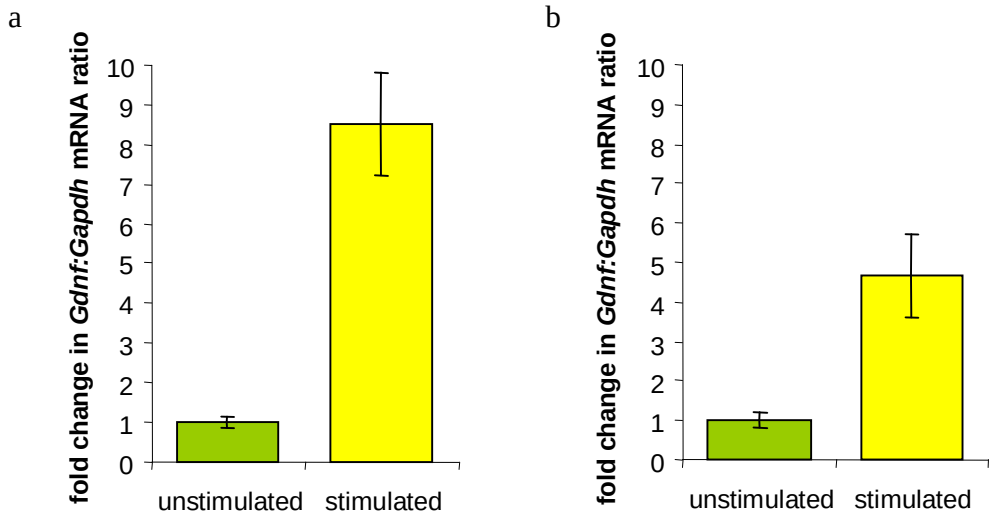

Figure 5.4 Comparison of *Gdnf* expression levels in unstimulated and NKC CM-stimulated cells using reverse transcription quantitative PCR. The reference gene is *Gapdh* and the error bars represents SE of the mean. (a) There was a significant increase in *Gdnf* following culture in NKC CM (*t*-test, $p<0.01$, n=6). (b) Up-regulation in *Gdnf* expression was also present in D1 cells 24 h following withdrawal of NKC CM (*t*-test, $p<0.05$, n=3).

As the stimulation with NKC CM resulted in a significant increase in *Gdnf* expression, it was investigated if *Gdnf* expression in D1 cells could be further enhanced by applying concentrated conditioned medium onto the cells. D1 cells were stimulated for 4 days with different concentrations of NKC CM. In order to obtain 1x, 2x or 10x NKC CM concentration in media used for stimulation, the conditioned medium was concentrated using a Vivaspin centrifugal concentrator and diluted with standard culture medium to reach the appropriate concentration. The expression levels after stimulation with concentrated NKC CM were compared to the expression levels found in unstimulated D1 cells. *Gdnf* expression was also evaluated in cells stimulated with the corresponding concentration of standard culture medium. The 1x condition, which was equivalent to a 1:1 mix of NKC CM and standard culture media, used in previous

experiments, elicited an increase in *Gdnf* expression after 4 days of stimulation (Figure 5.5). However, as demonstrated in Figure 5.5a, the use of concentrated NKC CM did not lead to any further increase in *Gdnf* levels in D1 cells. Furthermore, *Gdnf* expression following stimulation with 2x and 10x concentrated standard culture medium for the same period of time as with NKC CM, appeared to slightly up-regulate *Gdnf* expression levels in D1 cells (Figure 5.5b).

To investigate if CM derived from other cell types can induce *Gdnf* expression in D1 cells, the cells were cultured in a 1:1 mix of conditioned medium obtained from mouse embryonic fibroblasts derived from E11.5-E12.5 embryos (MEF CM) and standard culture media for 4 days. As shown in Figure 5.6a, the stimulation with MEF CM had a similar effect on *Gdnf* expression as NKC CM.

a

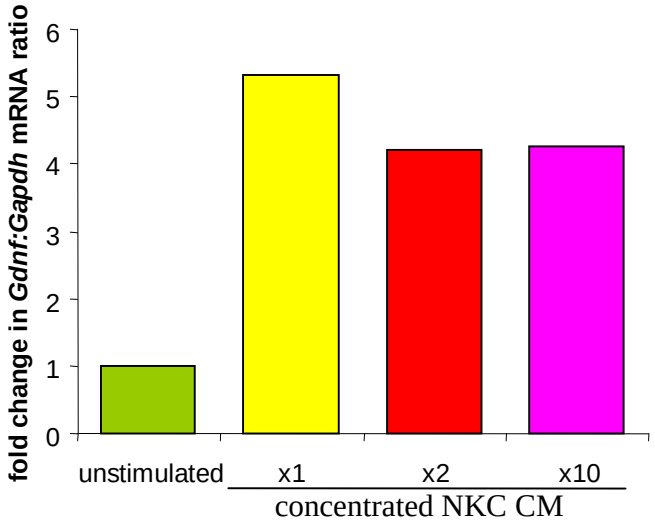

b

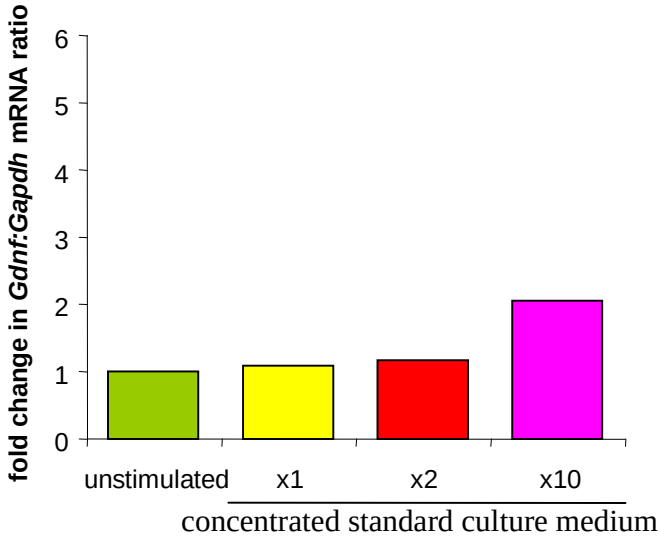

Figure 5.5 Comparison of *Gdnf* expression levels in unstimulated and KSC CM-stimulated D1 cells after 4 days using reverse transcription quantitative PCR. The following culture media were used: standard culture medium, 1x NKC CM in standard medium - an equivalent to 1:1 mix or 1x standard medium (1x), 2x NKC CM in standard medium or 2x standard medium in standard medium (2x), 10x NKC CM in standard medium or 10x standard medium in standard medium (10x). *Gapdh* was used as reference gene. (a) No further increase in *Gdnf* expression was detected when more concentrated NKC CM was applied, although D1 cells stimulated with different concentrations of NKC CM showed up-regulation of *Gdnf* in comparison to unstimulated cells. (b) D1 cells stimulated with correspondingly 10x concentrated standard culture medium showed also some up-regulation of *Gdnf* in comparison to unstimulated cells.

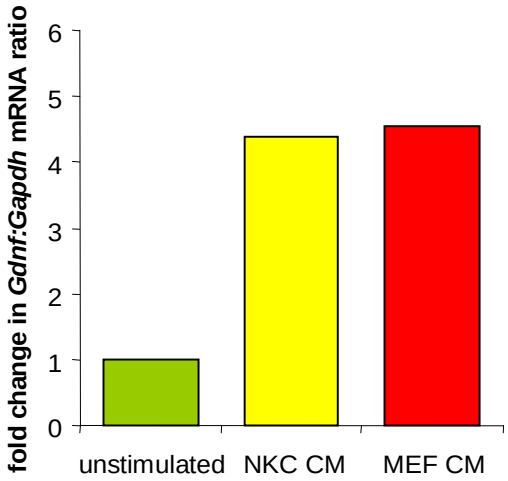

Figure 5.6 Comparison of *Gdnf* expression levels in unstimulated, MEF CM- and NKC CM-stimulated D1 cells using reverse transcription quantitative PCR. D1 cells stimulated with MEF CM showed similar up-regulation in *Gdnf* expression as with NKC CM. *Gapdh* was used as reference gene.

Finally, it has been described that stimulation with Gdnf results in induction of Gdnf expression in kidney-derived MSCs (Shi et al. 2008). The lowest concentration of Gdnf described to induce Gdnf expression in MSCs was 20ng/ml (Shi et al. 2008). Accordingly, in order to test if *Gdnf* expression may be induced by the presence of Gdnf in NKC CM or MEF CM, D1 cells were stimulated with different concentration of Gdnf (1ng/ml, 10ng/ml, and 50ng/ml) for 4 days. Exogenous Gdnf induces UB branching in metanephric kidney cultures (Vega et al. 1996; Sainio et al. 1997). Therefore the activity of Gdnf used for stimulation was confirmed by stimulating E11.5 kidney with 50ng/ml Gdnf for 4 days. Subsequently the UBs were visualized using calbindin staining (Davies 1994). Accordingly, kidneys stimulated with Gdnf demonstrated increased branching morphogenesis in comparison with unstimulated rudiments confirming that Gdnf used in this study is active (Figure 5.7a). However, as demonstrated in Figure 5.7b none of the Gdnf concentrations tested was able to elicit *Gdnf* up-regulation in D1 cells. It appeared

that D1 cells do not express *Ret* gene, which encodes the Ret receptor that is important in Gdnf signalling (Vega et al. 1996). Figure 5.7c demonstrates expression of *Ret* in E13.5 kidneys and its absence in D1 cells.

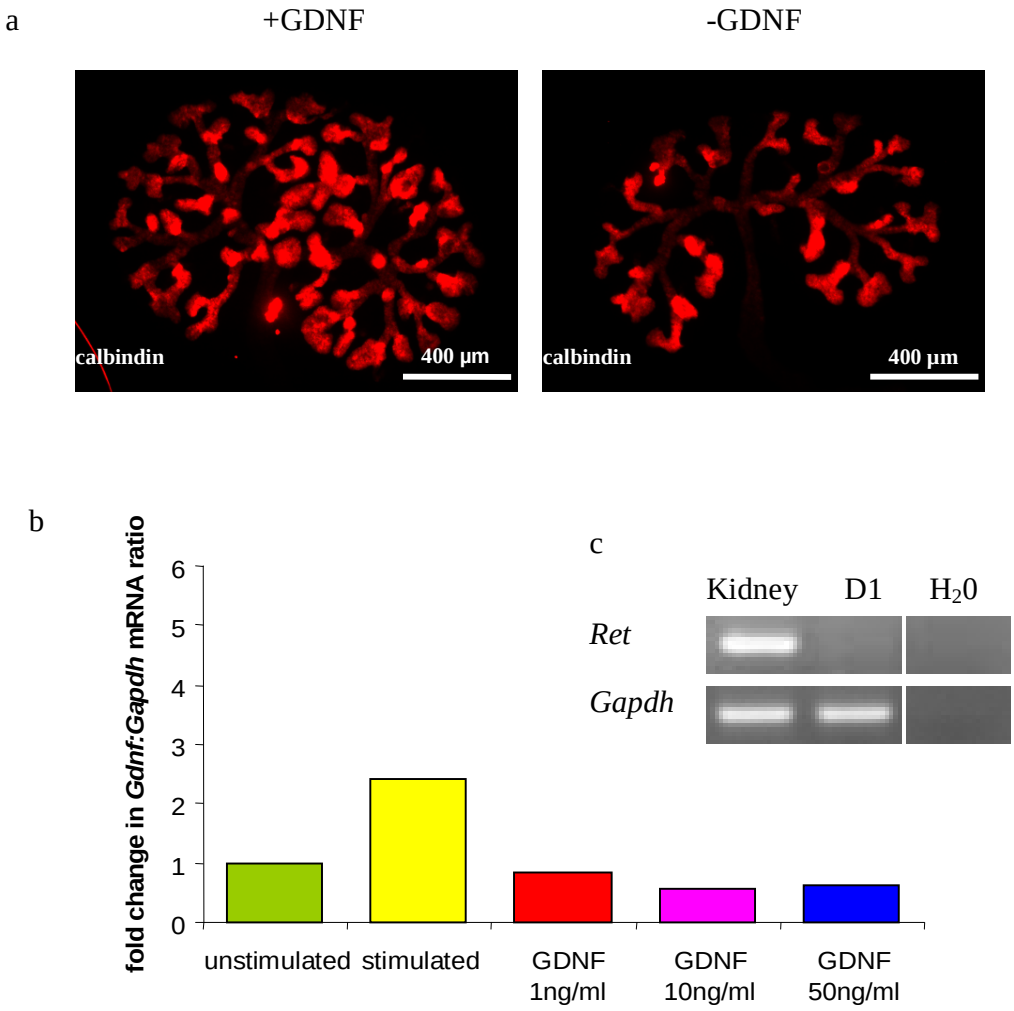

Figure 5.7 Comparison of *Gdnf* expression levels in unstimulated, NKC CM-stimulated D1 cells and D1 cells stimulated with different concentrations of Gdnf using reverse transcription quantitative PCR and subsequent analysis of *Ret* expression in D1 cells. *Gapdh* was used as reference gene for all experiments. (a) Increase in UB branching in E11.5 kidney after stimulation with Gdnf for 4 days demonstrating that Gdnf used for stimulation of D1 cells is active. Calbindin staining is visualising the UBs. (b) D1 cells stimulated with 1ng/ml, 10ng/ml and 50ng/ml of Gdnf showed no up-regulation in *Gdnf* expression in comparison with stimulated cells with NKC CM. (c) No expression of Gdnf receptor *Ret* was detected in D1 cells using semi-quantitative PCR. E13.5 kidney was used as a positive control and no template control was included (H2O).

Chimeric kidney assay using D1 cells stimulated with NKC CM

Next, D1 cells stimulated with NKC CM were assessed for their renogenic potential using the chimeric kidney culture system, described previously in Chapter 4. Both unstimulated and NKC CM-stimulated D1 cells were recombined with E11.5 kidney cell suspension in a 1 to 5 ratio. After 4 days of chimeric kidney culture, confocal microscopy was used to evaluate the localization of both unstimulated and stimulated QD-labelled D1 cells within renal structures. Although many labelled cells were still found in the Wt1- and laminin-negative compartment, incubation with NKC CM considerably improved the engraftment of QD-labelled D1 cells into condensing MM stained for Wt1, as demonstrated in Figure 5.8a-h.

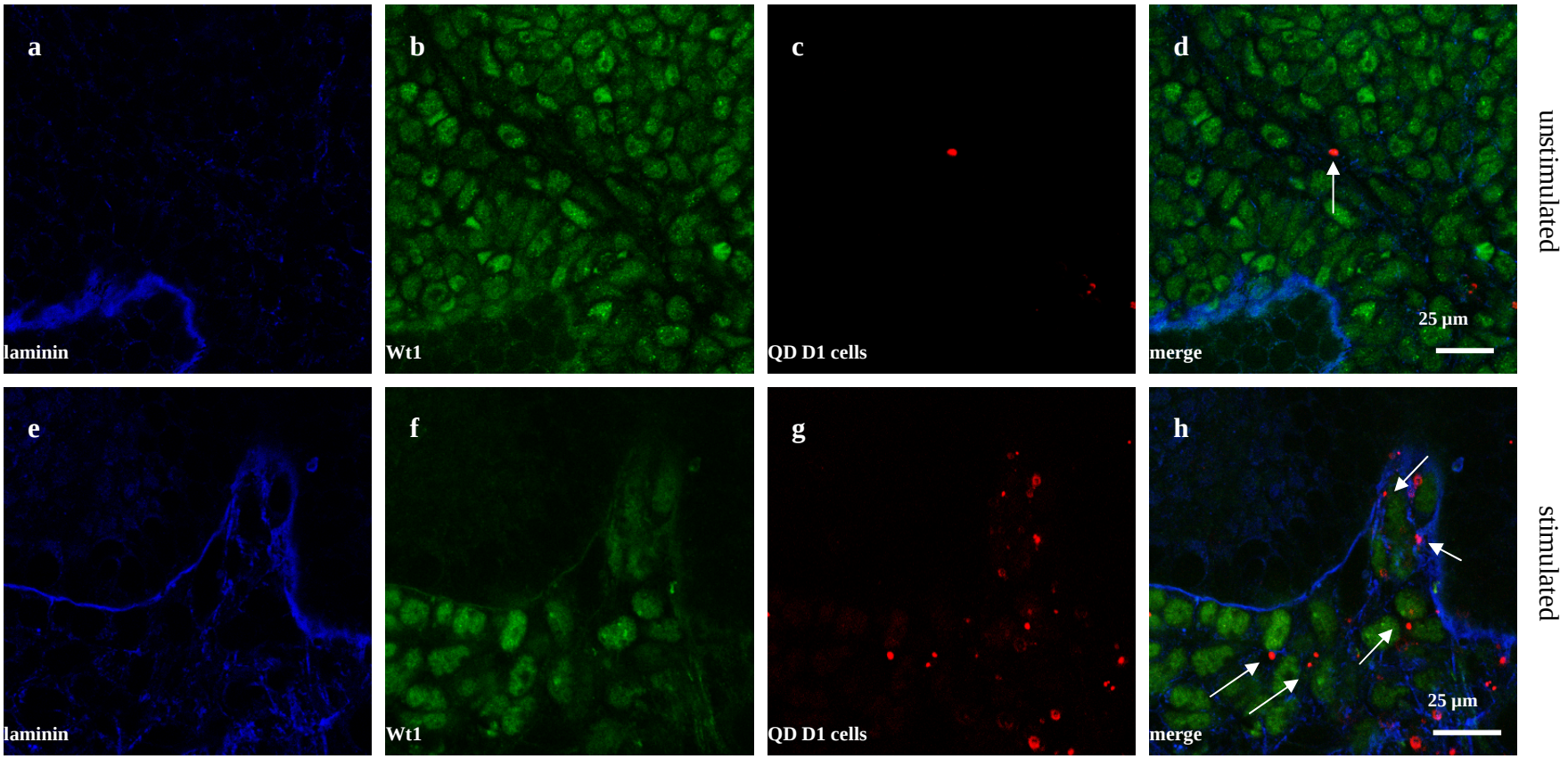

Figure 5.8 The contribution of QD-labelled D1 cells to nephrogenesis following treatment with NKC CM for 4 days in chimeric kidney rudiment assay. Considerably more stimulated D1 cells were found in Wt1-expressing mesenchyme in comparison with unstimulated cells after 4 days of culture. Representative images of kidney chimeras are shown (performed in at least in 3 independent experiments). (a-d) Engraftment potential of QD-labelled D1 cells cultured in standard medium into renal structures stained with Wt1 and laminin. Arrow indicates a D1 cell that has integrated into condensing mesenchyme. (e-h) Engraftment potential of NKC CM-stimulated QD-labelled D1 cells into renal structures stained with Wt1 and laminin. Arrows indicate NKC CM-stimulated D1 cells that have integrated into condensing mesenchyme.

In order to quantify the difference in incorporation rates into renal structures between stimulated and unstimulated QD D1 cells, a total number of cells counted in five random fields was assessed and compared against the number of cells found in different kidney compartments in the same five fields for both conditions. The following compartments have been considered: the Wt1-positive compartment representing the Wt1-expressing condensing MM; the laminin-positive compartment representing the UBs; the Wt1- and laminin-positive compartment representing the nephrons; and, finally, the Wt1- and laminin-negative compartment representing the stroma. Three separate experiments were performed for both conditions. As depicted in Figure 5.9a, most of the D1 cells in both conditions were localised in the Wt1- and laminin-negative compartment. Both unstimulated and NKC CM-stimulated D1 cells were also present to some extent in the Wt1-expressing compartment; however, more stimulated cells were found in the condensing MM. On average, 3.75% of all counted cells that were pre-treated with NKC CM before recombination, were found within Wt1-expressing mesenchyme, in comparison with only 1.18% for unstimulated D1 cells (Figure 5.9a). Occasionally both unstimulated and NKC CM-stimulated D1 cells were detected in the Wt1- and laminin-positive compartment (Figure 5.9a). There was also little engraftment into laminin-positive structures detected in both conditions (Figure 5.9a). Taken together, the integration rate of QD D1 cells into all Wt1-positive compartments, the condensing mesenchyme and nephron-like structures, upon stimulation with NKC CM increased significantly (i.e., up to 3.6 fold) ($p<0.05$, $n=3$) (Figure 5.6 b).

a

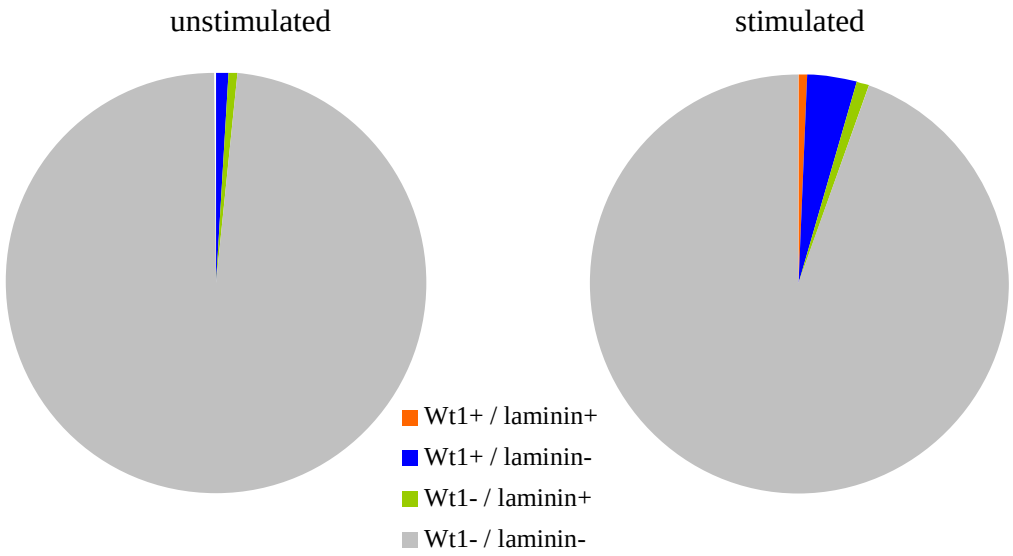

	unstimulated	stimulated
Wt1+ / laminin+	0,06	0,73
Wt1+ / laminin-	1,18	3,75
Wt1- / laminin+	0,41	1,19
Wt1- / laminin-	98,35	94,33

b

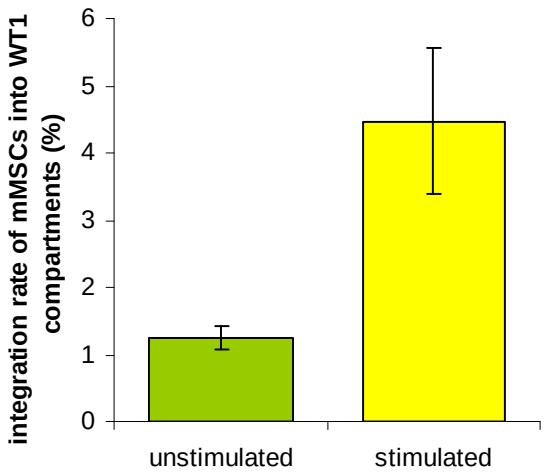

Figure 5.9 Statistical analysis of integration rate of unstimulated versus NKC CM-stimulated QD-labelled D1 cells into different compartments of chimeric kidney after 4 days of culture. (a) Percentage of unstimulated versus stimulated QD-labelled cells found in different kidney compartments counted in 3 separate experiments (b) QD D1 cells showed 3.6 fold increase in engraftment into condensing mesenchyme and nephron-like structures after 4 days of preconditioning with NKC CM in comparison with unstimulated QD D1 (*t*-test, $p<0.05$, $n=3$).

The recombination experiments were repeated with D1 cells labelled with GFP in order to confirm the results obtained with QD-labelled cells. Figure 5.10e-h shows that GFP D1 cells stimulated with NKC CM demonstrated considerable engraftment potential into the Wt1-positive MM. Occasionally, the presence of laminin around condensing mesenchyme harbouring pre-treated GFP-labelled cells was observed, indicating the possible start of nephron formation (Figure 5.10h arrowheads). In comparison, cells not stimulated with NKC CM displayed a lower integration potential into Wt1-positive MM, as shown in Figure 5.10a-d. In order to further confirm the presence of D1 cells within chimeric kidney structures, immunostaining was performed for Six2, which is expressed in nephron progenitor populations (Kobayashi et al. 2008), and calbindin, found mainly in ureteric buds (Davies 1994) (Figure 5.10a-h). Consequently, NKC CM-stimulated GFP D1 cells were found in higher numbers in Six2 positive MM than unstimulated cells, as shown in the Figure 5.11e-h. In both conditions, there was no engraftment into ureteric buds, stained for calbindin, confirming previous observations (Figure 5.11a-h).

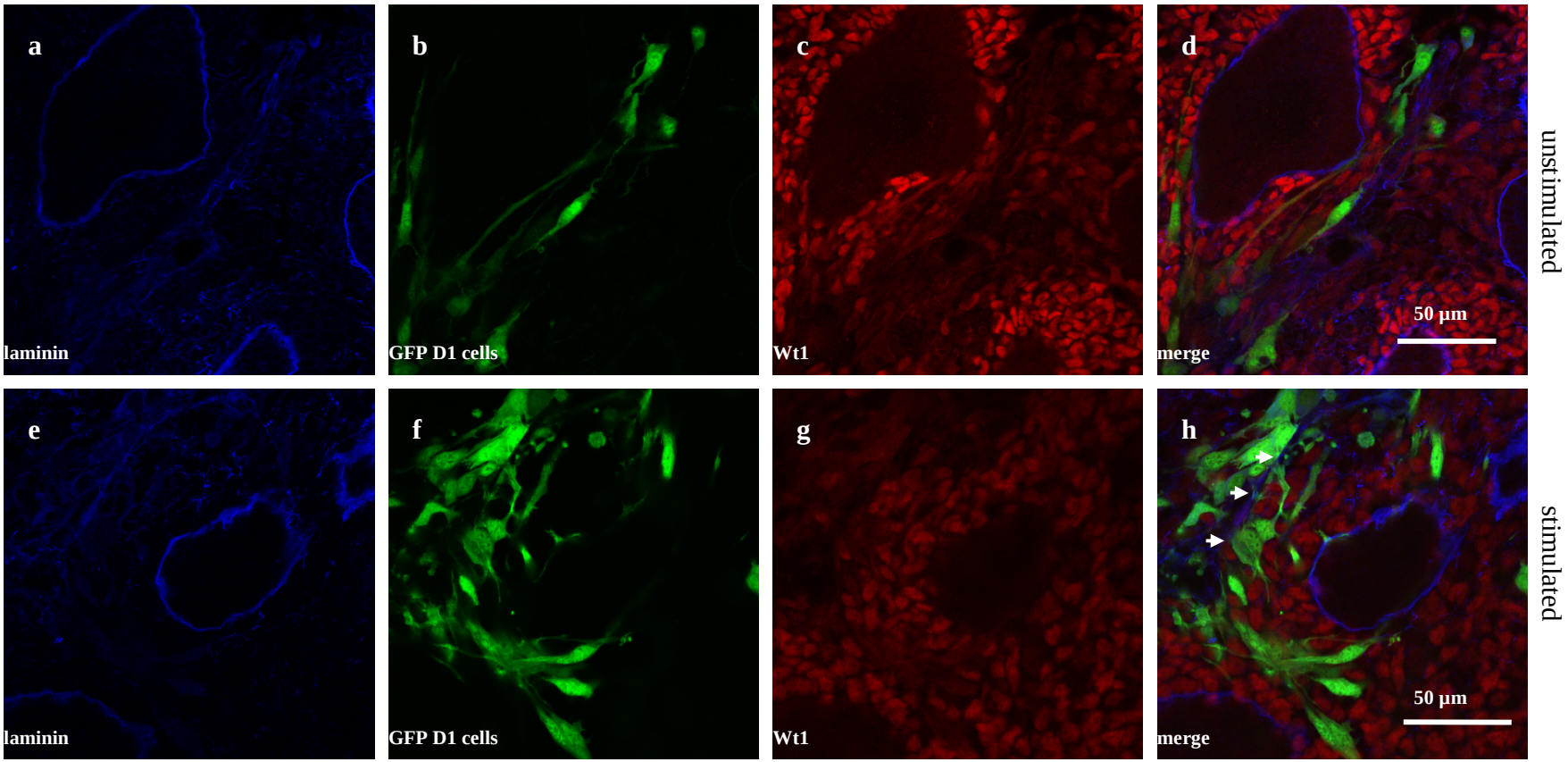

Figure 5.10 The contribution of GFP-labelled D1 cells to nephrogenesis following treatment with NKC CM for 4 days in chimeric kidney rudiment assay. Considerably more stimulated D1 cells were found in Wt1-expressing mesenchyme in comparison with unstimulated cells after 4 days of culture. Representative images of kidney chimeras are shown (performed in at least in 3 independent experiments). (a-d) Engraftment potential of GFP D1 cells not stimulated with NKC CM into developing renal structures stained with Wt1 and laminin. (e-h) Engraftment potential of GPF D1 cells stimulated with NKC CM into developing renal structures stained with Wt1 and laminin. Arrowheads indicate presence of laminin staining around Wt1-expressing region harbouring GFP cells.

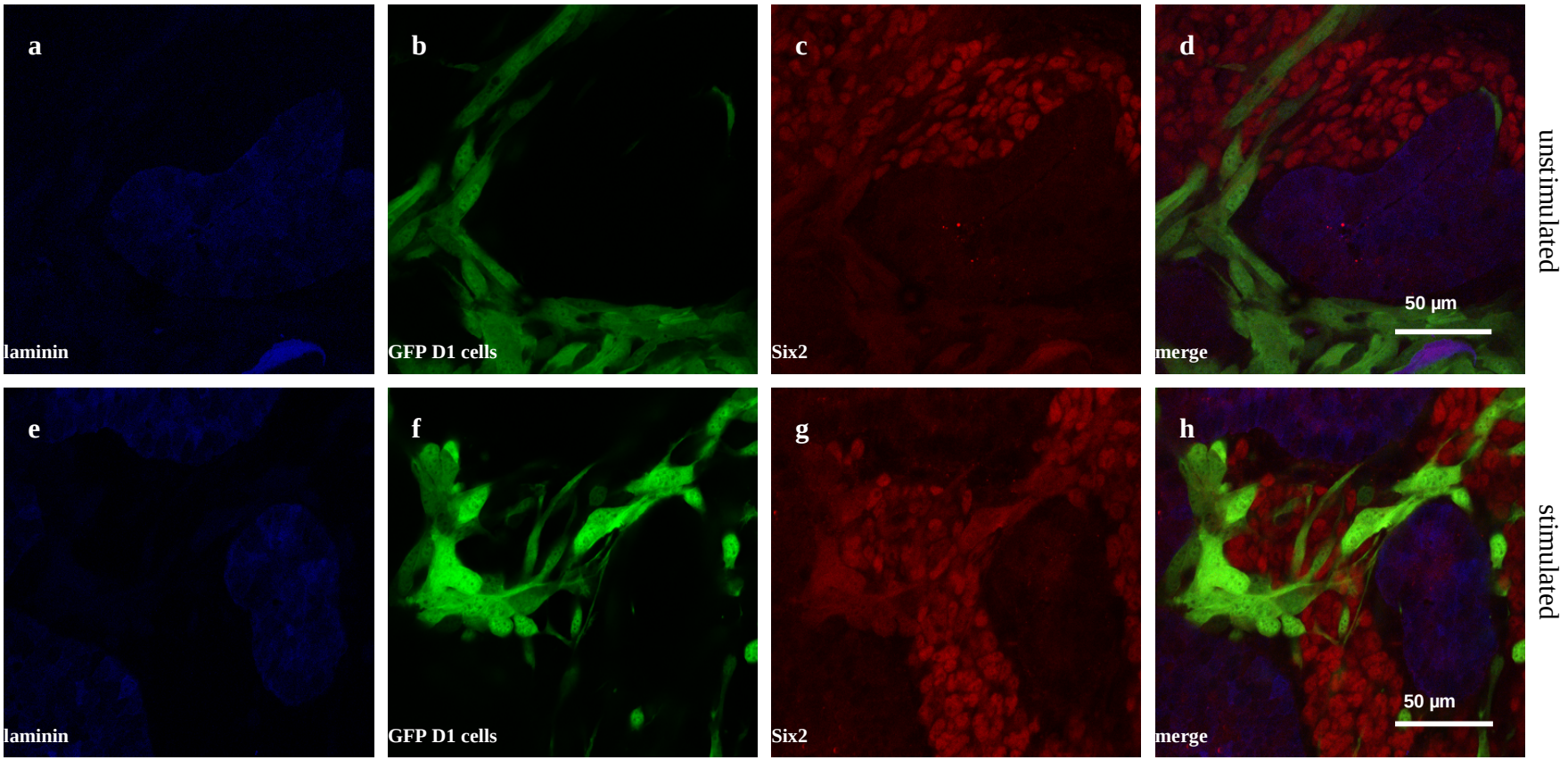

Figure 5.11 The contribution of GFP-labelled D1 cells to nephrogenesis following treatment with NKC CM in chimeric kidneys assay. It appeared that more stimulated D1 cells were found in Six2 expressing mesenchyme in comparison with unstimulated cells after 4 days of culture. No integration into calbindin positive ureteric buds was detected in any condition. Representative images of kidney chimeras are shown (performed in at least in 2 independent experiments). (a-d) Engraftment potential of GFP D1 cells not stimulated with NKC CM into developing renal structures stained with Six2 and calbindin. (e-h) Engraftment potential of GPF D1 cells stimulated with NKC CM into developing renal structures stained with Six2 and calbindin.

Accordingly, incorporation rates between NKC CM-stimulated and unstimulated D1 cells were evaluated. Similarly as for QD-labelled cells, a total number of GFP D1 cells counted in five random fields was assessed and compared against the number of GFP cells found in different kidney compartments in both conditions in three separate experiments (Figure 5.12a and b). Most GFP-labelled cells remained in the Wt1- and laminin-negative compartment of chimeric kidneys, as demonstrated in Figure 5.12a. On average, 13.29% of NKC CM-stimulated GFP D1 cells and 3.37% unstimulated GFP D1 cells was found within Wt1-expressing compartment in the kidney chimeras (Figure 5.12a). No integration into laminin-positive or Wt1- and laminin-positive structures was counted in any of the conditions (Figure 5.12a). As demonstrated in Figure 5.12b, the integration rate of GFP D1 cells into condensing mesenchyme upon stimulation increased up 3.9 fold. However the increase was not statistically significant ($p>0.05$, $n=3$).

In addition, it appeared that chimeric kidneys harbouring NKC CM-stimulated D1 cells developed better than kidneys that were reformed using unstimulated D1 cells. There were considerably more Wt1-positive regions as well as developing nephron-like structures in chimeras harbouring stimulated D1 cells. Accordingly, effects exerted by stimulated D1 cells on metanephric development are described in detail in the subsequent chapter.

a

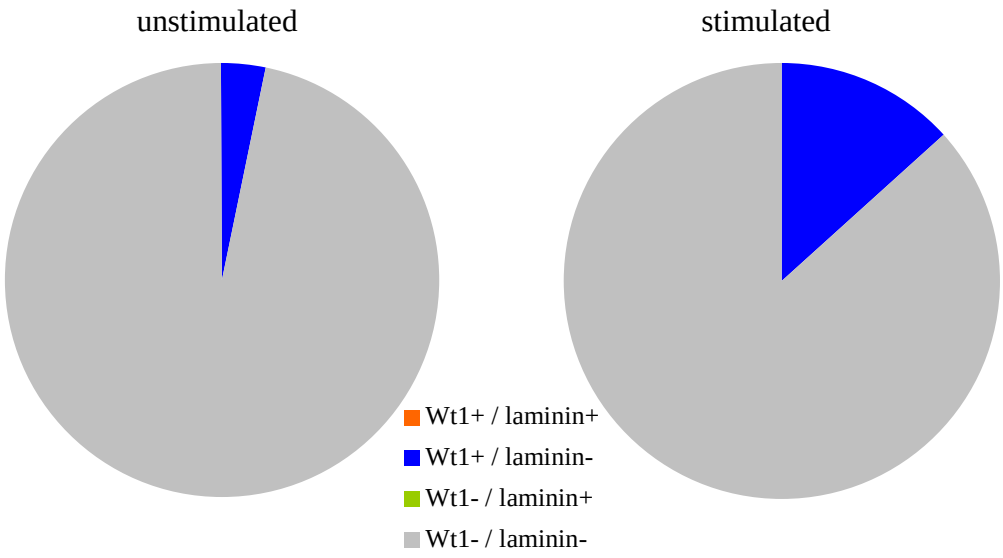

	unstimulated	stimulated
Wt1+ / laminin+	0	0
Wt1+ / laminin-	3,37	13,29
Wt1- / laminin+	0	0
Wt1- / laminin-	96,63	86,71

b

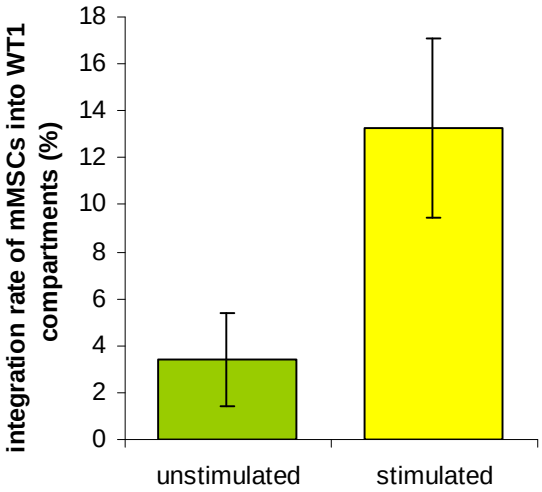

Figure 5.12 Statistical analysis of integration rate of unstimulated versus NKC CM-stimulated GFP-labelled D1 cells into different compartments of chimeric kidney after 4 days of culture. (a) Percentage of unstimulated versus stimulated GFP-labelled cells found in different kidney compartments counted in 3 separate experiments. (b) Stimulated GFP D1 cells showed considerable increase in engraftment into condensing mesenchyme after 4 days of culture, however this difference was not statistical significant (*t*-test, $p>0.05$, $n=3$).

In summary, the stimulation with NKC CM increased in D1 cells the expression of *Gdnf*, an important factor for UB development. It was demonstrated that the use of concentrated NKC CM does not induce any further increase in *Gdnf* expression in stimulated cells. Furthermore, exogenous Gdnf was not able to induce *Gdnf* up-regulation in D1 cells. Finally, conditioned medium derived from MEFs can similarly to NKC CM, increase expression of *Gdnf* in D1 cells after 4 days of stimulation. In addition, it has been demonstrated that stimulation of D1 cells for 4 days with NKC CM facilitates their integration into condensing MM in the chimeric kidney rudiment culture. However, there is a discrepancy in the number of integrated cells depending on the labelling method. Accordingly, 13.29% of NKC CM-stimulated D1 cells labelled with GFP were present in the condensing MM in the kidney chimeras after 4 days of culture in comparison with only 4.5% of NKC CM-stimulated D1 cells labelled with QDs.

5.2.3. Renogenic potential of human MSCs stimulation with NKC CM

In order to assess if human MSCs respond to NKC CM treatment in the same way as D1 cells, human MSCs were cultured in the presence of NKC CM for 4 days prior to the integration experiment. Figure 5.13a-h shows that stimulation with NKC CM had no effect on human MSC integration potential. Human MSCs did not integrate into condensing MM and developing nephron-like structures. Similarly as described in the previous chapter, recombination with human MSCs appeared to have a negative effect on the development of the chimeric kidneys, irrespective of whether the cells had been previously cultured in standard, or NKC CM media.

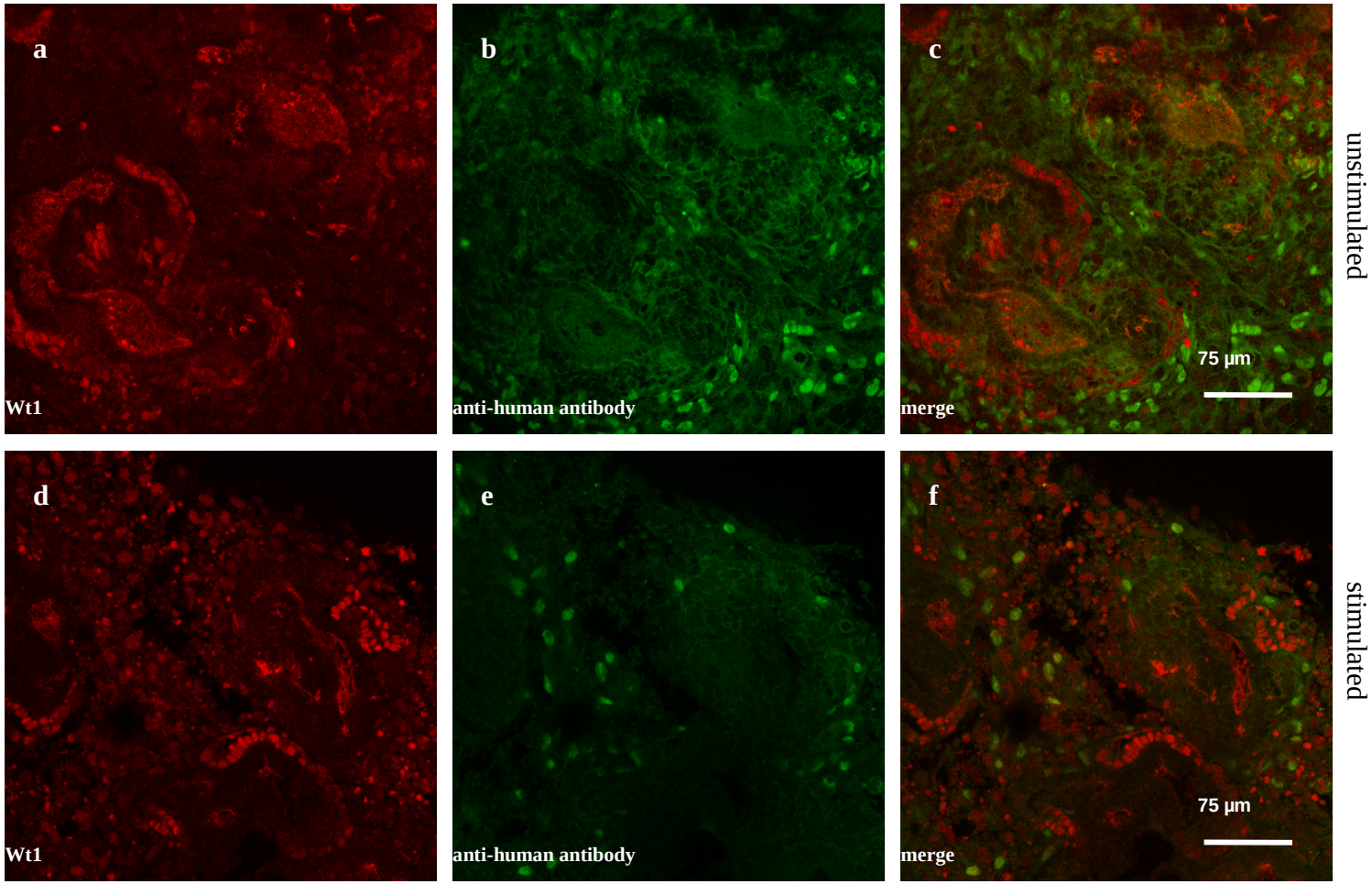

Figure 5.13 The contribution of human MSCs to nephrogenesis following treatment with NKC CM in chimeric kidney rudiment assay. Both unstimulated and NKC CM- stimulated human MSCs were mainly found in the Wt1 negative compartment of developing chimeras after 4 days of *in vitro* culture. Representative images of kidney chimeras are shown. (a-c) Engraftment potential of human MSCs labelled with anti-human nuclei antibody into developing renal structures stained for Wt1. (d-f) Engraftment potential of labelled human MSCs stimulated with NKC CM into developing renal structures stained for Wt1.

Taken together, pre-treatment with NKC CM could not increase the integration rate of human MSCs into chimeric kidney structures. The stimulation with NKC CM could not avert the negative effects exerted by human MSCs on metanephric development, although it seemed to prevent the detrimental action in mouse MSCs.

5.3. Discussion

Stimulation with conditioned medium from a particular culture can trigger changes in morphology and expression profile of MSCs and hence induce them to differentiate (Rivera et al. 2006; Pan et al. 2008; Baer et al. 2009; Schittini et al. 2010). In this chapter, mouse and human MSCs were stimulated with NKC CM in order to see if this treatment could induce a renal phenotype and subsequently increase their contribution to metanephric development. NKC CM-treated D1 cells maintained multilineage differentiation potential and similarly to D1 cells cultured in standard culture condition, expressed a number of MM-specific genes. In addition, the stimulation with NKC CM resulted in up-regulation in *Gdnf* expression in stimulated D1 cells. The pre-conditioning with NKC CM considerably increased the engraftment potential of D1 cells into the condensing MM and developing nephron-like structures of chimeric kidneys. In addition, stimulated D1 cells did not appear to have any detrimental effect on metanephric development of the chimeras. In contrast, stimulation with NKC CM did not facilitate integration of human MSCs into the developing structures of chimeric kidneys.

5.3.1. Characteristics of D1 cells stimulated with NKC CM

In this study, D1 cells were incubated with conditioned medium from a kidney cell population, in order to enhance their renogenic potential. As described by Baer *et al.*, stimulation with conditioned medium from human renal proximal tubular cells can initiate epithelial

differentiation in human adipose-derived MSCs. After 12 days of incubation with conditioned medium obtained from renal cells, human MSCs changed their morphology to become epithelial-like and started to express an early epithelial marker - cytokeratin 18 (Baer et al. 2009). After 4 days of stimulation with NKC CM, no change to epithelial-like morphology was observed in D1 cells. However, stimulated D1 cells appeared more aligned than unstimulated D1 cells. Further, D1 cells maintained multipotency after stimulation with NKC CM. Both unstimulated and stimulated D1 cells showed adipogenic, osteogenic and chondrogenic potential which is characteristic for MSC populations (Peister et al. 2004). However, fewer cells after NKC CM seemed to accumulate lipid vacuoles in comparison with unstimulated D1 cells. Following the osteogenic induction, both unstimulated and stimulated cells displayed calcium deposits. Unexpectedly, in this condition, some cells stimulated with NKC CM also exhibited lipid vacuoles, similar to those found during *in vitro* adipogenesis. However it is important to note that these vacuoles have not been stained to confirm the presence of lipids. Adipocytes and osteoblasts originate from a common mesenchymal progenitor and the presence of dexamethasone in inductive medium is modulating adipogenesis and osteogenesis in MSCs (Mikami et al. 2010). A similar but converse situation was described for adipose-derived human MSCs: adipose-derived MSCs at later passages were shown to form both lipid vacuoles and calcium deposits when induced with adipogenic medium (Wall et al. 2007).

5.3.2. Expression profile of D1 cells stimulated with NKC CM

In the previous chapter, the expression of embryonic kidney markers such as *Osr1*, *Sall1*, *Lim1* and *Gdnf* was described in D1 cells. D1 cells continued to express the aforementioned genes after stimulation with NKC CM. Further, no expression of *Wt1*, *Pax2* and *Six2* was induced by the pre-

conditioning. Similarly, no expression of *Rarβ2* has been induced in stimulated D1 cells. Nevertheless some weak expression of *Bf2* has been observed in NKC CM pre-treated cells. *Bf2* is expressed in stromal cells found around the condensing MM and at the periphery of the kidney rudiment (Hatini et al. 1996). This could suggest that the stimulated cells are triggered to become kidney stromal cells and consequently will more likely integrate into the stromal compartment of metanephric kidney. However, Bf2 expression during embryogenesis is not restricted to the kidney. Bf2 has been found also in the neuroepithelium during development of the central nervous system (Hatini et al. 1994). NKC CM-stimulated D1 cells showed also a significant up-regulation in *Gdnf* expression. Gdnf over-expression was shown to enhance the integration potential of human MSCs into metanephric kidney (Yokoo et al. 2005). Therefore it is possible that the stimulation with NKC CM could increase the engraftment potential of MSCs in the chimeric kidney rudiment assay.

Further, stimulation with concentrated NKC CM did not result in additional increase in *Gdnf* expression in D1 cells. Still, the expression remained higher than in unstimulated D1 cells. Surprisingly, stimulation with concentrated standard culture medium had also some positive effect on *Gdnf* expression. As a consequence, *Gdnf* expression in D1 cells following stimulation with 2x and 10x NKC CM was to some extent downregulated when *Gdnf* expression levels were compared against *Gdnf* expression levels found in cells stimulated with the corresponding concentration of standard culture medium for the same period of time. This could imply that standard culture medium already contains factors that are responsible for *Gdnf* up-regulation. Furthermore, conditioned medium derived from mouse embryonic fibroblasts had a similar effect on *Gdnf* expression as medium derived from NKCs. This medium, however, has not been used

for pre-conditioning of MSCs in the chimeric kidney assay.

It is not clear which factors present in the conditioned media induce *Gdnf* up-regulation in D1 cells. As it was shown that exogenous Gdnf triggers expression of Gdnf in kidney-derived MSCs (Shi et al. 2008), it was investigated if one of the factors inducing *Gdnf* expression could be Gdnf present in the conditioned medium. Accordingly, different concentrations of Gdnf were used to stimulate D1 cells for 4 days; however Gdnf was not able to induce *Gdnf* expression in the cells, irrespective of the concentration used, suggesting that the mechanism of *Gdnf* induction remains different in D1 cells than in kidney-derived MSCs.

5.3.3. Renogenic potential of MSCs stimulated with NKC CM

It has been demonstrated earlier by Yokoo *et al*. that MSCs can be reprogrammed to differentiate during metanephric development into the glomerular and tubular epithelium (Yokoo et al. 2005). Using the chimeric kidney rudiment system introduced in Chapter 4, D1 cells were shown only to contribute to nephrogenesis to a limited extent. In an attempt to increase the integration potential of MSCs, before performing the recombination assay, MSCs were stimulated with a mix of NKC CM and standard culture medium for 4 days. This was followed by 4 days of *in vitro* chimeric kidney culture. Consequently, the preconditioning with NKC CM improved the engraftment potential of D1 cells into condensing MM, characterised by the expression of Wt1 or Six2. At the same time, D1 cells pre-treated with NKC CM were also infrequently found in developing nephron-like structures characterised.

In addition, using the calbindin staining to visualise ureteric buds it has been possible to confirm that neither unstimulated nor stimulated GFP D1 cells integrate into the ureteric buds of chimeric kidneys. This is in accordance with previous data (Fukui et al. 2009). It has been

demonstrated that human bone marrow-derived MSCs expressing chicken Pax2 transplanted into a chicken embryo, can migrate along the elongating Wolffian duct and integrate into the Wolffian duct epithelia but do not engraft into the ureteric bud (Fukui et al. 2009).

Furthermore, the presence of numerous D1 cells in Wt1- and laminin-negative compartment was detected in both conditions. However, due to a lack of availability of an appropriate stromal marker, it was impossible to conclude if D1 cells found in this compartment are differentiating into stroma or rather represent a fraction of undifferentiated D1 cells. No study was also attempted to elucidate if cells found in the Wt1- and laminin-negative compartment are proliferating, which might explain the high numbers of D1 cells in the compartment.

Some human MSCs that were injected into rat embryos according to Yokoo`s protocol were expressing Wt1 when integrated into metanephric kidneys (Yokoo et al. 2005). Using QD-labelled D1 cells, it was possible to detect in the chimeric kidneys some D1 cells that expressed Wt1. However, the expression could not be confirmed using GFP labelling. Upon stimulation with NKC CM, the GFP cells did not acquire Wt1 expression, although stimulated QD-labelled cells were still found to be Wt1 positive when integrated into Wt1 expressing regions. There are several possibilities explaining this result which were discussed in the previous chapter (section 4.3.2).

Surprisingly, the stimulation with NKC CM did not facilitate integration of human MSCs. One explanation of this fact could be that the human MSCs are not able to respond to factors found in the conditioned medium obtained from mouse kidney cells. For instance, it has been described that mouse and human bone marrow cells differently respond to feeder layers from patients with acute granulocytic leukaemia. Accordingly, mouse marrow colony growth was stimulated by

the feeder layer while no colony growth occurred in normal human marrow (Lind et al. 1974). Another possibility is that the human cells require a different set of factors to trigger their engraftment than mouse MSCs, which possess some initial integration potential.

In conclusion, these data suggest that the pre-conditioning of D1 cells helps to increase the integration rate of the cells into condensing mesenchyme in the chimeric kidney model. In contrast, stimulation with NKC CM is insufficient to trigger engraftment of human MSCs. Accordingly, the difference in incorporation rates between stimulated and unstimulated D1 cells was evaluated and the outcomes of this analysis are discussed below.

5.3.4. Analysis of integration potential of D1 cells stimulated with NKC CM

In order to analyse the difference in incorporation between stimulated and unstimulated D1 cells, integration of the cells into different kidney compartments was assessed in three independent recombination experiments. Following stimulation with NKC CM, most D1 cells remained in the Wt1- and laminin-negative compartment of chimeric kidneys, similar to unstimulated cells. The second largest compartment, where stimulated D1 cells were localised upon recombination, was the Wt1-expressing MM. However, there is a discrepancy in the number of integrated cells depending on the labelling method used. On average, 3.75% of stimulated QD D1 cells and 1.18% of unstimulated QD D1 cells were found in the Wt1-positive compartment, whereas 13.29% of stimulated GFP D1 cells and 3.37% of unstimulated GFP D1 cells was localised within Wt1-positive compartment. This implies a 3.54-fold increase in the number of counted stimulated GFP cells versus stimulated QD cells, and a 2.86-fold increase in the number of counted unstimulated GFP cells versus unstimulated QD cells. One explanation for this result could be that some QDs were lost during the *in vitro* 4 day culture period. A quick loss of QD

labelling has been described in mouse embryonic stem cells (ESCs) and mouse embryonic fibroblasts (MEFs) (Pi et al. 2010). Also for human MSCs, a loss of QD labelling has been observed over a long period of time (Rosen et al. 2007). Indeed in section 3.2.1 it was demonstrated that D1 cells labelled with QDs remained stained *in vitro* for 5 days but fewer QDs were detected inside the cells on day 5 than directly after labelling. However, no quantification of D1 cells maintaining the labelling after 5 days of culture was attempted. Although a difference in the integration potential of D1 cells labelled with the two techniques was observed, both QD and GFP labelled D1 cells stimulated with NKC CM demonstrated a similar raise in engraftment into condensing mesenchyme, suggesting that if loss of labelling occurred it had to be similar in all cells.

A discrepancy between the integration rate of QD and GFP labelled D1 cells into laminin positive compartments highlights also the problems associated with labelling. While neither unstimulated nor stimulated GFP-labelled cells were detected in laminin positive tubular structures, both unstimulated and stimulated QD D1 cells were found in this compartment. Additionally, an increase in integration of stimulated QD cells versus unstimulated was detected in the laminin-positive compartment. In general, the renogenic potential of D1 cells seems to differ considerably depending on the labelling method used. While QD D1 cells show broad engraftment potential including stroma, condensing MM, nephron-like structures and UBs, GFP labelled cells display only integration potential into condensing MM. One explanation for those observations could be the fact that QDs can be excreted from D1 cells or remain in the structures after the cells underwent apoptosis, giving a false positive signal. Another possibility includes the transfer of QDs to kidney cells. It was shown that QDs found in the supernatant of labelled cells can be

further utilized for labelling of other cells (Pi et al. 2010). An additional labelling method should be considered to confirm the data using QD and GFP cells. Some other labelling methods for MSCs could include labelling with the lipophilic membrane dye Dil (Challen et al. 2006), sex chromosome staining (Morigi et al. 2004), as well as labelling with the analogue 5-bromo-2'deoxyuridine (BrdU) which only can be incorporated by proliferating cells (Kunter et al. 2006).

Although the integration of GFP-labelled cells increased upon stimulation, differently as for QD-labelled cells, the increase was not statistically significant. When reforming the embryonic kidneys some variability among the chimeras is observed that could lead to differences in integration rate. For example, the chimeras often have slightly different sizes as some cells are lost during the transfer onto the filter. Also since metal grids supporting the filter have to some extent different dimensions, differences in volume of culture medium used for culturing chimeras occur that can affect the growth of chimeras. As the number of samples used for the integration statistics was small, more experiments using D1 cells labelled with both techniques should be performed in order to confirm the statistical significance.

Finally, a difficulty in interpreting the integration results is the lack of information on apoptosis and proliferation of the cells in the chimeras. It has been suggested by Yokoo *et al*. that human MSCs in the kidney rudiments are undergoing cell division (Yokoo et al. 2005). It is possible that stimulated D1 cells in MM proliferate faster than unstimulated cells and this causes higher prevalence of stimulated D1 cells in the MM. Therefore the ratios obtained in these experiments do not reflect exact numbers of integrated cells but rather describe a trend in integration and cannot be used to fully describe the behaviour of the cells in chimeric kidneys.

5.3.5. Renogenic potential of D1 cells stimulated with NKC CM compared with other stem cells

It is difficult to compare the number of integrated stimulated D1 cells using the recombination method with the integration described by Yokoo *et al*. since no exact quantification of MSC engraftment was provided (Yokoo et al. 2005). However, it is possible to make some comparison in integration capability into different renal compartments between stimulated D1 cells and kidney cells. Challen *et al*. injected mouse kidney-derived cells into mouse E12.5 metanephroi followed by 3 days of *in vitro* culture, in order to evaluate their differentiation potential in the metanephric development (Challen et al. 2006). For the kidney side population, a renal progenitor population, 29% of cells were found in MM stained with Wt1, whereas 14% of the cells incorporated into UBs stained with calbindin. Further, 9% of cells derived from adult kidneys, which did not display the kidney side population characteristics, were detected in MM and 1% of these cells was present in the UBs (Challen et al. 2006). D1 cells, both unstimulated and stimulated with NKC CM, therefore have a lower engraftment potential into Wt1-expressing mesenchyme than kidney progenitors. Nevertheless, D1 cells stimulated with NKC CM possess a higher potential to integrate into Wt1-expressing mesenchyme when compared with adult kidney cells, according to the data obtained with GFP D1 cells. Since no quantitative analysis using calbindin was performed in the kidney chimeras it is difficult to directly compare the integration of D1 cells and kidney progenitors into UBs. However, according to the data obtained with calbindin staining and GFP labelled D1 cells, D1 cells have no potential to contribute to UB formation.

In addition, there exists also limited data on the extent of ESC integration into developing renal

structures. Steenhard *et al*. described that after injecting undifferentiated mouse ESCs into E13 mouse kidney rudiments, ESCs were forming tubules. By day 2, over 50% of all structures containing ESCs were identified as tubules, whereas the remaining cells were characterised as single cells, clusters of cells or dying cells (Steenhard et al. 2005). Further, it has been described that mouse ESC-derived cells injected into E12.5 kidney cultured for 4 to 5 days can be found in the tubules, the interstitium and peripheral mesenchyme. The percentage of surface area occupied by ESC-derived cells in the metanephroi was 60% and 40% for non-tubular and tubular structures, respectively (Kim and Dressler 2005). In comparison, mouse ESC-derived cells stimulated with nephrogenic factors exclusively formed tubular structures (Kim and Dressler 2005). Finally, no quantification of integration potential of amniotic fluid stem cells (AFSCs) into different kidney compartments was provided until now. However a recent report showed that modulation of mTOR activity in AFSCs decreases their ability to contribute to renal structures in the chimeric kidney assay (Siegel et al. 2010).

Finally, in the chimeric kidneys, both unstimulated and stimulated D1 cells were found frequently outside the MM, MM-derived structures and UBs. An important question remains: is this a feature of MSCs, or do all other stem cell types preferentially localise outside renal structures? The statistical data on integration of kidney progenitors and kidney-derived cells into MM and UBs demonstrated by Challen *et al*. implicates that both populations are mainly found within the Wt1- and calbindin-negative compartment of injected metanephroi (Challen et al. 2006), perhaps the stromal compartment. Furthermore, results obtained with label retaining tubular cells (LRTC) isolated from rat kidneys demonstrated that 60% of LRTC injected into E15 rat embryonic kidneys were localized in the interstitium after 5 days of culture (Maeshima et al. 2006). Also a

mouse embryonic renal stem cell population characterised by Lusis *et al*. was described to mostly reside in the interstitium of mouse embryonic kidneys after a similar experiment to formation of chimeric kidneys was performed using these cells (Lusis et al. 2010). Accordingly these data suggest that the high prevalence of D1 cells in the stroma and outside the renal structures in the metanephric kidney is not a unique feature of MSCs.

5.3.6. Mechanism of increased renogenic potential of D1 cells following preconditioning

As discussed above, the culture of D1 cells in NKC CM for 4 days prior to the integration assay increases the engraftment potential of the cells into MM of developing chimeric kidneys. However, it is not clear how the conditioned medium mediates this effect. Human MSCs transduced with an adenovirus to transiently over-express human Gdnf that were injected at the site of nephrogenesis prior to the start of kidney development were found in metanephroi to a greater extent than MSCs not transduced with Gdnf. Accordingly, transduction with Gdnf has been shown to lead to an approximately 6-fold increase in the incorporation rate. Ultimately, almost 30% of cells found in such developing kidneys were human MSCs over-expressing GDNF (Yokoo et al. 2005). Why GDNF expression increases the integration potential of human MSCs is not evident. Yokoo and co-workers state in their report only that GDNF is expressed in MM and takes part in epithelial-mesenchymal signalling (Yokoo et al. 2005). In the current study the pre-conditioning with NKC CM lead to a significant up-regulation in *Gdnf* expression in D1 cells. Subsequently, after the NKC CM was changed to standard culture medium, the increase in *Gdnf* expression was still detectable and significantly higher in comparison with unstimulated D1 cells. The up-regulation in *Gdnf* expression was accompanied by a higher integration rate in the chimeric kidney assay. These results suggest that pre-conditioning with NKC CM indeed may

help MSCs to incorporate into metanephric kidneys, acting similarly as transient transduction with Gdnf, and further corroborates the role of Gdnf in enhancing the integration potential of MSCs.

If Gdnf is increasing the renogenic potential of MSCs it is not clear if the up-regulation in *Gdnf* expression after stimulation with NKC CM is entirely responsible for the raise in incorporation rate. It might be possible that the increase in *Gdnf* expression only accompanies other mechanism. Still the factor that induces D1 to increasingly engraft has to be present in the NKC CM. One possibility to confirm the importance of Gdnf would be to knock-down its expression following stimulation and subsequently evaluate the integration ability of the stimulated cells. Another option could be to transiently over-express Gdnf in D1 cells and compare the effect of over-expression on engraftment potential of the cells with the effect exerted by NKC CM stimulation. Even if the up-regulation in *Gdnf* expression would be fully responsible for the improvement in integration potential of D1 cells, again it is difficult to assess which factors present in the NKC CM trigger the up-regulation. In this study in order to concentrate conditioned medium derived from NKCs Vivaspin centrifugal ultra-filtration device with 5kDa molecular weight cut off was used. In this way macromolecules with higher molecular weights dissolved in CM, such as growth factor, were retained in the concentrated CM, while salts and water passed through. For that reason it is difficult to speculate which factor present in both CM and concentrated CM is responsible for the increase in *Gdnf* expression and the enhanced engraftment. Nevertheless, elevated *Gdnf* expression has been shown to persist in cells stimulated with NKC CM that was concentrated. However, as the increase in concentration of NKC CM did not induce further increase in *Gdnf*, it can be assumed that a quasi optimal concentration of the

inducing factor has been reached already in the 1 to 1 mix. It is important to note that no analysis on diluted instead of concentrated NKC CM has been performed. Surprisingly, both concentrated culture media used for D1 and MEF CM induced also to some extent an increase in *Gdnf*. This suggests that the existence of factors responsible for *Gdnf* induction is not restricted to media derived from kidney cells. Nevertheless these results have not been quantified. Finally the possibility that Gdnf present in the NKC CM might induce *Gdnf* expression in D1 cells was evaluated, as MSCs were shown to increase *Gdnf* expression upon stimulation with Gdnf (Shi et al. 2008). Accordingly, no up-regulation in *Gdnf* expression in D1 cells has been achieved after Gdnf stimulation, possibly due to lack of expression of the *Ret* receptor. However, it is important to note that Gdnf can signal independently of Ret receptor (Popsueva et al. 2003), which might explain slight downregulation of *Gdnf* expression following Gdnf treatment.

Finally, in this study it was not possible to perform any analysis of Gdnf expression on protein level. All approaches aimed at detection of Gdnf at protein level, namely the use of commercial available anti-Gdnf antibody for immunofluorescence staining/Western blot analysis as well as the use of commercial available enzyme-linked immunoadsorbent assay (ELISA) detecting Gdnf, failed (data not shown). However, problems with detection of Gdnf have been reported before (Liu et al. 2001).

Chapter 6: Effects of MSCs on metanephric kidney development

6.1. Introduction

Bone marrow-derived MSCs were described to improve renal function in different experimental models of acute kidney injury (Herrera et al. 2004; Morigi et al. 2004; Togel et al. 2005; Kunter et al. 2006). Notably, the paracrine activity of MSCs appears to play an important role in achieving the enhanced recovery from kidney injury (Togel et al. 2005; Bi et al. 2007; Imberti et al. 2007; Semedo et al. 2007; Togel et al. 2007; Togel et al. 2009). Togel *et al*. demonstrated that administration of rat bone marrow-derived MSCs improved renal function in the model of ischemia-reperfusion acute renal failure, although only few MSCs were detected in the injured kidneys. Accordingly, 24h after administration of rat MSCs, injured kidneys showed reduced expression of pro-inflammatory cytokines such as *tumor necrosis factor-α* (*TNF-α*) and *interleukin-1β,* and an increase in expression of the anti-inflammatory molecule, *interleukin-10* (Togel et al. 2005). These results have been confirmed by another group which also demonstrated a change in cytokine expression following administration of rat MSC in the ischemia-reperfusion injury model (Semedo et al. 2007). Bone marrow-derived MSCs were also shown to have a protective effect in cisplatin-induced acute renal failure (Morigi et al. 2004; Bi et al. 2007). Later, it was demonstrated that administration of conditioned medium derived from mouse MSCs is able to decrease kidney injury in the cisplatin-induced acute renal failure in a similar manner as the injection of the cells (Bi et al. 2007). These results were also repeated in an *in vitro* model where conditioned medium derived from mouse MSCs was shown to increase the survival of immortalized mouse proximal tubule cells treated with cisplatin (Bi et al. 2007). Collectively, these results suggest that the beneficial action of MSCs during renal injury is mediated through

paracrine factors secreted by the cells.

Togel and co-workers subsequently showed that MSCs express various factors, such as *fibroblast growth factor 2* (*Fgf2*), *transforming growth factor-α* (*TGF-α)*, *insulin-like growth factor-1* (*IGF-1*) and different members of *vascular endothelial growth factor* (*VEGF*). In addition, the presence of VEGF-A, IGF-1 and TGF-β1 was confirmed in the conditioned medium from MSCs (Kunter et al. 2006; Togel et al. 2007). Ultimately, it has been described that inhibition of VEGF expression in bone marrow-derived rat MSCs prior to their administration in the ischemia-reperfusion kidney failure model results in reduced functional renal recovery (Togel et al. 2009). Similarly, IGF-1 was demonstrated to mediate the beneficial effects of MSC administration in the cisplatin-induced kidney injury (Imberti et al. 2007). Accordingly, Imberti *et al*. demonstrated that bone marrow-derived mouse MSCs do not protect from renal function deterioration when IGF-1 expression has been blocked. In addition, MSCs expressing IGF-1 were shown to induce proliferation of cisplatin-damaged proximal tubular epithelial cells *in vitro*. The inhibition of IGF-1 expression in MSCs resulted in reduced proliferation of cisplatin-damaged tubular cells (Imberti et al. 2007). A recent report, however, describes no protective action of porcine MSCs in the ischemia-reperfusion acute renal failure model despite the fact that cells were shown to secrete VEGF-A and IGF-1. From this study, it was concluded that porcine MSCs might produce other factors, like the pro-inflammatory interleukin-6, during kidney injury which do not induce functional improvement of kidneys (Brunswig-Spickenheier et al. 2010). Similar results were obtained with mice lacking the alpha3-chain of type IV collagen, a chronic kidney disease model. In the aforementioned study, although MSCs were shown *in vitro* to express *VEGF*, weekly administrations of mouse MSCs did not protect the animals from renal failure. Nevertheless

MSCs were described to reduce renal fibrosis in this model (Ninichuk et al. 2006).

In previous chapters, the contribution of MSC to nephrogenesis has been evaluated using the chimeric kidney model. Accordingly, D1 cells were shown to integrate infrequently into condensing metanephric mesenchyme (MM). Subsequently the engraftment potential was increased after pre-conditioning of the cells with conditioned medium derived from neonatal kidney cells (NKC CM). However, throughout the experiments it appeared that MSCs negatively affected the metanephric development of the chimeras. It also became evident that the stimulation with NKC CM may play a role in decreasing the negative action of D1 cells. Although the cells appeared to have a negative effect on the development of the chimeric rudiments, this was not directly investigated in previous chapters. If MSCs indeed negatively influence the metanephric development, their use in regenerative approaches aimed at recapitulating nephrogenesis would be very limited. The aforementioned results demonstrate that the renoprotective effect exerted by MSCs observed in experimental models of kidney injury can be mediated indirectly via a paracrine action of the cells. It is therefore likely that paracrine factors secreted by MSCs can affect chimeric kidney development. The aim of this chapter is to determine the effect of D1 cells on metanephric development and to investigate the mechanism of their action.

6.2. Results

In this chapter the effects exerted by MSCs on embryonic kidney development were examined. Accordingly, the outcome of recombination of D1 cells on chimeric kidney development was assessed and the putative mechanism of action is discussed.

6.2.1. Effect of integration of D1 cells and human MSCs on metanephric development following chimeric kidney culture

In previous experiments, the renogenic potential of MSCs was investigated following the recombination of MSCs with E11.5 kidney rudiment cells to form kidney chimeras. As mentioned in Chapter 4 and 5, some detrimental effect on metanephric kidney development in chimeras harbouring either D1 cells or human MSCs was observed which was not present in kidneys reformed in the absence of stem cells. Figure 6.1 and 6.2 highlight the differences between reformed embryonic kidneys in the absence and presence of MSCs. While the reformed kidneys in the absence of D1 cells contained aggregates of Wt1-expressing condensing mesenchyme and developing nephron-like structures (marked by high expression of Wt1) (Figure 6.1a-c), some regions of chimeric kidneys harbouring D1 cells entirely lacked condensing mesenchyme and nephron-like structures (Figure 6.1d-g).

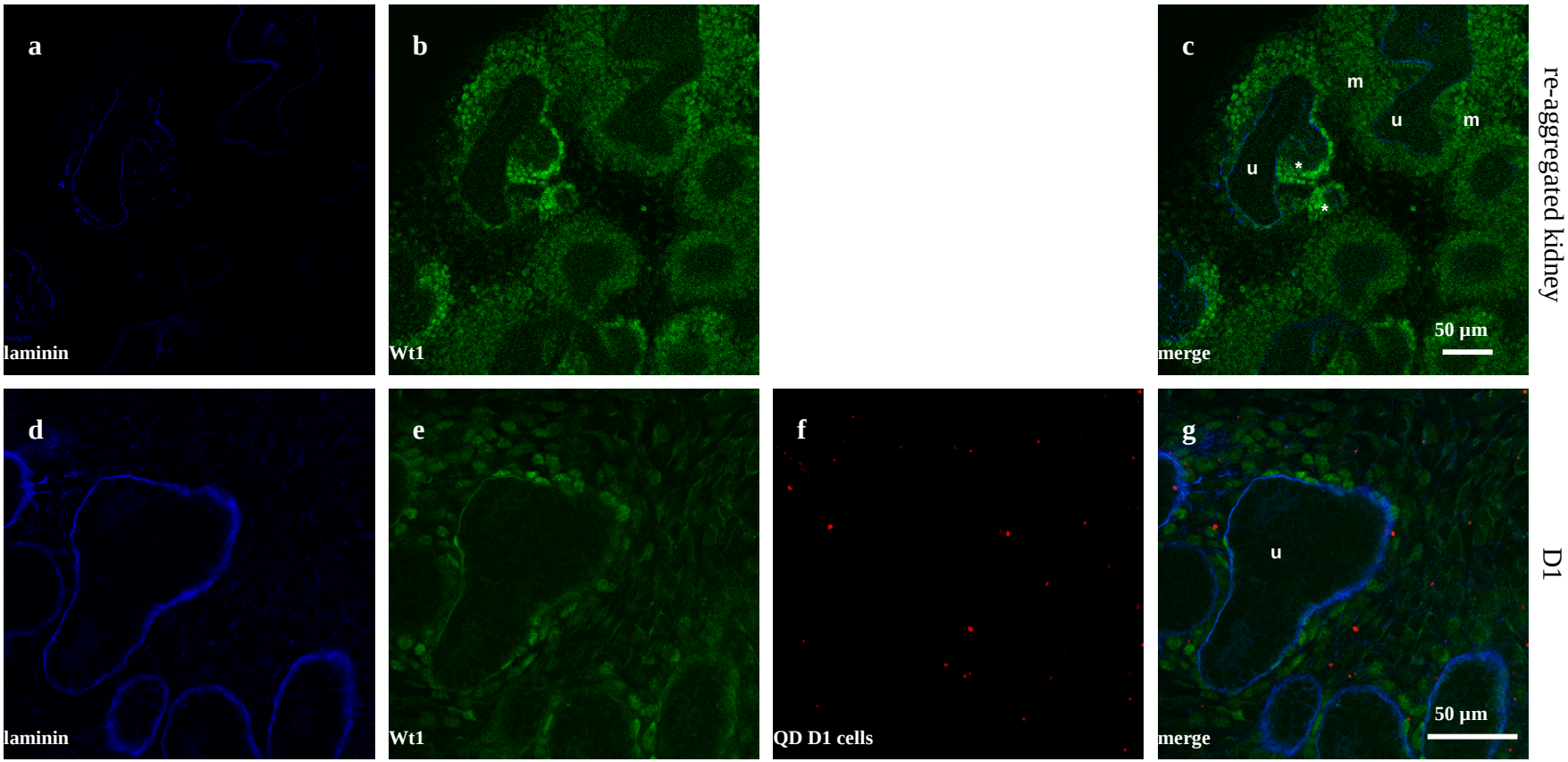

Figure 6.1 D1 cells impair the development of chimeric kidney after 4 days of culture. Representative images of chimeras are shown (from at least 3 independent experiments). (a-c) Re-aggregated kidney in the absence of D1 cells stained for Wt1 and laminin showed normal development characterised by condensation of mesenchyme (m) around UBs (u) and nephron-like structure formation (*). (d-g) Chimera recombined in the presence of QD-labelled D1 cells stained for Wt1 and laminin lacking condensing mesenchyme and developing nephrons.

A comparable impairment of development was observed in chimeras harbouring human MSCs. As shown in Figure 6.2b-d, chimeras harbouring human MSCs displayed disorganization of Wt1-expressing MM and lacked nephron-like structures. In comparison, reformed kidneys developing in the absence of human cells showed aggregates of Wt1-expressing condensing mesenchyme as well as highly Wt1-positive nephron-like structures (Figure 6.2a).

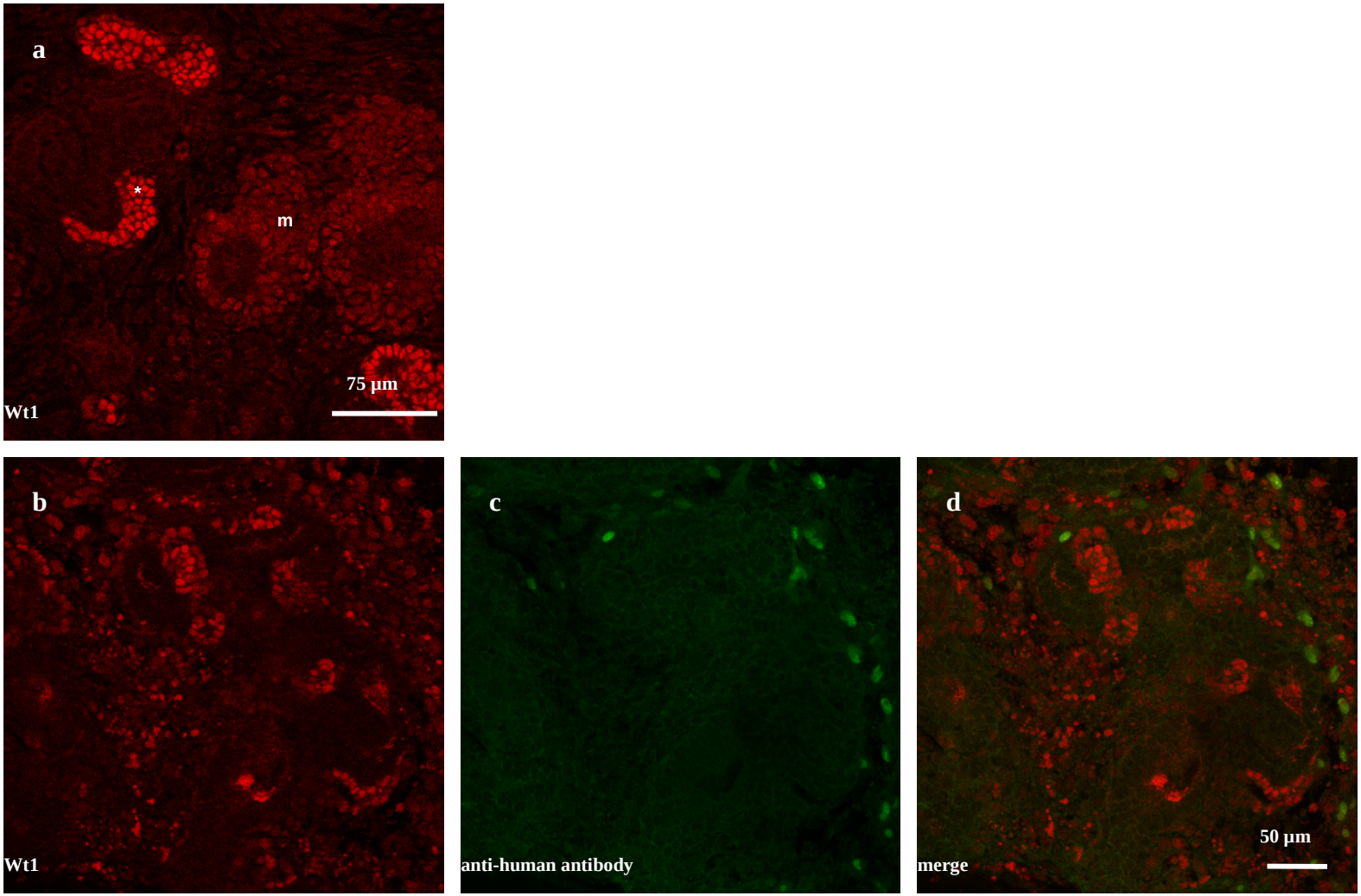

Figure 6.2 Human MSCs impair the development of chimeric kidney after 4 days of culture. Representative images of chimeras are shown (from at least 3 independent experiments). (a) Re-aggregated kidney in the absence of human MSCs showed normal development which is characterised by regions of condensing mesenchyme (m) expressing medium levels of Wt1 and nephron-like structures (*) expressing high levels of Wt1. (b-d) Chimera recombined in presence of human MSCs labelled with anti-human antibody and stained for Wt1 showing disorganization of condensing mesenchyme.

As described in the previous chapter, the stimulation with NKC CM increased the integration potential of D1 cells into condensing mesenchyme of rudiment chimeras after 4 days of culture. At the same time, it also appeared that the stimulation had some beneficial effect on chimeric kidney development. In Figure 6.3 the difference in overall development between reformed embryonic kidneys in the absence of stem cells, the presence of D1 cells and the presence of NKC CM pre-treated D1 cells is presented. Some inhibition in metanephric development characterised by reduction of condensing mesenchyme and fewer forming nephron-like structures occurred in chimeras harbouring D1 cells (Figure 6.3d-g). However, the development of kidneys recombined with D1 cells that were pre-treated with NKC CM (Figure 6.3h-k) and kidneys re-aggregated in the absence of D1 cells (Figure 6.3a-c) was similar. Both kidneys displayed Wt1-expressing condensing MM and nephron-like structures characterised by high expression of Wt1 and the presence of laminin.

In order to assess if stimulated D1 cells can exert long-term beneficial effects on kidney development, E11.5 kidney cells were recombined with unstimulated or NKC CM stimulated D1 cells in the same 1 to 5 ratio and cultured for 7 days. GFP-labelled D1 cells were used for this experiment as there was the risk that considerable number of cells might lose QDs after 7 days. It was demonstrated in section 3.2.1 that some D1 cells lost QD-labelling after 5 days of *in vitro* culture. Accordingly, the reduction of the D1-induced negative effect on metanephric development was detectable in chimeric kidneys containing NKC CM stimulated D1 cells after 7 days. As shown in Figure 6.4e-h, chimeras harbouring stimulated D1 cells appeared to contain more Wt1-exepressing mesenchyme in comparison with unstimulated D1 cells (Figure 6.4a-d). Surprisingly, no further increase in nephron development seemed to occur during this period of

time in any of the conditions. Ultimately, NKC CM stimulated D1 cells were found to a greater extent integrated into the Wt1-expressing condensing mesenchyme than unstimulated cells, confirming the previous experiment performed at day 4 (Figure 6.4a-h).

In summary, both D1 cells and human MSCs appear to exert a negative effect on chimeric kidney development. The pre-treatment of D1 cells with NKC CM seems to prevent the detrimental action of the cells in short- and long-term cultures.

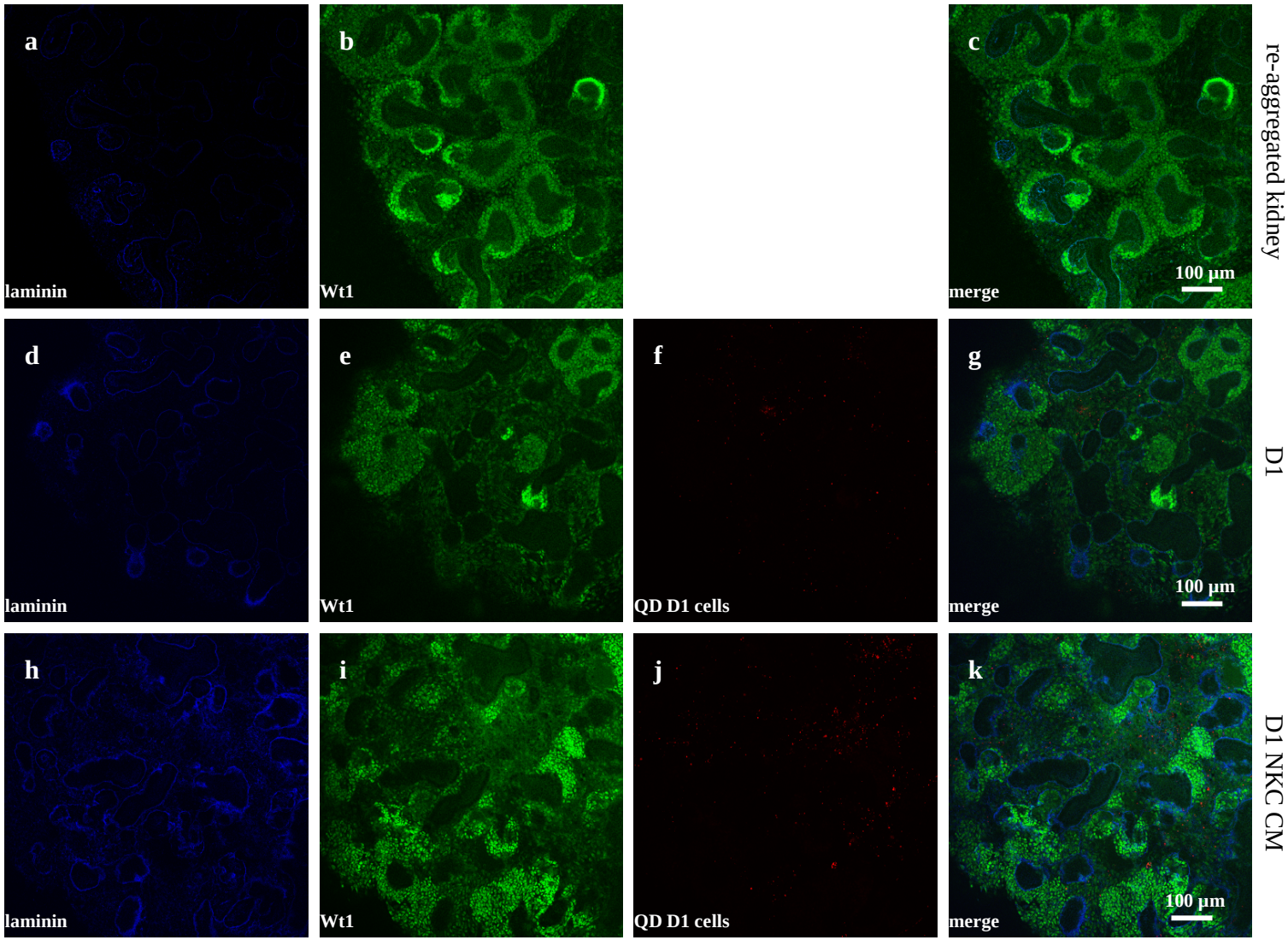

Figure 6.3 D1 cells impair the development of chimeric kidney after 4 days of culture; however, the pre-treatment with NKC CM for 4 days before the recombination experiment can avert this effect. Representative images of chimeras are shown (from at least 3 independent experiments). (a-c) Re-aggregated kidney in the absence of MSCs stained for Wt1 and laminin demonstrating presence of condensing mesenchyme around UBs and nephron-like structure formation. (d-g) Chimera recombined in presence of QD labelled D1 cells and stained for Wt1 and laminin appears to display less condensing mesenchyme and developing nephrons. (h-k) Chimera recombined in presence of QD labelled D1 cells pre-treated with NKC CM and stained for Wt1 and laminin demonstrates presence of condensing mesenchyme and developing nephrons.

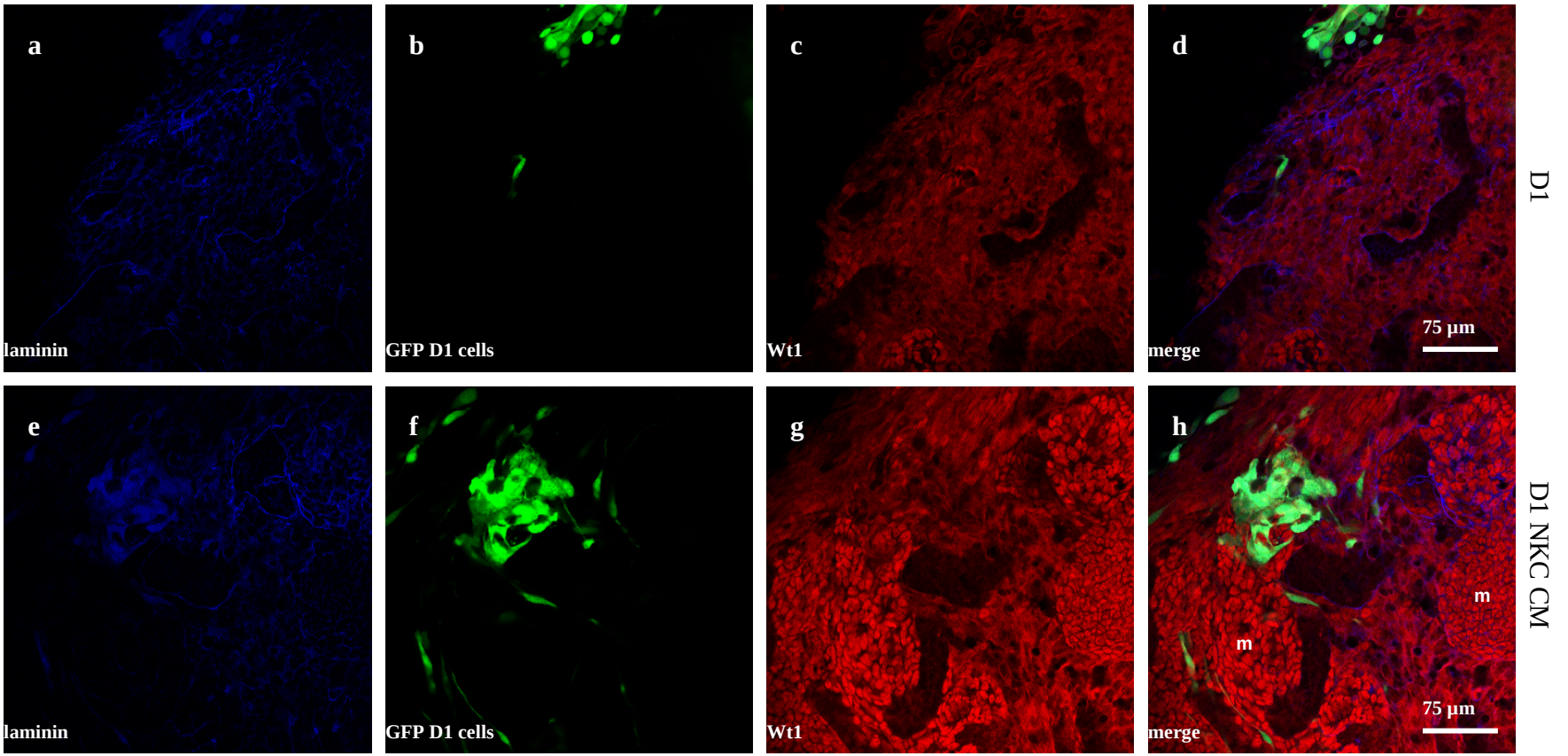

Figure 6.4 The pre-treatment of D1 cells with NKC CM can prevent loss of condensing mesenchyme in chimeras harbouring D1 cells after 7 days of culture. Representative images of chimeras are shown (from 2 independent experiments). (a-d) Chimera recombined in presence of GFP labelled D1 cells and stained for Wt1 and laminin appears to display less Wt1-positive mesenchyme. (e-h) Chimera recombined in presence of GFP labelled D1 cells pre-treated with NKC CM and stained for Wt1 and laminin demonstrates presence of Wt1-expressing condensing mesenchyme (m) and enhanced integration of the GFP cells.

6.2.2. Effect of conditioned medium derived from D1 cells on the development of intact kidney rudiments

To reduce condensation of metanephric mesenchyme or nephron formation in the chimeras, D1 cell have to either directly or indirectly interact with kidney cells. It is anticipated that the protective action and enhanced recovery in kidney injury models are achieved through the paracrine activity of MSCs (Togel et al. 2005; Togel et al. 2007; Bruno et al. 2009). In order to examine if MSCs may exert an indirect effect on chimeras by secreting paracrine factors that inhibit kidney development, *ex vivo* development of whole E11.5 rudiments in the presence of conditioned medium derived from D1 cells was assessed (MSC CM). Subsequently, the development of rudiments cultured with MSC CM was compared against kidneys cultured in standard culture medium and in conditioned medium from NKC CM stimulated D1 cells (sMSC CM), as it has been observed that pre-conditioning of D1 cells with NKC CM may reduce the negative effect on the development of reformed kidneys. Accordingly, E11.5 kidney rudiments were cultured for 3 days in the presence of standard culture medium mixed 1:1 with MSC CM or sMSC CM. In order to ensure that no NKC CM was present in the sMSC CM, the conditioned medium collection took place 24h after the medium had been changed to standard culture medium. Also, MSC CM was collected 24h after a medium change to maintain similar experimental conditions. To determine the influence of MSCs on the development of kidneys, branching morphogenesis was evaluated by staining with calbindin which is expressed in UBs (Davies 1994). A schematic representation of the experiment is presented in Figure 6.5. As demonstrated in Figure 6.6a-c, kidneys incubated with MSC CM, have impaired branching when compared with kidneys cultured in standard medium or sMSC CM. Moreover, the number of counted UB tips was similar in kidneys incubated in standard culture medium and in medium

from sMSC CM but was significantly reduced by MSC CM ($p<0.05$, $n=3$) (Figure 6.6d).

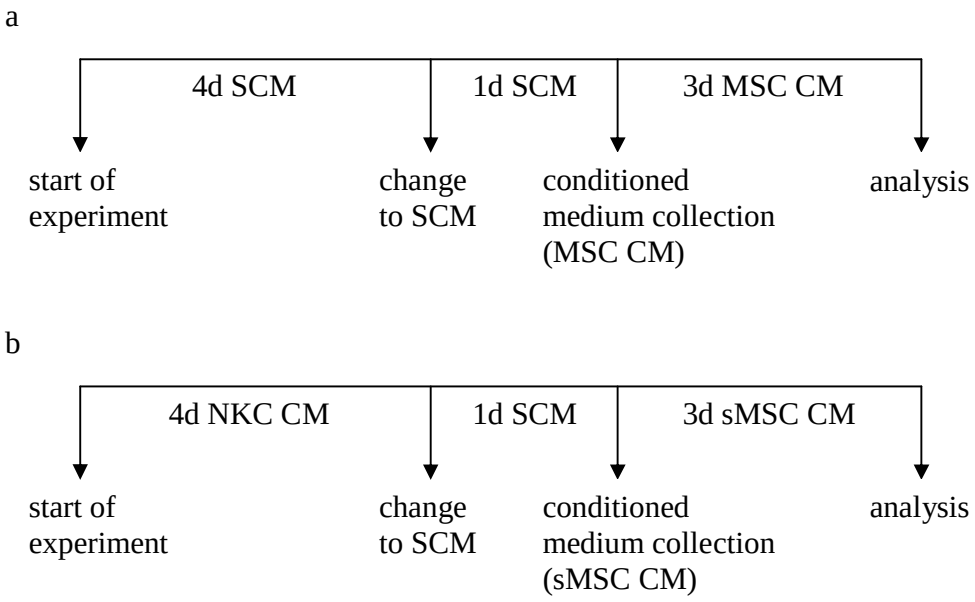

Figure 6.5. Schematic representation of an experiment elucidating the indirect effect of D1 cells on *ex vivo* development of intact E11.5 rudiments. D1 cells were cultured in standard culture medium (SCM) (a) or NKC CM (b) for 4 days. Subsequently the medium was changed to SCM for 24h in both conditions. Finally E11.5 kidney rudiments were cultured for 3 days in the presence of conditioned medium derived from D1 cells, either unstimulated (MSC CM) or previously stimulated with NKC CM (sMSC CM).

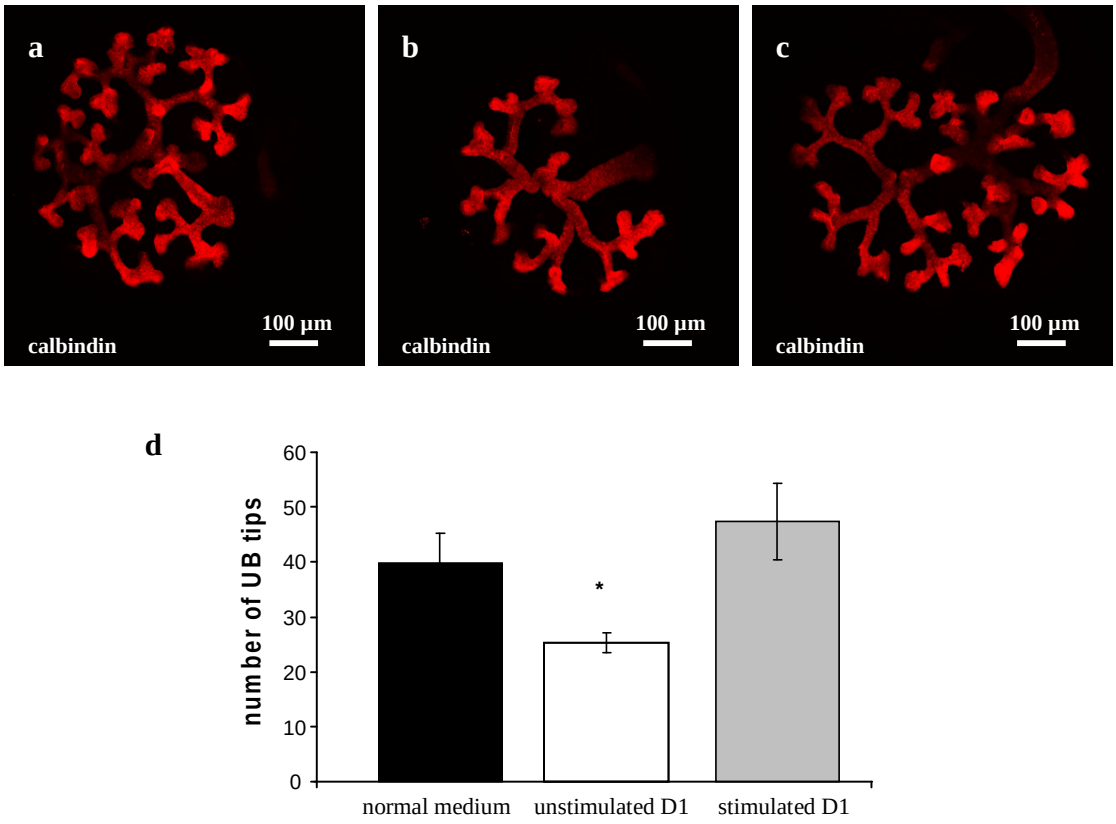

Figure 6.6 D1 cells exert an indirect negative effect on metanephric development and the pre-treatment of D1 cells with NKC CM can prevent this effect. Representative images showing whole E11.5 kidneys cultured in the presence of normal medium (a), medium from D1 cells (MSC CM) (b) and medium from stimulated D1 cells with NKC CM (sMSC CM) stained for calbindin after 3 days of *in vitro* culture. (d) UB tips count performed after 3 days on three different kidney rudiments cultured in normal medium, MSC CM and sMSC CM showing that the number of UB tips is significantly reduced in kidneys treated with MSC CM (*t*-test, $p<0.05$, n=3).

It has been shown that stimulation of E11.5 mouse kidney rudiments with exogenous bone morphogenetic protein 4 (Bmp4) inhibits branching of UB and condensation of MM (Miyazaki et al. 2003). As Bmp4 might be one of the factors implicated in inhibition of development in chimeras harbouring D1 cells, expression of *Bmp4* in D1 cells was evaluated. In Figure 6.7a, D1 cells were shown to express increased levels of *Bmp4* in comparison with E13.5 kidney ($p<0.01$, n=4). Furthermore, following stimulation with NKC CM, the expression levels of *Bmp4* in D1

cells were to some extent reduced.

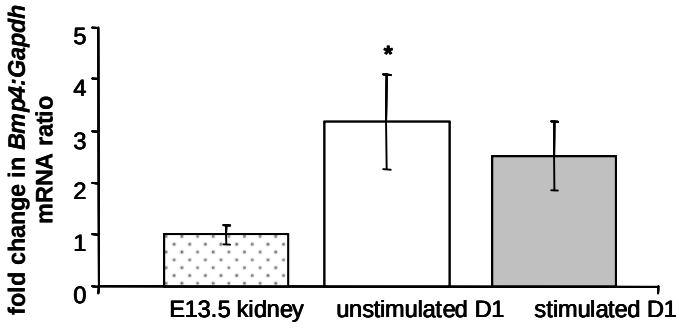

Figure 6.7 Comparison of *Bmp4* expression level in unstimulated and stimulated with NKC CM D1 cells using quantitative PCR. The reference gene is *Gapdh* and the error bars represent SE of the mean. In comparison with E13.5 kidney cells D1 cells showed higher expression of *Bmp4* (*t*-test, $p<0.01$, $n=4$). Expression of *Bmp4* was not significantly different in D1 cells stimulated with NKC CM from E13.5 kidney (*t*-test, $p>0.05$, $n=4$).

In conclusion, it was found that conditioned medium from D1 cultures has a negative effect on development of intact kidney rudiments, suggesting that inhibition of metanephric development in chimeras observed in previously experiments is indirectly mediated by MSCs. Further, D1 cells affect metanephric development possibly by secreting factors like Bmp4, which inhibit UB branching and condensation of MM.

6.3. Discussion

In this chapter the negative effect of recombination of MSCs on chimeric kidney development has been described. At the same time the stimulation with NKC CM was shown to prevent the detrimental effect on embryonic kidney development exerted by D1 cells. In order to examine if D1 cells influence kidney development in an indirect manner, intact metanephroi were cultured in the presence of conditioned medium derived from D1 cultures. It was found that conditioned medium from D1 cultures negatively affected the *ex vivo* development of intact kidney

rudiments. Finally, expression of *Bmp4*, a gene encoding a factor that inhibits nephrogenesis, was found to be highly expressed in D1 cells.

6.3.1. Effects exerted by MSCs on kidney development

So far it has been investigated if MSCs can contribute to nephrogenesis *in vitro*. The renogenic capacity of MSCs was determined by examining their integration potential into different compartments of chimeric kidneys. In this chapter, the effect of MSC recombination on metanephric development of the kidney chimeras was described. Accordingly, the chimeric kidneys were analysed for the presence of condensing mesenchyme and nephron formation. It appeared that chimeras harbouring either D1 cells or human MSCs displayed fewer areas of condensing mesenchyme or nephron-like structures in comparison with kidneys reformed in the absence of MSCs. This could be to some extent explained by the fact that chimeras reformed using MSCs contained fewer embryonic kidney cells. In the absence of MSCs the reformed kidneys were comprised only of kidney cells, whereas the chimeras harbouring MSCs were mixed in 1 to 5 ratios. Nevertheless, no such effect was observed when ESCs or NKCs were mixed in 1 to 5 ratios (see Chapter 4). Furthermore, chimeric kidneys harbouring D1 cells stimulated with NKC CM seemed to display similar levels of condensing mesenchyme and nephron-like structures when compared with kidneys without stem cells. It is not clear what factor in the NKC CM is responsible for the inhibition of detrimental effect on chimeric development in D1 cells upon stimulation. One option could be that NKC CM contains an inhibitor or an enzyme that inactivates a detrimental factor produced by MSCs. For example, it has been shown that matrix metalloproteinase-9 (MMP-9) secreted by embryonic kidneys are involved in UB branching (Lelongt et al. 1997). Nevertheless, MMP-9 can also induce epithelial

mesenchymal transition in tubular cells contributing to renal fibrosis (Tan et al. 2010). There exists a natural inhibitor of MMP-9, namely the tissue inhibitor of metalloproteinase 1, which is able to block the action of MMP-9 (Lelongt et al. 1997). NKC CM might contain such inhibitor. Together these results suggest that MSCs may have some negative impact on metanephric development in kidney chimeras.

In order to determine if the negative effect was due to paracrine factors secreted by MSCs, the action of D1 cells on intact E11.5 kidney rudiments was evaluated. MSCs were previously described to secrete various factors such as vascular endothelial growth factor (VEGF) and insulin growth factor-1 (IGF-1) *in vitro* (Kunter et al. 2006; Togel et al. 2007). Furthermore, it was shown that the paracrine factors released by MSC play a crucial role in enhancing recovery from kidney injury in animal models (Togel et al. 2005; Bi et al. 2007; Imberti et al. 2007; Togel et al. 2007; Togel et al. 2009). However, despite their positive role in renal injury models, it is possible that some of the paracrine factors secreted by D1 cells inhibit the emergence of condensing mesenchyme and formation of nephrons during kidney development. The inhibitory role of D1 paracrine factors was confirmed by showing that conditioned medium derived from D1 cells reduced UB branching of *in vitro* cultured intact E11.5 kidney rudiments. Interestingly, the incubation of kidney rudiments in medium derived from stimulated D1 cells sustained normal branching in the intact kidneys.

Together these results demonstrate that D1 cells can secrete factors that negatively influence metanephric development. Although it cannot be excluded that there might be some direct interaction between MSCs and kidney cells that contributes to observed negative effects on chimeric development, it is most likely the paracrine factors derived from MSCs that inhibit

nephrogenesis in the kidney chimeras. Furthermore, pre-treatment of D1 cells with NKC CM is able to avert this effect, probably by changing again the milieu of secreted factors. *Yokoo et al*. did not report any detrimental effect on kidney development when integrating human MSCs into rodent metanephroi (Yokoo et al. 2005). However there are reports describing toxic effects of conditioned medium derived from MSCs on hippocampal tissue *in vitro* (Horn et al. 2009; Horn et al. 2010). Accordingly, conditioned medium from rat bone marrow-derived MSCs was shown to induce reactive oxygen species formation and inflammation in organotypic cultures of rat hippocampus (Horn et al. 2010).

6.3.2. Putative mechanism of detrimental action of D1 cell on kidney development

Inductive interactions play a crucial role in early kidney morphogenesis (Horster et al. 1999; Dressler 2006). It is possible that MSCs interfere with these interactions and as a result, inhibit kidney development. One of the most important inductive interactions takes place when UB invades the MM and starts to branch and this is mediated through Gdnf signalling. Gdnf secreted by MM binds to the Ret receptor at the tips of UB inducing growth and branching of the UB (Vega et al. 1996; Sainio et al. 1997). D1 cells were shown to express *Gdnf;* however, no extensive UB branching was observed in chimeras harbouring D1 cells. On the contrary, it was observed that the conditioned medium derived from D1 cells reduced branching in the intact kidney rudiments. An explanation for this effect could be that although D1 cells express *Gdnf*, they do not secret the protein or that Gdnf secreted by D1 is not fully functional. In this study it has not been possible to measure Gdnf levels in supernatants obtained from D1 cell culture (data not shown). However, it has been reported that MSCs are able to produce and secrete Gdnf (Ye et al. 2005). Another possibility would be that D1 cells secrete simultaneously other factors or

molecules that inhibit Gdnf signalling in kidney cells. For example it has been reported that heparan sulphates are required to activate Ret receptor; nevertheless, exogenous heparan sulphates inhibit receptor activation and hence suppress Gdnf signalling (Barnett et al. 2002). Interestingly, D1 cells stimulated with NKC CM which do express higher levels of *Gdnf* than unstimulated D1 cells, do not induce impairment in branching morphogenesis. This can suggest that high expression of *Gdnf* may at least help sustain the number of UB tips. Blocking of *Gdnf* expression in stimulated cells would help to better understand the mechanism of protective action of D1 cells following treatment with NKC CM. Ultimately, the presence of Gdnf in the conditioned medium from stimulated cells has not been confirmed.

A range of factors has been described to modulate kidney development (Horster et al. 1999). Different members of transforming growth factor-β (TGF-β) superfamily such as TGF-β1, activin, and bone morphogenetic protein 2 or 4 were described to negatively act on growth and branching of UBs (Bush et al. 2004). Accordingly, bone morphogenetic protein 4 (Bmp4) might be one of the factors responsible for the inhibition of development in kidney chimeras harbouring MSCs or intact rudiments cultured in the presence of D1 derived conditioned medium. During metanephric development, *Bmp4* is expressed in mesenchymal cells surrounding the Wolffian duct when the UB starts invading the MM. Later, *Bmp4* expression is observed in stromal mesenchymal cells around the stalk of the UB and the smooth muscle layer around the developing ureter (Miyazaki et al. 2000). Although *in vitro* Bmp4 is able to promote survival of isolated MM in the absence of inducer tissue, the stimulation of E11.5 mouse kidney rudiments with Bmp4 for 48h results in inhibition of UB branching and MM condensation (Miyazaki et al. 2003). This is accompanied by down-regulation of expression of such markers like *Gdnf, Wt1*

and *Pax2* (Raatikainen-Ahokas et al. 2000; Miyazaki et al. 2003). In this chapter it has been confirmed that D1 cells express *Bmp4*. This is in accordance with previous data demonstrating *Bmp4* expression in mouse bone marrow-derived MSCs (Kondo et al. 2005). In addition, D1 cells were shown to express higher *Bmp4* levels than E13.5 mouse kidney rudiment. It is possible that release of additional Bmp4 by D1 cells results in development inhibition similarly to the one achieved by exogenous Bmp4 in *in vitro* experiments mentioned earlier. However, it has not been attempted in this study to determine the expression levels of Bmp4 protein in D1 cells. Nevertheless, the stimulation with NKC CM did result in slight down-regulation of *Bmp4* expression in D1 cells.

It is also likely that other members of TGF-β superfamily are implicated in the inhibition of the development of the chimeras or intact rudiments. Rat kidney rudiments treated with TGF-β1 for 5 days have demonstrated a reduced number of UB tips (Bush et al. 2004), whereas mouse embryonic kidneys cultured for 9 days in the presence of TGF-β2 were demonstrated to develop only rudimentary glomeruli (Sims-Lucas et al. 2010). Conditioned media from MSCs was shown to contain TGF-β1 (Salazar et al. 2009). Accordingly TGF-β1 derived from MSCs was described to be responsible for mediating immunosuppressive effects characteristic for these cells (Nemeth et al. 2010). Similarly, expression of TGF-β2 was also confirmed in MSCs (Sun et al. 2011). Moreover, inactivation of Wnt signalling in ureteric bud cells also impairs branching of UB during nephrogenesis and consequently leads to lower numbers of nephrons and collecting ducts in kidneys of new born mice (Bridgewater et al. 2008). It has been demonstrated that a secreted glycoprotein Dickkopf-1 (Dkk-1) is able to suppress Wnt signalling, inducing *in vitro* impairment of UB branching in E13.5 mouse kidneys (Iglesias et al. 2007). Human MSCs have been shown

to express Dkk-1 and accordingly, inhibit the Wnt pathway in tumor cells (Qiao et al. 2008; Zhu et al. 2009). Consequently it is possible, that kidney development inhibition may also be mediated by the secretion of other factors than Bmp4, such as TGF-β1, TGF-β2 or Dkk-1. However, the expression of factors has been investigated neither in D1 cells nor human MSCs in this study.

It is likely that MSCs may not only act on kidney development by secreting factors that inhibit UB or nephron development but also by facilitating stroma emergence. E11.5 mouse kidney rudiments treated with a mix of Bmp4 and fibroblast growth factor 2 (Fgf2) for 2 days showed expansion of stromal compartment at the periphery which was accompanied by the inhibition of MM condensation (Miyazaki et al. 2003). As mentioned before, D1 cells express *Bmp4*. It has been also demonstrated that Fgf2 is among the most prominent factors found in the supernatant of human bone marrow-derived MSCs (Schinkothe et al. 2008). A similar effect to Bmp4 and Fgf2 in metanephric kidney has been observed with bone morphogenetic protein 7 (Bmp7) and Fgf2 (Dudley et al. 1999). E11.5 kidney rudiments treated for 2 days with Bmp7 demonstrate impaired nephron formation. Consequently some UB tips remain surrounded by condensed MM but lack developing nephrons. The combination of Bmp7 and Fgf2 resulted in severe impairment in nephron formation which was accompanied by emergence of additional peripheral mesenchyme positive for the stromal marker *Bf2* (Dudley et al. 1999). In addition, Weller *et al*. showed that epidermal growth factor (EGF) promotes emergence of interstitial cells in isolated MM. Treatment of intact E12 mouse embryonic kidneys with EGF led to formation of fewer epithelial structures and expansion of mesenchymal tissue (Weller et al. 1991). Unfortunately the expression of Bmp7 and EGF has not been investigated in MSCs.

Finally it is also possible that MSCs by secreting factors like TGF-β2 can induce renal cells to differentiate towards other cell types not found during normal nephrogenesis in the kidney. It has been shown that stimulation with TGF-β2 for 6 days induces two types of mesenchymal cells in mouse metanephroi which neither expressed the MM-specific markers *Wt1* and *Pax2,* nor the stromal marker, *Foxd1*. Furthermore, in the presence of TGF-β2, some kidney cells started to resemble chondrocytes as they were expressing collagen found in the cartilage and after 9 days of culture, stained with Alcian blue. Another mesenchymal population induced by TGF-β2 was located at the periphery of the kidneys. These cells were positive for α-smooth muscle actin and did not stain for Alcian blue (Sims-Lucas et al. 2010).

In conclusion, D1 cells affect kidney development by secreting various factors. Possibly some of the factors may support development and at the same time, different sets of factors may act antagonistically on nephrogenesis. D1 cells express both *Gdnf,* which induces UB branching (Vega et al. 1996), and *Bmp4,* described to suppress UB branching and MM condensation (Miyazaki et al. 2003). In addition, D1 cells may secrete simultaneously several factors that negatively act on kidney morphogenesis, such as Bmp4 and Fgf2. The combination of Bmp4 and Fgf2 may induce not only inhibition of MM condensation but as well expansion of the stromal compartment in the chimeras harbouring D1 cells as described for mouse kidney rudiments (Miyazaki et al. 2003). Finally, NKC CM stimulation of D1 cells helps to prevent the observed negative effects, possibly by modulating the expression profile of the cells.

Chapter 7: Final discussion

There exist several approaches to renal regeneration in patients with kidney injury, which may involve stem cells or progenitor cells. One possibility would be to stimulate endogenous progenitors to induce more rapid renal regeneration following the injury. Another option would be to transplant exogenous stem cells/progenitors to enhance the functional and structural recovery of the injured kidneys. In patients with severely damaged kidneys that require a renal transplant, the above mentioned treatment options, however, would not be feasible. In this case, stem cells might be used to generate *de novo* renal tissue for transplantation (Little 2006). Previous research suggests that MSCs can be considered as potential candidates for therapies aimed at renal tissue regeneration. Along with renoprotective effects in different acute kidney injury models, occasional integration of MSCs into tubules of injured kidneys was observed (Herrera et al. 2004; Morigi et al. 2004; Qian et al. 2008; Li et al. 2010). Some reports have also described *in vitro* acquisition of kidney specific phenotypes by MSCs (Singaravelu and Padanilam 2009; Matsushita et al. 2010). Finally, MSCs were demonstrated to contribute to kidney development by integrating into glomeruli and tubules of metanephric kidneys (Yokoo et al. 2005). The purpose of the current study was to examine the renogenic potential of mouse and human MSCs using a novel approach that involves formation of mouse embryonic kidney chimeras. The study was also intended to compare the renogenic capacity of MSCs and other cell types as well as to evaluate the possibility of increasing the ability of MSCs to contribute to renal development. In addition, an attempt was made to elucidate the action of MSCs on metanephric development. Accordingly, using the kidney chimeras, MSCs were demonstrated to have low renogenic potential. In addition, their incorporation into metanephric kidneys led to inhibited kidney development. Subsequently, incubation of embryonic kidneys with conditioned

medium obtained from mouse MSCs culture was demonstrated to decrease branching morphogenesis of the kidney rudiments, suggesting that MSCs have indeed a detrimental effect on metanephric development. Pre-conditioning of mouse MSCs with medium derived from mouse neonatal kidney cells facilitated their engraftment into developing renal structures and prevented the negative action of the cells on kidney development. In addition, the renogenic potential of MSCs was compared to the renogenic potential of embryonic stem cells and neonatal kidney cells using the same approach. Consequently all objectives of the study have been addressed. In this chapter the outcomes of the study are summarised and discussed in view of existing evidence.

Chimeric kidney assay

Previously, human MSCs were demonstrated to contribute to kidney development by integrating into renal structures and expressing kidney-specific markers (Yokoo et al. 2005). Consequently metanephroi with integrated MSCs were shown to produce fluid similar to urine following transplantation into the omentum of recipient animals (Yokoo et al. 2006). Nevertheless, in order to achieve integration of human MSCs into metanephric kidneys, a sophisticated protocol had to be developed, as direct injection of MSCs into the kidney rudiment was demonstrated to be insufficient to trigger their integration. The protocol involved demanding experimental procedures, like injection of MSCs into the intermediate mesoderm of rat embryos and subsequent *ex utero* culture of the embryos (Yokoo et al. 2005; Yokoo et al. 2006). In order to accurately evaluate the suitability of MSCs for renal tissue generation a much simpler and more reproducible protocol is required. In the current study, a modified procedure developed by Unbekandt and Davies which involves disaggregation of mouse metanephroi followed by re-

aggregation of kidney cells to form *de novo* kidney rudiments was used to assess renogenic potential of MSCs (Unbekandt and Davies 2010). It was shown previously that the re-formed kidney rudiments display features of developing metanephroi, with the same morphology and marker expression observed in intact rudiments, thus mimicking normal metanephric development (Unbekandt and Davies 2010). The suitability of re-aggregated kidney to act as a model of nephrogenesis was also confirmed here. In order to make kidney chimeras, kidney rudiments were disaggregated and subsequently re-aggregated in the presence of labelled MSCs, creating chimeras containing both kidney rudiment cells and MSCs. Recently, this protocol was used to incorporate human amniotic fluid stem cells (AFSCs) into embryonic kidneys in order to test their contribution to kidney development. Subsequently, the cells were detected in Pax2 and Wt1 positive renal structures (Siegel et al. 2010). Ultimately, an alternative chimeric kidney assay for testing MSCs contribution to kidney structures could be employed. A recent report describes the use of a similar technique to integrate embryonic renal stem cells, derived from dissociated E12.5 mouse kidney rudiments and subsequently cultured as nephrospheres, into metanephric kidneys. Accordingly, the cells were mixed with a suspension of kidney cells obtained from disaggregated E12.5 mouse kidney rudiments, subsequently pelletted and cultured in the presence of NIH3T3 cells expressing Wnt4 on a collagen IV coated filter. After 4 days of culture, embryonic renal stem cells were found to a great extent in the interstitium of the developing chimeras; however, some cells were detected in tubular structures (Lusis et al. 2010).

Renogenic potential of MSCs

In the first part of this study, the multilineage potential of the employed MSCs was confirmed and the most appropriate labelling methods for further experiments were determined. The

adipogenic, osteogenic and chondrogenic capacity of MSCs was assessed using standard differentiation protocols (Peister et al. 2004) and both mouse and human cells were shown to undergo adipo- and osteogenesis. In addition, mouse MSCs were also confirmed to undergo chondrogenesis. Previously, it has been demonstrated that transient labelling with QDs, GFP transduction and staining with species-specific antibodies are suitable for MSCs labelling (Azizi et al. 1998; Lu et al. 2005; Muller-Borer et al. 2007). Subsequently, all abovementioned methods were confirmed to be appropriate for tracking MSCs, hence investigating their integration into chimeric kidneys.

Before introducing MSCs into the embryonic kidney environment, the cells were analysed for their expression of early kidney development markers. Mouse MSCs showed expression of some genes involved in metanephric development, such as *Gdnf, Sall1, Lim1* and *Osr1*; however, they did not express *Pax2* and *Wt1*. At the same time Lusis *et al.* demonstrated that primary bone marrow-derived MSCs do not express markers like *Sall1* and *Lim1*. A discrepancy observed between the expression profile of mouse MSCs employed in this study and the profile described previously for bone-marrow derived mouse MSCs (Lusis et al. 2010) might be explained by the fact that the mouse cells used in current study were a MSC line derived from BALB/c mice in comparison to the primary MSCs isolated form C57BL/6 mice used by Lusis *et al*.. Also, a difference between the expression profile of mouse MSC line and human primary MSCs was observed, as human MSCs were shown not to express *SALL1* detected earlier in mouse cells. Similarly to mouse cells, human MSCs did not express *PAX2* and *WT1*.

Finally, in the current study, MSCs were recombined with a kidney cell suspension derived from mouse embryonic kidneys at the onset of metanephric development at E11.5. After 4 days of

culture the chimeras were analysed. Mouse MSCs were found integrated into condensing metanephric mesenchyme (MM) but not into ureteric buds (UBs). Despite the fact that some MSCs were detected in the condensing mesenchyme, no cells were found in developing nephron-like structures. Regarding the human MSCs, they were found in the proximity of condensing MM or developing nephron-like structures, but no definitive integration was detected. Those result are contradictory to the observation made by Yokoo and co-workers showing integration of human MSCs into nephrons of rat metanephric kidneys (Yokoo et al. 2005). One of the main differences between this study and Yokoo *et al* is that MSCs were integrated into kidney rudiments at the onset of metanephric development and not prior to the start of nephrogenesis, as described before (Yokoo et al. 2005). In addition, it was demonstrated that high expression of GDNF in human MSCs is essential for enhancing the number of integrated cells (Yokoo et al. 2005). Gdnf is an important factor for outgrowth and branching of UBs during metanephric development (Vega et al. 1996; Sainio et al. 1997). Nevertheless, the mouse and human MSCs employed in this study did not over-express Gdnf. Finally, the absence of MSCs from UBs is with agreement with previous results showing lack of integration of human MSCs into the developing colleting duct of embryonic kidneys (Fukui et al. 2009).

Moreover, the integration of mouse and human MSCs also had some negative effect on the development of the chimeras. The presence of MSCs affected the condensation of MM and subsequent nephron formation in the kidney chimeras, as fewer areas of condensing mesenchyme and nephron-like structures were formed in chimeras harbouring MSCs in comparison with kidneys reformed in the absence of MSCs. The inhibitory role of MSCs was confirmed in intact kidney rudiments. Accordingly, it was demonstrated that conditioned medium derived from

mouse MSCs decreased UB branching of *in vitro* cultured intact E11.5 kidney rudiments. Apparently others did not observe any detrimental effect on kidney development when integrating human MSCs (Yokoo et al. 2005; Yokoo et al. 2006; Fukui et al. 2009), although there exists reports demonstrating negative effects of conditioned medium derived from MSCs on hippocampal tissue (Horn et al. 2009; Horn et al. 2010). It is not clear which factors secreted by MSCs are responsible for this effect. Possibly, high expression of *Bmp4* in MSCs can mediate the developmental inhibition in the chimeras and intact kidney rudiments. Bmp4 was shown to inhibit *in vitro* UB branching and MM condensation in mouse kidney rudiments (Raatikainen-Ahokas et al. 2000; Miyazaki et al. 2003). In conclusion, despite the fact that MSCs secrete paracrine factors that play a crucial role in enhancing recovery from kidney injury (Imberti et al. 2007; Togel et al. 2007; Togel et al. 2009), they exert an indirect negative effect on metanephric development.

Ultimately, embryonic stem cells (ESCs) and neonatal kidney cells (NKCs) were integrated into chimeric kidneys in order to compare renogenic potential of MSCs with other cells. A previous study has shown that undifferentiated mouse ESCs were found in large tubule-like structures surrounded by basement membranes following injection into embryonic kidneys (Steenhard et al. 2005). Using the chimeric kidney, in the current study, mouse ESCs were detected in both laminin positive tubular structures, possibly confirming previous results, and within condensing MM, but not in the developing nephron-like structures. When compared with MSCs, ESCs seemed to have a broader integration potential. In addition, no negative effect on metanephric development was noted. However, both stem cells types were absent from forming nephrons despite their presence in the condensing MM. In contrast, NKCs were rarely found integrated into

laminin positive structures in the chimeric kidneys. Accordingly, they were present in condensing MM and to some extent in developing nephron-like structures. Behaviour of NKCs in the chimeric kidneys was similar to the adult kidney progenitor populations, namely the side population, which after injection into metanephric kidney was detected in MM-derived structures rather than UBs (Challen et al. 2006). When compared with MSCs, NKCs seemed to have a similar integration potential, as both MSCs and NKCs were found in condensing MM but not in the laminin positive structures. However, the main difference between MSCs and NKCs was that the latter were also found in developing nephrons, marked in those experiments by presence of laminin and Wt1. Finally, NKCs did not appear to have any detrimental effect on kidney development. ESCs and NKCs were also present to a great extent in the stroma of developing chimeras, similar to MSCs.

Increasing renogenic potential of MSCs

Several studies demonstrated that MSCs can adopt the characteristics of the particular cell population following stimulation with conditioned medium derived from this population (Rivera et al. 2006; Pan et al. 2008; Baer et al. 2009; Schittini et al. 2010). Accordingly, the conditioned medium derived from cardiac explants, foetal liver culture, adult neural tissue, proximal tubular cells were demonstrated to induce phenotypic changes in the MSCs (Rivera et al. 2006; Pan et al. 2008; Baer et al. 2009; Schittini et al. 2010). In order to enhance the contribution of MSCs to kidney development, conditioned medium from NKCs (NKC CM) was used to increase the renogenic potential of MSCs in the chimeric kidneys. After 4 days of stimulation with NKC CM, the cells were recombined with kidney cell suspension to form chimeric kidneys. In comparison with cells not pre-treated with the conditioned medium, the engraftment into condensing MM of

stimulated mouse MSCs increased significantly. The integration into Wt1-expressing compartment of chimeric kidneys was almost four times higher for stimulated mouse MSCs.

The mechanism of action of conditioned medium on mouse MSCs is not clear. However, it was demonstrated that the stimulated cells significantly up-regulated *Gdnf* expression. In Yokoo`s experiments, transduction with GDNF has been shown to lead to an approximately 6-fold increase in the incorporation rate of human MSCs into metanephroi following injection into intermediate mesoderm (Yokoo et al. 2005). Possibly the pre-conditioning with NKC CM facilitates the incorporation of mouse MSCs into condensing MM by inducing high levels of Gdnf.

Importantly, these results could not be replicated with human MSCs, as stimulation with NKC-derived conditioned medium did not result in an increase of integration of human MSCs. Accordingly, human MSCs do not express *SALL1* and, differently from mouse cells, were not integrating into any renal structures before pre-conditioning which may explain why human MSCs did not respond to NKC CM stimulation. Other possibility could be that human MSCs were not able to respond to factors found in the conditioned medium since they were derived from mouse cells.

Interestingly, the pre-treatment of mouse MSCs with NKC conditioned medium prevented any negative effect on the development of the chimeras. In the presence of stimulated MSCs, condensation of MM and subsequent nephron formation in the chimeric kidneys occurred in the same way as in kidneys reformed in the absence of MSCs. Consequently, it was demonstrated that conditioned medium derived from stimulated cells did not inhibit UB branching of *in vitro* cultured intact E11.5 kidney rudiments. As mentioned earlier, the stimulation with NKC CM

led to an increase in *Gdnf* expression in the cells. In addition, some downregulation of *Bmp4* expression was also detected following the pre-treatment with NKC CM. These results indicate that the stimulation with NKC CM might change the secretion profile of mouse MSCs preventing the detrimental effects on metanephric kidneys.

In this study it was possible to increase the engraftment potential of mouse MSCs using the NKC CM. Nevertheless, still only a very small number of MSCs was found in the nephron-like structures in the chimeras. Therefore in order to obtain engraftment of MSCs into nephrons it might be necessary to permanently change the expression profile of MSCs, similarly as it was shown by Yokoo and co-workers (Yokoo et al. 2005). One idea would be to transduce MSCs with Wt1. AFSCs which expressed Wt1 before the recombination with embryonic kidney cells have been shown to readily integrate into developing renal structures in the chimeric kidney assay (Siegel et al. 2010). Also, NKCs which integrated into condensing mesenchyme and nephron-like structures were demonstrated to express Wt1 (Mora 2009). On the other hand, permanent expression of Wt1 could become problematic later in the development. In addition, for both mouse and human bone marrow-derived MSCs, subpopulations with higher plasticity exist (D'Ippolito et al. 2004; Kucia et al. 2006; Anjos-Afonso and Bonnet 2007). Their engraftment potential could be determined using the chimeric kidney assay as possibly these cells would more efficiently contribute to chimeric kidney development.

Future directions

In this study it was demonstrated that the chimeric kidney culture assay is a useful tool for investigating the renogenic potential of MSCs. This approach can be also used to assess renogenic potential of other cells like ESCs or kidney progenitors. In the long term perspective,

the chimeric kidneys could be utilized as a scaffold for generating renal tissue with the help of exogenous stem cells. Recent advances in kidney rudiment culture may be used to improve the kidney chimera culture. For instance, despite the emergence of forming nephrons and UB branching, no distinct cortical and medullary zones were observed in the chimeras performed in this study. Lately, it has been shown that culture of mouse metanephroi in a low volume of medium facilitates the development of cortico-medullary zones in the kidney rudiments, dividing the kidneys into cortex containing the glomeruli and ureteric bud tips, and medulla containing collecting ducts and the loops of Henle (Sebinger et al. 2010). Furthermore, in order to generate fully functional renal tissue from chimeric kidneys, a blood supply is required. To allow vascularisation, chimeras could be transplanted into host animals, for example under the renal capsule of a host rat (Rogers et al. 1998; Rosines et al. 2007). Previously, it has been attempted to transplant intact embryonic kidneys (Rogers et al. 1998) or *in vitro* engineered kidney rudiments consisting of recombined T-shaped UB and uninduced MM (Rosines et al. 2007).

As discussed here, ESC, NKC and MSC populations have different abilities to contribute to kidney development. These observations can have crucial implications in approaches aimed at *de novo* generation of renal tissue. According to data presented in this study and by others, MSCs do not have a potential to contribute to the duct system (Yokoo et al. 2005; Fukui et al. 2009). For that reason it is rather unlikely that MSCs will be used in the future for generation of collecting ducts. On the contrary, kidney progenitors (Challen et al. 2006; Maeshima et al. 2006) or AFSCs (Perin et al. 2007; Siegel et al. 2010) were demonstrated to engraft into UBs and accordingly they might be used for this purpose. Numerous stem cell/progenitor types were demonstrated to engraft into MM-derived structures (Kim and Dressler 2005; Steenhard et al. 2005; Yokoo et al.

2005; Challen et al. 2006; Maeshima et al. 2006; Perin et al. 2007; Vigneau et al. 2007; Siegel et al. 2010). Nevertheless, it is difficult to decide which would be the most appropriate for *de novo* nephron formation as different methodologies were used to characterise the engraftment and subsequent differentiation towards kidney-like phenotype. So far no common standard has been established to evaluate performance of the various stem cells and progenitors in the metanephric environment, either following injection into the rudiment or following recombination with embryonic kidney cells. Accordingly, the following areas require standardization in order to effectively assess renogenic potential of stem cells and progenitors in the future: (i) labelling methods for detecting integrated cells; (ii) methods of calculating the number of engrafted cells into renal structures; and (iii) methods for determining their subsequent differentiation towards both renal phenotypes and non-renal phenotypes.

Many reports showing a contribution of different cell types to nephrogenesis *in vitro*, including MSCs, do not use more then one labelling method to confirm the observations. Accordingly, this may result in misleading statements regarding their renogenic potential.

As demonstrated in this study, a discrepancy between integration potential of QD- and GFP-labelled MSCs into chimeric kidneys was observed. While QD-labelled cells showed broad engraftment potential encompassing all compartments found in the chimeric kidney, GFP-labelled cells were found mainly in stroma and condensing MM. Also, the number of integrated cells into condensing MM differed depending on the labelling method, with less QD-labelled MSCs being engrafted into the condensing MM in comparison with GFP-labelled cells. It is likely that QD signal detected in some structures was not genuine. Some QDs might be also lost from cells in the condensing MM due to cell death or transferred to other cells. It is also possible

that GFP expression prevents MSCs integration in some compartments but facilitates the presence of MSCs in the condensing MM. All scenarios might be possible as loss of QD labelling has been described in different cell types, including MSCs (Rosen et al. 2007; Pi et al. 2010). QDs were also demonstrated to have some potential to transfer to other cells, as it was possible to use supernatants collected from labelled ESCs to label other cells again (Pi et al. 2010). Similarly, GFP labelling could have some effect on MSCs, since GFP expression was shown to negatively affect kidney cells by inducing renal defects *in vivo* and interfering with common signalling pathways *in vitro* (Baens et al. 2006; Guo et al. 2007). In conclusion, the number of observed integrated cells and their location may strongly depend on the labelling method. Further, using the GFP and species-specific antibody it became also clear that the majority of the MSCs were forming different sized clusters inside of chimeric kidneys, despite the fact that the cells were homogonously distributed at day 0, which could not be observed using QDs. Taken together, it is crucial to identify better labelling methods that give consistent results when assessing renogenic potential of cells in the future. Possibly, more than one tracking method should be employed to evaluate results.

In order to be used for renal tissue engineering, a sufficient number of stem cells/progenitor cells would need to engraft and subsequently commit into kidney-specific cell types. Sporadic contribution of some cells would be unlikely to generate *de novo* renal structures. Although Yokoo *et al*. described contribution of human MSCs to glomeruli and tubules (Yokoo et al. 2005), no quantification was provided, which could imply rather infrequent engraftment. Similarly, in the report of Siegel *et al*. which used the same chimeric kidney system to test renogenic potential of AFSCs, no quantification of the engraftment was shown (Siegel et al.

2010), which may again suggest only occasional integration of the cells. In the current study it was shown that following NKC CM pre-treatment, on average, 13% of GFP-labelled mouse MSCs were found engrafted into condensing MM. In addition, it appeared that stimulated mouse MSCs have a similar integration potential into Wt1-expressing mesenchyme as the neonatal kidney cells used in this study, and adult kidney cells (Challen et al. 2006). The engraftment into MM, however, does not implicate that all the cells initially found in this compartment will become integrated into developing nephron-like structures. On the contrary, in this study it was demonstrated that despite a high integration rate of GFP mouse MSCs into condensing MM, only occasionally the cells were found in the nephron-like structures at day 4 and no integration into nephron-like structures was detected on day 7 of chimeric kidney culture. This result can also be interpreted as a lack of proliferation of engrafted MSCs. Finally, one of the limitations of this study, but also other studies elucidating renogenic potential of stem cells, is the lack of a negative control, namely a population of cells that should not harbour any renogenic potential which could be used to compare the renogenic potential of MSCs. Ultimately, a suitable positive control should be established to elucidated renogenic potential of all stem cells and progenitors. In conclusion, in order to accurately assess the renogenic potential of different stem cells/progenitors, including MSCs, more quantitative studies should be performed in the future. Satisfactory levels of engraftment should be determined beforehand, in order to allow accurate analysis of renogenic potential of different cells types.

Another important issue regarding the putative renogenic capacity of stem cells/progenitors is the acquisition of expression of kidney markers upon integration into kidney rudiment structures. The acquisition of expression of such markers by the engrafted cells suggests their differentiation

towards kidney phenotype. Previously, human MSC were demonstrated to express Wt1 when integrated into metanephric kidneys (Yokoo et al. 2005). In this study, QD-labelled mouse MSCs appeared to be stained with Wt1 when integrated into the condensing MM of chimeric kidneys implying that mouse MSCs might differentiate into MM-like cells that give rise to nephron. No expression of Wt1 was, however, detected when GFP-labelled MSCs were used instead of QD-labelled cells. Again, it could be claimed that GFP expression prevents the Wt1 expression in the engrafted cells. One aspect that was not considered previously is the fusion potential of MSCs. Accordingly, mouse MSCs could infrequently fuse with kidney cells, which might explain the acquisition of renal markers by the QD-labelled cells. Nevertheless, in a model of folic acid induced kidney injury in mice, no conclusive evidence was found for fusion between bone marrow-derived cells and kidney cells (Fang et al. 2005). In addition, human MSCs were demonstrated to possess multilineage transdifferentiation potential *in vitro*. Accordingly they were shown to differentiate into osteoblasts but upon adipogenic or chondrogenic induction they could reverse their phenotype and become adipocytes or chondrocytes, respectively (Song and Tuan 2004). The transdifferentiation potential of engrafted MSCs as well as other stem cells needs to be considered in studies on renogenic potential. In conclusion, the expression of given renal markers may depend on the labelling method or other factors, like possible fusion events. For this reason, acquisition of renal expression should not be the only criterion for differentiation of engrafted cells. Long-term follow up studies should be performed to assess the commitment of the cells to renal lineages.

MSCs, ESCs and NKCs were found predominantly in the stroma of the chimeric kidneys. These results are in accordance with some data from experiments with adult kidney-derived progenitors

injected into metanephric kidney which were shown to reside to a great extent in the stromal compartment (Challen et al. 2006; Maeshima et al. 2006). Similarly embryonic renal progenitors were shown to mainly localise in the interstitium following a similar recombination experiment involving chimeric kidney formation (Lusis et al. 2010). These results demonstrate that apart from MSCs, other stem cells/progenitors can be found in the stroma of developing kidneys. The behaviour of the cells in the stromal compartment has not yet been determined, and for this reason it cannot be concluded if such cells remain undifferentiated or become embryonic kidney stroma. In any case, the high proportion of stem cells/progenitors not contributing to any renal structures can make efficient generation of *de novo* renal tissue difficult. For the future regenerative therapies it might be important to assess the prevalence of the cells in the stroma and their characteristics.

Ultimately, it is possible that undifferentiated stem cells/progenitors which do not contribute to nephrons, collecting ducts or interstitium in the developing kidneys, could differentiate towards non-renal phenotypes within the kidney. MSCs were demonstrated to improve renal function in acute mesangioproliferative glomerulonephritis in rats, a model of acute renal failure; however, at the same time they were also shown to maldifferentiate into adipocytes. Administration of MSCs led as well to glomerular expression of smooth muscle actin which was accompanied by expression of collagen I, III and IV suggesting a fibrotic response in MSC-treated kidneys (Kunter et al. 2007). Recently, cells found in Wilms tumor, a childhood kidney cancer, were shown to resemble MSCs. Accordingly, Wilms tumor cells demonstrated a similar differentiation potential and expression profile as MSCs (Royer-Pokora et al. 2010). Finally, a recent report showing angiomyeloproliferative lesions in a patient receiving renal injection of hematopoietic

stem cells demonstrates possible risks associated with other stem cell (Thirabanjasak et al. 2010). In conclusion, integration of stem cells/progenitors could have harmful effects in the long term regenerative application. Further experiments are required to assess if MSCs and other cell types do not maldifferentiate when integrated into kidney structures.

In this study the renogenic potential of MSCs, and thus their suitability for renal regeneration, was evaluated using the chimeric kidney assay. It was demonstrated that MSCs have low renogenic potential despite the fact that they expressed some genes involved in metanephric development. However, the integration potential of MSCs in the chimeric kidneys could be enhanced by pre-conditioning of the cells with medium derived from neonatal kidney cell culture. MSCs are possibly not the best candidates for *de novo* renal tissue generation due to their limited integration into nephrons, lack of contribution to UBs and negative indirect effect on kidney development. However, as no common standards exists to evaluate performance of the stem cells/progenitors in the metanephric environment it is difficult to assess if any of the stem cells/progenitors has sufficient renogenic potential to be used for *de novo* kidney formation. Above-mentioned issues should to be considered when evaluating renogenic potential of MSCs and other cells in the future.

Bibliography

Abecassis, M., S. T. Bartlett, et al. (2008). "Kidney transplantation as primary therapy for end-stage renal disease: a National Kidney Foundation/Kidney Disease Outcomes Quality Initiative (NKF/KDOQITM) conference." Clin J Am Soc Nephrol **3**(2): 471-80.

Anjos-Afonso, F. and D. Bonnet (2007). "Nonhematopoietic/endothelial SSEA-1+ cells define the most primitive progenitors in the adult murine bone marrow mesenchymal compartment." Blood **109**(3): 1298-306.

Armstrong, J. F., K. Pritchard-Jones, et al. (1993). "The expression of the Wilms' tumour gene, WT1, in the developing mammalian embryo." Mech Dev **40**(1-2): 85-97.

Azizi, S. A., D. Stokes, et al. (1998). "Engraftment and migration of human bone marrow stromal cells implanted in the brains of albino rats--similarities to astrocyte grafts." Proc Natl Acad Sci U S A **95**(7): 3908-13.

Baddoo, M., K. Hill, et al. (2003). "Characterization of mesenchymal stem cells isolated from murine bone marrow by negative selection." J Cell Biochem **89**(6): 1235-49.

Baens, M., H. Noels, et al. (2006). "The dark side of EGFP: defective polyubiquitination." PLoS One **1**: e54.

Baer, P. C., J. Bereiter-Hahn, et al. (2009). "Conditioned medium from renal tubular epithelial cells initiates differentiation of human mesenchymal stem cells." Cell Prolif **42**(1): 29-37.

Barnes, J. D., J. L. Crosby, et al. (1994). "Embryonic expression of Lim-1, the mouse homolog of Xenopus Xlim-1, suggests a role in lateral mesoderm differentiation and neurogenesis." Dev Biol **161**(1): 168-78.

Barnett, M. W., C. E. Fisher, et al. (2002). "Signalling by glial cell line-derived neurotrophic factor (GDNF) requires heparan sulphate glycosaminoglycan." J Cell Sci **115**(Pt 23): 4495-503.

Baxter, M. A., R. F. Wynn, et al. (2004). "Study of telomere length reveals rapid aging of human marrow stromal cells following in vitro expansion." Stem Cells **22**(5): 675-82.

Bi, B., R. Schmitt, et al. (2007). "Stromal cells protect against acute tubular injury via an endocrine effect." J Am Soc Nephrol **18**(9): 2486-96.

Braun, G. S., R. W. Veh, et al. (2002). "Developmental expression and functional significance of Kir channel subunits in ureteric bud and nephron epithelia." Pflugers Arch **445**(3): 321-30.

Bridgewater, D., B. Cox, et al. (2008). "Canonical WNT/beta-catenin signaling is required for ureteric branching." Dev Biol **317**(1): 83-94.

Brignier, A. C. and A. M. Gewirtz (2010). "Embryonic and adult stem cell therapy." J Allergy Clin Immunol **125**(2 Suppl 2): S336-44.

Brodbeck, S., B. Besenbeck, et al. (2004). "The transcription factor Six2 activates expression of the Gdnf gene as well as its own promoter." Mech Dev **121**(10): 1211-22.

Brophy, P. D., L. Ostrom, et al. (2001). "Regulation of ureteric bud outgrowth by Pax2-dependent activation of the glial derived neurotrophic factor gene." Development **128**(23): 4747-56.

Bruno, S., B. Bussolati, et al. (2009). "Isolation and characterization of resident mesenchymal stem cells in human glomeruli." Stem Cells Dev **18**(6): 867-80.

Bruno, S., C. Grange, et al. (2009). "Mesenchymal stem cell-derived microvesicles protect against acute tubular injury." J Am Soc Nephrol **20**(5): 1053-67.

Brunswig-Spickenheier, B., J. Boche, et al. (2010). "Limited immune-modulating activity of porcine mesenchymal stromal cells abolishes their protective efficacy in acute kidney injury." Stem Cells Dev **19**(5): 719-29.

Burst, V. R., M. Gillis, et al. (2010). "Poor cell survival limits the beneficial impact of mesenchymal stem cell transplantation on acute kidney injury." Nephron Exp Nephrol **114**(3): e107-16.

Bush, K. T., H. Sakurai, et al. (2004). "TGF-beta superfamily members modulate growth, branching, shaping, and patterning of the ureteric bud." Dev Biol **266**(2): 285-98.

Bussolati, B., S. Bruno, et al. (2005). "Isolation of renal progenitor cells from adult human kidney." Am J Pathol **166**(2): 545-55.

Cai, Q., N. I. Dmitrieva, et al. (2005). "Pax2 expression occurs in renal medullary epithelial cells in vivo and in cell culture, is osmoregulated, and promotes osmotic tolerance." Proc Natl Acad Sci U S A **102**(2): 503-8.

Campagnoli, C., I. A. Roberts, et al. (2001). "Identification of mesenchymal stem/progenitor cells in human first-trimester fetal blood, liver, and bone marrow." Blood **98**(8): 2396-402.

Challen, G. A., I. Bertoncello, et al. (2006). "Kidney side population reveals multilineage potential and renal functional capacity but also cellular heterogeneity." J Am Soc Nephrol **17**(7): 1896-912.

Cheng, H. T., M. Kim, et al. (2007). "Notch2, but not Notch1, is required for proximal fate acquisition in the mammalian nephron." Development **134**(4): 801-11.

Cullen-McEwen, L. A., G. Caruana, et al. (2005). "The where, what and why of the developing renal stroma." Nephron Exp Nephrol **99**(1): e1-8.

D'Ippolito, G., S. Diabira, et al. (2004). "Marrow-isolated adult multilineage inducible (MIAMI) cells, a unique population of postnatal young and old human cells with extensive expansion and differentiation potential." J Cell Sci **117**(Pt 14): 2971-81.

da Silva Meirelles, L., P. C. Chagastelles, et al. (2006). "Mesenchymal stem cells reside in virtually all post-natal organs and tissues." J Cell Sci **119**(Pt 11): 2204-13.

Davies, J. (1994). "Control of calbindin-D28K expression in developing mouse kidney." Dev Dyn **199**(1): 45-51.

Davies, J. A. (2010). "The embryonic kidney: isolation, organ culture, immunostaining and RNA interference." Methods Mol Biol **633**: 57-69.

De Coppi, P., G. Bartsch, Jr., et al. (2007). "Isolation of amniotic stem cell lines with potential for therapy." Nat Biotechnol **25**(1): 100-6.

Dekel, B., L. Zangi, et al. (2006). "Isolation and characterization of nontubular sca-1+lin- multipotent stem/progenitor cells from adult mouse kidney." J Am Soc Nephrol **17**(12): 3300-14.

Dezawa, M., H. Ishikawa, et al. (2005). "Bone marrow stromal cells generate muscle cells and repair muscle degeneration." Science **309**(5732): 314-7.

Diduch, D. R., M. R. Coe, et al. (1993). "Two cell lines from bone marrow that differ in terms of collagen synthesis, osteogenic characteristics, and matrix mineralization." J Bone Joint Surg Am **75**(1): 92-105.

Digirolamo, C. M., D. Stokes, et al. (1999). "Propagation and senescence of human marrow stromal cells in culture: a simple colony-forming assay identifies samples with the greatest potential to propagate and differentiate." Br J Haematol **107**(2): 275-81.

Dominici, M., K. Le Blanc, et al. (2006). "Minimal criteria for defining multipotent mesenchymal stromal cells. The International Society for Cellular Therapy position statement."

Cytotherapy **8**(4): 315-7.
Donovan, M. J., T. A. Natoli, et al. (1999). "Initial differentiation of the metanephric mesenchyme is independent of WT1 and the ureteric bud." Dev Genet **24**(3-4): 252-62.
Dressler, G. R. (2006). "The cellular basis of kidney development." Annu Rev Cell Dev Biol **22**: 509-29.
Dressler, G. R. (2009). "Advances in early kidney specification, development and patterning." Development **136**(23): 3863-74.
Dressler, G. R., U. Deutsch, et al. (1990). "Pax2, a new murine paired-box-containing gene and its expression in the developing excretory system." Development **109**(4): 787-95.
Dressler, G. R. and E. C. Douglass (1992). "Pax-2 is a DNA-binding protein expressed in embryonic kidney and Wilms tumor." Proc Natl Acad Sci U S A **89**(4): 1179-83.
Dudley, A. T., R. E. Godin, et al. (1999). "Interaction between FGF and BMP signaling pathways regulates development of metanephric mesenchyme." Genes Dev **13**(12): 1601-13.
Ekblom, P. (1981). "Formation of basement membranes in the embryonic kidney: an immunohistological study." J Cell Biol **91**(1): 1-10.
Ekblom, P., P. Lonai, et al. (2003). "Expression and biological role of laminin-1." Matrix Biol **22**(1): 35-47.
Enomoto, H., T. Araki, et al. (1998). "GFR alpha1-deficient mice have deficits in the enteric nervous system and kidneys." Neuron **21**(2): 317-24.
Fang, T. C., M. R. Alison, et al. (2005). "Proliferation of bone marrow-derived cells contributes to regeneration after folic acid-induced acute tubular injury." J Am Soc Nephrol **16**(6): 1723-32.
Fang, T. C., W. R. Otto, et al. (2008). "Haematopoietic lineage-committed bone marrow cells, but not cloned cultured mesenchymal stem cells, contribute to regeneration of renal tubular epithelium after HgCl 2 -induced acute tubular injury." Cell Prolif **41**(4): 575-91.
Fiorina, P., M. Jurewicz, et al. (2009). "Immunomodulatory function of bone marrow-derived mesenchymal stem cells in experimental autoimmune type 1 diabetes." J Immunol **183**(2): 993-1004.
Fogelgren, B., M. C. Kuroyama, et al. (2008). "Misexpression of Six2 is associated with heritable frontonasal dysplasia and renal hypoplasia in 3H1 Br mice." Dev Dyn **237**(7): 1767-79.
Friedenstein, A. J., R. K. Chailakhyan, et al. (1974). "Stromal cells responsible for transferring the microenvironment of the hemopoietic tissues. Cloning in vitro and retransplantation in vivo." Transplantation **17**(4): 331-40.
Fukui, A., T. Yokoo, et al. (2009). "Integration of human mesenchymal stem cells into the Wolffian duct in chicken embryos." Biochem Biophys Res Commun **385**(3): 330-5.
Golden, J. P., J. A. DeMaro, et al. (1999). "Expression of neurturin, GDNF, and GDNF family-receptor mRNA in the developing and mature mouse." Exp Neurol **158**(2): 504-28.
Gong, K. Q., A. R. Yallowitz, et al. (2007). "A Hox-Eya-Pax complex regulates early kidney developmental gene expression." Mol Cell Biol **27**(21): 7661-8.
Guillaume, R., M. Bressan, et al. (2009). "Paraxial mesoderm contributes stromal cells to the developing kidney." Dev Biol **329**(2): 169-75.
Guillot, P. V., H. T. Cook, et al. (2008). "Transplantation of human fetal mesenchymal stem cells improves glomerulopathy in a collagen type I alpha 2-deficient mouse." J Pathol **214**(5): 627-36.
Guo, J. K., E. C. Cheng, et al. (2007). "The commonly used beta-actin-GFP transgenic mouse strain develops a distinct type of glomerulosclerosis." Transgenic Res **16**(6): 829-34.

Gupta, S., C. Verfaillie, et al. (2002). "A role for extrarenal cells in the regeneration following acute renal failure." Kidney Int **62**(4): 1285-90.
Gupta, S., C. Verfaillie, et al. (2006). "Isolation and characterization of kidney-derived stem cells." J Am Soc Nephrol **17**(11): 3028-40.
Hatini, V., S. O. Huh, et al. (1996). "Essential role of stromal mesenchyme in kidney morphogenesis revealed by targeted disruption of Winged Helix transcription factor BF-2." Genes Dev **10**(12): 1467-78.
Hatini, V., W. Tao, et al. (1994). "Expression of winged helix genes, BF-1 and BF-2, define adjacent domains within the developing forebrain and retina." J Neurobiol **25**(10): 1293-309.
Hauser, P. V., R. De Fazio, et al. (2010). "Stem cells derived from human amniotic fluid contribute to acute kidney injury recovery." Am J Pathol **177**(4): 2011-21.
Herrera, M. B., B. Bussolati, et al. (2004). "Mesenchymal stem cells contribute to the renal repair of acute tubular epithelial injury." Int J Mol Med **14**(6): 1035-41.
Herrera, M. B., B. Bussolati, et al. (2007). "Exogenous mesenchymal stem cells localize to the kidney by means of CD44 following acute tubular injury." Kidney Int **72**(4): 430-41.
Hooper, M., K. Hardy, et al. (1987). "HPRT-deficient (Lesch-Nyhan) mouse embryos derived from germline colonization by cultured cells." Nature **326**(6110): 292-5.
Horn, A. P., A. Bernardi, et al. (2010). "Mesenchymal stem cell conditioned medium triggers neuroinflammation and reactive species generation in organotypic cultures of rat hippocampus." Stem Cells Dev.
Horn, A. P., R. L. Frozza, et al. (2009). "Conditioned medium from mesenchymal stem cells induces cell death in organotypic cultures of rat hippocampus and aggravates lesion in a model of oxygen and glucose deprivation." Neurosci Res **63**(1): 35-41.
Horster, M. F., G. S. Braun, et al. (1999). "Embryonic renal epithelia: induction, nephrogenesis, and cell differentiation." Physiol Rev **79**(4): 1157-91.
Iglesias, D. M., P. A. Hueber, et al. (2007). "Canonical WNT signaling during kidney development." Am J Physiol Renal Physiol **293**(2): F494-500.
Imberti, B., M. Morigi, et al. (2007). "Insulin-like growth factor-1 sustains stem cell mediated renal repair." J Am Soc Nephrol **18**(11): 2921-8.
in 't Anker, P. S., W. A. Noort, et al. (2003). "Mesenchymal stem cells in human second-trimester bone marrow, liver, lung, and spleen exhibit a similar immunophenotype but a heterogeneous multilineage differentiation potential." Haematologica **88**(8): 845-52.
Ito, T., A. Suzuki, et al. (2001). "Bone marrow is a reservoir of repopulating mesangial cells during glomerular remodeling." J Am Soc Nephrol **12**(12): 2625-35.
Jaiswal, J. K., H. Mattoussi, et al. (2003). "Long-term multiple color imaging of live cells using quantum dot bioconjugates." Nat Biotechnol **21**(1): 47-51.
James, R. G., C. N. Kamei, et al. (2006). "Odd-skipped related 1 is required for development of the metanephric kidney and regulates formation and differentiation of kidney precursor cells." Development **133**(15): 2995-3004.
Jendelova, P., V. Herynek, et al. (2004). "Magnetic resonance tracking of transplanted bone marrow and embryonic stem cells labeled by iron oxide nanoparticles in rat brain and spinal cord." J Neurosci Res **76**(2): 232-43.
Jeong, J. H., E. S. Jin, et al. (2009). "Human mesenchymal stem cells implantation into the degenerated coccygeal disc of the rat." Cytotechnology **59**(1): 55-64.
Juffroy, O., D. Noel, et al. (2009). "Subcutaneous graft of D1 mouse mesenchymal stem cells

leads to the formation of a bone-like structure." Differentiation **78**(4): 223-31.
Karavanov, A. A., I. Karavanova, et al. (1998). "Expression pattern of the rat Lim-1 homeobox gene suggests a dual role during kidney development." Int J Dev Biol **42**(1): 61-6.
Karlsson, C., C. Brantsing, et al. (2007). "Differentiation of human mesenchymal stem cells and articular chondrocytes: analysis of chondrogenic potential and expression pattern of differentiation-related transcription factors." J Orthop Res **25**(2): 152-63.
Karner, C. M., R. Chirumamilla, et al. (2009). "Wnt9b signaling regulates planar cell polarity and kidney tubule morphogenesis." Nat Genet **41**(7): 793-9.
Kern, S., H. Eichler, et al. (2006). "Comparative analysis of mesenchymal stem cells from bone marrow, umbilical cord blood, or adipose tissue." Stem Cells **24**(5): 1294-301.
Kim, D. and G. R. Dressler (2005). "Nephrogenic factors promote differentiation of mouse embryonic stem cells into renal epithelia." J Am Soc Nephrol **16**(12): 3527-34.
Kispert, A., S. Vainio, et al. (1998). "Wnt-4 is a mesenchymal signal for epithelial transformation of metanephric mesenchyme in the developing kidney." Development **125**(21): 4225-34.
Kobayashi, A., K. M. Kwan, et al. (2005). "Distinct and sequential tissue-specific activities of the LIM-class homeobox gene Lim1 for tubular morphogenesis during kidney development." Development **132**(12): 2809-23.
Kobayashi, A., M. T. Valerius, et al. (2008). "Six2 defines and regulates a multipotent self-renewing nephron progenitor population throughout mammalian kidney development." Cell Stem Cell **3**(2): 169-81.
Kohlhase, J., A. Wischermann, et al. (1998). "Mutations in the SALL1 putative transcription factor gene cause Townes-Brocks syndrome." Nat Genet **18**(1): 81-3.
Kondo, T., S. A. Johnson, et al. (2005). "Sonic hedgehog and retinoic acid synergistically promote sensory fate specification from bone marrow-derived pluripotent stem cells." Proc Natl Acad Sci U S A **102**(13): 4789-94.
Koshman, Y. E., S. B. Waters, et al. (2008). "Delivery and visualization of proteins conjugated to quantum dots in cardiac myocytes." J Mol Cell Cardiol **45**(6): 853-6.
Kreidberg, J. A., H. Sariola, et al. (1993). "WT-1 is required for early kidney development." Cell **74**(4): 679-91.
Kretlow, J. D., Y. Q. Jin, et al. (2008). "Donor age and cell passage affects differentiation potential of murine bone marrow-derived stem cells." BMC Cell Biol **9**: 60.
Kucerova, L., V. Altanerova, et al. (2007). "Adipose tissue-derived human mesenchymal stem cells mediated prodrug cancer gene therapy." Cancer Res **67**(13): 6304-13.
Kucia, M., R. Reca, et al. (2006). "A population of very small embryonic-like (VSEL) CXCR4(+)SSEA-1(+)Oct-4+ stem cells identified in adult bone marrow." Leukemia **20**(5): 857-69.
Kunter, U., S. Rong, et al. (2007). "Mesenchymal stem cells prevent progressive experimental renal failure but maldifferentiate into glomerular adipocytes." J Am Soc Nephrol **18**(6): 1754-64.
Kunter, U., S. Rong, et al. (2006). "Transplanted mesenchymal stem cells accelerate glomerular healing in experimental glomerulonephritis." J Am Soc Nephrol **17**(8): 2202-12.
Lazzeri, E., C. Crescioli, et al. (2007). "Regenerative potential of embryonic renal multipotent progenitors in acute renal failure." J Am Soc Nephrol **18**(12): 3128-38.
Le Blanc, K. and O. Ringden (2007). "Immunomodulation by mesenchymal stem cells and clinical experience." J Intern Med **262**(5): 509-25.
LeBleu, V., H. Sugimoto, et al. (2009). "Stem cell therapies benefit Alport syndrome." J Am Soc

Nephrol **20**(11): 2359-70.
Lee, P. T., H. H. Lin, et al. (2010). "Mouse kidney progenitor cells accelerate renal regeneration and prolong survival after ischemic injury." Stem Cells **28**(3): 573-84.
Lelongt, B., G. Trugnan, et al. (1997). "Matrix metalloproteinases MMP2 and MMP9 are produced in early stages of kidney morphogenesis but only MMP9 is required for renal organogenesis in vitro." J Cell Biol **136**(6): 1363-73.
Li, K., Q. Han, et al. (2010). "Not a process of simple vicariousness, the differentiation of human adipose-derived mesenchymal stem cells to renal tubular epithelial cells plays an important role in acute kidney injury repairing." Stem Cells Dev **19**(8): 1267-75.
Lin, S., X. Xie, et al. (2007). "Quantum dot imaging for embryonic stem cells." BMC Biotechnol **7**: 67.
Lind, D. E., M. L. Bradley, et al. (1974). "The non-equivalence of mouse and human marrow culture in the assay of granulopoietic stimulatory factors." J Cell Physiol **83**(1): 35-41.
Little, M. H. (2006). "Regrow or repair: potential regenerative therapies for the kidney." J Am Soc Nephrol **17**(9): 2390-401.
Liu, H., R. P. Iacono, et al. (2001). "Detection of GDNF secretion in glial cell culture and from transformed cell implants in the brains of live animals." Mol Genet Genomics **266**(4): 614-23.
Lu, P., L. L. Jones, et al. (2005). "BDNF-expressing marrow stromal cells support extensive axonal growth at sites of spinal cord injury." Exp Neurol **191**(2): 344-60.
Luppen, C. A., R. L. Chandler, et al. (2008). "BMP-2 vs. BMP-4 expression and activity in glucocorticoid-arrested MC3T3-E1 osteoblasts: Smad signaling, not alkaline phosphatase activity, predicts rescue of mineralization." Growth Factors **26**(4): 226-37.
Lusis, M., J. Li, et al. (2010). "Isolation of clonogenic, long-term self renewing embryonic renal stem cells." Stem Cell Res **5**(1): 23-39.
Lyons, A. B. and C. R. Parish (1994). "Determination of lymphocyte division by flow cytometry." J Immunol Methods **171**(1): 131-7.
Mackay, A. M., S. C. Beck, et al. (1998). "Chondrogenic differentiation of cultured human mesenchymal stem cells from marrow." Tissue Eng **4**(4): 415-28.
Maeshima, A., H. Sakurai, et al. (2006). "Adult kidney tubular cell population showing phenotypic plasticity, tubulogenic capacity, and integration capability into developing kidney." J Am Soc Nephrol **17**(1): 188-98.
Maretto, S., M. Cordenonsi, et al. (2003). "Mapping Wnt/beta-catenin signaling during mouse development and in colorectal tumors." Proc Natl Acad Sci U S A **100**(6): 3299-304.
Matsushita, K., F. Morello, et al. (2010). "Mesenchymal stem cells differentiate into renin-producing juxtaglomerular (JG)-like cells under the control of liver X receptor-alpha." J Biol Chem **285**(16): 11974-82.
Mavilio, F. and G. Ferrari (2008). "Genetic modification of somatic stem cells. The progress, problems and prospects of a new therapeutic technology." EMBO Rep **9 Suppl 1**: S64-9.
Mendelsohn, C., E. Batourina, et al. (1999). "Stromal cells mediate retinoid-dependent functions essential for renal development." Development **126**(6): 1139-48.
Mendelsohn, C., D. Lohnes, et al. (1994). "Function of the retinoic acid receptors (RARs) during development (II). Multiple abnormalities at various stages of organogenesis in RAR double mutants." Development **120**(10): 2749-71.
Mikami, Y., M. Lee, et al. (2010). "Dexamethasone modulates osteogenesis and adipogenesis with regulation of osterix expression in rat calvaria-derived cells." J Cell Physiol **226**(3):

739-48.
Min, J. Y., M. F. Sullivan, et al. (2002). "Significant improvement of heart function by cotransplantation of human mesenchymal stem cells and fetal cardiomyocytes in postinfarcted pigs." Ann Thorac Surg **74**(5): 1568-75.
Miyazaki, Y., K. Oshima, et al. (2000). "Bone morphogenetic protein 4 regulates the budding site and elongation of the mouse ureter." J Clin Invest **105**(7): 863-73.
Miyazaki, Y., K. Oshima, et al. (2003). "Evidence that bone morphogenetic protein 4 has multiple biological functions during kidney and urinary tract development." Kidney Int **63**(3): 835-44.
Mora, C. F. (2009). Isolation and characterisation of a novel population of potential kidney stem cells from postnatal mouse kidney University of Liverpool. **PhD**.
Morigi, M., B. Imberti, et al. (2004). "Mesenchymal stem cells are renotropic, helping to repair the kidney and improve function in acute renal failure." J Am Soc Nephrol **15**(7): 1794-804.
Morigi, M., C. Rota, et al. (2010). "Life-sparing effect of human cord blood-mesenchymal stem cells in experimental acute kidney injury." Stem Cells **28**(3): 513-22.
Mugford, J. W., P. Sipila, et al. (2008). "Hoxd11 specifies a program of metanephric kidney development within the intermediate mesoderm of the mouse embryo." Dev Biol **319**(2): 396-405.
Mugford, J. W., P. Sipila, et al. (2008). "Osr1 expression demarcates a multi-potent population of intermediate mesoderm that undergoes progressive restriction to an Osr1-dependent nephron progenitor compartment within the mammalian kidney." Dev Biol **324**(1): 88-98.
Muller-Borer, B. J., M. C. Collins, et al. (2007). "Quantum dot labeling of mesenchymal stem cells." J Nanobiotechnology **5**: 9.
Mundlos, S., J. Pelletier, et al. (1993). "Nuclear localization of the protein encoded by the Wilms' tumor gene WT1 in embryonic and adult tissues." Development **119**(4): 1329-41.
Nemeth, K., A. Keane-Myers, et al. (2010). "Bone marrow stromal cells use TGF-beta to suppress allergic responses in a mouse model of ragweed-induced asthma." Proc Natl Acad Sci U S A **107**(12): 5652-7.
Ninichuk, V., O. Gross, et al. (2006). "Multipotent mesenchymal stem cells reduce interstitial fibrosis but do not delay progression of chronic kidney disease in collagen4A3-deficient mice." Kidney Int **70**(1): 121-9.
Nishinakamura, R., Y. Matsumoto, et al. (2001). "Murine homolog of SALL1 is essential for ureteric bud invasion in kidney development." Development **128**(16): 3105-15.
Nussbaum, J., E. Minami, et al. (2007). "Transplantation of undifferentiated murine embryonic stem cells in the heart: teratoma formation and immune response." FASEB J **21**(7): 1345-57.
Pan, R. L., Y. Chen, et al. (2008). "Fetal liver-conditioned medium induces hepatic specification from mouse bone marrow mesenchymal stromal cells: a novel strategy for hepatic transdifferentiation." Cytotherapy **10**(7): 668-75.
Parish, C. R. (1999). "Fluorescent dyes for lymphocyte migration and proliferation studies." Immunol Cell Biol **77**(6): 499-508.
Peister, A., J. A. Mellad, et al. (2004). "Adult stem cells from bone marrow (MSCs) isolated from different strains of inbred mice vary in surface epitopes, rates of proliferation, and differentiation potential." Blood **103**(5): 1662-8.
Pellegrini, M., S. Pantano, et al. (1997). "Emx2 developmental expression in the primordia of the

reproductive and excretory systems." Anat Embryol (Berl) **196**(6): 427-33.
Perin, L., S. Giuliani, et al. (2007). "Renal differentiation of amniotic fluid stem cells." Cell Prolif **40**(6): 936-48.
Perin, L., S. Sedrakyan, et al. (2010). "Protective effect of human amniotic fluid stem cells in an immunodeficient mouse model of acute tubular necrosis." PLoS One **5**(2): e9357.
Pfaffl, M. W. (2001). "A new mathematical model for relative quantification in real-time RT-PCR." Nucleic Acids Res **29**(9): e45.
Phinney, D. G., G. Kopen, et al. (1999). "Plastic adherent stromal cells from the bone marrow of commonly used strains of inbred mice: variations in yield, growth, and differentiation." J Cell Biochem **72**(4): 570-85.
Pi, Q. M., W. J. Zhang, et al. (2010). "Degradation or excretion of quantum dots in mouse embryonic stem cells." BMC Biotechnol **10**: 36.
Pinaud, F., X. Michalet, et al. (2006). "Advances in fluorescence imaging with quantum dot bio-probes." Biomaterials **27**(9): 1679-87.
Pittenger, M. F., A. M. Mackay, et al. (1999). "Multilineage potential of adult human mesenchymal stem cells." Science **284**(5411): 143-7.
Ponte, A. L., E. Marais, et al. (2007). "The in vitro migration capacity of human bone marrow mesenchymal stem cells: comparison of chemokine and growth factor chemotactic activities." Stem Cells **25**(7): 1737-45.
Popsueva, A., D. Poteryaev, et al. (2003). "GDNF promotes tubulogenesis of GFRalpha1-expressing MDCK cells by Src-mediated phosphorylation of Met receptor tyrosine kinase." J Cell Biol **161**(1): 119-29.
Poulsom, R., S. J. Forbes, et al. (2001). "Bone marrow contributes to renal parenchymal turnover and regeneration." J Pathol **195**(2): 229-35.
Prockop, D. J. (1997). "Marrow stromal cells as stem cells for nonhematopoietic tissues." Science **276**(5309): 71-4.
Prodromidi, E. I., R. Poulsom, et al. (2006). "Bone marrow-derived cells contribute to podocyte regeneration and amelioration of renal disease in a mouse model of Alport syndrome." Stem Cells **24**(11): 2448-55.
Qian, H., H. Yang, et al. (2008). "Bone marrow mesenchymal stem cells ameliorate rat acute renal failure by differentiation into renal tubular epithelial-like cells." Int J Mol Med **22**(3): 325-32.
Qiao, L., Z. L. Xu, et al. (2008). "Dkk-1 secreted by mesenchymal stem cells inhibits growth of breast cancer cells via depression of Wnt signalling." Cancer Lett **269**(1): 67-77.
Raatikainen-Ahokas, A., M. Hytonen, et al. (2000). "BMP-4 affects the differentiation of metanephric mesenchyme and reveals an early anterior-posterior axis of the embryonic kidney." Dev Dyn **217**(2): 146-58.
Raimondo, S., C. Penna, et al. (2006). "Morphological characterization of GFP stably transfected adult mesenchymal bone marrow stem cells." J Anat **208**(1): 3-12.
Ren, X., J. Zhang, et al. (2010). "Differentiation of murine embryonic stem cells toward renal lineages by conditioned medium from ureteric bud cells in vitro." Acta Biochim Biophys Sin (Shanghai) **42**(7): 464-71.
Ripoll, C. B. and B. A. Bunnell (2009). "Comparative characterization of mesenchymal stem cells from eGFP transgenic and non-transgenic mice." BMC Cell Biol **10**: 3.
Rivera, F. J., W. D. Sierralta, et al. (2006). "Adult hippocampus derived soluble factors induce a neuronal-like phenotype in mesenchymal stem cells." Neurosci Lett **406**(1-2): 49-54.

Rogers, S. A., J. A. Lowell, et al. (1998). "Transplantation of developing metanephroi into adult rats." Kidney Int **54**(1): 27-37.
Ronconi, E., C. Sagrinati, et al. (2009). "Regeneration of glomerular podocytes by human renal progenitors." J Am Soc Nephrol **20**(2): 322-32.
Rosen, A. B., D. J. Kelly, et al. (2007). "Finding fluorescent needles in the cardiac haystack: tracking human mesenchymal stem cells labeled with quantum dots for quantitative in vivo three-dimensional fluorescence analysis." Stem Cells **25**(8): 2128-38.
Rosines, E., R. V. Sampogna, et al. (2007). "Staged in vitro reconstitution and implantation of engineered rat kidney tissue." Proc Natl Acad Sci U S A **104**(52): 20938-43.
Royer-Pokora, B., M. Busch, et al. (2010). "Wilms tumor cells with WT1 mutations have characteristic features of mesenchymal stem cells and express molecular markers of paraxial mesoderm." Hum Mol Genet **19**(9): 1651-68.
Saavedra, A., G. Baltazar, et al. (2008). "Driving GDNF expression: the green and the red traffic lights." Prog Neurobiol **86**(3): 186-215.
Sagrinati, C., G. S. Netti, et al. (2006). "Isolation and characterization of multipotent progenitor cells from the Bowman's capsule of adult human kidneys." J Am Soc Nephrol **17**(9): 2443-56.
Sainio, K., D. Nonclercq, et al. (1994). "Neuronal characteristics in embryonic renal stroma." Int J Dev Biol **38**(1): 77-84.
Sainio, K., P. Suvanto, et al. (1997). "Glial-cell-line-derived neurotrophic factor is required for bud initiation from ureteric epithelium." Development **124**(20): 4077-87.
Sajithlal, G., D. Zou, et al. (2005). "Eya 1 acts as a critical regulator for specifying the metanephric mesenchyme." Dev Biol **284**(2): 323-36.
Salazar, K. D., S. M. Lankford, et al. (2009). "Mesenchymal stem cells produce Wnt isoforms and TGF-beta1 that mediate proliferation and procollagen expression by lung fibroblasts." Am J Physiol Lung Cell Mol Physiol **297**(5): L1002-11.
Sanchez, M. P., I. Silos-Santiago, et al. (1996). "Renal agenesis and the absence of enteric neurons in mice lacking GDNF." Nature **382**(6586): 70-3.
Saxen, L., Ed. (1987). Organogenesis of the kidney, Cambridge University Press
Schinkothe, T., W. Bloch, et al. (2008). "In vitro secreting profile of human mesenchymal stem cells." Stem Cells Dev **17**(1): 199-206.
Schittini, A. V., P. F. Celedon, et al. (2010). "Human cardiac explant-conditioned medium: soluble factors and cardiomyogenic effect on mesenchymal stem cells." Exp Biol Med (Maywood) **235**(8): 1015-24.
Schroeder, T. (2008). "Imaging stem-cell-driven regeneration in mammals." Nature **453**(7193): 345-51.
Schuchardt, A., V. D'Agati, et al. (1994). "Defects in the kidney and enteric nervous system of mice lacking the tyrosine kinase receptor Ret." Nature **367**(6461): 380-3.
Sebinger, D. D., M. Unbekandt, et al. (2010). "A novel, low-volume method for organ culture of embryonic kidneys that allows development of cortico-medullary anatomical organization." PLoS One **5**(5): e10550.
Sekiya, I., B. L. Larson, et al. (2002). "Expansion of human adult stem cells from bone marrow stroma: conditions that maximize the yields of early progenitors and evaluate their quality." Stem Cells **20**(6): 530-41.
Self, M., O. V. Lagutin, et al. (2006). "Six2 is required for suppression of nephrogenesis and progenitor renewal in the developing kidney." EMBO J **25**(21): 5214-28.

Semedo, P., P. M. Wang, et al. (2007). "Mesenchymal stem cells ameliorate tissue damages triggered by renal ischemia and reperfusion injury." Transplant Proc **39**(2): 421-3.
Shah, B. S., P. A. Clark, et al. (2007). "Labeling of mesenchymal stem cells by bioconjugated quantum dots." Nano Lett **7**(10): 3071-9.
Shawlot, W. and R. R. Behringer (1995). "Requirement for Lim1 in head-organizer function." Nature **374**(6521): 425-30.
Shen, F. H., J. M. Visger, et al. (2002). "Systemically administered mesenchymal stromal cells transduced with insulin-like growth factor-I localize to a fracture site and potentiate healing." J Orthop Trauma **16**(9): 651-9.
Shi, H., D. Patschan, et al. (2008). "Glial cell line-derived neurotrophic growth factor increases motility and survival of cultured mesenchymal stem cells and ameliorates acute kidney injury." Am J Physiol Renal Physiol **294**(1): F229-35.
Siegel, N., M. Rosner, et al. (2010). "Contribution of human amniotic fluid stem cells to renal tissue formation depends on mTOR." Hum Mol Genet **19**(17): 3320-31.
Simpson, D. A., S. Feeney, et al. (2000). "Retinal VEGF mRNA measured by SYBR green I fluorescence: A versatile approach to quantitative PCR." Mol Vis **6**: 178-83.
Sims-Lucas, S., R. J. Young, et al. (2010). "Redirection of renal mesenchyme to stromal and chondrocytic fates in the presence of TGF-beta2." Differentiation **79**(4-5): 272-84.
Singaravelu, K. and B. J. Padanilam (2009). "In vitro differentiation of MSC into cells with a renal tubular epithelial-like phenotype." Ren Fail **31**(6): 492-502.
So, P. L. and P. S. Danielian (1999). "Cloning and expression analysis of a mouse gene related to Drosophila odd-skipped." Mech Dev **84**(1-2): 157-60.
Solanki, A., J. D. Kim, et al. (2008). "Nanotechnology for regenerative medicine: nanomaterials for stem cell imaging." Nanomedicine (Lond) **3**(4): 567-78.
Song, L. and R. S. Tuan (2004). "Transdifferentiation potential of human mesenchymal stem cells derived from bone marrow." FASEB J **18**(9): 980-2.
Stark, K., S. Vainio, et al. (1994). "Epithelial transformation of metanephric mesenchyme in the developing kidney regulated by Wnt-4." Nature **372**(6507): 679-83.
Steenhard, B. M., K. S. Isom, et al. (2005). "Integration of embryonic stem cells in metanephric kidney organ culture." J Am Soc Nephrol **16**(6): 1623-31.
Sun, Z., Q. Han, et al. (2011). "NANOG Has a Role in Mesenchymal Stem Cells' Immunomodulatory Effect." Stem Cells Dev **20**(9): 1521-8.
Sweetman, D. and A. Munsterberg (2006). "The vertebrate spalt genes in development and disease." Dev Biol **293**(2): 285-93.
Swenson, E. S., J. G. Price, et al. (2007). "Limitations of green fluorescent protein as a cell lineage marker." Stem Cells **25**(10): 2593-600.
Takahashi, M. (2001). "The GDNF/RET signaling pathway and human diseases." Cytokine Growth Factor Rev **12**(4): 361-73.
Tan, T. K., G. Zheng, et al. (2010). "Macrophage matrix metalloproteinase-9 mediates epithelial-mesenchymal transition in vitro in murine renal tubular cells." Am J Pathol **176**(3): 1256-70.
Tao, W., B. G. Evans, et al. (2007). "Enhanced green fluorescent protein is a nearly ideal long-term expression tracer for hematopoietic stem cells, whereas DsRed-express fluorescent protein is not." Stem Cells **25**(3): 670-8.
Thirabanjasak, D., K. Tantiwongse, et al. (2010). "Angiomyeloproliferative lesions following autologous stem cell therapy." J Am Soc Nephrol **21**(7): 1218-22.

Togel, F., A. Cohen, et al. (2009). "Autologous and allogeneic marrow stromal cells are safe and effective for the treatment of acute kidney injury." Stem Cells Dev **18**(3): 475-85.
Togel, F., Z. Hu, et al. (2005). "Administered mesenchymal stem cells protect against ischemic acute renal failure through differentiation-independent mechanisms." Am J Physiol Renal Physiol **289**(1): F31-42.
Togel, F., K. Weiss, et al. (2007). "Vasculotropic, paracrine actions of infused mesenchymal stem cells are important to the recovery from acute kidney injury." Am J Physiol Renal Physiol **292**(5): F1626-35.
Torres, M., E. Gomez-Pardo, et al. (1995). "Pax-2 controls multiple steps of urogenital development." Development **121**(12): 4057-65.
Trupp, M., E. Arenas, et al. (1996). "Functional receptor for GDNF encoded by the c-ret proto-oncogene." Nature **381**(6585): 785-9.
Tsang, T. E., W. Shawlot, et al. (2000). "Lim1 activity is required for intermediate mesoderm differentiation in the mouse embryo." Dev Biol **223**(1): 77-90.
Ulven, S. M., T. E. Gundersen, et al. (2000). "Identification of endogenous retinoids, enzymes, binding proteins, and receptors during early postimplantation development in mouse: important role of retinal dehydrogenase type 2 in synthesis of all-trans-retinoic acid." Dev Biol **220**(2): 379-91.
Unbekandt, M. and J. A. Davies (2010). "Dissociation of embryonic kidneys followed by reaggregation allows the formation of renal tissues." Kidney Int **77**(5): 407-16.
Vega, Q. C., C. A. Worby, et al. (1996). "Glial cell line-derived neurotrophic factor activates the receptor tyrosine kinase RET and promotes kidney morphogenesis." Proc Natl Acad Sci U S A **93**(20): 10657-61.
Vigneau, C., K. Polgar, et al. (2007). "Mouse embryonic stem cell-derived embryoid bodies generate progenitors that integrate long term into renal proximal tubules in vivo." J Am Soc Nephrol **18**(6): 1709-20.
Vize Peter, W. A., Bard Jonathan Ed. (2003). The Kidney. From normal development to congenital disease, Amsterdam-Tokyo, Academic Press.
Wall, M. E., S. H. Bernacki, et al. (2007). "Effects of serial passaging on the adipogenic and osteogenic differentiation potential of adipose-derived human mesenchymal stem cells." Tissue Eng **13**(6): 1291-8.
Wang, Q., Y. Lan, et al. (2005). "Odd-skipped related 1 (Odd 1) is an essential regulator of heart and urogenital development." Dev Biol **288**(2): 582-94.
Ward, H. H., E. Romero, et al. (2011). "Adult human CD133/1(+) kidney cells isolated from papilla integrate into developing kidney tubules." Biochim Biophys Acta **1812**(10): 1344-57.
Weir, C., M. C. Morel-Kopp, et al. (2008). "Mesenchymal stem cells: isolation, characterisation and in vivo fluorescent dye tracking." Heart Lung Circ **17**(5): 395-403.
Weller, A., L. Sorokin, et al. (1991). "Development and growth of mouse embryonic kidney in organ culture and modulation of development by soluble growth factor." Dev Biol **144**(2): 248-61.
Wellik, D. M., P. J. Hawkes, et al. (2002). "Hox11 paralogous genes are essential for metanephric kidney induction." Genes Dev **16**(11): 1423-32.
Woodbury, D., E. J. Schwarz, et al. (2000). "Adult rat and human bone marrow stromal cells differentiate into neurons." J Neurosci Res **61**(4): 364-70.
Xie, Q. P., H. Huang, et al. (2009). "Human bone marrow mesenchymal stem cells differentiate

into insulin-producing cells upon microenvironmental manipulation in vitro." Differentiation **77**(5): 483-91.
Xu, P. X., J. Adams, et al. (1999). "Eya1-deficient mice lack ears and kidneys and show abnormal apoptosis of organ primordia." Nat Genet **23**(1): 113-7.
Yamamoto, M., L. Cui, et al. (2006). "Branching ducts similar to mesonephric ducts or ureteric buds in teratomas originating from mouse embryonic stem cells." Am J Physiol Renal Physiol **290**(1): F52-60.
Yang, H. N., J. S. Park, et al. (2009). "The use of green fluorescence gene (GFP)-modified rabbit mesenchymal stem cells (rMSCs) co-cultured with chondrocytes in hydrogel constructs to reveal the chondrogenesis of MSCs." Biomaterials **30**(31): 6374-85.
Ye, M., S. Chen, et al. (2005). "Glial cell line-derived neurotrophic factor in bone marrow stromal cells of rat." Neuroreport **16**(6): 581-4.
Yokoo, T., A. Fukui, et al. (2006). "Xenobiotic kidney organogenesis from human mesenchymal stem cells using a growing rodent embryo." J Am Soc Nephrol **17**(4): 1026-34.
Yokoo, T., T. Ohashi, et al. (2005). "Human mesenchymal stem cells in rodent whole-embryo culture are reprogrammed to contribute to kidney tissues." Proc Natl Acad Sci U S A **102**(9): 3296-300.
Zhao, T., Z. N. Zhang, et al. (2011). "Immunogenicity of induced pluripotent stem cells." Nature **474**(7350): 212-5.
Zhu, Y., Z. Sun, et al. (2009). "Human mesenchymal stem cells inhibit cancer cell proliferation by secreting DKK-1." Leukemia **23**(5): 925-33.